

**Investigation of Sweeping as a Sample Enrichment  
Method in Micellar Electrokinetic Chromatography  
in the Analysis of Pharmaceutical Preparations and  
Biological Fluids**

**Kumulative Dissertation**

zur

Erlangung des Doktorgrades

der Naturwissenschaften

(Dr. rer. nat.)

dem

Fachbereich Chemie der Philipps-Universität Marburg

vorgelegt von

**M.Sc. Mohamed Ibraheem Mohamed El-Awady**

aus

Ägypten

Marburg an der Lahn 2013



Die vorliegende Dissertation wurde in der Zeit von August 2009 bis Juli 2013 am Fachbereich Chemie der Philipps-Universität Marburg unter der Leitung von Prof. Dr. Ute Pyell angefertigt.

Vom Fachbereich Chemie der Philipps-Universität Marburg als Dissertation am 16.07.2013 angenommen.

Erstgutachter: Prof. Dr. Ute Pyell

Zweitgutachter: Prof. Dr. Gerhard K. E. Scriba (Friedrich-Schiller-Universität Jena)

Tag der mündlichen Prüfung: 17.07.2013

Hochschulkennziffer: 1180



## **Erklärung**

Ich erkläre, dass eine Promotion noch an keiner anderen Hochschule als der Philipps-Universität Marburg, Fachbereich Chemie, versucht wurde.

Ich versichere, dass ich meine vorgelegte Dissertation

*“Investigation of sweeping as a sample enrichment method in micellar electrokinetic chromatography in the analysis of pharmaceutical preparations and biological fluids”*

selbst und ohne fremde Hilfe verfasst, nicht andere als die in ihr angegebenen Quellen oder Hilfsmittel benutzt, alle vollständig oder sinngemäß übernommenen Zitate als solche gekennzeichnet sowie die Dissertation in der vorliegenden oder einer ähnlichen Form noch bei keiner anderen in- oder ausländischen Hochschule anlässlich eines Promotionsgesuchs oder zu anderen Prüfungszwecken eingereicht habe.

Marburg, June 2013

Unterschrift

(Mohamed El-Awady)



*To My Family*



# Preface

This cumulative dissertation is concerned with the investigation of sweeping as a sample enrichment method in micellar electrokinetic chromatography in the analysis of pharmaceutical preparations and biological fluids. The dissertation is based on the following four **publications**, which are referred to within the text by the Roman numerals I-IV:

Publication I: Processes involved in sweeping under inhomogeneous electric field conditions as sample enrichment procedure in micellar electrokinetic chromatography.

Mohamed El-Awady, Carolin Huhn, Ute Pyell,

*Journal of Chromatography A*, 1264 (2012) 124-136 [doi: 10.1016/j.chroma.2012.09.044].

Publication II: Sweeping as a multistep enrichment process in micellar electrokinetic chromatography: The retention factor gradient effect.

Mohamed El-Awady, Ute Pyell,

*Journal of Chromatography A*, 1297 (2013) 213-225 [doi: 10.1016/j.chroma.2013.04.069].

Publication III: Processes involved in sweeping as sample enrichment method in cyclodextrin-modified micellar electrokinetic chromatography of hydrophobic basic analytes.

Mohamed El-Awady, Ute Pyell,

*Submitted to: Electrophoresis.*

Publication IV: Robust analysis of hydrophobic basic analytes in pharmaceutical preparations and biological fluids by sweeping-micellar electrokinetic chromatography with retention factor gradient effect and dynamic pH junction.

Mohamed El-Awady, Fathalla Belal, Ute Pyell,

*Submitted to: Journal of Chromatography A.*

In addition, the results of this work were presented in 3 different **posters** in the following scientific conferences:

- CE Forum: Capillary Electromigration Separation Techniques in Chemistry, Food Chemistry and Pharmacy, October 12-13, 2010, Jülich Research Center, Jülich, Germany.
- The 27<sup>th</sup> International Symposium on MicroScale Bioseparations and Analyses (MSB2012), February 12-15, 2012, Geneva, Switzerland.
- The 39<sup>th</sup> International Symposium on High Performance Liquid Phase Separations and Related Techniques (HPLC2013), June 16-20, 2013, Amsterdam, the Netherlands.

A summary of the major part of the obtained results was introduced as an **oral presentation** in the weekly seminar of the research groups of analytical chemistry in the Department of Chemistry, University of Marburg, February 7, 2012, Marburg, Germany.

# List of abbreviations and symbols

## Abbreviations

BGE	Background electrolyte
BNZ	Benzamide
CAE	Capillary affinity electrophoresis
CCD	Charge-coupled device
CD	Cyclodextrin
CD-MEKC	Cyclodextrin-modified micellar electrokinetic chromatography
CE	Capillary electrophoresis
CEC	Capillary electrochromatography
CGE	Capillary gel electrophoresis
CIEF	Capillary isoelectric focusing
CITP	Capillary isotachopheresis
CMC	Critical micelle concentration
CSE	Capillary sieving electrophoresis
CZE	Capillary zone electrophoresis
DL	Detection limit
DSL	Desloratadine
EF	Enrichment factor
EKC	Electrokinetic chromatography
EOF	Electroosmotic flow
EP	Ethylparaben
FASS	Field-amplified sample stacking
HPLC	High performance liquid chromatography
HP- $\beta$ -CD	Hydroxypropyl- $\beta$ -cyclodextrin
HP- $\beta$ -CD	Hydroxypropyl- $\beta$ -cyclodextrin
I.D.	Inner diameter
I.S.	Internal standard
ICH	International conference on harmonisation
IHP	Inner Helmholtz plane
ITP	Isotachopheresis
IUPAC	International union of pure and applied chemistry

LIF	Laser-induced fluorescence
LOR	Loratadine
MEEKC	Microemulsion electrokinetic chromatography
MEKC	Micellar electrokinetic chromatography
MS	Mass spectrometry
MSS	Micelle to solvent stacking
mtITP	Micellar transient isotachopheresis
O.D.	Outer diameter
OHP	Outer Helmholtz plane
PP	Propylparaben
PSP	Pseudostationary phase
QC	Quality control
QL	Quantitation limit
R&D	Research and development
RFGE	Retention factor gradient effect
RM-MEKC	Reversed direction mode micellar electrokinetic chromatography
RSD	Relative standard deviation
SD	Standard deviation
SDS	Sodium dodecyl sulfate
SE	Sweeping efficiency
SSE	Sum of squared errors
tITP	Transient isotachopheresis
TLC	Thin layer chromatography
TTAB	Tetradecyltrimethylammonium bromide
UV	Ultraviolet

## Symbols

$\alpha_{mic}$	Degree of micellization
$C_{BGE}$	Concentration of the analyte in the separation zone (final zone)
$C_M$	Molar concentration of the micelles
$CMC_{app}$	Apparent critical micelle concentration
$c_s$	Concentration of the analyte in the swept sample zone (primary zone after sweeping)

$c_s$	Molar concentration of monomer surfactant
$c_T$	Total surfactant concentration
$\delta$	Thickness of the ion cloud or of the electric double layer (Debye length)
$E$	Electric field strength
$E_{BGE}$	Electric field strength in the separation zone (BGE)
$E_S$	Electric field strength in the sample zone
$\epsilon_0$	Electric permittivity of vacuum
$\epsilon_r$	Dielectric constant
$f$	Additional focusing/defocusing factor
$F$	Faraday constant
$f_{exp}$	Experimentally measured focusing/defocusing factor
$f_{theo}$	Theoretically predicted focusing/defocusing factor
$\gamma$	Field-strength enhancement factor
$h$	Peak height
$I$	Ionic strength
$\varphi_{BGE}$	Phase ratio in the separation zone (BGE)
$\varphi_S$	Phase ratio in the sample zone
$\kappa$	Debye-Hückel parameter
$K$	Partition coefficient
$k_{app}$	Apparent retention factor
$\kappa_{BGE}$	Electric conductivity of the background electrolyte
$K_{BGE}$	Retention factor of the analyte in the background electrolyte
$k_{BGE,app}$	Apparent retention factor in the background electrolyte
$K_D$	Distribution coefficient
$K_{D,app}$	Apparent distribution coefficient
$K_{mic}$	Micelle-formation equilibrium constant
$\kappa_S$	Electric conductivity of the sample solution

$k_S$	Retention factor of the analyte in the sample zone
$K_{S,app}$	Apparent retention factor in the sample zone
$L_{eff}$	Effective length of the capillary or length to the detector
$l_{focus}$	Length of the focused analyte zone
$l_{grad}$	Final length of the sample zone after sweeping with retention factor gradient effect
$l_{inj}$	Initial sample plug length
$l_{sweep}$	Length of the analyte zone after sweeping
$L_T$	Total length of the capillary
$\mu$	Pseudoeffective electrophoretic mobility of the analyte in micellar background electrolyte
$\mu_a$	Electrophoretic mobility of the analyte
$\mu_{eo}$	Electroosmotic mobility
$\mu_{ep}$	Electrophoretic mobility
$\mu_{ep,eff}$	Effective electrophoretic mobility
$\mu_{PSP}$	Electrophoretic mobility of the pseudostationary phase
$\mu_{PSP,BGE}$	Effective electrophoretic mobility of the pseudostationary phase in the separation zone (BGE)
$\mu_{PSP,S}$	Effective electrophoretic mobility of the pseudostationary phase in the sample zone
$N_C$	Carbon number
$P$	Octanol/water partition coefficient
$pK_a$	Acid dissociation constant
$\theta$	Phase ratio shift factor
$q$	Electric charge
$R$	Gas constant
$r$	Radius
$r$	Correlation coefficient
$R_s$	Peak resolution
$S_a$	Standard deviation of intercept
$S_b$	Standard deviation of slope

$S_{y/x}$	Standard deviation of residuals
T	Temperature
$t_0$	Migration time of the EOF marker
$t_{eo}$	Electroosmotic hold-up time
$t_{mc}$	Migration time of the micelle marker
$t_{mob}$	Residence time in the mobile phase
$t_r$	Retention time or migration time
$t_{rmc}$	Residence time associated with the micellar pseudophase
$t_s$	Migration time of the solute
U	Applied voltage
$V_{aq}$	Volume of aqueous phase
$v_{BGE}$	Velocity of the analyte in the BGE
$v_{eo}$	Electroosmotic velocity
$v_{ep,mc}$	Electrophoretic velocity of micelles
$v_{mc}$	Observed velocity of micelles
$V_{mic}$	Volume of micellar phase
$v_{PSP,BGE}$	Velocity of the pseudostationary phase in the separation zone (BGE)
$v_{PSP,S}$	Velocity of the pseudostationary phase in the sample zone
$v_s$	Velocity of the analyte in the sample zone
$\zeta$	Electrokinetic potential or zeta potential
$\Delta t_r$	Difference in migration time
$\eta$	Viscosity
$\mu_{ob}$	Observed electrophoretic mobility
$\sigma$	Surface charge density

# Table of Contents

<b>Preface</b> .....	i
<b>List of abbreviations and symbols</b> .....	ii
<b>Table of contents</b> .....	vii
<b>1. General introduction</b> .....	1
1.1. Theoretical background of capillary electromigration separation techniques .....	3
1.1.1. Capillary zone electrophoresis or capillary electrophoresis .....	4
1.1.2. Micellar electrokinetic chromatography .....	8
1.1.2.1. Overview .....	8
1.1.2.2. Interaction between micelle and analyte .....	11
1.1.2.3. Retention factor in MEKC .....	11
1.1.2.4. Experimental aspects in MEKC .....	13
1.1.3. Microemulsion electrokinetic chromatography .....	14
1.2. Online sample enrichment in capillary electromigration techniques .....	14
1.2.1. Stacking .....	15
1.2.2. Sweeping .....	16
1.3. Pharmaceutical applications of capillary electromigration techniques .....	18
1.4. References .....	20
<b>2. Aim of the work</b> .....	25
<b>3. Summary</b> .....	27
<b>4. Zusammenfassung</b> .....	29
<b>5. Cumulative part (publications)</b> .....	33
<b>5.1. Publication I</b> .....	35
5.1.1. Summary and discussion .....	37
5.1.2. Author contribution .....	38
5.1.3. Main article .....	39
5.1.4. Supplementary data .....	53
5.1.5. Copyright license agreement .....	63

<b>5.2. Publication II</b> .....	65
5.2.1. Summary and discussion .....	67
5.2.2. Author contribution .....	68
5.2.3. Main article .....	69
5.2.4. Supplementary data .....	83
5.2.5. Copyright license agreement .....	111
<b>5.3. Publication III</b> .....	113
5.3.1. Summary and discussion .....	115
5.3.2. Author contribution .....	116
5.3.3. Main manuscript .....	117
5.3.4. Supporting information .....	151
<b>5.4. Publication IV</b> .....	171
5.4.1. Summary and discussion .....	173
5.4.2. Author contribution .....	174
5.4.3. Main manuscript .....	175
5.4.4. Supplementary data .....	215
<b>6. Acknowledgement</b> .....	225
<b>7. Curriculum Vitae</b> .....	227

# **1. General introduction**



## 1.1. Theoretical background of capillary electromigration separation techniques

Electrophoresis is the migration of charged particles under the influence of an electric field. The technique of moving boundary electrophoresis was reported for the first time by Tiselius [1] for the separation of different serum proteins. Later, the efficiency of the moving boundary method was improved by the development of other techniques such as gel electrophoresis and paper electrophoresis. Paper electrophoresis is now obsolete; however, gel electrophoresis is still used in biochemistry for the determination of proteins and nucleic acids [2]. In 1967, Hjerten [3] was the first to apply electrophoresis using glass tubes with an internal diameter around 3 mm coated with methyl cellulose (free zone electrophoresis). In 1981, Jorgensen and Lukacs [4] created the first operational system that used fused-silica capillaries with an internal diameter of 75  $\mu\text{m}$  and voltages up to 30 kV for the separations of proteins and dansylated amino acids, with plate heights of less than 1  $\mu\text{m}$  (capillary zone electrophoresis). Since then, many papers of highly efficient separations have been published.

The term “capillary electromigration techniques” is a collective term that includes all modes in which electrokinetic phenomena are used for the separation within a capillary [5]. The separations in capillary electromigration techniques are achieved in narrow capillaries by applying a high electric field strength. These techniques include capillary electrophoretic techniques and electrically driven capillary chromatographic techniques, based on different separation principles. In some cases, these principles overlap. Capillary electromigration techniques have proven to be a highly effective tool for the analysis of a large number of substances in different application fields, e.g. the separation of small organic and inorganic ions, pharmaceuticals, explosives, dyes, polymers, proteins and peptides, DNA and RNA, cells, particles, etc. These techniques are characterized by their high speed, an extremely high efficiency and minimum solvent consumption [6,7]. Figure 1 illustrates the basic components of the instrument used in capillary electromigration separation techniques.

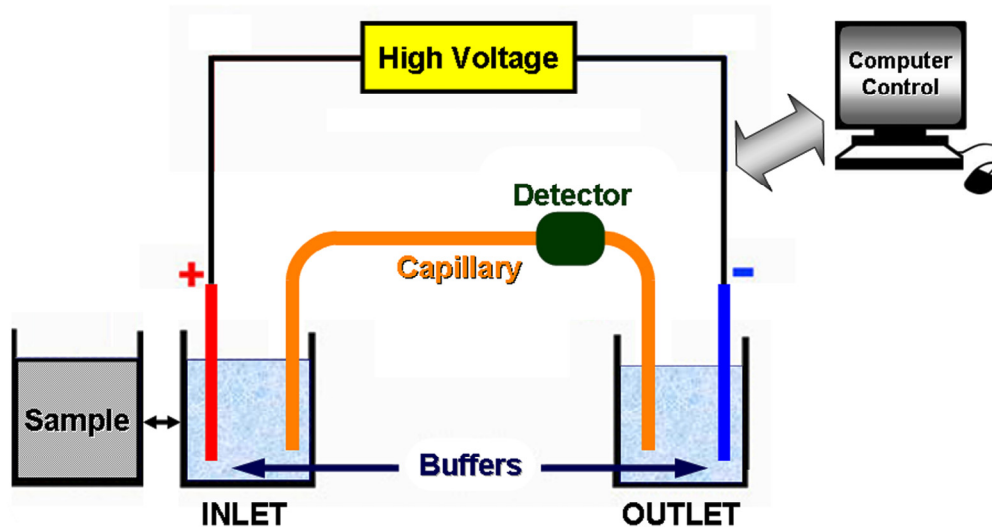


**Figure 1:** basic components of capillary electromigration separation instrument.

The main components of the instrument include a sample vial, inlet and outlet buffer vials, capillary, detector, high-voltage power supply and data handling device such as an integrator or a computer. Upon application of voltage, the analytes migrate through the capillary and they are online detected. Then the signal is handled by the data handling device. The output is displayed as an electropherogram, which is a plot of the detector response versus time [6].

Several modes of capillary electromigration techniques have been reported in the literature such as: capillary zone electrophoresis (CZE), micellar electrokinetic chromatography (MEKC), microemulsion electrokinetic chromatography (MEEKC), capillary affinity electrophoresis (CAE), capillary sieving electrophoresis (CSE), capillary gel electrophoresis (CGE), capillary isoelectric focusing (CIEF), capillary isotachopheresis (CITP) and capillary electrochromatography (CEC).

### **1.1.1. Capillary zone electrophoresis or capillary electrophoresis**

Capillary zone electrophoresis (CZE) or capillary electrophoresis (CE) is the simplest form of capillary electromigration separation techniques. Discussion of this mode permits the presentation of a generic design for the instrumentation for other capillary electromigration modes. The addition of specialized reagents to the separation buffer readily allows the same instrumentation to be used with the other modes [8]. CZE is defined as a separation technique carried out in capillaries based solely on the differences in the electrophoretic mobilities of charged species (analytes) either in aqueous or non-aqueous background electrolyte solutions [5]. The background electrolyte (BGE) can contain additives, which can interact with the analytes and alter their electrophoretic mobility. According to the International Union of Pure and Applied Chemistry (IUPAC), the use of the term capillary electrophoresis (CE) as a collective term for all capillary electromigration techniques is not recommended as some of these techniques involve other separation mechanisms than electrophoresis [5]. The separation principle in CZE is based on the difference between analytes in their effective electrophoretic mobility. Two main aspects are involved in the separation process in CZE; electrophoretic mobility  $\mu_{ep}$  and electroosmotic mobility  $\mu_{eo}$ .

**The electrophoretic mobility  $\mu_{ep}$**  is defined as the electrophoretic velocity  $v$  of an ion normalized on the electric field strength  $E$ . In capillary electrophoresis,  $E$  is calculated by dividing the applied voltage  $U$  by the total length of the capillary  $L_T$ .

$$\mu_{ep} = \frac{v}{E} = \frac{v L_T}{U} \quad (1)$$

For most of the analytical applications,  $\mu_{ep}$  of a charged molecular species can be deduced from a simplified model regarding the ions as charged spheres in a viscous medium:

$$\mu_{ep} = \frac{1}{6 \pi \eta r} q \quad (2)$$

where  $q$  is the charge of the species,  $r$  is the hydrodynamic radius of the charged species,  $\eta$  is the bulk solution viscosity. From this equation, it is evident that small, highly charged species (i.e. high charge to size ratio) have higher mobilities compared to large, less charged species [8].

**The electroosmotic mobility  $\mu_{eo}$**  is defined as the electroosmotic velocity  $v_{eo}$  normalized on the electric field strength  $E$ . If  $L_{eff}$  is the effective length of the capillary (length to the detector),  $t_{eo}$  is the electroosmotic hold-up time,  $U$  is the applied voltage and  $L_T$  is the total length of the capillary, then  $v_{eo}$  and  $\mu_{eo}$  can be calculated as follows [5]:

$$v_{eo} = \frac{L_{eff}}{t_{eo}} \quad (3)$$

$$\mu_{eo} = \frac{v_{eo}}{E} = \frac{L_{eff} L_T}{t_{eo} U} \quad (4)$$

The term “electroosmosis” in capillary electromigration techniques refers to the motion of a liquid through a capillary as a consequence of the application of an electric field across the capillary [5]. To understand electroosmosis, the structure of the electric double layer formed onto the capillary wall should be discussed. Figure 2 shows a schematic illustration of the electrical double layer.

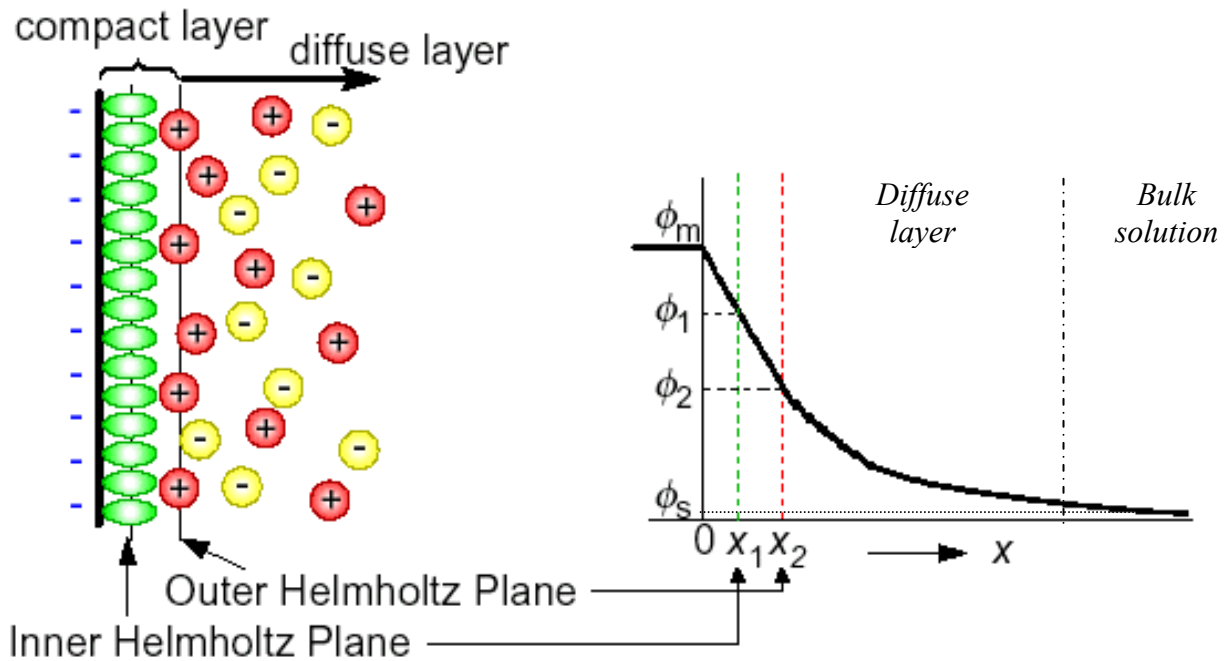


**Figure 2:** Schematic representation of the structure of the electric double layer modified from [9].

Different models have been reported in the literature for describing the structure of the electric double layer [10]. In the Helmholtz layer model, the solvated ions arrange themselves along the charged surface but are held away from it by their hydration spheres. The location of the sheet of ionic charge, which is called the outer Helmholtz plane (OHP), is identified as the plane running through the solvated ions. In this simple model, the electrical potential changes linearly within the layer confined by the charged surface on one side and the OHP on the other. The Helmholtz layer model ignores the disrupting effect of thermal motion, which tends to break up and disperse the rigid outer plane of charge. In the Gouy-Chapman model of the diffuse double layer, the disordering effect of thermal motion is taken into account in the same way as the Debye-Hückel model describes the ionic atmosphere of an ion with the latter's single central ion replaced by an infinite plane charged surface. The local concentrations of cations and anions differ in the Gouy-Chapman model from their bulk concentrations. Ions of opposite charge cluster close to the charged surface and ions of the same charge are repelled from it. Neither the Helmholtz nor the Gouy-Chapman models can adequately describe the structure of the double layer. The former overemphasizes the rigidity of the local solution; the latter underemphasizes its structure. Both models are combined in the Stern model, in which the ions closest to the charged surface are constrained into a rigid Helmholtz plane while outside that plane the ions are dispersed as in the Gouy-Chapman model. In the Grahame model an inner Helmholtz plane (IHP) was added to the Stern model. The IHP is formed from ions that have discarded their solvating molecules and have become attached to the charged surface by chemical bonds [10].

The mechanism of the electroosmotic flow (EOF) is generally described using the electrical double-layer model, in which the counterions are pictured as forming two distinct layers near the solid wall (compact layer and diffuse layer) as shown in Figure 2. In a fused-silica capillary filled with a buffer, the silanol groups (-Si-OH) on the surface of the capillary dissociate into negatively charged (Si-O<sup>-</sup>) groups. Two distinct layers are formed; the first one is a layer of positively charged counter-ions that are strongly adsorbed to the wall resulting in an immobilized compact layer of tightly bound cations. This compact layer is also called the Stern layer. The second layer, known as the diffuse layer, contains cations and anions that arrange themselves in a mobile loosely held layer of solvated ions. As shown in Figure 2, the electric potential is assumed to decrease in a linear fashion across the compact layer while across the diffuse layer and into the bulk solution, the decrease in the electric potential is assumed to be exponential (according to the linearized Poisson-Boltzmann equation). The thickness of the electric double layer (Debye length  $\delta$ ) or its reciprocal (Debye-Hückel parameter  $\kappa$ ) is then given by the following equation [8]:

$$\kappa = \frac{1}{\delta} = \sqrt{\frac{2 I F^2}{R T \varepsilon_0 \varepsilon_r}} \quad (5)$$

where  $\kappa$  is the Debye-Hückel parameter,  $\delta$  is the double layer thickness (Debye length),  $I$  is the ionic strength of the background electrolyte,  $F$  is Faraday constant,  $R$  is the gas constant,  $\varepsilon_0$  is the electric permittivity of vacuum, and  $\varepsilon_r$  is the dielectric constant.

The electric potential at the plane of shear (the interface between the compact and diffuse layers) is called electrokinetic potential or zeta potential  $\zeta$ . The zeta potential depends on the surface charge density  $\sigma$  and on the double layer thickness  $\delta$ . When the radius of the capillary  $r$  is very large compared to the thickness of the electric double layer  $\delta$  ( $r \gg \delta$ ), the EOF linear velocity  $v_{eo}$  and the electroosmotic mobility  $\mu_{eo}$  are given by the Smoluchowski equation [8]:

$$v_{eo} = \frac{\varepsilon_0 \varepsilon_r \zeta E}{\eta} \quad (6)$$

$$\mu_{eo} = \frac{\varepsilon_0 \varepsilon_r \zeta}{\eta} \quad (7)$$

where  $\varepsilon_0$  is the electric permittivity of vacuum,  $\varepsilon_r$  is the dielectric constant,  $\zeta$  is the zeta potential,  $E$  is the electric field strength and  $\eta$  is the viscosity of the background electrolyte.

It is now clear that the EOF velocity is independent of the capillary diameter. It depends on the surface charge density, the ionic strength, the type of solvent, the electric field strength, and via the viscosity of the separation medium on the temperature. When a voltage is applied longitudinally along the capillary, cations in the diffuse layer migrate toward the cathode, mobilizing the bulk solution. This type of mobilization results in a characteristic flat flow profile of the BGE in the direction of the cathode.

An important factor affecting the electroosmotic mobility is the pH of the BGE. The EOF mobility is significantly higher at high pH. At high pH ( $\text{pH} > 9$ ), the silanol groups on the capillary surface are completely ionized and hence, the electroosmotic mobility is very high. However, at low pH ( $\text{pH} < 4$ ) the degree of ionization of the silanol groups is very low and the EOF mobility is nearly negligible [8].

**The observed electrophoretic mobility  $\mu_{ob}$**  of an analyte is determined from the sum of the movement via electrophoretic migration and transport via electroosmotic flow. In other words,  $\mu_{ob}$  can be calculated as follows:

$$\mu_{ob} = \mu_{eo} + \mu_{ep,eff} \quad (8)$$

where  $\mu_{eo}$  is the electroosmotic mobility and  $\mu_{ep,eff}$  is the effective electrophoretic mobility.

The parameter  $\mu_{ob}$ ,  $\mu_{eo}$  and  $\mu_{ep,eff}$  can be obtained from an electropherogram, provided the following magnitudes are known:  $t_{eo}$  (migration time of a neutral EOF marker),  $t_{ob}$  (migration time of the analyte),  $L_T$  (total length of the capillary),  $L_{eff}$  (effective length of the capillary or length to the detector) and  $U$  (applied voltage). Generally, the mobility is positive if the migration is towards the cathode (positively charged species), and the mobility is negative if the migration is towards the anode (negatively charged species).

$$\mu_{ep,eff} = \frac{L_{eff} L_T}{t_{ob} U} - \frac{L_{eff} L_T}{t_{eo} U} \quad (9)$$

In general, capillary electromigration techniques are suitable methods for the determination of different equilibrium constants. For example, because of the dependence of the effective electrophoretic mobility  $\mu_{ep,eff}$  on the pH of the solution, acid dissociation constants can be determined. It is also possible to calculate complex-formation constants from the dependence of  $\mu_{ep,eff}$  on the ligand concentration in the separation electrolyte [11].

### 1.1.2. Micellar electrokinetic chromatography

#### 1.1.2.1. Overview

Micellar electrokinetic chromatography (MEKC) is a capillary electromigration separation technique based on a combination of electrophoresis and interactions of the analytes with dissolved micelles (separation carrier). In order to achieve separation either the analytes or the micellar phase should be charged [5]. Generally, the term “Electrokinetic chromatography (EKC)” refers to the use of different PSPs in capillary electromigration techniques [12]. Several PSPs other than micelles have been used in EKC, for example microemulsions [13-15], charged cyclodextrins [12,16], charged polymers [17,18], proteins [19,20], nanoparticles [21,22] and tetraalkylammonium ions [23,24]. Several books, book chapters, and reviews about MEKC have been published in the literature [11,12,25-29].

MEKC was first introduced by Terabe *et al.* [30] in 1985. In this approach a surfactant is added to the BGE of CZE in a concentration above the critical micelle concentration (CMC) resulting in a formation of micelles that act as a separation carrier that transforms CZE into MEKC. Charged micelles migrate with a velocity different from that of the bulk aqueous phase due to their electrophoretic mobility, whereas the bulk solution migrates with the velocity of the EOF. As in CZE, even a negatively charged micelle can be transported toward the cathode in the case of a strong EOF under either neutral or alkaline conditions. In CZE, neutral analytes can not be separated and they usually migrate at the same velocity as does the bulk solution while in MEKC the separation of neutral analytes is possible.

In general, the micellar pseudophase has an effective electrophoretic mobility and is able to interact with the solutes of interest. In Figure 3 the separation mechanism in MEKC for a neutral solute and a micellar pseudophase of an anionic surfactant is illustrated. In MEKC the micelle acts like the stationary phase in chromatography. However, the micelle is not immobilized, and hence can have an observed velocity different from zero. Therefore, the micellar pseudophase in MEKC is termed pseudostationary phase (PSP). The observed velocity of a solute zone (neutral solute) is the weighted mean of the velocity of the mobile phase (the surrounding aqueous phase) and of the observed velocity of micelles:

$$v_s = \frac{t_{mob}}{t_{mob} + t_{rnc}} v_{mob} + \frac{t_{rnc}}{t_{mob} + t_{rnc}} v_{mc} = \frac{1}{k + 1} v_{mob} + \frac{k}{k + 1} v_{mc} \quad (10)$$

where  $v_s$  is the observed velocity of the solute zone (neutral solute),  $t_{mob}$  is the residence time in the mobile phase,  $t_{rnc}$  is the residence time associated with the micellar pseudophase,  $v_{mob}$  is the velocity of the mobile phase,  $v_{mc}$  is the observed velocity of micelles ( $v_{mc} = v_{ep,mc} + v_{eo}$ ) and  $k$  is the retention factor ( $t_{rnc}/t_{mob}$ ) [11].

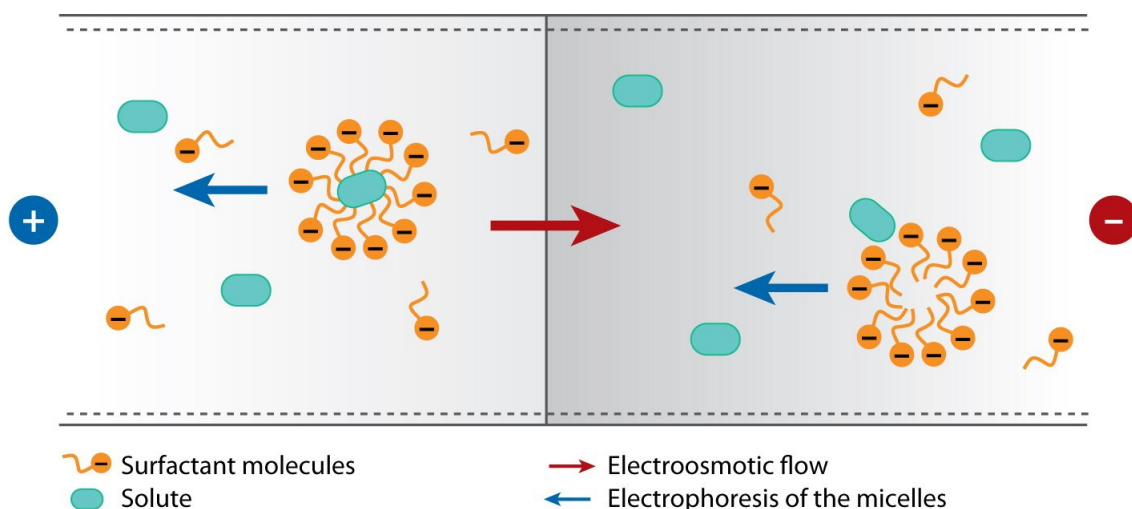


**Figure 3:** Schematic illustration of the separation principle in MEKC [28].

The migration behavior of an imaginary mixture of an EOF marker, a neutral solute and a marker of the micelles of an anionic surfactant is schematically shown in Figure 4. Here, the neutral solute is assumed to be equally distributed between the micelle and the surrounding aqueous phase. As shown in Figure 4a, the aqueous phase is transported at the EOF velocity, and the micellar pseudophase is transported in a much slower velocity due to the effect of its electrophoretic mobility in the opposite direction to the EOF. The neutral solute zone migrates at an average velocity between

that of the EOF marker and the micelle marker. The three components in the proposed mixture are assumed to be detectable, resulting in an electropherogram (Figure 4b).

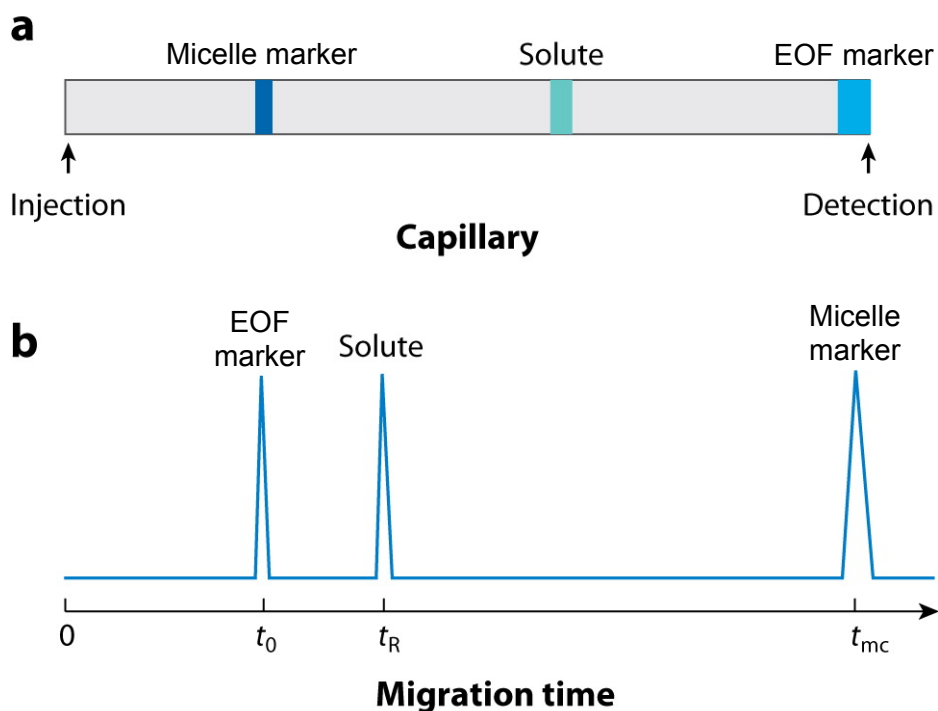


**Figure 4:** Migration behavior of zones (a) and MEKC electropherogram (b) of an imaginary mixture of an EOF marker, a neutral solute and a micelle marker.  $t_0$ ,  $t_R$ , and  $t_{mc}$  are migration times of the EOF marker, the solute and the micelle marker, respectively [28].

Micelles are molecular aggregates of surfactant molecules formed in dynamic equilibrium with single molecules if the surfactant is present in solution at a concentration higher than the critical micelle concentration (CMC). In MEKC, sodium dodecyl sulfate (SDS) is the most widely employed anionic surfactant used to generate the PSP because it has several advantages over other surfactants, including its well-characterized properties, high solubilization capability, easy availability, low ultraviolet absorbance, and high solubility in aqueous solutions. Minor disadvantages of SDS are its relatively high CMC (about 8 mmol L<sup>-1</sup> in pure water, less in buffer solutions) and its liability to be precipitated at low temperatures. Tetradecyltrimethylammonium bromide (TTAB) is an example of a popular cationic surfactant used in MEKC. Cationic surfactants offer a complementary selectivity to anionic surfactants. An important feature of cationic surfactants is their tendency to be strongly adsorbed onto the surface of the capillary and to reverse the EOF. Two different surfactants can be also combined in MEKC to form mixed micelles. Mixed micelles consisting of ionic and nonionic surfactants are also useful PSPs because they provide a significantly different separation selectivity compared to micelles formed from a single ionic surfactant [28].

### 1.1.2.2. Interaction between micelle and analyte

Three types of interaction are known between micelles and analytes: (1) incorporation of the analyte into the hydrophobic core of the micelle, (2) adsorption of the analyte on the surface of the micelle by electrostatic or dipole interaction and (3) incorporation of the analyte as a cosurfactant by participating in the formation of the micelle (Figure 5a). In case of mixed micelles, an additional interaction between analyte and the non-ionic surface is also possible (Figure 5b) [27].

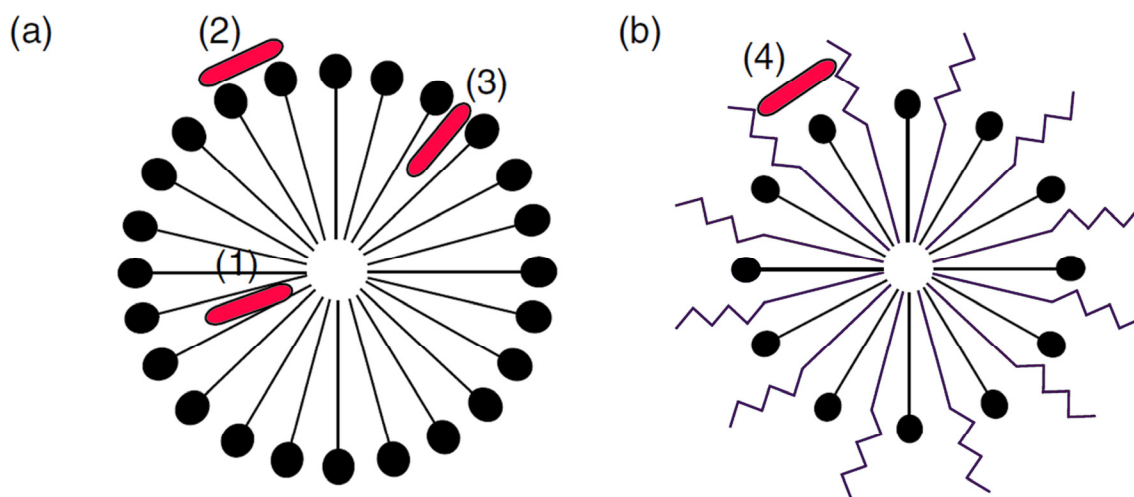


**Figure 5:** Schematic illustration of micellar solubilization.

(a) Ionic micelle and (b) mixed micelle of ionic and nonionic surfactants interacting (1) with the hydrophobic core, (2) on the surface, (3) as a cosurfactant, and (4) with nonionic surface [27].

The effect of the molecular structure of the surfactant on the separation selectivity differs according to the type of interaction involved. The hydrophilic, or ionic group, is generally more important in determining selectivity than is the hydrophobic group since most analytes interact with the micelle at the surface. Different polar groups of various surfactants can show different selectivity for analytes, even if the surfactants have identical alkyl chain groups [31].

### 1.1.2.3. Retention factor in MEKC

Similar to chromatography the retention factor  $k$  (older term: capacity factor  $k'$ ) in MEKC is defined as the residence time in the micellar pseudophase (pseudostationary phase) divided by the residence time in the surrounding liquid phase. If we assume the micelles to be a homogeneous pseudophase, the separation process can be understood to be due to distribution between two distinct phases having two different observed mobilities [11]:

$$k = K_D \frac{V_{mic}}{V_{aq}} \quad (11)$$

where  $K_D$  is the distribution coefficient,  $V_{mic}/V_{aq}$  is the phase ratio (= volume of micellar phase/volume of aqueous phase). By replacing the velocities with the respective distance-over-time and rearranging the results, the following equation is obtained:

$$k = \frac{t_s - t_0}{t_0(1 - t_s / t_{mc})} \quad (12)$$

where  $t_0$  = migration time of the EOF marker,  $t_s$  = migration time of the solute,  $t_{mc}$  = migration time of the micelle marker.

This equation is valid only in the normal elution mode where the electroosmotic velocity  $v_{eo}$  and the velocity of micelles  $v_{mc}$  have identical direction and  $|v_{eo}| > |v_{mc}|$  [32]. Gareil [33] has shown that in the case that the observed velocity of the solute zone is opposite to that of the  $v_{eo}$  (reversed direction mode),  $k$  has to be determined using the following equation:

$$k = \frac{t_s + t_0}{t_0(t_s / t_{mc} - 1)} \quad (13)$$

For measuring the retention factor for charged solutes in MEKC, a different approach is needed. The calculation is then based on following equation [34]:

$$k = \frac{\mu - \mu_{ep,eff}}{\mu_{mc} - \mu} \quad (14)$$

where  $\mu$  = pseudoeffective electrophoretic mobility of the analyte in micellar BGE,  $\mu_{ep,eff}$  = effective electrophoretic mobility of the analyte in micelle-free BGE, and  $\mu_{mc}$  = electrophoretic mobility of the micelles in micellar BGE.

In the presence of an organic solvent or a cyclodextrin in the micellar BGE, the direct measurement of retention factors using a single compound as a micelle marker is no longer reliable [35]. That is because the prerequisite that the micelle marker should have a retention factor of infinity is no longer fulfilled [35]. Therefore, in these cases the iterative procedure published by Bushey and Jorgenson [36,37] should be used for the determination of the electrophoretic mobility of the micelles. This method is based on the Martin equation valid for the retention factors of the members of a homologous series. For example, Chen *et al.* [35] used the homologous series of alkyl phenyl ketones for measuring  $t_{mc}$  values in BGEs containing methanol, acetonitrile, 1-propanol and tetrahydrofuran. Further experimental details about the procedure of this approach are discussed within the cumulative part of the dissertation.

#### **1.1.2.4. Experimental aspects in MEKC**

MEKC is performed with a conventional capillary electrophoresis instrument simply by using a micellar BGE consisting of a surfactant dissolved in a buffer at a concentration higher than its CMC. The CMC of SDS, the most popular surfactant used in MEKC, is about 8 mmol L<sup>-1</sup> in pure water but can range from 2.8 to 6.4 mmol L<sup>-1</sup>, depending on the buffer composition and the temperature [38]. Therefore, experimental parameters must be kept constant to obtain precise data. Usually, untreated or bare fused-silica capillaries are employed in MEKC. The inner surface of the capillary is negatively charged due to ionization of the silanol group above a pH of 2, and the direction of the EOF is toward the cathode [28]. However, if a cationic surfactant such as TTAB is used as PSP, the EOF is directed toward the anode because the inner capillary surface becomes positively charged due to the adsorption of the cationic surfactant [39]. To suppress the EOF, polyacrylamide- or polyethylene glycol-coated capillaries can be utilized, but it is difficult to completely suppress the EOF with cationic surfactants [28].

The right choice of the detection technique in MEKC depends on the type and concentration of analytes, the complexity of the sample and the potential interferences from the sample matrix. In addition, the commercial availability of the detector, and the cost and ease of operation should also be considered. Optical detection techniques, including UV spectrophotometric and laser-induced fluorescence (LIF) detection, are widely used in MEKC. The sensitivity of spectrophotometric detectors is relatively low while LIF detection is very sensitive and can detect concentrations down to the nanomolar scale. Other detection techniques based on the measurement of electrochemical properties of analytes (conductometric or amperometric detection) are less often used, but their sensitivity is in many cases better than the sensitivity of UV spectrophotometric detectors [40]. Mass spectrometry (MS) is an important detection method for capillary electromigration techniques, as well as for gas and liquid chromatography. MS is difficult to be routinely used in MEKC because PSPs used in MEKC are often incompatible with MS, as they interfere with the ionization process necessary for detection [41]. Different approaches have been proposed to solve this problem [42]. One solution of this problem is the partial filling technique [43,44], where only a part of the capillary is filled with an electrolyte solution containing the PSP, which allows the separation avoiding the entrance of the PSP into the ion source of the mass spectrometer. In order to lower the detection limit of MEKC methods, several online sample preconcentration techniques have been developed and will be discussed in Section 1.2.

Besides the capillary format of MEKC, chip technologies have emerged in the last decade, triggering new rapid developments in this field and offering several advantages over capillaries such as the possibility to use higher electric field strength and shorter separation lengths in addition to the suitability to use more sophisticated detection techniques [45].

### 1.1.3. Microemulsion electrokinetic chromatography

Microemulsion electrokinetic chromatography (MEEKC) is a special case of electrokinetic chromatography, where a microemulsion is employed as the dispersed phase (pseudostationary phase). Microemulsions (oil in water) consisting of a surfactant, an oil, a cosurfactant, and water were first used as a PSP in EKC by Watarai [13] and Watarai *et al.* [14]. Very soon, the technique is termed microemulsion electrokinetic chromatography or MEEKC [15]. The theoretical background of MEEKC and its comparison with MEKC have been discussed in the literature [15,46]. Because microemulsions contain additional oil and cosurfactant components, their separation selectivity seems to be very different from that of MEKC. However, since both methods use the same surfactant, their separation selectivities do not differ significantly [13-15]. The component that most affects selectivity in MEEKC is the cosurfactant, as its polar group is located on the surface of the microemulsion. The oil effect on the microemulsion is not very significant because most analytes cannot be incorporated into the core oil, but rather remain on the surface [28]. An advantage of MEEKC over MEKC is that its migration time window can be widened by changing the surfactant concentration [15]. Although MEEKC usually employs an oil-in-water microemulsion, a water-in-oil microemulsion in butanol has been also used with different selectivity compared to oil-in-water microemulsion [47].

### 1.2. Online sample enrichment in capillary electromigration techniques

One disadvantage of capillary electromigration techniques is the low detection sensitivity because of the small loaded sample volume (few nanoliters) and the narrow optical pathlength. This problem is more challenging in case of trace analysis [48]. Different approaches have been investigated to overcome this problem such as the use of a capillary with longer path length (e.g. Z-shape [49] and bubble cells [50]), the use of high-sensitivity detectors like laser-induced fluorescence detectors [51], off-line concentration of the analyte through liquid-liquid extraction [52] or solid phase extraction [53], and the employment of online sample preconcentration (enrichment) methods [48,54].

Online sample preconcentration techniques are focusing techniques that preconcentrate the analyte within the capillary before separation and detection. In these approaches, either a large volume of the sample solution is injected into the capillary via pressurized injection then the analyte is concentrated inside the capillary before separation or the analyte is electrokinetically injected from the sample solution and concentrated at the injection end of the capillary before separation [28]. Several review articles about online sample preconcentration methods have been published in the literature [55-64]. Currently, sample stacking and sweeping are the most widely used techniques for online sample preconcentration in capillary electromigration techniques.

### 1.2.1. Stacking

One of the simplest methods for sample preconcentration is to induce “stacking” of analytes by exploiting the electric conductivity differences between the sample matrix and the BGE [65,66]. The sample is prepared in a matrix having an electric conductivity lower than that of the BGE. Stacking results from the fact that the analytes have an enhanced velocity in a lower electric conductivity (high electric field strength) zone. When the voltage is applied to the system, the charged analytes in the sample plug migrate toward the adjacent BGE compartment. Upon crossing the sample/BGE boundary, the higher conductivity zone induces a decrease in the electrophoretic velocity and subsequent “stacking” of the sample components into a smaller zone than the original sample plug (see Figure 6). Stacking can be achieved with either hydrodynamic or electrokinetic injection of the sample [8]. Several stacking modes have been reported in the literature [56,65].

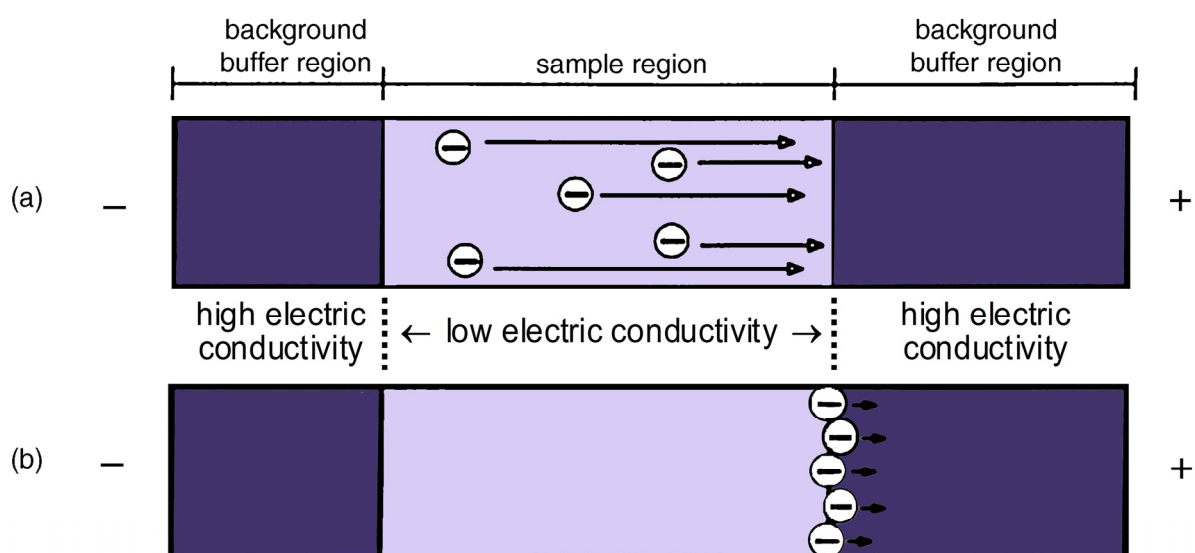


**Figure 6:** Schematic illustration of sample stacking for negatively charged analyte modified from [67]. (a) Fast migration of analyte in the sample zone (high electric field strength). (b) Abrupt decrease in the analyte velocity when crossing the sample/BGE boundary resulting in focusing of the analyte zone.

In MEKC, analytes having an effective electrophoretic mobility, e.g. due to protonation or dissociation, can be also preconcentrated by stacking [68,69]. Liu *et al.* [70] have presented the concept of field-amplified sample stacking for online enrichment of neutral hydrophobic molecules in MEKC. They used an aqueous sample matrix having a low electric conductivity and containing micelles in a concentration just above the CMC. The analytes investigated were extremely hydrophobic (tetrachlorodibenzo-*p*-dioxins and polynuclear aromatic hydrocarbons). In this case, the retention factor is very high so that the effective electrophoretic mobility of the analytes equals in first approximation the electrophoretic mobility of the micelles, which are stacked at the sample/BGE boundary. With this concept, Liu *et al.* [70]

succeeded in combining on-line enrichment with the separation of a mixture of polycyclic aromatic hydrocarbons with a BGE containing 100 mmol L<sup>-1</sup> sodium borate, 100 mmol L<sup>-1</sup> SDS, 5 mol L<sup>-1</sup> urea, and 10 mmol L<sup>-1</sup>  $\gamma$ -cyclodextrin, while the sample solution consisted of 9 mmol L<sup>-1</sup> SDS in aqueous buffer. Quirino and Terabe [71] extensively developed sample preconcentration techniques for neutral analytes using the field-amplified stacking technique.

### 1.2.2. Sweeping

Sweeping is one of the most important sample preconcentration techniques in MEKC. It is based on the accumulation of analyte molecules by the PSP that penetrates the sample zone being void of PSP [72]. The principle of sweeping is illustrated in Figure 7.

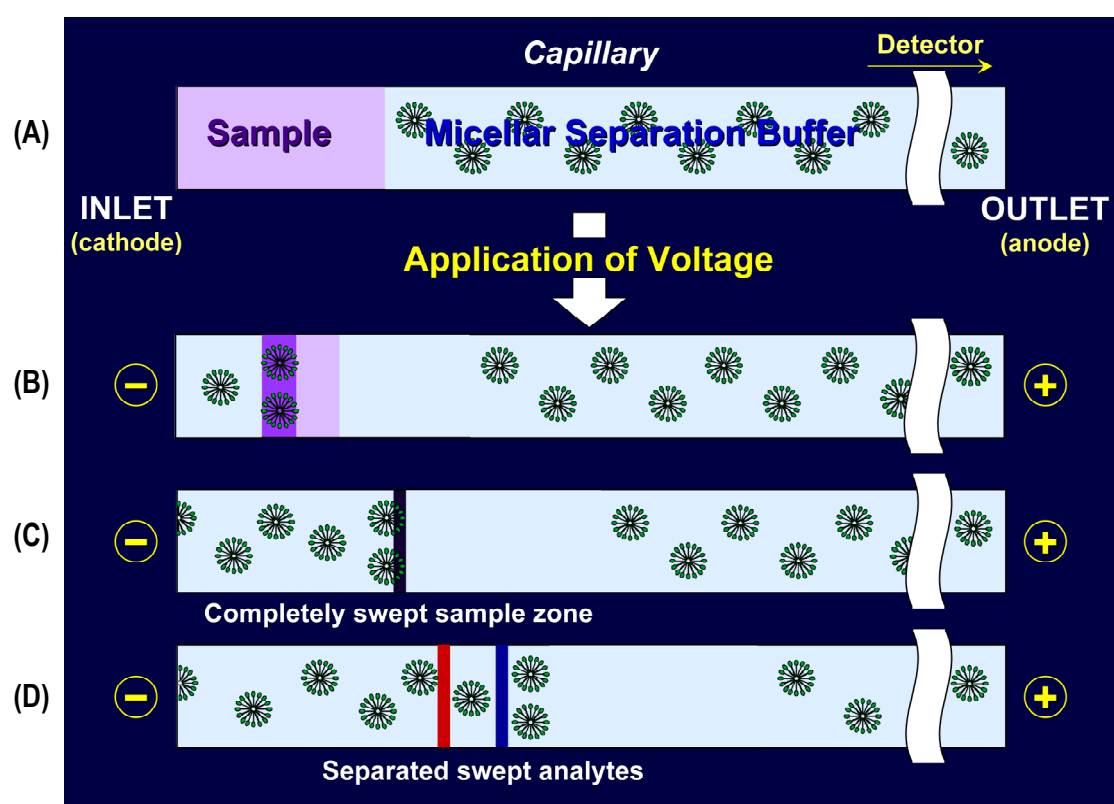


**Figure 7:** Schematic illustration of the sweeping process using negatively charged micelles under homogeneous electric field and zero EOF conditions. (A) Starting situation: injection of a large volume of the sample solution prepared in a matrix with an electric conductivity similar to that of the micellar BGE. (B) Application of voltage (reversed polarity mode) associated with the entrance of micelles into the sample zone and sweeping of the analyte molecules. (C) Formation of the final swept analyte zone when the micelles have filled the sample zone. (D) Separation of analytes by MEKC.

Investigations related to sweeping have been early described by some authors but under different names [70,73]. In 1998, the concept of sweeping was introduced by Quirino and Terabe [72]. Their

study included neutral analytes dissolved in matrices having the same electric conductivity as the BGE using SDS as anionic surfactant. In 1999, more investigations on the sweeping phenomenon and the role of analyte charge and electroosmotic flow were performed by the same authors including sweeping under homogeneous and inhomogeneous electric field conditions [74,75]. Very soon, sweeping was further applied by Kim *et al.* [76] using cationic surfactants. In a similar approach, Palmer *et al.* [77] used electokinetic injection of a sample containing neutral analytes dissolved in BGE void of micelles. Since the first introduction of sweeping as a sample enrichment method in MEKC [72] and until now, several publications have been emerged in the literature studying the fundamentals of sweeping and its application in different analytical fields. A summary of the number of publications dealing with sweeping in MEKC methods is presented in Figure 8.

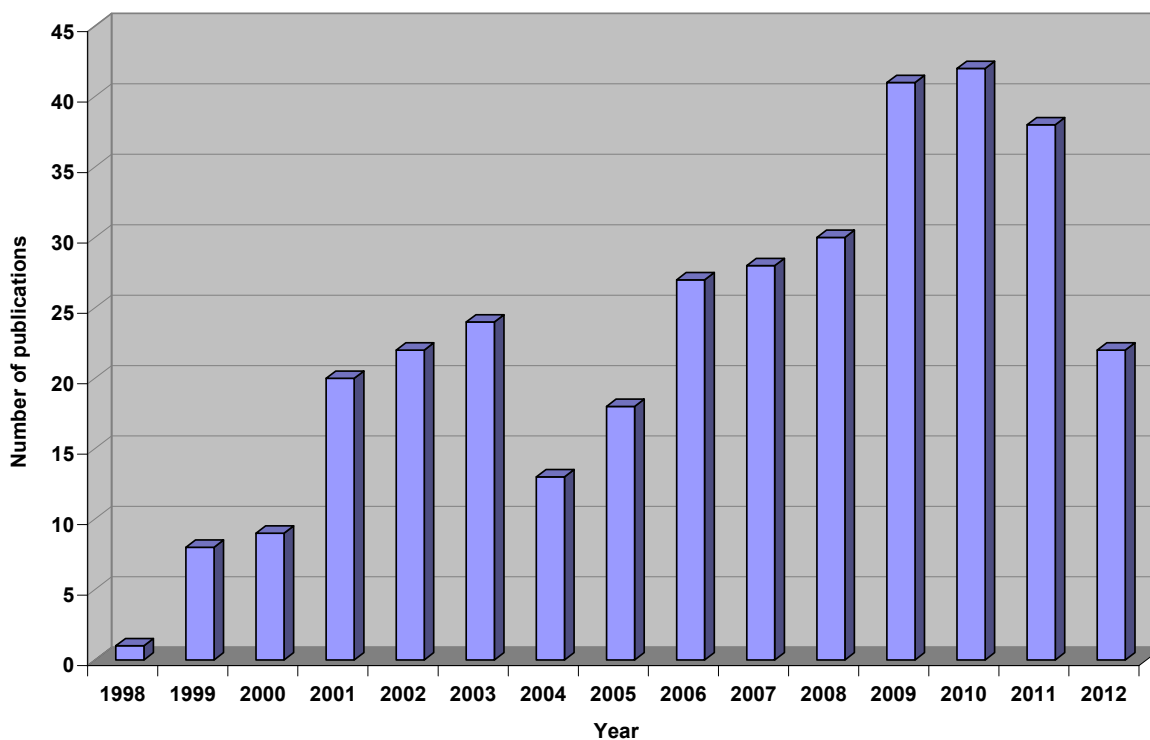


**Figure 8:** Statistical diagram of the number of publications about sweeping in capillary electromigration methods from 1998 to 2012 based on the research records in SciFinder® database.

According to the concept, presented by Quirino and Terabe [72], the length of the sample zone after sweeping  $l_{\text{sweep}}$  depends only on the initial sample-plug length  $l_{\text{inj}}$  and on the retention factor in the sample zone  $k_S$  during sweeping. The enrichment factor ( $= l_{\text{inj}}/l_{\text{sweep}}$ ) is then directly proportional to  $k_S$ :

$$l_{\text{sweep}} = \frac{1}{1 + k_S} l_{\text{inj}} \quad (15)$$

However, we showed experimentally and theoretically that the focusing process due to sweeping is not only influenced by the retention factor of the analyte in the sample zone, but also by the retention factor of the analyte in the BGE [78].

Additional information about the sweeping technique as well as the underlying processes are included in the cumulative part (publications) of this dissertation.

### **1.3. Pharmaceutical applications of capillary electromigration techniques**

Capillary electromigration techniques are powerful separation tools that are widely used in research and development (R&D), quality control (QC), and stability studies of pharmaceuticals. They offer several advantages over high-performance liquid chromatography (HPLC) methods like simplicity, rapid analysis, automation, ruggedness, different mechanisms for selectivity, and low cost. In addition, they offer higher efficiency and thus greater resolution power than HPLC even if only a small sample size is available [2]. Several publications were concerned with the strategies that can be employed for the development, optimization and validation of capillary electrophoretic methods [79-83].

Capillary electromigration techniques have been found particularly useful for different separation problems in the pharmaceutical field. Different application areas have been explored by these techniques including the analysis of peptides, enantiomeric separation, analysis of small molecules such as amino acids or drug counter-ions, pharmaceutical assay, related substances determinations, and physicochemical measurements such as log P and pKa of compounds of peptides, proteins, carbohydrates, inorganic ions, chiral compounds, and other numerous pharmaceutical applications [2]. Several comprehensive review articles can be found in the literature covering the pharmaceutical applications of capillary electromigration techniques [84-95].

The international pharmacopoeias such as the United States Pharmacopeia (USP), the European Pharmacopeia (EP) and the Japanese Pharmacopeia (JP), being responsible for the quality of drugs, are continuously revising their monographs. Nowadays the pharmacopoeias make use of chromatographic methods in identification and purity evaluation purposes and try to replace the less sensitive thin layer chromatography (TLC) methods with HPLC tests. However, capillary electromigration separation methods can offer a more selective, efficient and rapid alternative to HPLC methods and therefore they are often more appropriate for the impurity evaluation of a drug than HPLC. In addition, capillary electrophoretic assay methods are currently applied in the USP and the EP for the analysis of peptides and proteins [96].

In the field of pharmaceutical analysis, the sensitivity is a very important issue especially in case of trace analysis like the analysis of impurities or metabolites. Because one of the major challenges in capillary electromigration separation techniques is the low sensitivity compared to HPLC methods, the use of sample enrichment methods is of great importance in this field [48]. This was one of the most important motivations of the present study.

#### 1.4. References

- [1] A. Tiselius, *Trans. Faraday Soc.* 33 (1937) 524.
- [2] S. Ahuja, in S.Ahuja, M.I.Jimidar (Editors), *Capillary Electrophoresis Methods for Pharmaceutical Analysis*, Elsevier, San Diego, 2008, p. 1.
- [3] S. Hjerten, *Chromatogr Rev* 9 (1967) 122.
- [4] J.W. Jorgenson, K.D. Lukacs, *Anal. Chem.* 53 (1981) 1298.
- [5] M.L. Riekkola, J.A. Joensuu, R.M. Smith, D. Moore, F. Ingman, K.J. Powell, R. Lobinski, G.G. Gauglitz, V.P. Kolotov, K. Matsumoto, R.M. Smith, Y. Umezawa, Y. Vlasov, A. Fajgelj, H. Gamsjaeger, D.B. Hibbert, W. Kutner, K. Wang, E.A.G. Zagatto, M.L. Riekkola, H. Kim, A. Sanz-Medel, *T. Ast, Pure Appl. Chem.* 76 (2004) 443.
- [6] D.R. Baker, *Capillary Electrophoresis*, John Wiley, New York, 1995.
- [7] W. Kok, *Chromatographia* 51 (2000) S1-S89.
- [8] J.P. Landers, in J.P.Landers (Editor), *Handbook of Capillary and Microchip Electrophoresis and Associated Microtechniques*, Third Edition, CRC Press, New York, 2008, p. 3.
- [9] [http://web.nmsu.edu/~snsm/classes/chem435/Lab14/double\\_layer.html](http://web.nmsu.edu/~snsm/classes/chem435/Lab14/double_layer.html) (accessed 15.06.2013)
- [10] P. Atkins, J. De Paula, *Physical Chemistry*, 9th Edition, Oxford University Press, Oxford, UK, 2010.
- [11] U. Pyell, in U.Pyell (Editor), *Electrokinetic Chromatography - Theory, Instrumentation and Applications*, John Wiley & Sons, Ltd, Chichester, 2006, p. 3.
- [12] S. Terabe, *TrAC Trends Anal. Chem.* 8 (1989) 129.
- [13] H. Watarai, *Chem. Lett.* (1991) 391.
- [14] H. Watarai, K. Ogawa, M. Abe, T. Monta, I. Takahashi, *Anal. Sci.* 7 (1991) 245.
- [15] S. Terabe, N. Matsubara, Y. Ishihama, Y. Okada, *J. Chromatogr.* 608 (1992) 23.
- [16] S. Terabe, H. Ozaki, K. Otsuka, T. Ando, *J. Chromatogr.* 332 (1985) 211.
- [17] S. Terabe, T. Isemura, *J. Chromatogr.* 515 (1990) 667.
- [18] S. Terabe, T. Isemura, *Anal. Chem.* 62 (1990) 650.
- [19] G.E. Barker, P. Russo, R.A. Hartwick, *Anal. Chem.* 64 (1992) 3024.
- [20] Y. Tanaka, N. Matsubara, S. Terabe, *Electrophoresis* 15 (1994) 848.
- [21] K. Bächmann, B. Göttlicher, *Chromatographia* 45 (1997) 249.
- [22] C. Nilsson, S. Nilsson, *Electrophoresis* 27 (2006) 76.

- [23] Y. Walbroehl, J.W. Jorgenson, *Anal. Chem.* 58 (1986) 479.
- [24] S. Pedersen-Bjergaard, R. Einar, T. Tilander, *J. Chromatogr. A* 807 (1998) 285.
- [25] S. Terabe, N. Chen, K. Otsuka, *Adv. Electrophor.* 7 (1994) 87.
- [26] U. Pyell, *Fresenius' J. Anal. Chem.* 371 (2001) 691.
- [27] S. Terabe, *Anal. Chem.* 76 (2004) 240A.
- [28] S. Terabe, *Annu. Rev. Anal. Chem.* 2 (2009) 99.
- [29] S. Terabe, *Procedia Chem.* 2 (2010) 2.
- [30] S. Terabe, K. Otsuka, T. Ando, *Anal. Chem.* 57 (1985) 834.
- [31] L. Jia, S. Terabe, in U.Pyell (Editor), *Electrokinetic Chromatography - Theory, Instrumentation and Applications*, John Wiley & Sons, Ltd, Chichester, 2006, p. 79.
- [32] J. Vindevogel, P. Sandra, *Introduction to micellar electrokinetic chromatography*, Hüthig, Heidelberg, 1992.
- [33] P. Gareil, *Chromatographia* 30 (1990) 195.
- [34] K. Otsuka, S. Terabe, T. Ando, *J. Chromatogr.* 348 (1985) 39.
- [35] N. Chen, S. Terabe, T. Nakagawa, *Electrophoresis* 16 (1995) 1457.
- [36] M.M. Bushey, J.W. Jorgenson, *J. Microcolumn Sep.* 1 (1989) 125.
- [37] M.M. Bushey, J.W. Jorgenson, *Anal. Chem.* 61 (1989) 491.
- [38] S. Terabe, T. Katsura, Y. Okada, Y. Ishihama, K. Otsuka, *J. Microcolumn Sep.* 5 (1993) 23.
- [39] K. Otsuka, S. Terabe, T. Ando, *J. Chromatogr.* 332 (1985) 219.
- [40] J. Fischer, P. Jandera, in U.Pyell (Editor), *Electrokinetic Chromatography - Theory, Instrumentation and Applications*, John Wiley & Sons, Ltd, Chichester, 2006, p. 235.
- [41] J.P. Quirino, S. Terabe, *J. Chromatogr. A* 856 (1999) 465.
- [42] G.W. Somsen, R. Mol, J. de, *J. Chromatogr. A* 1217 (2010) 3978.
- [43] L.K. Amundsen, J.T. Kokkonen, H. Siren, *J. Sep. Sci.* 31 (2008) 803.
- [44] M. Molina, S.K. Wiedmer, M. Jussila, M. Silva, M.L. Riekkola, *J. Chromatogr. A* 927 (2001) 191.
- [45] O. Gustafsson, J.r. Kutter, in U.Pyell (Editor), *Electrokinetic Chromatography - Theory, Instrumentation and Applications*, John Wiley & Sons, Ltd, Chichester, 2006, p. 337.
- [46] K.D. Altria, *J. Chromatogr. A* 892 (2000) 171.
- [47] K.D. Altria, M.F. Broderick, S. Donegan, J. Power, *Electrophoresis* 25 (2004) 645.

- [48] Y. Wen, J. Li, J. Ma, L. Chen, *Electrophoresis* 33 (2012) 2933.
- [49] S.E. Moring, R.T. Reel, R.E.J. van Soest, *Anal. Chem.* 65 (1993) 3454.
- [50] A. Rodat, P. Gavard, F.-J. Couderc, *Biomed. Chromatogr.* 23 (2009) 42.
- [51] B. Nickerson, J.W. Jorgenson, *J. High Resolut. Chromatogr.* 11 (1988) 878.
- [52] S. Pedersen-Bjergaard, K.E. Rasmussen, H. Gronhaug, *J. Chromatogr. A* 902 (2000) 91.
- [53] M.A. Strausbauch, S.J. Xu, J.E. Ferguson, M.E. Nunez, D. Machacek, G.M. Lawson, P.J. Wettstein, J.P. Landers, *J. Chromatogr. A* 717 (1995) 279.
- [54] J.P. Quirino, in U. Pyell (Editor), *Electrokinetic Chromatography - Theory, Instrumentation and Applications*, John Wiley & Sons, Ltd, Chichester, 2006, p. 207.
- [55] D.M. Osbourn, D.J. Weiss, C.E. Lunte, *Electrophoresis* 21 (2000) 2768.
- [56] J.B. Kim, S. Terabe, *J. Pharm. Biomed. Anal.* 30 (2003) 1625.
- [57] S.L. Simpson, J.P. Quirino, S. Terabe, *J. Chromatogr. A* 1184 (2008) 504.
- [58] A.T. Aranas, A.M. Guidote, Jr., J.P. Quirino, *Anal. Bioanal. Chem.* 394 (2009) 175.
- [59] M.C. Breadmore, J.R.E. Thabano, M. Dawod, A.A. Kazarian, J.P. Quirino, R.M. Guijt, *Electrophoresis* 30 (2009) 230.
- [60] M.C. Breadmore, M. Dawod, J.P. Quirino, *Electrophoresis* 32 (2011) 127.
- [61] A.A. Kazarian, E.F. Hilder, M.C. Breadmore, *J. Sep. Sci.* 34 (2011) 2800.
- [62] B.C. Giordano, D.S. Burgi, S.J. Hart, A. Terray, *Anal. Chim. Acta* 718 (2012) 11.
- [63] F. Kitagawa, T. Kawai, K. Sueyoshi, K. Otsuka, *Anal. Sci.* 28 (2012) 85.
- [64] M.C. Breadmore, A.I. Shallan, H.R. Rabanes, D. Gstoettenmayr, K. Abdul, A. Gaspar, M. Dawod, J.P. Quirino, *Electrophoresis* 34 (2013) 29.
- [65] R.L. Chien, D.S. Burgi, *Anal. Chem.* 64 (1992) 489A.
- [66] R.L. Chien, D.S. Burgi, *Anal. Chem.* 64 (1992) 1046.
- [67] J.P. Quirino, S. Terabe, *J. Chromatogr. A* 902 (2000) 119.
- [68] J.J. Berzas Nevado, J. Rodriguez Flores, G. Castaneda Penalvo, N. Rodriguez Farinas, *J. Chromatogr. A* 953 (2002) 279.
- [69] B.F. Liu, X.H. Zhong, Y.T. Lu, *J. Chromatogr. A* 945 (2002) 257.
- [70] Z. Liu, P. Sam, S.R. Sirimanne, P.C. McClure, J. Grainger, D.G. Patterson, Jr., *J. Chromatogr. A* 673 (1994) 125.
- [71] J.P. Quirino, S. Terabe, *J. Capillary Electrophor.* 4 (1997) 233.

- [72] J.P. Quirino, S. Terabe, *Science* 282 (1998) 465.
- [73] M. Gilges, *Chromatographia* 44 (1997) 191.
- [74] J.P. Quirino, S. Terabe, *Anal. Chem.* 71 (1999) 1638.
- [75] J.P. Quirino, S. Terabe, *J. High Resolut. Chromatogr.* 22 (1999) 367.
- [76] J.B. Kim, J.P. Quirino, K. Otsuka, S. Terabe, *J. Chromatogr. A* 916 (2001) 123.
- [77] J. Palmer, D.S. Burgi, J.P. Landers, *Anal. Chem.* 74 (2002) 632.
- [78] M. El-Awady, U. Pyell, *J. Chromatogr. A* 1297 (2013) 213.
- [79] J.P. Foley, *Anal. Chem.* 62 (1990) 1302.
- [80] C. Quang, J.K. Strasters, M.G. Khaledi, *Anal. Chem.* 66 (1994) 1646.
- [81] K.D. Altria, H. Fabre, *Chromatographia* 40 (1995) 313.
- [82] H. Wätzig, M. Degenhardt, A. Kunkel, *Electrophoresis* 19 (1998) 2695.
- [83] M.I. Jimidar, N. Van, A. Van, S. De, *Sep. Sci. Technol. (San Diego, CA, U. S. )* 9 (2008) 63.
- [84] A. Amini, *Electrophoresis* 22 (2001) 3107.
- [85] G.K.E. Scriba, *Electrophoresis* 24 (2003) 2409.
- [86] T.K. Natishan, *J. Liq. Chromatogr. Relat. Technol.* 28 (2005) 1115.
- [87] I. Ali, H.Y. Aboul-Enein, V.K. Gupta, S.F.Y. Li, *J. Capillary Electrophor. Microchip Technol.* 9 (2006) 85.
- [88] K. Altria, A. Marsh, d.G.C. Sanger-van, *Electrophoresis* 27 (2006) 2263.
- [89] P.T.T. Ha, J. Hoogmartens, S. Van, *J. Pharm. Biomed. Anal.* 41 (2006) 1.
- [90] H. Wätzig, G. Scriba, *Electrophoresis* 27 (2006) 2261.
- [91] I. Ali, H.Y. Aboul-Enein, V.K. Gupta, *Egypt. J. Chem.* (2007) 1.
- [92] A. Marsh, M. Broderick, K. Altria, J. Power, S. Donegan, B. Clark, *Methods Mol. Biol. (Totowa, NJ, U. S. )* 384 (2008) 205.
- [93] G.K.E. Scriba, *J. Pharm. Biomed. Anal.* 55 (2011) 688.
- [94] B.S. Sekhon, *J. Pharm. Educ. Res.* 2 (2011) 2.
- [95] H. Wätzig, G. Scriba, *Electrophoresis* 33 (2012) 1493.
- [96] U. Holzgrabe, in S.Ahuja, M.I.Jimidar (Editors), *Capillary Electrophoresis Methods for Pharmaceutical Analysis*, Elsevier, San Diego, 2008, p. 245.



## **2. Aim of the work**

The objective of the present study was to thoroughly investigate sweeping as one of the most important sample preconcentration techniques in MEKC. The study includes an intensive theoretical discussion of the fundamentals of sweeping and the underlying processes involved in sweeping under homogeneous and under inhomogeneous electric field conditions as well as the processes involved in CD-MEKC analysis of hydrophobic basic analytes. In addition, the study aimed to investigate different factors affecting the sweeping efficiency including the effect of the salt content and the electric conductivity of the sample solution, the effect of organic solvent in the sample and/or the BGE, the effect of pH variation of the sample and the BGE, the effect of adsorption and the addition of dynamic coating agents and the effect of cyclodextrins (CD-MEKC). For doing this, it was important to develop an accurate reliable method for the assessment of sweeping efficiency to be used during this work for studying the effect of different experimental parameters on the final enrichment factor. A special focus was given to the effect of sample matrix composition, which is usually under-estimated in the literature. The study aimed also to derive suitable equations, whenever possible, to express the processes involved in the sweeping procedure and to check the validity of these equations experimentally and theoretically. The analytes selected for the present study represent different chemical classes including *p*-hydroxybenzoates (parabens), benzamide and aromatic amines as examples of acidic, neutral and basic analytes, respectively. In all cases, SDS was used as an anionic surfactant.

In addition, the present study aimed to develop a method for the determination of different pharmaceutical compounds based on the results achieved in the fundamental part of the dissertation. This was applied for the analysis of loratadine and desloratadine in pharmaceutical preparations and spiked urine. We aimed to develop a robust, precise and accurate method for the simultaneous determination of these drugs as examples of hydrophobic basic analytes which are usually difficult to analyze by capillary electromigration separation methods. Official validation protocols were followed to confirm the reliability of the developed method.



### 3. Summary

The present thesis deals with the study of sweeping as one of the most important sample preconcentration techniques in micellar electrokinetic chromatography (MEKC). The work includes the study of the fundamentals of sweeping as well as their application in the pharmaceutical field. The thesis is divided into four main parts based on four different publications.

**In the first part of the thesis**, the processes involved in sweeping under homogeneous and under inhomogeneous electric field conditions are theoretically discussed. These processes include stacking or destacking of micelles when entering the sample zone, sweeping of analytes by the stacked or destacked micelles, and destacking or stacking of the swept analyte zone. Equations describing sweeping are revisited and a factor  $\theta$  (phase ratio shift factor) is defined to quantitatively describe the change of the retention factor between the sample and separation zones. A new robust and reliable method for the assessment of the sweeping efficiency is developed based on recording the peak height dependent on the injected sample volume. The values obtained via this method agree well with theoretically predicted ones. Weakly acidic *p*-hydroxybenzoates (parabens), neutral benzamide, and weakly basic anilines are taken as model analytes using SDS as anionic surfactant. The effect of both the buffer and the added salt concentrations (in the sample solution) on the obtainable sweeping efficiency is intensively studied. The results obtained show that the sweeping efficiency for neutral analytes is independent of the electric conductivity of the sample matrix. It is also shown that under specific conditions unexpectedly high enrichment factors are obtained which are attributed to the focusing of neutral analytes by micellar transient isotachopheresis.

**In the second part of the thesis**, our developed method for the assessment of sweeping efficiency was extended to the general case, in which the distribution coefficient and the electric conductivity is varied in the sample and BGE compartments. The same test analytes as in the first part are studied with SDS as anionic surfactant. It is shown that in the general case – in contrast to the classical description of sweeping – the obtainable enrichment factor is not only dependent on the retention factor of the analyte in the sample zone but also dependent on the retention factor in the BGE. An additional focusing/defocusing step is confirmed and the term “Retention factor gradient effect (RFGE)” is introduced. A suitable quantitative description of this effect is performed by extending the classical equation employed for the description of the sweeping process with an additional focusing/defocusing factor. The validity of the derived equation is confirmed experimentally and theoretically under variation of the organic solvent content (in the sample and/or the BGE), the type of organic solvent (in the sample and/or the BGE), the electric conductivity (in the sample), the pH (in the sample), and the concentration of surfactant (in the BGE). High enrichment factors

are obtained when the pH in the sample zone makes possible to convert the analyte into a charged species that has a high distribution coefficient with respect to an oppositely charged micellar phase, while the pH in the BGE enables separation of the neutral species under moderate retention factor conditions.

**In the third part of the thesis**, the processes involved in sweeping in cyclodextrin-modified micellar electrokinetic chromatography (CD-MEKC) are theoretically discussed with a special focus on dynamic pH junction and adsorption of the analyte onto the capillary wall (especially with hydrophobic basic analytes). The new method for the assessment of sweeping efficiency is further extended to CD-MEKC. Ethylparaben (pharmaceutical preservative) as an example of acidic analytes and desloratadine (antihistaminic drug) as an example of basic analytes are investigated using different types of  $\beta$ -cyclodextrins. The presence of RFGE as an additional focusing/defocusing effect in sweeping-CD-MEKC is confirmed under the conditions of different content of cyclodextrin and different pH between the sample and the BGE. Desloratadine shows an unexpectedly low enrichment factor compared to the less hydrophobic ethylparaben. This unexpected behavior is ascribed to the strong adsorption of the protonated species of this drug onto the inner capillary wall in the sample zone that significantly counteracts the sweeping process. This effect is confirmed by the improvement in the enrichment factor achieved by the addition of a dynamic coating agent to the sample solution.

**In the fourth part of the thesis**, a CD-MEKC method is developed for the simultaneous determination of the antihistaminic drugs loratadine and desloratadine (the major metabolite and an impurity of loratadine). The tendency of these drugs (hydrophobic basic analytes) to be adsorbed onto the inner capillary wall and the difficulty to separate them due to the extremely high retention factors make the present study challenging. The effect of the sample matrix on the reachable enrichment factor is studied. The use of a low pH sample solution overcomes problems associated with the low solubility of the studied analytes in aqueous solution while having advantages with regard to online focusing. In addition, the use of a basic BGE and the presence of cyclodextrin reduce the adsorption of these analytes in the separation compartment. Different experimental parameters are investigated in order to achieve the highest resolution within a short run time. The separation is achieved in less than 7 min using a BGE consisting of 10 mmol L<sup>-1</sup> sodium borate buffer, pH 9.30 containing 40 mmol L<sup>-1</sup> SDS and 20 mmol L<sup>-1</sup> hydroxypropyl- $\beta$ -CD while the sample solution is composed of 10 mmol L<sup>-1</sup> phosphoric acid, pH 2.15. All validation parameters are thoroughly investigated based on the ICH guidelines. The developed method is successfully applied to the determination of the studied drugs in tablets and in spiked human urine. Moreover, desloratadine is detected at the stated pharmacopeial limit (0.1% w/w) as an impurity in loratadine bulk powder. In addition, the developed method achieves excellent separation from the co-formulated drug pseudoephedrine. The obtained results are compared with those of the official liquid chromatographic method and are found in a good agreement.

## 4. Zusammenfassung

Die vorliegende Arbeit untersucht Sweeping als eine der wichtigsten Probenvorbereitungstechniken in der Mizellaren Elektrokinetischen Chromatographie (MEKC). Sie beinhaltet eine Studie der Grundlagen des Sweeping und ihrer Anwendung im Bereich der pharmazeutischen Analytik. Die Arbeit ist (in Anlehnung an die vier darin enthaltenen Publikationen) in vier Teilbereiche unterteilt.

**Im ersten Teil der Arbeit** werden die Prozesse diskutiert, die in das Sweeping unter den Bedingungen des homogenen und inhomogenen elektrischen Feldes einbezogen sind. Diese Prozesse beinhalten Stacking oder Destacking der Mizellen, die in die Probenzone hineinmigrieren, Sweeping der Analyte durch die angereicherten oder abgereicherten Mizellen und Stacking oder Destacking der vorangereicherten Analytzone. Den Sweepingprozess beschreibende Gleichungen werden überprüft und ein Faktor  $\theta$  (Phasenverhältnis-Shift-Faktor) wird definiert, um die Änderung des Retentionsfaktors (bezogen auf Proben- und Trennzone) quantitativ zu erfassen. Eine neue robuste und verlässliche Methode zur Bestimmung der Sweeping-Effizienz wird entwickelt. Diese basiert auf der Erfassung der Abhängigkeit der Peakhöhe vom Probeaufgabevolumen. Die so erhaltenen Werte stimmen gut mit den theoretisch vorhergesagten überein. Schwach saure p-Hydroxybenzoesäureester (Parabene), neutrales Benzamid und schwach basische Aniline werden als Modellanalyte unter Verwendung von SDS als anionischem Tensid eingesetzt. Studiert wird der Einfluss von Puffer- und hinzugefügter Salzkonzentration (in der Probenlösung) auf die erreichbare Sweeping-Effizienz. Die erhaltenen Ergebnisse zeigen, dass die Sweeping-Effizienz für neutrale Analyte unabhängig ist von der elektrischen Leitfähigkeit in der Probenmatrix. Es wird ebenfalls gezeigt, dass in manchen Fällen unerwartet hohe Anreicherungs-Faktoren erhalten werden, die durch Fokussierung der Mizellen durch transiente Isotachophorese erklärt werden können.

**Im zweiten Teil der Arbeit** wird die entwickelte Methode zur Bestimmung der Sweeping-Effizienz auf den allgemeinen Fall bezogen. In diesem Fall werden sowohl der Verteilungskoeffizient als auch die elektrische Leitfähigkeit in der Probenzone und in der Trennzone variiert. Hierzu werden dieselben Testanalyte wie im ersten Teil unter Verwendung von SDS als anionischem Tensid herangezogen. Es wird gezeigt, dass im allgemeinen Fall – im Gegensatz zur klassischen Beschreibung des Sweeping – der erreichbare Anreicherungs-faktor nicht nur vom Retentionsfaktor des Analyten in der Probenzone sondern auch vom Retentionsfaktor in der Trennzone abhängt. Die Existenz eines zusätzlichen Fokussierungs-/Defokussierungsschritts wird nachgewiesen. Dieser zusätzliche Schritt wird als „Retentionsfaktor-Gradient-Effekt“ [retention factor gradient effect (RFGE)] bezeichnet. Eine geeignete quantitative Beschreibung

dieses Effekts wird durch Erweiterung der klassischen Gleichung für den Sweeping-Prozess durch Einführung eines zusätzlichen Fokussierungs/Defokussierungs-Faktors erreicht. Die Gültigkeit der so hergeleiteten Gleichung wird experimentell und theoretisch unter Variation des Volumenanteils an organischem Lösungsmittel (in der Probe und/oder im Trennelektrolyten), der Art des organischen Lösungsmittels (in der Probe und/oder im Trennelektrolyten), der elektrischen Leitfähigkeit (in der Probe), des pH (in der Probe) und der Konzentration des Tensids (im Trennelektrolyten) bestätigt. Hohe Anreicherungsfaktoren werden dann erreicht, wenn der pH der Probe die Überführung des Analyten in eine geladene Spezies ermöglicht. Diese weist einen hohen Verteilungskoeffizienten bezogen auf die entgegengesetzt geladene Mizellare Phase auf, während der pH im Trennelektrolyten eine Trennung der neutralen Spezies bei moderaten Retentionsfaktoren ermöglicht.

**Im dritten Teil der Arbeit** werden die Prozesse, die in das Sweeping bei Cyclodextrin-modifizierter MEKC (CD-MEKC) einbezogen sind, mit einem Schwerpunkt auf "dynamic pH junction" und Adsorption der Analyte an der Kapillarwand diskutiert (insbesondere bei hydrophoben basischen Analyten). Die neue Methode der Bestimmung der Sweeping-Effizienz wird im Rahmen der CD-MEKC eingesetzt. Untersucht werden Ethylparaben (ein für pharmazeutische Formulierungen eingesetztes Konservierungsmittel) als ein Beispiel für saure Analyte und Desloratadin (ein Antihistaminikum) als ein Beispiel für basische Analyte unter Verwendung unterschiedlicher  $\beta$ -Cyclodextrine. Der Einfluss von RFGE als ein zusätzlicher Fokussierungs-/Defokussierungs-Effekt wird unter den Bedingungen unterschiedlicher Konzentration an Cyclodextrin und unterschiedlichen pH-Werts von Probenzone und Trennzone bestätigt. Desloratadin weist einen unerwartet niedrigen Anreicherungsfaktor auf, verglichen mit dem Anreicherungsfaktor, der für das weitaus weniger hydrophobe Ethylparaben erreicht wurde. Dieses unerwartete Verhalten wird starker Adsorption der protonierten Spezies dieses Wirkstoffs an der Kapillar-Innenwand in der Probenzone (welche dem Sweeping-Prozess entgegenwirkt) zugeschrieben. Diese Zuschreibung wird durch Verbesserung des Anreicherungs-Faktors durch Zusatz eines dynamischen Coating-Agens zur Probenlösung bestätigt.

**Im vierten Teil der Arbeit** wird ein CD-MEKC Verfahren zur Bestimmung der Antihistaminika Loratadin und Desloratadin (Hauptmetabolit und Verunreinigung von Loratadin) entwickelt. Die Neigung dieser Wirkstoffe (hydrophobe basische Analyte), an der Kapillar-Innenwand adsorbiert zu werden, und das Problem, sie trotz ihrer hohen Retentionsfaktoren zu trennen, erschweren die Lösung dieser Aufgabe. Untersucht wird der Einfluss der Probenmatrix auf den erreichbaren Anreicherungsfaktor. Die Verwendung einer Probenlösung mit niedrigem pH vermeidet die Probleme, die mit der niedrigen Löslichkeit der untersuchten Analyte verbunden sind, während sie Vorteile hat in Bezug auf die online-Fokussierung. Zusätzlich verringert die Verwendung eines basischen Trennelektrolyten die Adsorption dieser Analyte im

## *Zusammenfassung*

---

Bereich der Trennzone. Unterschiedliche experimentelle Parameter werden untersucht, um höchstmögliche Auflösung innerhalb einer kurzen Laufzeit zu erreichen. Eine Trennung wird innerhalb von weniger als 7 min unter Verwendung eines Trennelektrolyten bestehend aus 10 mmol L<sup>-1</sup> Natriumborat-Puffer (pH 9,30), 40 mmol L<sup>-1</sup> SDS und 20 mmol L<sup>-1</sup> Hydroxypropyl-β-CD erreicht, während die Probenlösung 10 mmol L<sup>-1</sup> Phosphorsäure (pH 2,15) enthält. Alle erforderlichen Validierungsparameter werden entsprechend den ICH Richtlinien bestimmt. Das entwickelte Verfahren wird auf die Bestimmung der untersuchten Wirkstoffe in Tabletten und in gespiktem menschlichem Urin eingesetzt. Desloratadin wird als Verunreinigung im Reinstoff Loratadin beim (durch das Arzneibuch zugelassenen) Grenzwert von 0,1% (m/m) bestimmt. Das entwickelte Verfahren erreicht zusätzlich eine hervorragende Trennung vom co-formulierten Wirkstoff Pseudoephedrin. Die erhaltenen Ergebnisse zeigen gute Übereinstimmung mit denen des offiziell zugelassenen flüssigchromatographischen Verfahrens.



# **5. Cumulative Part (Publications)**



## **5.1. Publication I**

**Processes involved in sweeping under inhomogeneous electric field conditions as sample enrichment procedure in micellar electrokinetic chromatography**

Mohamed El-Awady, Carolin Huhn, Ute Pyell

*Journal of Chromatography A, 1264 (2012) 124-136*

*doi: 10.1016/j.chroma.2012.09.044*



## 5.1.1. Summary and discussion

In this publication, we first theoretically discuss sweeping under homogeneous and under inhomogeneous electric field conditions as a multistep process that includes stacking or destacking of the micelles when entering the sample zone, sweeping of analytes by the stacked or destacked micelles, and destacking or stacking of the swept analyte zone. We introduce the phase ratio shift factor  $\theta$  to quantitatively describe the change of the retention factor between the sample and BGE compartments assuming a constant distribution coefficient in the two zones. This factor is used in the derivation of equations that describe sweeping under homogeneous and inhomogeneous electric field conditions. The final length of the focused sample zone  $l_{\text{focus}}$  after completion of the sweeping process can be calculated from the initial sample-plug length  $l_{\text{inj}}$  as follows:

$$l_{\text{focus}} = \frac{1}{\gamma \theta (1 + k_{\text{BGE}})} l_{\text{inj}} \quad (1)$$

where  $\gamma$  = field-strength enhancement factor (= ratio of the electric field strengths in the sample zone and in the BGE ( $E_{\text{S}}/E_{\text{BGE}}$ ) or ratio of the electric conductivities of the BGE and the sample solution ( $\kappa_{\text{BGE}}/\kappa_{\text{S}}$ ));  $\theta$  = phase ratio shift factor or quotient of phase ratios in the sample zone during sweeping and in the BGE ( $\varphi_{\text{S}}/\varphi_{\text{BGE}}$ ).

A new method is developed for the assessment of sweeping efficiency based on plotting the peak height against the injected sample volume. This method offers highly accurate and precise results that agree well with theoretically predicted values. The method is successfully applied within a detailed study to investigate the influence of the sample matrix composition on the experimentally obtained sweeping efficiency. Weakly acidic parabens, neutral benzamide, and weakly basic anilines separated in SDS containing phosphate buffer (pH = 7.00), borate buffer (pH = 9.00 or pH = 9.37), respectively, are taken as model analytes. The results obtained for varied buffer concentration, varied concentration of added NaCl (at fixed buffer concentration) and varied concentration of NaCl without buffer in the sample solution show that under the conditions of our experimental study, the approximation of assuming  $\theta$  to be equal to the reciprocal value of the field strength enhancement factor  $\gamma$  is valid. Consequently, the sweeping efficiency for neutral analytes is in first approximation independent of the electric conductivity of the sample matrix. Under specific conditions unexpectedly high enrichment factors are obtained which are ascribed to the focusing of neutral analytes by micellar transient isotachopheresis (mtITP). This effect takes place in case of low retention factor analytes via the migration of micelles in an isotachopheretically stacked zone, which is possible if a salt with a co-ion (with respect to the charge of the micelles) having a high electrophoretic mobility is added to the sample solution in a concentration above a critical value. The results of this publication allow better understanding of the sweeping process and the factors affecting the sweeping efficiency in MEKC.

## **5.1.2. Author contribution**

The experimental part of this publication was conducted by me. This includes the measurement of sweeping efficiency under the studied experimental conditions and comparison with theoretically predicted values. Dr. Pablo Kler (Forschungszentrum Jülich) performed the computer simulations of micellar transient isotachopheresis. The introduction and theoretical considerations of the manuscript were written by me, Dr. Carolin Huhn (Forschungszentrum Jülich) and Prof. Ute Pyell. Other parts of the manuscript were written by me. The draft of the manuscript was corrected by Dr. Huhn and Prof. Pyell before submission to the journal. Prof. Ute Pyell was responsible for the supervision of this work.



## Processes involved in sweeping under inhomogeneous electric field conditions as sample enrichment procedure in micellar electrokinetic chromatography

Mohamed El-Awady<sup>a</sup>, Carolin Huhn<sup>b</sup>, Ute Pyell<sup>a,\*</sup>

<sup>a</sup> University of Marburg, Department of Chemistry, Hans-Meerwein-Straße, D-35032 Marburg, Germany

<sup>b</sup> Central Division of Analytical Chemistry, Forschungszentrum Jülich, D-52425 Jülich, Germany

### ARTICLE INFO

#### Article history:

Received 6 June 2012

Received in revised form

13 September 2012

Accepted 18 September 2012

Available online 23 September 2012

#### Keywords:

Micellar electrokinetic chromatography

Sweeping

Assessment of sweeping efficiency

Matrix effects

Micellar transient isotachopheresis

### ABSTRACT

Sweeping under inhomogeneous electric field conditions has been described as a process that includes stacking or destacking of the micelles when entering the sample zone, sweeping of analytes by the stacked or destacked micelles, and destacking or stacking of the swept analyte zone. However, there is ongoing debate that not only the retention factor of the analyte but also the electric conductivity of the sample solution or the concentration of an added salt can have an impact on the enrichment efficiency. Revisiting the equations describing sweeping, a factor  $\theta$  (phase ratio shift factor) is defined to quantitatively describe the change of the retention factor between the sample and separation zones. The influence of the sample matrix composition on the experimentally obtained sweeping efficiency is studied with SDS as pseudostationary phase taking parabens, benzamide and anilines as model analytes. To this end, a robust and reliable method for the assessment of the sweeping efficiency is developed. The values obtained via this method are very precise and agree well with theoretically predicted ones. The results obtained for varied buffer concentration and varied concentration of NaCl in the sample solution show that under the conditions of our experimental study, the approximation of assuming  $\theta$  to be equal to the reciprocal value of the field strength enhancement factor  $\gamma$  is valid. Accordingly, the sweeping efficiency for neutral analytes is independent of the electric conductivity of the sample matrix. It is also shown that under specific conditions unexpectedly high enrichment factors are obtained which are ascribed to the focusing of neutral analytes by micellar transient isotachopheresis (mtITP). The results obtained in this study can be used as a guide for better understanding of the sweeping process and the factors affecting the sweeping efficiency in micellar electrokinetic chromatography (MEKC).

© 2012 Elsevier B.V. All rights reserved.

### 1. Introduction

In combination with capillary electromigration separation techniques, detection is often performed with a photometric detector. Due to the short optical path length inherently present when using on-column detection, on-line preconcentration techniques are very desirable. In case of analytes having an effective electrophoretic mobility due to protonation or dissociation, those preconcentration techniques which have been introduced for CE can also be applied in MEKC [1,2]. These techniques comprise proportional and boundary stacking [3]. However, it is not possible to use these techniques for analytes with negligible effective electrophoretic mobility.

Liu et al. [4] have presented the concept of field-amplified stacking in MEKC for on-column sample concentration of neutral hydrophobic molecules. They used an aqueous sample matrix having a low electric conductivity and containing micelles in

a concentration just above the CMC. The analytes investigated were extremely hydrophobic (tetrachlorodibenzo-*p*-dioxins and polynuclear aromatic hydrocarbons). In this case, the retention factor is very high so that the effective electrophoretic mobility of the analytes equals in first approximation the electrophoretic mobility of the micelles, which are stacked at the sample/BGE boundary. With this concept Liu et al. [4] succeeded in combining on-line enrichment with the separation of a mixture of polynuclear aromatic hydrocarbons with a BGE containing 100 mmol L<sup>-1</sup> sodium borate, 100 mmol L<sup>-1</sup> SDS, 5 mol L<sup>-1</sup> urea, and 10 mmol L<sup>-1</sup>  $\gamma$ -cyclodextrin, while the sample solution consisted of 9 mmol L<sup>-1</sup> SDS in aqueous buffer.

In case of neutral (or charged) analytes, on-line preconcentration can also be performed by a process which has been termed sweeping. The concept of sweeping was developed by Quirino and Terabe [5]. Sweeping can be regarded as the most important sample preconcentration technique in MEKC. It is based on the accumulation of analyte molecules by the pseudostationary phase (PSP) that penetrates the sample zone being void of PSP. This concept has been visualized in a very illustrative manner with a charge-coupled

\* Corresponding author. Tel.: +49 6421 2822192; fax: +49 6421 2822124.  
E-mail address: [pyellu@staff.uni-marburg.de](mailto:pyellu@staff.uni-marburg.de) (U. Pyell).

device (CCD) camera for MEKC on a microchip [6]. (The basic principle of the sweeping process is also illustrated in the animation file included in supplementary material). Within the process of sweeping, the effective electrophoretic mobility of neutral analytes changes from zero to  $\mu_a$  [7,8]:

$$\mu_a = \frac{k_S}{1 + k_S} \mu_{\text{PSP}} \quad (1)$$

where  $\mu_{\text{PSP}}$  is the electrophoretic mobility of the PSP and  $k_S$  is the retention factor of the analyte in the sample zone during sweeping. Although described here as abrupt change in the effective electrophoretic mobility of the analyte, this process can also be regarded to be due to chromatographic effects comparable to the enrichment of an analyte at the top of a chromatographic column during the process of sample injection. Because of this analogy sweeping was also denoted chromatographic stacking [3].

According to Quirino and Terabe [9], sweeping was initially observed by Gilges [10] who reported a focusing effect for neutral analytes separated by MEKC. He was able to determine impurities in a drug substance with SDS as PSP (in borate buffer/acetonitrile (65:35, v/v)) whereas the sample matrix was void of micelles (only borate buffer/acetonitrile (65:35, v/v), or (80:20, v/v)). Although sweeping occurs whenever the sample matrix is void of micelles while the BGE contains micelles, independent of the electric conductivity of the sample solution [9], the mechanism of the focusing effect reported by Gilges [10] was not understood until 1998.

In 1998 Quirino and Terabe [5] presented the concept of sweeping (with hydrodynamic injection) which is applicable to neutral and charged analytes and samples having the same electric conductivity as the BGE [5,11,12] (sweeping under homogeneous electric field conditions). Very soon also sweeping under inhomogeneous electric field conditions was investigated [13]. In a similar approach Palmer et al. [14] injected the sample (containing neutral analytes) dissolved in BGE void of micelles electrokinetically where the analytes were retarded in the injected zone by the micelles migrating opposite to the direction of the EOF. Employing this procedure, it was possible to inject a large volume of the sample solution, about seven times the capillary inner volume [14].

Sweeping is most efficient for analytes with high partition coefficients regarding partitioning between the micellar phase (or another PSP) and the surrounding phase. The length of the sample zone after sweeping  $l_{\text{sweep}}$  depends on the initial sample plug length  $l_{\text{inj}}$  and on the retention factor in the sample zone during sweeping  $k_S$  [5,11]. It is in first approximation independent of the velocity of the EOF [9]:

$$l_{\text{sweep}} = \frac{1}{1 + k_S} l_{\text{inj}} \quad (2)$$

This equation can be a guide for the further improvement of enrichment factors ( $l_{\text{inj}}/l_{\text{sweep}}$ ), which is expected to be obtained by following means: (1) increase of the retention factor (in the sample zone) and (2) modification of the electric conductivity of the sample solution. Another option focuses on the combination of sweeping with an optimization of the direction and the velocity of the EOF in order to remove the sample matrix [15].

An increase of the retention factor (in the sample zone) reflected by an increase in the enrichment factor was obtained when using mixed micelles by adding SB-12 (a zwitterionic surfactant) to a BGE containing SDS, enabling also the efficient enrichment of polar analytes due to their increased retention factor [16]. To the same end, ion pairing reagents were added to the sample solution [17]. It is also possible to select a sample solution with lower content of an organic modifier compared to that of the BGE [10] or to increase the phase ratio prior to sweeping.

A modification of the electric conductivity of the sample solution (with respect to the electric conductivity of the BGE) will change

not only the retention factor but also evoke stacking or destacking effects at the boundaries BGE/sample and sample/BGE [13]. The effects of different electric conductivity in the sample zone (compared to that of the BGE), are still not fully understood and contradicting results have been published. In combination with sweeping, either the decrease or the increase of the electric conductivity of the sample solution have been proposed as means to improve the on-line enrichment efficiency by sweeping (compared to that obtainable with a sample solution with an electric conductivity identical to that of the BGE) [7,12,13,18–21]. In studying the observed phenomena, possibly some authors have underestimated the influence of other secondary parameters (e.g. pH of the sample and of the BGE, effect of organic solvents, etc.).

The enrichment process during sweeping is complex with the resulting combination of enrichment at the (moving) concentration boundary [22] and stacking/destacking phenomena taking place at the (stationary) electrolyte boundaries BGE/sample and sample/BGE [13]. In other words, with respect to the micelles, sweeping can be regarded as a complex multistep process that includes stacking or destacking of the micelles at the boundary BGE/sample, sweeping of the neutral analytes by stacked or destacked micelles at the moving concentration boundary and destacking or stacking of the micelles and hence the swept analyte zone at the boundary sample/BGE. All these “steps” contribute to the overall process.

Making the simplifying assumption that the concentration of the (micellar) PSP in the sample zone equals the concentration of the PSP in the separation zone multiplied with the ratio of the electric conductivities in the sample and in the separation zone (the reciprocal value of the so-called field-strength enhancement factor  $\gamma$ ), Quirino et al. [23] were able to show that the length of the sample zone after sweeping  $l_{\text{sweep}}$  should be independent of the electric conductivity of the sample solution (or the concentration of the added salt, respectively), as stacking and destacking processes balance each other. They supported their calculations with an experimental study, in which they demonstrated the stacking and destacking of UV-absorbing micelles. However, they also observed for some selected analytes slightly better focused zones if the electric conductivity of the sample solution is increased compared to the electric conductivity of the BGE.

Against this background, we first theoretically discuss the possible underlying enrichment effects not taken into account in previous concepts and experimentally investigate in detail the effect of both the buffer and the added salt concentrations (in the sample solution) on the obtainable sweeping efficiency. Weakly acidic parabens, neutral benzamide, and weakly basic anilines separated in SDS containing phosphate buffer (pH = 7.00), borate buffer (pH = 9.00) and borate buffer (pH = 9.37), respectively, are taken as model analytes. In order to eliminate influences due to varied migration times and hydrodynamic dispersion as a consequence of local EOF velocity differences [24–26], we present a new method for the determination of the enrichment efficiency. This new method is based on recording the peak height dependent on the injected plug length. It is successfully applied within a detailed study on the influence of varied buffer concentration, varied concentration of added NaCl and varied concentration of NaCl without buffer in the sample solution on the obtainable sweeping efficiency. Moreover, conditions under which micellar transient ITP (mtITP) might have an impact on the measurable enrichment efficiency are discussed.

## 2. Theoretical considerations

### 2.1. Sweeping under inhomogeneous electric field conditions

The classical description of sweeping under inhomogeneous electric field conditions [23] (neglecting transient ITP) is based on

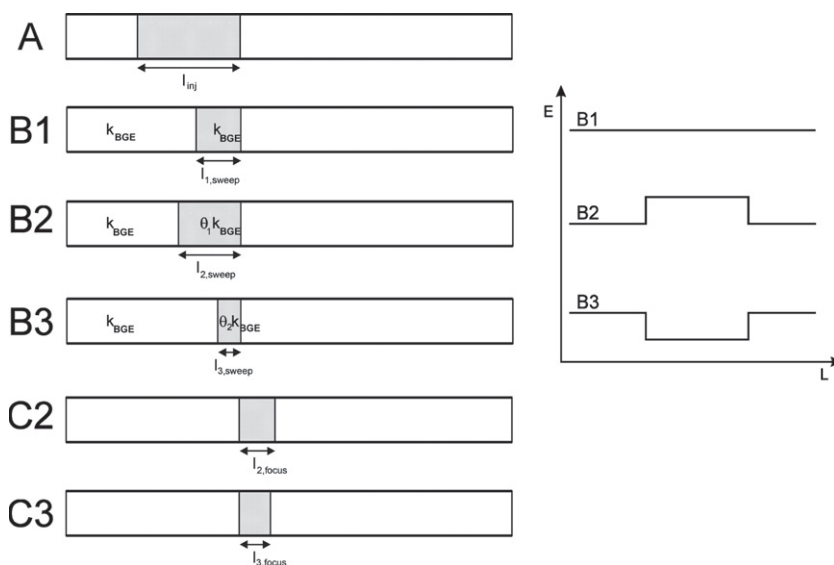


**Fig. 1.** Schematic view of the preconcentration processes: (A) sample injected in a capillary filled with BGE, sample zone length =  $l_{inj}$ . (B) sweeping process: (B1) sweeping under homogeneous electric field conditions (with retention factor  $k_S = k_B$ ), (B2) sweeping under enhanced field strength in the sample zone with retention factor  $k_S = \theta_1 k_B$ , (B3) sweeping under reduced electric field strength in the sample solution with retention factor  $k_S = \theta_2 k_B$ . (C2) sample zone after additional stacking. (C3) sample zone after additional destacking. The insert shows a schematic view of the electric field strength distribution along the column.

considerations made by Quirino and Terabe [5,13] and by Chien and Burgi [27]. It takes into account that sweeping under inhomogeneous electric field conditions is (with respect to the PSP) a multistep enrichment process including: (1) stacking or destacking of the PSP when entering the sample zone, (2) sweeping of the neutral analytes by the stacked or destacked PSP, and (3) destacking or stacking of the swept analyte zone.

Chien and Burgi [27] described the stacking process for charged analytes in capillary electrophoresis and introduced the so-called field-strength enhancement factor  $\gamma$  which is identical to the ratio of the electric field strengths in the sample zone and in the separation zone. The field-strength enhancement factor  $\gamma$  can be regarded to be identical to the ratio of the electric conductivities of the BGE and the sample solution:

$$\gamma = \frac{E_S}{E_{BGE}} = \frac{\kappa_{BGE}}{\kappa_S} \quad (3)$$

where  $E_S$  is the electric field strength in the sample zone,  $E_{BGE}$  is the electric field strength in the separation zone (containing BGE),  $\kappa_{BGE}$  is the electric conductivity of the BGE and  $\kappa_S$  is the electric conductivity of the sample solution.

If  $\gamma = 1$  (identical electric conductivities of the sample solution and the BGE), Eq. (2) quantitatively describes zone focusing by sweeping [5,11]. However, in order to describe zone focusing by sweeping if  $\gamma \neq 1$ , more steps have to be taken into account [13,28] (see Fig. 1).

## 2.2. Processes involved in sweeping

In order to simplify the derived equations, the following assumptions were made: the velocity of the EOF is assumed to be close to zero and is therefore neglected. The anionic surfactant SDS is used as PSP in the reversed direction mode (RM-MEKC). The analyte is neutral. The sample is injected hydrodynamically as a zone of the length  $l_{inj}$ . In the further interpretation, it should be, however, noted that the sweeping efficiency – in principle – is independent of the EOF velocity. Based on the studies and considerations made by Quirino and Terabe [5,13], Quirino et al. [23,28] and by Chien and Burgi [27], sweeping can be described as a complex process that includes the following “steps”.

### 2.2.1. Stacking or destacking of the PSP at the boundary BGE/sample

At the boundary BGE/sample (at the capillary inlet in RM-MEKC) micelles migrate into the sample zone and stacking or destacking takes place. Stacking or destacking will change the phase ratio  $\varphi$  (=volume of PSP/volume of aqueous phase). For a quantitative description of the change in the phase ratio  $\varphi_S/\varphi_{BGE}$ , we introduce the phase ratio shift factor  $\theta$  (see Eq. (4)). The phase ratio shift factor  $\theta$  is defined as the phase ratio  $\varphi_S$  ( $=V_{PSP,S}/V_{aq,S}$ ) in the sample zone during sweeping divided by the phase ratio  $\varphi_{BGE}$  ( $=V_{PSP,BGE}/V_{aq,BGE}$ ) in the BGE. If the partition coefficient  $K$  can be regarded to be independent of the phase ratio shift factor  $\theta$ , the retention factor of the analyte in the sample zone during sweeping  $k_S$  will correspond to the retention factor in the separation zone  $k_{BGE}$  multiplied by  $\theta$ .

$$\theta = \frac{\varphi_S}{\varphi_{BGE}} = \frac{k_S}{k_{BGE}} \quad (4)$$

where  $\varphi_S$  is the phase ratio in the sample zone during sweeping,  $\varphi_{BGE}$  is the phase ratio in the separation zone (containing BGE),  $k_S$  is the retention factor in the sample zone during sweeping and  $k_{BGE}$  is the retention factor in the separation zone (containing BGE).

### 2.2.2. Sweeping

Zone focusing by sweeping takes place with the stacked or destacked PSP. The length of the swept zone can be calculated employing Eq. (2) taking the modified phase ratio into account.

$$l_{sweep} = \frac{1}{1 + \theta k_{BGE}} l_{inj} \quad (5)$$

A schematic representation of the processes taking place in sweeping under homogeneous and inhomogeneous electric field conditions is shown in Fig. 1 based on the model developed by Quirino et al. [23]. Fig. 1A shows the initial sample zone having the length  $l_{inj}$ . After the sweeping step the sample zone length is lowered to  $l_{sweep}$ . Fig. 1B1 shows the situation under homogeneous electric field conditions (Case 1). Fig. 1B2 shows the situation when an enhanced electric field is present in the sample zone (Case 2). Here, the micelles are destacked when they enter the sample zone and thus lower retention factors are obtained yielding a lower sweeping efficiency and thus a sample zone of the length  $l_{2,sweep}$ . In

contrast to this,  $l_{3,sweep}$  is obtained at lowered electric field strength in the sample (Fig. 1B3, Case 3). Thus, after the sweeping process  $l_{3,sweep} < l_{1,sweep} < l_{2,sweep}$ .

### 2.2.3. Destacking or stacking of the swept zone at the boundary sample/BGE

For Cases 2 and 3 (see Fig. 1), a further step has to be considered: for Case 2, there is a stacking of the micelles at the boundary sample/BGE and thus a reduced final focused sample zone length  $l_{2,focus}$  ( $l_{2,focus} < l_{2,sweep}$ , Fig. 1C2). The opposite is true for Case 3, where destacking of the micelles at the boundary sample/BGE has to be taken into account and thus the resulting zone length  $l_{3,focus}$  will be larger than  $l_{3,sweep}$  (Fig. 1C3).

According to the method of Chien and Burgi [27] the concentration of the analyte in the separation zone  $c_{BGE}$  can be calculated from the concentration of the analyte in the swept sample zone  $c_S$  provided that the velocity increase/decrease of the analyte zone at the boundary between the sample and the BGE is known ( $c_{BGE}v_{BGE} = c_S v_S$ ). In MEKC the migration velocity of a neutral analyte zone is related to the migration velocity of the PSP and the retention factor of the analyte [8,13]:

$$v_S = \frac{\theta k_{BGE}}{1 + \theta k_{BGE}} v_{PSP,S} \quad (6a)$$

$$v_{BGE} = \frac{k_{BGE}}{1 + k_{BGE}} v_{PSP,BGE} \quad (6b)$$

where  $v_S$  is the velocity of the analyte in the sample zone,  $v_{BGE}$  is the velocity of the analyte in the BGE,  $v_{PSP,S}$  is the velocity of PSP in the sample zone and  $v_{PSP,BGE}$  is the velocity of PSP in the BGE.

The migration velocity of the PSP in the two zones results from its effective electrophoretic mobility and the electric field strength:

$$v_S = \frac{\theta k_{BGE}}{1 + \theta k_{BGE}} \mu_{PSP,S} E_S \quad (7a)$$

$$v_{BGE} = \frac{k_{BGE}}{1 + k_{BGE}} \mu_{PSP,BGE} E_{BGE} \quad (7b)$$

where  $\mu_{PSP,S}$  is the effective electrophoretic mobility of the PSP in the sample zone,  $\mu_{PSP,BGE}$  is the effective electrophoretic mobility of the PSP in the separation zone (BGE),  $E_S$  is the electric field strength in the sample zone and  $E_{BGE}$  is the electric field strength in the separation zone.

If the effective electrophoretic mobility of the PSP is regarded to be equal in both zones ( $\mu_{PSP,S} = \mu_{PSP,BGE}$ ), the following approximation is possible:

$$c_{BGE} = \frac{\theta k_{BGE}/(1 + \theta k_{BGE})}{k_{BGE}/(1 + k_{BGE})} \frac{\mu_{PSP,S}}{\mu_{PSP,BGE}} \frac{E_S}{E_{BGE}} c_S = \frac{\theta k_{BGE}/(1 + \theta k_{BGE})}{k_{BGE}/(1 + k_{BGE})} \gamma c_S \quad (8)$$

where  $c_{BGE}$  is the concentration of analyte in the final zone and  $c_S$  is the concentration of analyte in the primary sample zone after sweeping. The length of the sample zone after the second destacking or stacking process  $l_{focus}$  can be calculated from  $l_{sweep}$  multiplied with the concentration ratio  $c_S/c_{BGE}$ :

$$l_{focus} = \frac{(1/(1 + \theta k_{BGE})) l_{inj} c_S}{c_{BGE}} \quad (9)$$

$$l_{focus} = \frac{(1/(1 + \theta k_{BGE})) l_{inj}}{((\theta k_{BGE}/1 + \theta k_{BGE})/(k_{BGE}/1 + k_{BGE})) \gamma} = \frac{1}{\gamma \theta (1 + k_{BGE})} l_{inj} \quad (10)$$

With Eq. (10), a direct comparison of classical sweeping and sweeping with inhomogeneous electric field conditions is possible. Eq.

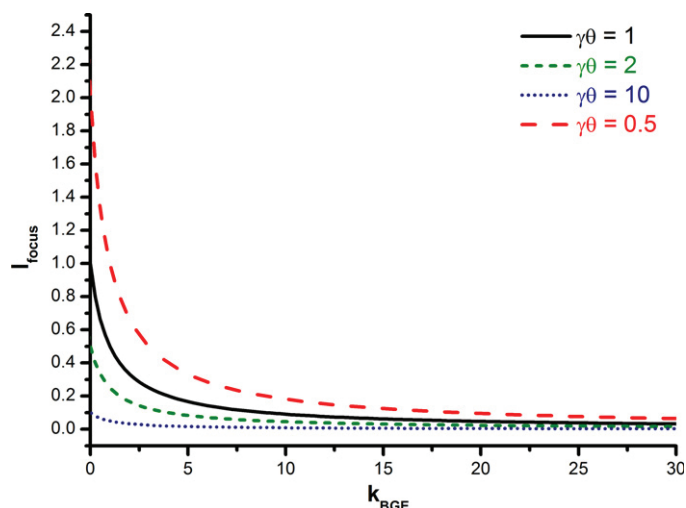


Fig. 2. Length of the focused sample zone  $l_{focus}$  dependent on the retention factor of the analyte in the BGE for different values of  $\gamma\theta$  (Eq. (10));  $l_{inj}$  was set to 1.

(10) differs from Eq. (2) only in the factor  $1/\gamma\theta$  (in case that in Eq. (2)  $k_S = k_{BGE}$ ). This equation corresponds to the equation derived by Quirino and Terabe [13] (in their publication: Eq. (8)) provided that  $\theta$  is identified by the ratio  $k_S/k_{BGE}$  (see Eq. (4)). This equation also shows why focusing of a neutral analyte by sweeping can be regarded to be independent of the electric conductivity of the sample solution if  $\theta$  can be approximated by  $1/\gamma$  [23]. In that case  $l_{1,sweep} = l_{2,focus} = l_{3,focus}$  (Fig. 1).

### 2.3. Discussion of the phase ratio shift factor $\theta$

A difference in the electric conductivity of the sample solution from the electric conductivity of the BGE has an impact on the final enrichment factor ( $l_{focus}/l_{inj}$ ) if  $\gamma\theta \neq 1$ . Only in this case  $l_{focus} \neq l_{1,sweep}$  (Fig. 1). In Fig. 2 the length of the focused zone  $l_{focus}$  (normalized to  $l_{inj} = 1$ ) calculated via Eq. (10) is plotted against the retention factor of the analyte in the BGE for different values of  $\gamma\theta$ . The impact of  $\gamma\theta$  on the peak width will be more pronounced for analytes of low to moderate  $k_{BGE}$  than for those with high  $k_{BGE}$ .

In their pioneering paper on sweeping of neutral analytes under inhomogeneous electric field conditions, Quirino and Terabe [13] have investigated for analytes of low to moderate  $k_{BGE}$  (several phenol derivatives separated at pH=2.5) the influence of the retention factor  $k_{BGE}$  and the field strength enhancement factor  $\gamma$  on the peak width keeping the length of the injected zone  $l_{inj}$  constant at 3.82 cm. In Fig. 3 these data are compared to predicted curves (calculated via Eq. (10)).

For  $0.6 \leq \gamma \leq 4.1$  there is excellent agreement of the experimental data with the predicted curve for  $\gamma\theta = 1.0$  showing that the assumption made by Quirino et al. [23] that the phase shift factor  $\theta$  can be approximated in the general case by  $1/\gamma$  is confirmed by experimental results. However, under the conditions selected for solutes with  $k_{BGE} \leq 5$ , reducing strongly the buffer concentration of the sample solution ( $\gamma \geq 10$ ) has advantages over working with sample solutions which have an electric conductivity similar to that of the BGE. The observed peak width is smaller than that with  $\gamma = 1$ . Possibly, this effect can be ascribed to pH differences between the sample compartment and the separation compartment at low buffer concentration, so that dynamic pH-junction/sweeping [29,30] is present.

However, in spite of the general conclusion that for sweeping of neutral solutes (neutral in the sample and in the separation compartment) under moderate conditions the obtainable enrichment factor can be expected to be independent of the electric

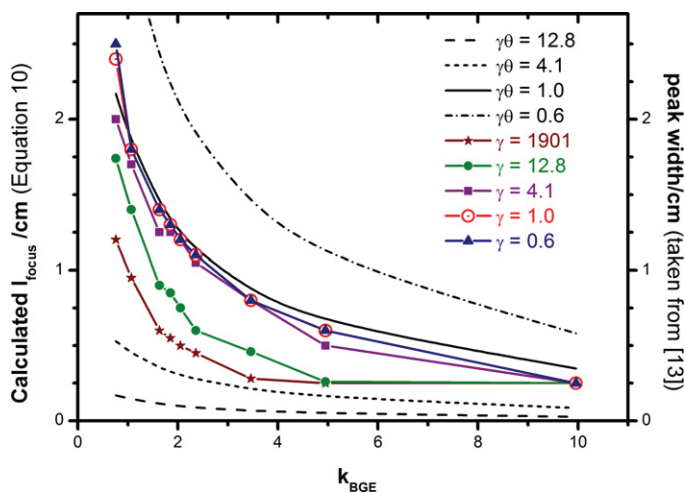


Fig. 3. Comparison of theoretically predicted curves to experimentally determined peak widths ( $l_{inj} = 3.82$  cm), experimental data taken from [13].

conductivity of the sample solution, Quirino et al. [23] have reported that for analytes with low  $k_{BGE}$  the use of high-conductivity sample matrices ( $0.3 < \gamma < 1$ ) seems to be beneficial over the use of a sample matrix with identical electric conductivity (compared to that of the BGE). This observation suggests that there are cases in which  $\theta \neq 1/\gamma$ . Following considerations support this conclusion:

- (1) In MEKC the PSP is an association colloid, which consists of dynamic units (micelles) permanently forming and dissociating on a time-scale in the microsecond to millisecond range [31]. Micelles are in equilibrium with dissolved surfactant monomer. According to the closed association model [31] the equilibrium constant  $K_{mic}$  of the process ( $n$  monomer  $\rightarrow$  micelle) equals to:

$$K_{mic} = \frac{c_M}{c_S^n} = \frac{c_M}{(c_T - nc_M)^n} \quad (11)$$

where  $c_M$  is the molar concentration of the micelles,  $c_S$  is the molar concentration of monomer surfactant,  $c_T$  is the total surfactant concentration and  $n$  is the aggregation number. Above the critical micelle concentration (CMC)  $c_T$  is given by  $c_T = c_S + nc_M$ . For reasonable values of  $K_{mic}$  and  $n$  this equation gives rise to a sharp transition from a system in which the surfactant is exclusively present as monomer ( $c_T < CMC$ ) to a system in which  $c_S$  remains essentially constant and all added surfactant contributes to an increase in  $c_M$  ( $c_T > CMC$ ) [31].

Accordingly, the degree of micellization  $\alpha_{mic}$  can be defined to be:

$$\alpha_{mic} \equiv \frac{nc_M}{c_T} \quad (12)$$

The assumption  $\theta = 1/\gamma$  is only correct, if  $\alpha_{mic}$  remains constant. However, according to Eqs. (11) and (12) the degree of micellization  $\alpha_{mic}$  is dependent on  $c_T$ . If we assume for the BGE  $c_T = 50 \text{ mmol L}^{-1}$  and  $CMC = 3 \text{ mmol L}^{-1}$  the following values for  $\alpha_{mic}$  will be obtained in the sample compartment:  $\gamma = 4$  (four times dilution or lower conductivity of the sample)  $\rightarrow \alpha_{mic} = 76\%$ ;  $\gamma = 1 \rightarrow \alpha_{mic} = 94\%$ ;  $\gamma = 0.25$  (four times concentration or higher conductivity of the sample)  $\rightarrow \alpha_{mic} = 98.5\%$ . The effects are clearly more pronounced when the conductivity is reduced, but less pronounced increasing the conductivity.

Destacking of the micellar pseudostationary phase in the first step will result in an “overproportional” decrease in  $\theta$  (via reduction in  $\alpha_{mic}$ ). Stacking of the micellar pseudostationary

phase will result in an “overproportional” increase in  $\theta$  (via increase of  $\alpha_{mic}$ ). If  $\gamma \gg 1$  (corresponding to a large destacking of the micellar pseudostationary phase in the first step) it can be expected that  $c_T < CMC$  and  $\theta = 0$ . This expectation is fulfilled in the method introduced by Quirino and Haddad [32]. Online sample preconcentration via analyte focusing by micelle collapse uses destacking of the micelles (resulting in a  $c_T < CMC$ ) into a low-conductivity focusing zone. In this technique, focusing is due to the abrupt local absence of transporting micelles.

- (2) The CMC of ionic surfactants is strongly dependent on the concentration of ionic constituents in the solution and on the effective charge number of the counter-ion. Differences in the salt content in different zones will cause differences in the CMC of the PSP in the different zones. In case of higher electric conductivity in the sample zone (higher ionic strength) a decrease of the CMC can be expected and vice versa. Listed data [33] for the CMC of SDS show a constant decrease from 8.1 to 0.52  $\text{mmol L}^{-1}$  when increasing  $c(\text{NaCl})$  from 0 to 400  $\text{mmol L}^{-1}$  (e.g. for  $c(\text{NaCl}) = 100 \text{ mmol L}^{-1} \rightarrow CMC(\text{SDS}) = 1.39 \text{ mmol L}^{-1}$ ). Additionally, with varied  $c(\text{NaCl})$  the aggregation number  $n$  is increased from 60 to 130 [33]. From the dependence of the CMC of an ionic surfactant on the concentration of ionic constituents following predictions can be made: a lowered electric conductivity in the sample zone (compared to the electric conductivity in the separation zone) will result in an “overproportional” decrease in  $\theta$  (via increase in the CMC). An increased electric conductivity in the sample zone will result in an “overproportional” increase in  $\theta$  (via decrease in the CMC).
- (3) Micelle formation of ionic surfactants includes charge condensation, i.e. the effective charge number of a micelle formed by an ionic surfactant is considerably lower than the aggregation number. A significant fraction of the counter-ions remains strongly bound to the head groups of the ionic surfactant [32]. The type and concentration of counter-ions will strongly influence the degree of dissociation of the micellar phase varying also the effective charge number. Consequently, the assumption that the effective electrophoretic mobility of the PSP can be regarded to be equal in the sample zone and in the separation zone ( $\mu_{PSP,S} = \mu_{PSP,BGE}$ ) is imprecise. While the sweeping efficiency is not dependent on the velocity of the PSP, the change in the effective charge number has an impact on the stacking or destacking process (Eq. (8)). It should also not be forgotten that the ionic strength of the electrolyte solution defines the thickness of the ion cloud  $\delta$  around the micelles and consequently the Debye-Hückel parameter  $\kappa_{DH}$  ( $\kappa_{DH} = 1/\delta$ ). It can be expected that for spherical aggregates having a hydrodynamic radius  $a$  in the range of a few nm the electrophoretic mobility will increase with decreasing  $a\kappa$  [34]. The impact of the sample composition on the effective electrophoretic mobility of the micelles  $\mu_{PSP,S}$  will have an effect on  $\theta$  which is counterbalanced by an opposite effect on the destacking or stacking of the swept zone at the boundary sample/BGE.
- (4) The partition coefficient  $K$  of a neutral solute between the micellar pseudostationary phase and the surrounding aqueous phase is not independent of the concentration of an added salt. Quirino et al. [28] reported an increase of the retention factor of progesterone from about 24 at 25  $\text{mmol L}^{-1}$  NaCl to about 40 at 150  $\text{mmol L}^{-1}$  NaCl with 80  $\text{mmol L}^{-1}$  sodium cholate in 10  $\text{mmol L}^{-1}$  tetraborate buffer. This increase in  $k$  with increasing  $c(\text{NaCl})$  can be ascribed to an increase in the partition coefficient  $K$  which is predicted from solvophobic theory [35]. This dependence of  $K$  on the concentration of ionic constituents “in the mobile phase” will additionally result in an “overproportional” decrease in  $\theta$  in the case of a lowered electric conductivity in the sample zone. A higher electric

conductivity in the sample zone than in the BGE will result in an “overproportional” increase in  $\theta$  via increase in  $K$ .

- (5) Different electric conductivities in different sections of the capillary will induce local differences in the electric field strength which results in a discontinuity of the electroosmotic velocity even when the dependence of the electroosmotic mobility on the ionic strength (via variation in  $\zeta$ ) is neglected. As liquids are quasi-incompressible, the overall bulk flow velocity must be constant inside the capillary. This requirement can only be fulfilled if differences in the local electroosmotic flow are counteracted by hydrodynamic flow velocities inside the capillary. However, this superimposed laminar flow induces additional band broadening which can be identified as a dispersion mechanism corresponding to Taylor dispersion (coupling of the non-uniformity of the convective flow velocity inside a cylindrical tube with radial molecular diffusion) [24,26].

As a summary, increasing the conductivity of the sample solution ( $\gamma < 1$ ) may result in an overproportional increase of  $\theta$  due to an increase in the degree of micellization, a decrease in the CMC, and an increase in the partition coefficient  $K$ . These considerations strongly suggest that increasing the electric conductivity of the sample solution has advantages over reducing its electric conductivity (with respect to that of the BGE) resulting in  $\theta \geq 1/\gamma$  (see Fig. 2). Increasing the electric conductivity of the sample solution also has advantages from another point of view, which was highlighted by Palmer et al. [18], as it can be applied to samples containing ionic constituents in high concentration. However, EOF velocity differences in the electric conductivity between sample and BGE will induce band broadening by hydrodynamic dispersion [24,26]. This explains why, according to Quirino et al. [23],  $\gamma$  should not exceed the range  $0.3 < \gamma < 1$ .

A quantitative treatment of the described phenomena and calculation of the resulting phase ratio shift factor  $\theta$  from thermodynamic magnitudes is difficult, because many of the data needed for these calculations are not available.

#### 2.4. Micellar transient isotachopheresis (mtITP)

Křivánková et al. [36] have shown that conditions for the existence of transient isotachopheresis (tITP) in capillary electrophoresis are quite common. They distinguish several cases of tITP. One case is tITP induced by the sample composition. In this case, the sample solution contains an ionic component (in a concentration higher than a critical value) which acts as leader or terminator, while the co-ion of the BGE acts as transient terminator or leader, respectively. This ionic component (contained in the sample solution in high concentration) can be either a constituent of the sample or an added modifier. The analytes (which are present in the sample in much lower concentration than the ionic component) are stacked (boundary stacking [3], isotachopheretic stacking [37]) either behind the transient leader or in front of the transient terminator (before they reach separation conditions), provided that the effective electrophoretic mobility of the analyte is between the effective electrophoretic mobility of the transient leader/terminator (in the sample) and the effective electrophoretic mobility of the co-ion of the BGE acting as transient terminator/leader, respectively.

It is obvious that neutral analytes cannot be stacked via tITP as they never fulfill these requirements. However, in the case that the PSP is an ionic surfactant, the micelles migrating across the sample zone can be isotachopheretically stacked provided that the requirements for tITP are fulfilled. Asakawa et al. [38] and Ogino et al. [39] have demonstrated for sodium alkyl sulfate micelles and other anionic micelles that ionic micelles can form correct isotachopheretic zones [40]. If the concentration of the surfactant

in the migrating zone exceeds the CMC, the authors observe a zone of micelles and monomers and an additional monomer zone. Separation into two zones is due to the fact that the effective electrophoretic mobilities are different for the surfactant monomer and the surfactant micelle. The authors have used the developed isotachopherograms for the determination of the CMC of selected surfactants. In these studies, chloride was used as the leading ion.

These results suggest the possibility of a micellar transient ITP (mtITP) step, e.g. with chloride as transient leading anion and the sample being devoid of background electrolyte co-ions such as borate or phosphate. In this case, mtITP acts as an on-line enrichment process in which an isotachopheretically stacked zone of the micelles will migrate through the sample zone enriching the analytes. Such an mtITP system has been described, simulated and experimentally verified by Foteeva et al. [41], who have effectively enriched metalloodrugs in a MEKC system composed of SDS and borate with sodium chloride as sample matrix with  $\mu_{\text{Cl}} > \mu_{\text{SDS}} > \mu_{\text{borate}}$ . A similar phenomenon, termed micelle-mediated ITP, was observed by Quirino [42] during his study of neutral analyte focusing by micelle collapse where an ITP state is induced by the presence of NaCl in the sample.

According to the moving boundary equation [40], an effective enrichment of the micelles will take place if there is a sufficiently high concentration of the leading ion, which will lead to an associated increase of the phase ratio shift factor  $\theta$ . The final concentration of the micelles in the boundary region is then regulated by the concentration of the transient leader. Also because of charge condensation at the surface of the ionic micelles [31], the micelle concentration reached via tITP can be much higher than that achieved via proportional stacking [3]. A moving boundary of chloride followed by the isotachopheretically enriched micelles is then migrating through the sample zone, and therefore a very efficient zone focusing via sweeping is expected to be obtained even for analytes of moderate to low retention factors. Regarding the fact that the PSP is present in an unlimited amount in the BGE, it is a point of view, if one wants to regard the BGE co-ion or the PSP as the terminating ion in this PSP-overloaded tITP system (see simulations performed by Foteeva et al. [41]). From another point of view the developed zones can also be regarded as an ITP train with trailing electrolyte impurity (in the micellar zone) [43].

There is an important difference to classical sweeping with a high-salt containing matrix [23] in which the sample contains a high concentration of a salt together with BGE co-ions like phosphate: whereas in the classical sweeping mechanism, two stationary boundaries exist at both ends of the sample plug, in mtITP, the sample/BGE boundary is a moving boundary. Thus, no destacking takes place at the original position of this boundary. Instead, in mtITP the micelle/leading ion boundary is moving and does not disappear at the original sample/BGE boundary. Based on these considerations it can be expected that very efficient sweeping can be obtained for all analytes regardless of their retention factors. However, stacking of micelles at a moving boundary is temporary and the transient ITP stack will disappear as a consequence of electromigration dispersion (see simulations performed by Foteeva et al. [41]). The enrichment efficiency then depends on the temporal evolution of the mtITP stack vs. the migration velocity of the analyte, regulated by its retention factor. Analytes of high retention factor are present at the front of the micelle/leading ion boundary and will thus experience the electromigration dispersion of the micellar front. This process will counteract the enrichment process which has taken place in the first step of mtITP. However, analytes of low retention factor have already been left behind the front, before the electromigration dispersion takes place, and therefore with this type of analytes the acquired high enrichment efficiency can be expected to be maintained.

The whole process can also be regarded to be a chromatographic enrichment mechanism, because neutral analytes are enriched by partitioning between the isotachophoretically focused micelles and the surrounding aqueous phase. Dependent on the lifetime of the moving boundary, the “general elution problem” (as it is defined in the chromatographic literature [44]) also comes into play, and the unavoidable “elution step” can counteract focusing by micellar tITP.

### 3. Experimental

#### 3.1. Apparatus

All measurements were done with a Beckman (Fullerton, CA, USA) P/ACE™ MDQ CE system equipped with a UV-detector. Temperatures of the capillary and the sample tray were kept at 25 °C by liquid cooling. Separations of parabens, benzamide and anilines were carried out at a voltage of 20, 15 and 22 kV, respectively and a detection wavelength of 254 nm. Data were recorded with Beckman 32 Karat software (v. 5.0). Fused silica-capillaries (50 μm I.D., 362 μm O.D.) were obtained from Polymicro Technologies (Phoenix, AZ, USA). New capillaries were conditioned by flushing them first with 0.2 mol L<sup>-1</sup> NaOH solution for 60 min, then with water for 30 min and then with BGE for 30 min. A rinsing step with BGE for 5 min was performed between runs. HI 8817 pH meter (Hanna Instruments, Kehl, Germany) was used for pH measurements, and LF 191 conductometer (WTW, Weinheim, Germany) was used to measure the electric conductivity of the sample solutions. Origin 8.5 software (OriginLab Corporation, Northampton, USA) or GraphPad Prism 4.03 software (GraphPad Software, Inc., San Diego, USA) were used for performing non-linear regression needed for the assessment of sweeping efficiencies.

#### 3.2. Chemicals and background electrolytes

Ethylparaben, quinine hydrochloride, sodium dodecyl sulfate and disodium hydrogen phosphate were from Fluka, Buchs, Switzerland. Propylparaben, aniline and 4-ethylaniline were from Sigma, St. Louis, USA. Benzamide was from Acros Organics, Geel, Belgium. Boric acid, disodium tetraborate decahydrate, sodium chloride and sodium dihydrogen phosphate were from Merck, Darmstadt, Germany. Thiourea was from Riedel-de Haën, Seelze, Germany. 1-Butanol, HPLC grade was from VWR-BDH-Prolabo, Leuven, Belgium. N-octane, 97% was available at the department of chemistry, Marburg, Germany. All analytes were dissolved in water and their concentrations in the sample solution were 20, 40 and 50 mg L<sup>-1</sup> for parabens, benzamide and anilines, respectively.

Stock solutions of phosphate and borate buffers were prepared and further diluted for the preparation of background electrolytes. Stock phosphate buffer (40 mmol L<sup>-1</sup>, pH 7.00) was prepared by mixing 20 mmol L<sup>-1</sup> sodium dihydrogen phosphate and 20 mmol L<sup>-1</sup> disodium hydrogen phosphate and adjusting the pH by sodium hydroxide or phosphoric acid if necessary. Stock boric acid buffer (20 mmol L<sup>-1</sup>, pH 9.00) was prepared by dissolving 1.236 g boric acid in 500 mL of water, adjusting the pH with 1 mol L<sup>-1</sup> sodium hydroxide (about 10 mL) and then diluting to 1000 mL with water. Stock disodium tetraborate buffer (20 mmol L<sup>-1</sup>, pH 9.37) was prepared by dissolving 7.627 g disodium tetraborate decahydrate in 500 mL of water and diluting to 1000 mL with water.

The BGE was 20 mmol L<sup>-1</sup> phosphate buffer, pH 7.00 containing 25, 50 or 75 mmol L<sup>-1</sup> SDS for parabens, 10 mmol L<sup>-1</sup> borate buffer, pH 9.00 containing 75 or 100 mmol L<sup>-1</sup> SDS for benzamide and 10 mmol L<sup>-1</sup> borate buffer, pH 9.37 containing 50 mmol L<sup>-1</sup> SDS, for anilines.

### 4. Results and discussion

#### 4.1. Assessment of sweeping efficiency

Three groups of analytes were selected for the present study; ethylparaben (EP) and propylparaben (PP) as examples of weakly acidic analytes, benzamide as an example of a neutral analyte and aniline and 4-ethylaniline as examples of weakly basic analytes. These analytes were selected to have moderate retention factors and adequate water solubility so that they can be dissolved in aqueous solutions.

The online enrichment by sweeping was achieved by dissolving the analyte in the same solution as the BGE, however, without micelles and without modification of the electric conductivity of the sample solution. The advantage of using sweeping as a sample enrichment method can be illustrated in Fig. 4 showing the marked enhancement of sensitivity and improvement of peak shape (with constant injection parameters) due to sweeping. Different definitions have been proposed to express the enrichment efficiency in capillary electromigration separation techniques. Many papers used the ratio of peak heights obtained under sample preconcentration conditions to that obtained with the conventional injection procedure multiplied with the dilution factor [5,16,45]. Simpson et al. [46] emphasized that this definition is somewhat arbitrary because there is no exact definition of the injection parameters to be employed [46]. Another definition is the ratio of the length of the sample zone to that of the analyte zone at the detection cell, called the detector-to-injection bandwidth ratio [46,47]. This definition, however, requires an exact measurement of the zone lengths. According to Simpson et al. [46] a more practical definition is to compare the limits of detection which are obtained under conventional and under preconcentration conditions [48,49]. However, all the previously published methods for the assessment of sweeping efficiency do not offer a compensation of secondary effects (e.g. induced hydrodynamic dispersion, variation in mean EOF velocity). For experimental verification of the theoretical considerations made in Section 2, there is a strong need to develop an accurate, robust and reliable method for the assessment of the sweeping efficiency.

The principle of the method developed by us is illustrated in Fig. 5. It depends on measuring the peak height ratio of the analyte peak obtained under sweeping conditions and under conventional conditions using injection conditions in the volume overload region. This can be achieved by recording the (peak height) vs. (injection pressure × injection time) plot and then performing non-linear regression by Origin 8.5 software using *BoxLucas1* function or by GraphPad Prism 4.03 software using *Zero to Top* function. Both functions achieve the best curve fitting for the obtained results based on using the equation  $Y = a(1 - e^{-bX})$  for regression where “a” and “b” are coefficients and “a” represents the limiting peak height (plateau region of the curve). With this approach, the limiting peak heights in the volume overload (plateau) regions under sweeping and under conventional conditions are determined. The sweeping efficiency can then be calculated using the following equation:

$$\text{Sweeping efficiency} = \frac{h_2}{h_1} \quad (13)$$

where  $h_2$  is the limiting peak height in the plateau region under sweeping conditions (analyte dissolved in BGE void of PSP) and  $h_1$  is the limiting peak height in the plateau region under conventional conditions (analyte dissolved in BGE) as illustrated in Fig. 5. The values of  $h_1$  and  $h_2$  are calculated from the fit where the coefficient “a” in the regression equation is taken as the value of  $h_1$  or  $h_2$ . The peak height in case of regular sharp narrow peaks was measured automatically using the algorithm implemented in the Beckman 32 Karat software while in case of almost rectangular broad peaks

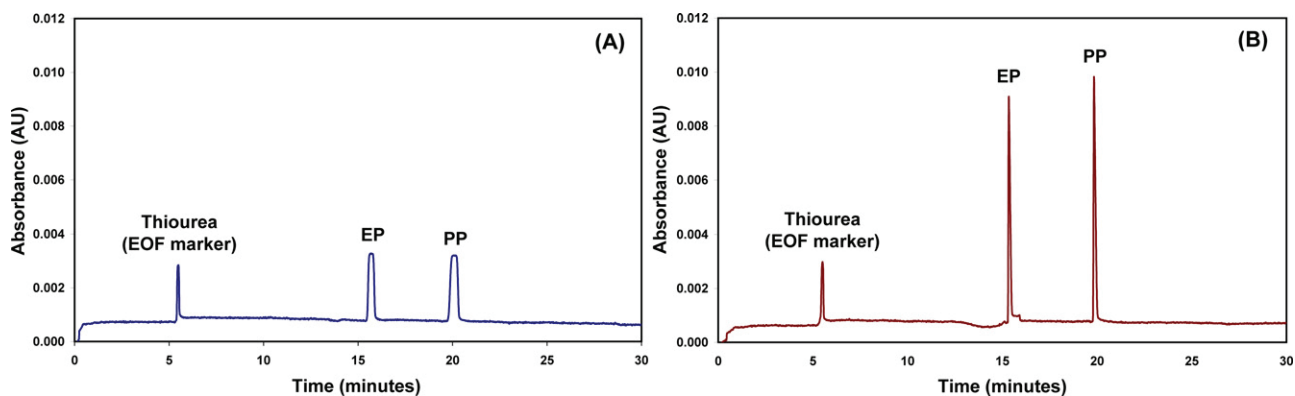


**Fig. 4.** Electropherograms of ethylparaben (EP) and propylparaben (PP) under (A) conventional conditions (analyte dissolved in BGE), (B) sweeping conditions (analyte dissolved in phosphate buffer) with constant injection parameters (1 psi for 10 s). BGE: 50 mmol L<sup>-1</sup> SDS, 20 mmol L<sup>-1</sup> phosphate buffer, pH 7.00; capillary: fused silica-capillaries (50  $\mu$ m I.D., 362  $\mu$ m O.D.) with a total length of 60.9 cm and a length to the detector of 50.7 cm; temperatures of the capillary and the sample tray: 25 °C; voltage: +20 kV; detection wavelength: 254 nm.

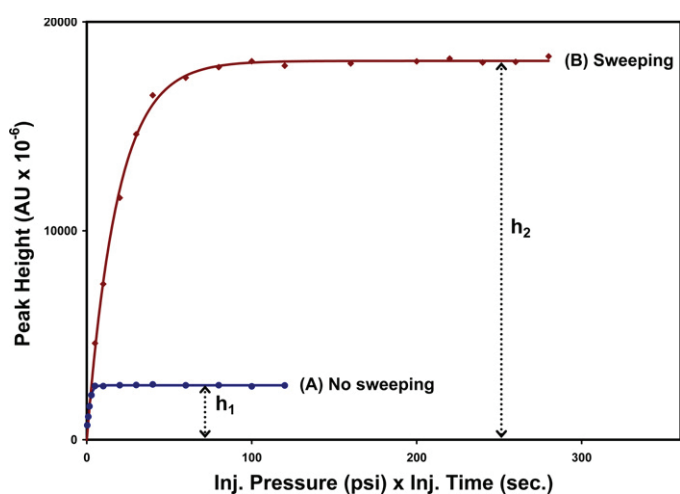


**Fig. 5.** Peak height plotted against injected volume for ethylparaben under (A) conventional conditions and (B) sweeping conditions. For experimental parameters refer to Fig. 4.

the peak height is measured indirectly using the scale on the y-axis of the electropherogram and simply calculating the difference between the peak maximum (located as the middle horizontal line between all points within the upper flat part of the peak, rejecting outliers) and the baseline close to the peak. For illustration of the principle, selected electropherograms corresponding to increasing injection volumes of EP under conventional and under sweeping conditions are shown in Fig. 6.

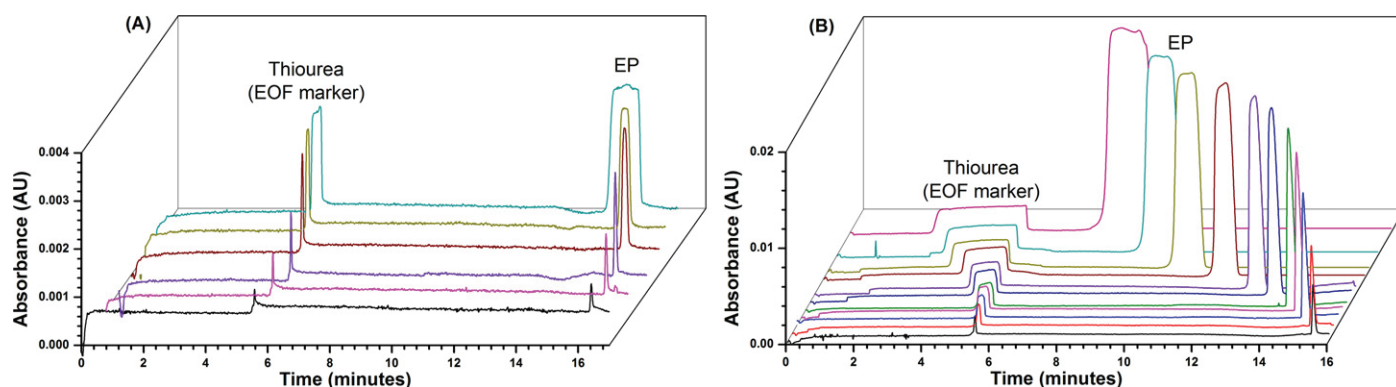


**Fig. 6.** Electropherograms for ethylparaben (EP) obtained with varied injected sample volume under (A) conventional conditions and (B) sweeping conditions. For experimental parameters refer to Fig. 4.

This procedure was successfully applied to the analytes ethylparaben, propylparaben, benzamide, aniline, and 4-ethylaniline using different SDS concentrations and different buffer types. Selected examples of the regression curves recorded are illustrated in Fig. 7 showing data for benzamide as an example of analytes with low retention factor and for PP as an example of analytes with high retention factor (additional regression curves for other analytes are included in supplementary data). The results obtained for all analytes are summarized in Table 1 which illustrates the direct relationship between the sweeping efficiency and the retention factor in the BGE. More details about the experimental measurement of retention factors are discussed in Section 4.2. The higher the retention factor, the higher is the sweeping efficiency and vice versa. For a selected analyte, the sweeping efficiency increases with increasing the concentration of PSP. Table 1 confirms the applicability of the proposed method for the determination of sweeping efficiency for different acidic, basic and neutral analytes under variable separation conditions.

In addition, the method was also tested for the assessment of sweeping efficiency in MEEKC and the measured sweeping efficiencies were 3.63 and 4.10 for EP and PP, respectively. The MEEKC separation conditions were as follows: BGE: 20 mmol L<sup>-1</sup> phosphate buffer, pH 7 containing 3.3% (w/w) SDS, 0.8% (w/w) n-octane and 6.6% (w/w) 1-butanol, sample: 20 mg L<sup>-1</sup> EP or PP in water, detection wavelength: 254 nm, voltage: +25 kV, capillary: fused silica-capillaries (50  $\mu$ m I.D., 362  $\mu$ m O.D.) with a total length of 60.9 cm and a length to the detector of 50.7 cm, kept at 40 °C (corresponding regression curve is included in supplementary data (Fig. S5 and S6)).

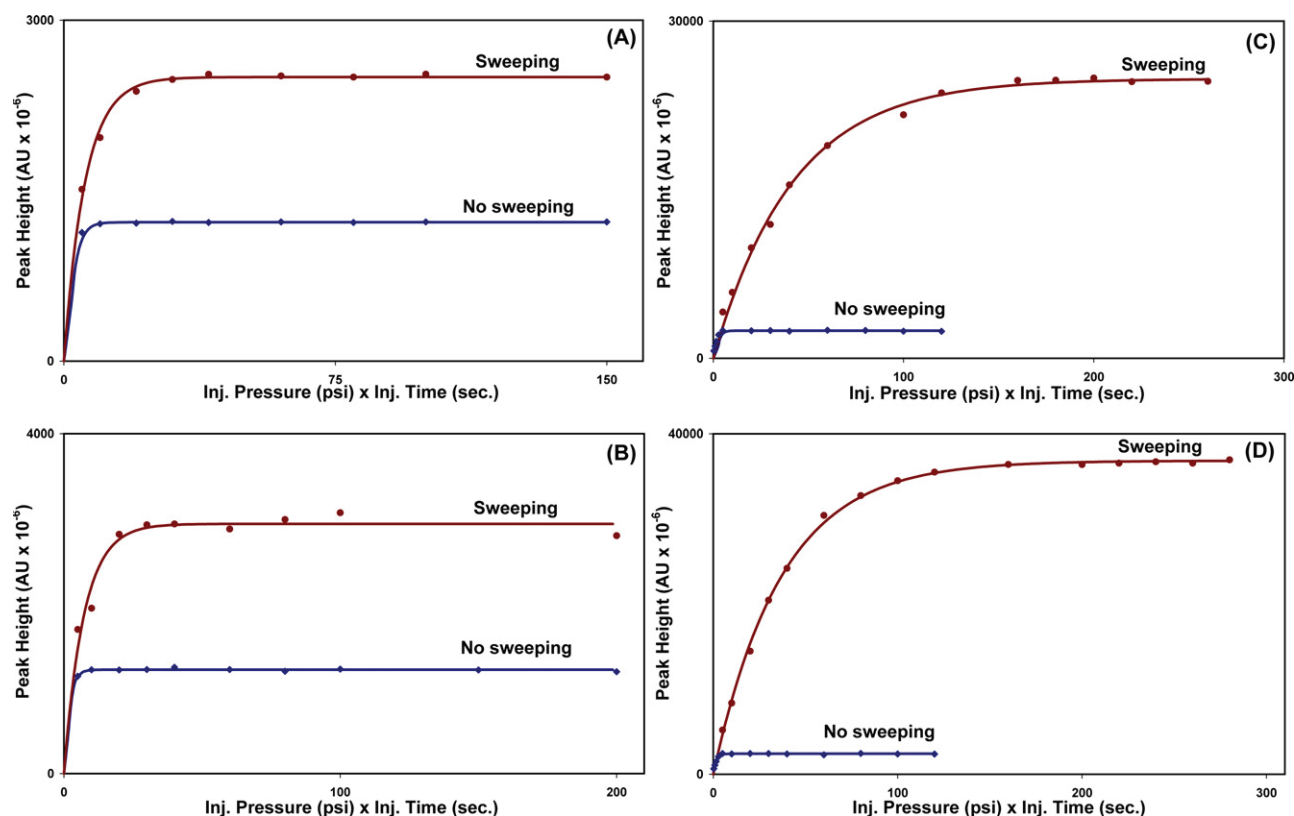


**Fig. 7.** Assessment of sweeping efficiency for benzamide with (A) 75 mmol L<sup>-1</sup> and (B) 100 mmol L<sup>-1</sup> SDS in the BGE and for propylparaben with (C) 25 mmol L<sup>-1</sup> and (D) 50 mmol L<sup>-1</sup> SDS in the BGE. Capillary: fused silica-capillaries (50 μm I.D., 362 μm O.D.) with a total length of 60.9 cm and a length to the detector of 50.7 cm; temperatures of the capillary and the sample tray: 25 °C; voltage: +15 kV for benzamide and +20 kV for propylparaben; detection wavelength: 254 nm.

The developed procedure for the assessment of sweeping efficiency can also be applied for the assessment of enrichment efficiency in other online sample preconcentration methods employed in capillary electromigration techniques (e.g. field-amplified sample stacking, or dynamic pH junction). The only drawback of this method is that it will be difficult to reach the volume overload region under enrichment conditions with very high enrichment factors (e.g. sweeping conditions with extremely hydrophobic analytes) due to the limited capillary volume available for sample injection. In this case, the highest possible peak height corresponding to the maximum allowed injection volume for a specified capillary under sweeping conditions can be used as  $h_2$  in Eq. (13).

The value obtained in this case represents the actual sweeping efficiency that can be achieved experimentally rather than the true value which is difficult to be reached under real conditions. Generally, the developed method for the assessment of sweeping efficiency is very ideal for studies that investigate the factors affecting sample enrichment techniques because such studies are usually performed on moderately hydrophobic analytes to avoid solubility problems.

A simplified procedure of the method developed for measuring the sweeping efficiency was also tested. This method depends on the peak heights of only two or three pre-selected injection volumes which are known to be in the volume overload region.

**Table 1**  
Application of the proposed method for the assessment of sweeping efficiency in MEKC using different SDS concentrations.

Analyte	BGE	Retention factor ( $k_{BGE}$ ) <sup>a</sup>	Sweeping efficiency	
			Experimentally measured	Theoretically predicted <sup>a</sup> (Eq. (14))
Ethylparaben	25 mmol L <sup>-1</sup> SDS in phosphate buffer, pH 7.00	2.46 (±0.02)	4.16 (±0.03) <sup>b</sup>	3.46 (±0.02)
	50 mmol L <sup>-1</sup> SDS in phosphate buffer, pH 7.00	5.15 (±0.07)	7.08 (±0.19) <sup>b</sup>	6.15 (±0.07)
	75 mmol L <sup>-1</sup> SDS in phosphate buffer, pH 7.00	7.83 (±0.12)	9.65	8.83 (±0.12)
Propylparaben	25 mmol L <sup>-1</sup> SDS in phosphate buffer, pH 7.00	6.53 (±0.10)	10.11 (±0.02) <sup>b</sup>	7.53 (±0.10)
	50 mmol L <sup>-1</sup> SDS in phosphate buffer, pH 7.00	13.99 (±0.18)	15.08 (±0.25) <sup>b</sup>	14.99 (±0.18)
	75 mmol L <sup>-1</sup> SDS in phosphate buffer, pH 7.00	21.40 (±0.41)	23.20	22.40 (±0.41)
Benzamide	75 mmol L <sup>-1</sup> SDS in borate buffer, pH 9.00	0.83 (±0.01)	2.05	1.83 (±0.01)
	100 mmol L <sup>-1</sup> SDS in borate buffer, pH 9.00	1.09 (±0.01)	2.40	2.09 (±0.01)
Aniline	50 mmol L <sup>-1</sup> SDS in borate buffer, pH 9.37	0.41 (±0.00)	1.38	1.41 (±0.00)
4-Ethylaniline	50 mmol L <sup>-1</sup> SDS in borate buffer, pH 9.37	2.90 (±0.02)	3.92	3.90 (±0.02)

<sup>a</sup> Each value is the mean of at least three repetitions, standard deviations given in brackets.

<sup>b</sup> Each value is the mean of three repetitions, standard deviations given in brackets.

**Table 2**

Comparison of the sweeping efficiency values obtained by the “selected points” and the “plateau curve” procedures for EP and PP.

Analyte		Ethylparaben		Propylparaben	
		25 mmol L <sup>-1</sup>	50 mmol L <sup>-1</sup>	25 mmol L <sup>-1</sup>	50 mmol L <sup>-1</sup>
Plateau curve procedure	1st trial	4.14	6.96	10.13	15.28
	2nd trial	4.14	6.99	10.10	15.15
	3rd trial	4.20	7.30	10.10	14.80
	Mean	4.16	7.08	10.11	15.08
	SD <sup>a</sup>	0.03	0.19	0.02	0.25
	RSD <sup>b</sup>	0.72%	2.68%	0.20%	1.66%
Selected points procedure	1st trial	4.03	6.57	10.26	15.43
	2nd trial	4.35	6.92	10.32	15.91
	3rd trial	4.01	6.44	9.99	15.93
	4th trial	4.02	6.55	9.99	14.12
	Mean	4.10	6.62	10.14	15.35
	SD	0.17	0.21	0.17	0.85
RSD	4.15%	3.17%	1.68%	5.54%	

<sup>a</sup> SD: standard deviation.

<sup>b</sup> RSD: relative standard deviation.

This assumption can easily be confirmed by the recorded peak shape, which in case of volume overload is broad and nearly rectangular. Although the precision of this simplified “selected points” procedure is somewhat lower than that of the original “plateau curve” procedure, it still provides reliable data and is a time-saving alternative to the regression analysis method. Table 2 shows a comparison of different trials for measuring the sweeping efficiency using both procedures. Each value represents a separate independent measurement for each analyte. The results confirm the precision and robustness of the developed method as indicated by the small values of the standard deviations.

#### 4.2. Comparison with the theoretically predicted sweeping efficiency

The accuracy of the proposed method for the assessment of sweeping efficiency (Section 4.1.) was confirmed by comparing the results obtained experimentally with those which are predicted by Eq. (2). The theoretically predicted values were calculated directly from the retention factors *k* of the analytes, which had to be measured experimentally. As the sweeping efficiency can be defined as the ratio of the initial sample plug length *l<sub>inj</sub>* to the length of the sample zone after sweeping *l<sub>sweep</sub>*, according to Eq. (2), it can be calculated as follows:

$$\text{Sweeping efficiency} = \frac{l_{inj}}{l_{sweep}} = 1 + k_s \quad (14)$$

The retention factors were determined experimentally by MEKC with the corresponding separation electrolyte using marker compounds: thiourea as EOF marker and quinine hydrochloride as micelle marker. All analytes can be regarded to be neutral under

the conditions of enrichment. Therefore, the following equation was applied [11]:

$$k = \frac{t_s - t_0}{t_0(1 - t_s/t_{mc})} \quad (15)$$

where *t<sub>0</sub>* is the migration time of the EOF marker, *t<sub>s</sub>* is the migration time of the solute and *t<sub>mc</sub>* is the migration time of the micelle marker.

In Table 1 the experimentally measured values of the sweeping efficiency using the proposed method of variation of injection volume are compared to those values calculated according to Eq. (14). The results obtained via the two methods are in very close agreement. Differences can be attributed to unavoidable measuring errors, to the simplified assumptions in deriving Eq. (2) in which the authors assume that the peaks have a perfect rectangular shape, and to deviations from the simplification that the value of *γθ* in Eq. (10) equals 1 (whereas our considerations outlined in Section 2.3 predict that the approximation *θ* = 1/*γ* is not permitted in all cases). In addition, the differences found between the experimentally measured and theoretically predicted values were also observed by Quirino and Terabe [11]. It is interesting to note that those values determined via the developed method have the tendency to be slightly higher than those calculated on the basis of Eq. (2). Principally, according to the best of our knowledge, our results that are presented here constitute the first precise experimental verification of the validity of Eq. (2) for neutral analytes with moderate retention factors.

#### 4.3. Effect of salt content and electric conductivity of the sample matrix

For performing this study, the simplified “selected points” procedure was utilized for measuring the sweeping efficiency by using

**Table 3**

Effect of decreasing the concentration of phosphate buffer on the sweeping efficiencies of EP and PP.

Sample matrix	Water	5 mmol L <sup>-1</sup> phosphate buffer	10 mmol L <sup>-1</sup> phosphate buffer	15 mmol L <sup>-1</sup> phosphate buffer	20 mmol L <sup>-1</sup> phosphate buffer
Electric conductivity (mS/cm)	0.01	0.64	1.23	1.82	2.36
<i>γ</i> in case of 25 mmol L <sup>-1</sup> SDS <sup>a</sup>	352.00	5.50	2.86	1.93	1.49
<i>γ</i> in case of 50 mmol L <sup>-1</sup> SDS <sup>a</sup>	407.00	6.36	3.31	2.24	1.72
Sweeping efficiency					
For EP (using 25 mmol L <sup>-1</sup> SDS)	4.20	4.35	3.83	4.02	4.16
For EP (using 50 mmol L <sup>-1</sup> SDS)	6.82	8.77	8.05	8.08	7.08
For PP (using 25 mmol L <sup>-1</sup> SDS)	8.23	9.18	10.99	10.29	10.11
For PP (using 50 mmol L <sup>-1</sup> SDS)	8.91	14.16	15.52	18.20	15.08

<sup>a</sup> *γ* = field-strength enhancement factor (electric conductivities of background electrolytes *κ<sub>BCE</sub>* are 3.52 and 4.07 for 25 and 50 mmol L<sup>-1</sup> SDS, respectively).



**Table 5**

Effect of using pure NaCl solutions as sample matrix on the sweeping efficiencies of EP and PP ( $k_{BGE}$  = retention factor in BGE).

Sample matrix	20 mmol L <sup>-1</sup> phosphate buffer	50 mmol L <sup>-1</sup> NaCl	100 mmol L <sup>-1</sup> NaCl	150 mmol L <sup>-1</sup> NaCl
Electric conductivity (mS/cm)	2.36	5.80	10.53	15.23
$\gamma$ in case of 25 mmol L <sup>-1</sup> SDS <sup>a</sup>	1.49	0.61	0.33	0.23
$\gamma$ in case of 50 mmol L <sup>-1</sup> SDS <sup>a</sup>	1.72	0.70	0.39	0.27
Sweeping efficiency				
For EP (using 25 mmol L <sup>-1</sup> SDS) ... [ $k_{BGE}$ = 2.46 ± 0.02]	4.16	<b>(18.53)</b>	<b>(15.65)</b>	Not determined
For EP (using 50 mmol L <sup>-1</sup> SDS) ... [ $k_{BGE}$ = 5.15 ± 0.07]	7.08	8.09	7.14	6.83
For PP (using 25 mmol L <sup>-1</sup> SDS) ... [ $k_{BGE}$ = 6.53 ± 0.10]	10.11	8.13	6.73	Not determined
For PP (using 50 mmol L <sup>-1</sup> SDS) ... [ $k_{BGE}$ = 13.99 ± 0.18]	15.08	14.88	11.14	8.56

<sup>a</sup>  $\gamma$  = field-strength enhancement factor (electric conductivities of background electrolytes  $\kappa_{BGE}$  are 3.52 and 4.07 for 25 and 50 mmol L<sup>-1</sup> SDS, respectively).

“irregular conditions” a higher sweeping efficiency can be reached for an analyte of lower retention factor  $k_{BGE}$ .

Electropherograms obtained for different injection volumes and different concentrations of NaCl in the sample solution (using 25 mmol L<sup>-1</sup> SDS in 20 mmol L<sup>-1</sup> phosphate buffer, pH 7.00 as a BGE) are shown in Fig. 8 (another independent measurement series of these electropherograms is included in supplementary data indicating precision of the obtained data). The experimental data reported here are in full agreement with the assumption that the on-line focusing process includes transient isotachophoretic stacking of micelles (mtITP) as described in Section 2.4. In this case of a sample matrix containing only NaCl (no buffer co-ion), chloride would be the transient leading ion.

The effective electrophoretic mobility of the micelles in BGE was experimentally determined, by MEKC employing quinine hydrochloride as micelle marker, to be  $-3.79 \times 10^{-4} \text{ cm}^2 \text{ V}^{-1} \text{ s}^{-1}$  for 25 mmol L<sup>-1</sup> SDS which is very close to the effective electrophoretic mobility predicted for phosphate at pH 7.00 which is

$-3.75 \times 10^{-4} \text{ cm}^2 \text{ V}^{-1} \text{ s}^{-1}$  (from Peakmaster Program [50]). Simulation of the mtITP process (data not shown) reveals that an ITP zone of phosphate evolves directly after the chloride zone, followed by an isotachophoretically adapted SDS zone. In this system, the SDS micelles represent the terminating ion (instead of the BGE co-ion). Also in this case, a clear transient ITP stack evolves. However, regarding the very similar effective electrophoretic mobilities of phosphate and the PSP (both determined in BGE), it is not clear, which zone will evolve directly after the chloride zone. It can be expected that the effective electrophoretic mobility of the isotachophoretically enriched PSP will differ from that in the BGE. It should be noted, however, that in both cases (i.e. phosphate has higher or lower effective electrophoretic mobility than the PSP in the mtITP stack), an efficient isotachophoretic enrichment of the PSP will occur and a zone of a high concentration of SDS will migrate through the sample plug.

The evolved micelle/chloride (or micelle/phosphate) boundary is a moving boundary. Therefore, mtITP should result in high

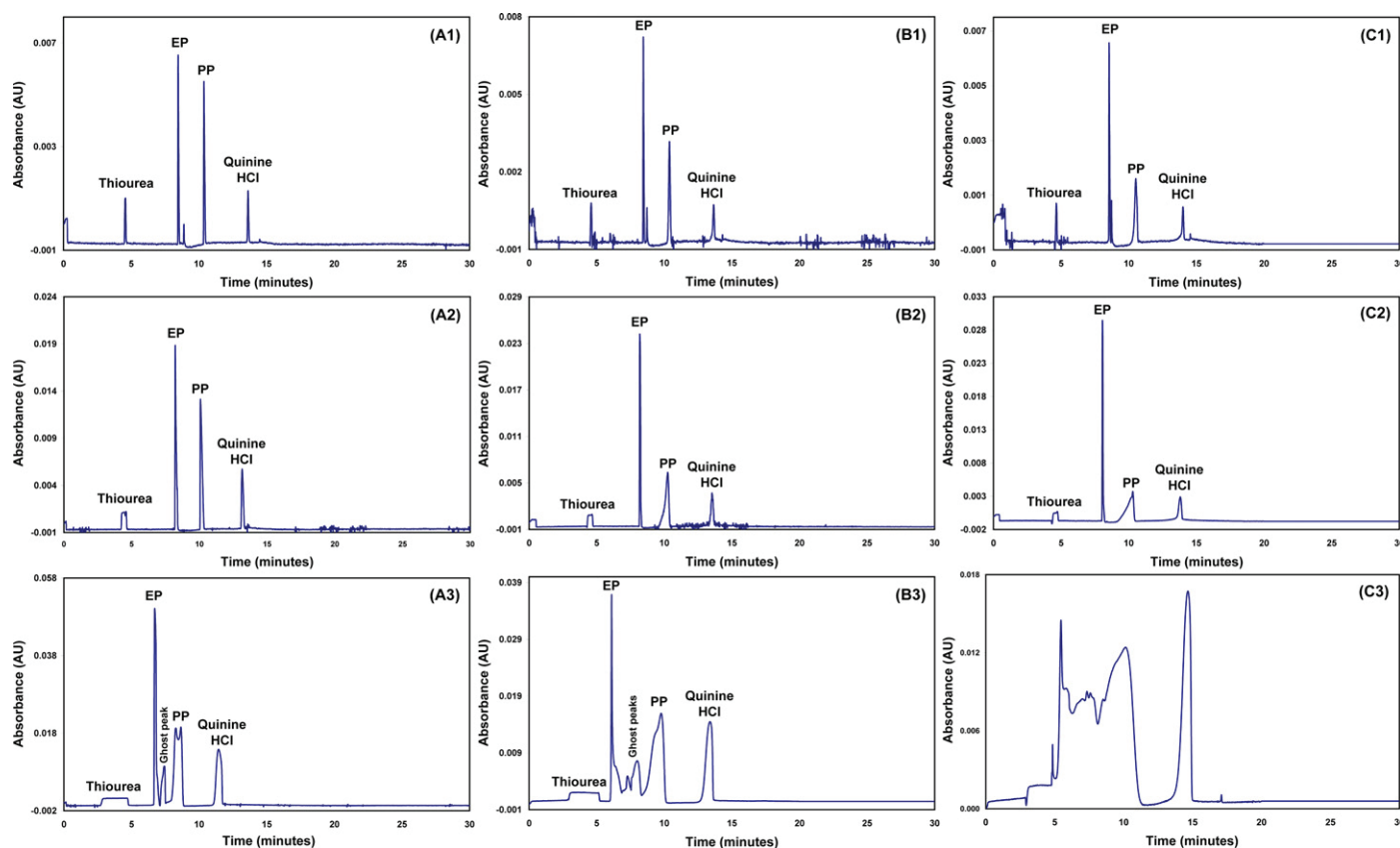


**Fig. 8.** Electropherograms obtained for different sample injection volumes with (A) 50 mmol L<sup>-1</sup>, (B) 100 mmol L<sup>-1</sup>, and (C) 150 mmol L<sup>-1</sup> NaCl in the sample solution. Injection: hydrodynamic using pressure (A1, B1, C1) 1 psi for 10 s, (A2, B2, C2) 1 psi for 40 s, (A3, B3, C3) 5 psi for 40 s; BGE: 25 mmol L<sup>-1</sup> SDS, 20 mmol L<sup>-1</sup> phosphate buffer, pH 7.00. For other experimental parameters refer to Fig. 4.

enrichment efficiency for all analytes independent of their retention factor. However, our results show that analytes of higher  $k_{\text{BGE}}$  like PP are not effectively enriched while analytes with lower  $k_{\text{BGE}}$  like EP are very effectively preconcentrated. This observation can be explained by the considerations made in Section 2.4. Analytes with high  $k_{\text{BGE}}$  are kept in the enriched micellar zone within the time frame of its electromigration dispersion, thus they will experience band broadening. Contrarily, EP with its very low retention factor has already been “eluted” from this zone and thus the acquired high enrichment efficiency can be kept. This may also explain the different peak shapes observed for EP and PP. For EP, sharp peaks are recorded even for large injection volumes, whereas the peaks recorded for PP are highly asymmetric without showing the typical rectangular shape resulting from volume overload. Their asymmetric triangular shape points to band broadening due to electromigration dispersion of the isotachophoretically stacked micellar zone. In addition, the signal of EP is directly followed by a ghost peak which might be due to isotachophoretic focusing of BGE ions or impurities in the sample solution [5] or due to peak splitting resulting from transient processes induced by the injection of salt-containing samples [51].

The possible contribution of mtITP to on-line enrichment processes in MEKC for neutral analytes with low retention factor was already predicted and observed by Foteeva et al. [41]. It can be concluded from our data that mtITP can be distinguished from ordinary sweeping by the phenomenon that the reachable sweeping efficiency is exceeding (up to several times) the sweeping efficiency which would be expected from Eq. (10). Sweeping with an isotachophoretically stacked micellar zone corresponds to an increase in the phase ratio shift factor  $\theta$  which will be much higher than the increase expected from the simple field-amplified sample stacking of micelles. Consequently, the product  $\gamma\theta$  will be increased to a high extent ( $\gamma\theta \gg 1$ ). As can be seen from Fig. 2, this increase in  $\gamma\theta$  will influence the focused zone length considerably for those analytes having a  $k_{\text{BGE}}$  lower than 10. The lower is the retention factor; the more important will be the focusing effect due to mtITP. If we also take into consideration that in case of mtITP band broadening takes place due to electrophoretic dispersion of the stacked micellar zone and due to the “elution” of the analyte from the isotachophoretically stacked PSP zone (see Section 2.4), the prediction can be made that focusing by mtITP is only applicable for analytes having a relatively low retention factor, which is supported by our experimental data.

## 5. Conclusions

The developed method for the assessment of sweeping efficiency offers high accuracy and precision. With this method the validity of the theoretical considerations regarding sweeping can be shown. We have verified the assumptions of Quirino et al. [23] that in first approximation the introduced phase ratio shift factor  $\theta$  equals  $1/\gamma$  (the reciprocal field-strength enhancement factor). Consequently, the sweeping efficiency for neutral analytes is quasi-independent of the electric conductivity or the salt content of the sample matrix, which is very important for the application of sweeping in the analysis of real samples. In this case, the sweeping efficiency can only be improved by other means like increasing the concentration of the pseudostationary phase in the BGE or using a different pseudostationary phase. In case of a low retention factor of the analyte and a strong (positive) deviation of the measured sweeping efficiency from the theoretically predicted value, micellar transient ITP (mtITP) can be assumed to take place via the migration of micelles in an isotachophoretically stacked (concentration adapted) zone, which is possible if a salt with a co-ion (with respect to the charge of the micelles) having a high electrophoretic mobility

is added to the sample solution in a concentration above a critical value.

## Acknowledgements

M. El-Awady thanks Yousef-Jameel foundation for the financial support of this work. C. Huhn thanks for financial support from the Hessian Ministry of Science and Art and the Helmholtz Initiative and Networking Fund. We thank P. Kler for discussions and simulations on micellar transient ITP. We thank M. Bauerfeind for his valuable assistance in drawing some of the figures.

## Appendix A. Supplementary data

Supplementary data associated with this article can be found, in the online version, at <http://dx.doi.org/10.1016/j.chroma.2012.09.044>.

## References

- [1] J.J. Berzas Nevado, J. Rodriguez Flores, G. Castaneda Penalvo, N. Rodriguez Fariñas, J. Chromatogr. A 953 (2002) 279.
- [2] B.F. Liu, X.H. Zhong, Y.T. Lu, J. Chromatogr. A 945 (2002) 257.
- [3] Z. Mala, L. Krivankova, P. Gebauer, P. Bocek, Electrophoresis 28 (2007) 243.
- [4] Z. Liu, P. Sam, S.R. Sirimanne, P.C. McClure, J. Grainger, D.G. Patterson Jr., J. Chromatogr. A 673 (1994) 125.
- [5] J.P. Quirino, S. Terabe, Science 282 (1998) 465.
- [6] Y. Sera, N. Matsubara, K. Otsuka, S. Terabe, Electrophoresis 22 (2001) 3509.
- [7] J.P. Quirino, S. Terabe, J. Chromatogr. A 781 (1997) 119.
- [8] K. Ghowsi, J.P. Foley, R.J. Gale, Anal. Chem. 62 (1990) 2714.
- [9] J.P. Quirino, S. Terabe, J. Chromatogr. A 856 (1999) 465.
- [10] M. Gilges, Chromatographia 44 (1997) 191.
- [11] J.P. Quirino, S. Terabe, Anal. Chem. 71 (1999) 1638.
- [12] J.B. Kim, J.P. Quirino, K. Otsuka, S. Terabe, J. Chromatogr. A 916 (2001) 123.
- [13] J.P. Quirino, S. Terabe, J. High Resolut. Chromatogr. 22 (1999) 367.
- [14] J. Palmer, D.S. Burgi, J.P. Landers, Anal. Chem. 74 (2002) 632.
- [15] J.P. Quirino, in: U. Pyell (Ed.), Electrokinetic Chromatography—Theory, Instrumentation and Applications, John Wiley & Sons, Ltd., Chichester, 2006, p. 207.
- [16] M.R. Monton, K. Otsuka, S. Terabe, J. Chromatogr. A 985 (2003) 435.
- [17] J.B. Kim, K. Otsuka, S. Terabe, J. Chromatogr. A 979 (2002) 131.
- [18] J. Palmer, N.J. Munro, J.P. Landers, Anal. Chem. 71 (1999) 1679.
- [19] M. Molina, M. Silva, Electrophoresis 21 (2000) 3625.
- [20] R. Carabias-Martinez, E. Rodriguez-Gonzalo, P. Revilla-Ruiz, J. Dominguez-Alvarez, J. Chromatogr. A 990 (2003) 291.
- [21] E.A. Pereira, A.A. Cardoso, M.F.M. Tavares, Electrophoresis 24 (2003) 700.
- [22] J.P. Quirino, S. Terabe, J. Microcolumn Sep. 11 (1999) 513.
- [23] J.P. Quirino, S. Terabe, P. Bocek, Anal. Chem. 72 (2000) 1934.
- [24] R.L. Chien, J.C. Helmer, Anal. Chem. 63 (1991) 1354.
- [25] D.S. Burgi, R.L. Chien, Anal. Chem. 63 (1991) 2042.
- [26] C. Huhn, U. Pyell, J. Chromatogr. A 1217 (2010) 4476.
- [27] R.L. Chien, D.S. Burgi, Anal. Chem. 64 (1992) 489A.
- [28] J.P. Quirino, J.B. Kim, S. Terabe, J. Chromatogr. A 965 (2002) 357.
- [29] P. Britz-McKibbin, K. Otsuka, S. Terabe, Anal. Chem. 74 (2002) 3736.
- [30] P. Britz-McKibbin, M.J. Markuszewski, T. Iyanagi, K. Matsuda, T. Nishioka, S. Terabe, Anal. Biochem. 313 (2003) 89.
- [31] R.J. Hunter, Foundations of Colloid Science, 2nd edition, Oxford University Press, Oxford, 2001.
- [32] J.P. Quirino, P.R. Haddad, Anal. Chem. 80 (2008) 6824.
- [33] J.P. Kratochvil, J. Colloid Interface Sci. 75 (1980) 271.
- [34] P.H. Wiersema, A.L. Loeb, J.T. Overbeek, J. Colloid Interface Sci. 22 (1966) 78.
- [35] C.F. Poole, The Essence of Chromatography, Elsevier, Amsterdam, 2003.
- [36] L. Krivankova, P. Pantuckova, P. Bocek, J. Chromatogr. A 838 (1999) 55.
- [37] M. Urbanek, L. Krivankova, P. Bocek, Electrophoresis 24 (2003) 466.
- [38] T. Asakawa, S. Sunazaki, S. Miyagishi, Colloid Polym. Sci. 270 (1992) 259.
- [39] K. Ogino, T. Kakiyama, M. Abe, Colloid Polym. Sci. 265 (1987) 604.
- [40] P. Bocek, M. Deml, P. Gebauer, V. Dolnik, Analytical Isotachopheresis, Wiley-VCH Verlag, Weinheim, 1988.
- [41] L.S. Foteeva, Z. Huang, A.R. Timerbaev, T. Hirokawa, J. Sep. Sci. 33 (2010) 637.
- [42] J.P. Quirino, J. Chromatogr. A 1214 (2008) 171.
- [43] E.V. Dose, G.A. Guiochon, Anal. Chem. 63 (1991) 1063.
- [44] E.J. Guthrie, J.W. Jorgenson, Anal. Chem. 56 (1984) 483.
- [45] F.K. Liu, J. Chromatogr. A 1215 (2008) 194.
- [46] S.L. Simpson, J.P. Quirino, S. Terabe, J. Chromatogr. A 1184 (2008) 504.
- [47] P. Britz-McKibbin, D.D.Y. Chen, Anal. Chem. 72 (2000) 1242.
- [48] F. Kitagawa, T. Tsuneka, Y. Akimoto, K. Sueyoshi, K. Uchiyama, A. Hattori, K. Otsuka, J. Chromatogr. A 1106 (2006) 36.
- [49] C.M. Shih, C.H. Lin, Electrophoresis 26 (2005) 3495.
- [50] M. Jaros, V. Hruska, M. Stedry, I. Zuskova, B. Gas, Electrophoresis 25 (2004) 3080.
- [51] Z. Mala, P. Gebauer, P. Bocek, Electrophoresis 30 (2009) 866.



**5.1.4. Processes involved in sweeping under inhomogeneous electric field conditions as sample enrichment procedure in micellar electrokinetic chromatography**

Mohamed El-Awady<sup>1</sup>, Carolin Huhn<sup>2</sup>, Ute Pyell<sup>1\*</sup>

<sup>1</sup>University of Marburg, Department of Chemistry, Hans-Meerwein-Straße, D-35032 Marburg, Germany

<sup>2</sup>Central Division of Analytical Chemistry, Forschungszentrum Jülich, D-52425 Jülich, Germany

\* corresponding author

**Supplementary data**

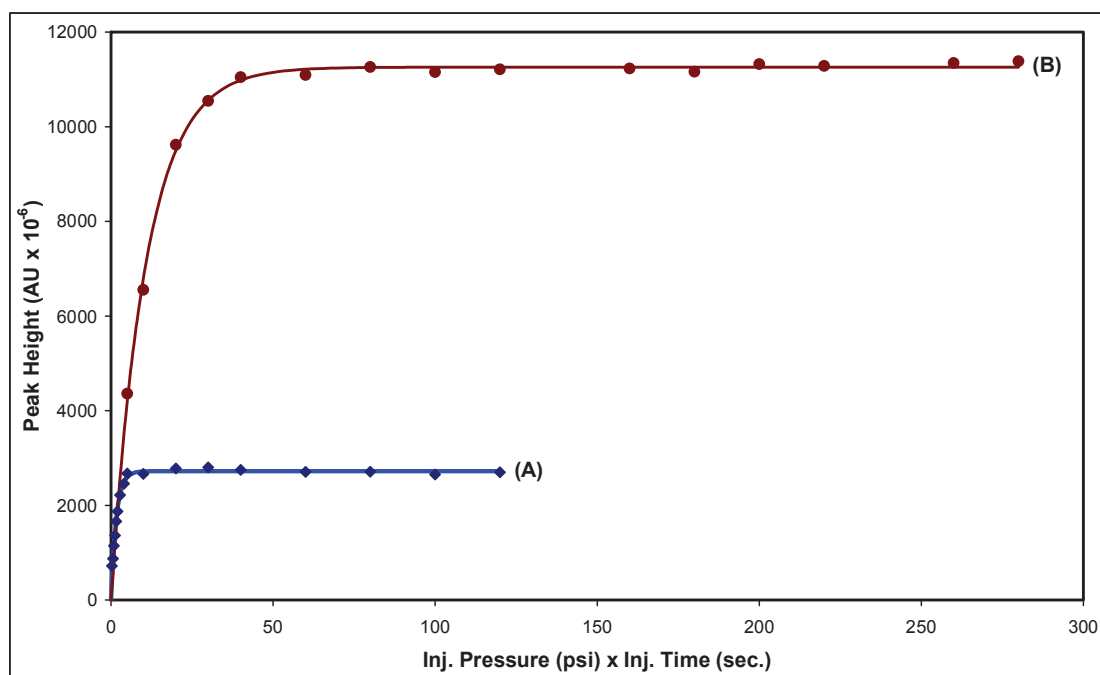


**Figure S1:** Peak height plotted against injected volume for **ethylparaben** under (A) conventional conditions, (B) sweeping conditions, using **25 mmol L<sup>-1</sup> SDS**, 20 mmol L<sup>-1</sup> phosphate buffer, pH 7 as a BGE. Injection: hydrodynamic; capillary: fused-silica capillary (50  $\mu\text{m}$  I.D., 362  $\mu\text{m}$  O.D.) with a total length of 60.9 cm and a length to the detector of 50.7 cm; temperature of the capillary and the sample tray: 25°C; voltage: +20 kV; detection wavelength: 254 nm.

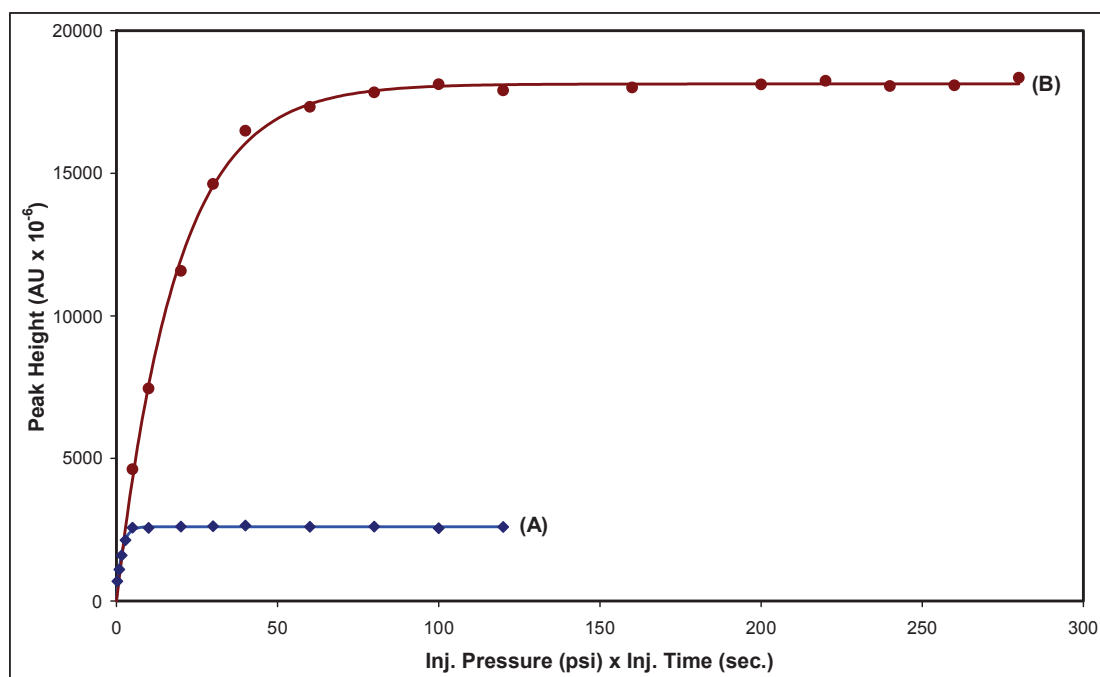


**Figure S2:** Peak height plotted against injected volume for **ethylparaben** under (A) conventional conditions, (B) sweeping conditions, using **50 mmol L<sup>-1</sup> SDS**, 20 mmol L<sup>-1</sup> phosphate buffer, pH 7 as a BGE. For other experimental parameters refer to Figure S1.

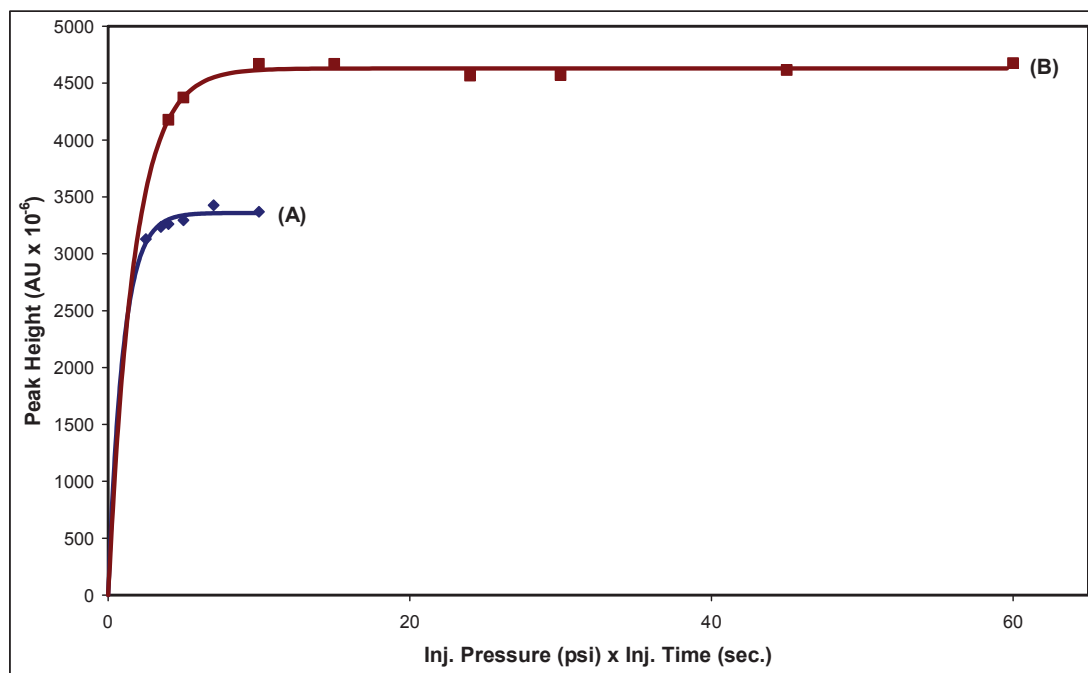


**Figure S3:** Peak height plotted against injected volume for **aniline** under (A) conventional conditions, (B) sweeping conditions, using **50 mmol L<sup>-1</sup> SDS**, 10 mmol L<sup>-1</sup> borate buffer, pH 9.37 as a BGE. Injection: hydrodynamic; capillary: fused-silica capillary (50  $\mu\text{m}$  I.D., 362  $\mu\text{m}$  O.D.) with a total length of 50.65 cm and a length to the detector of 40.25 cm; temperature of the capillary and the sample tray: 25°C; voltage: +22 kV; detection wavelength: 254 nm.

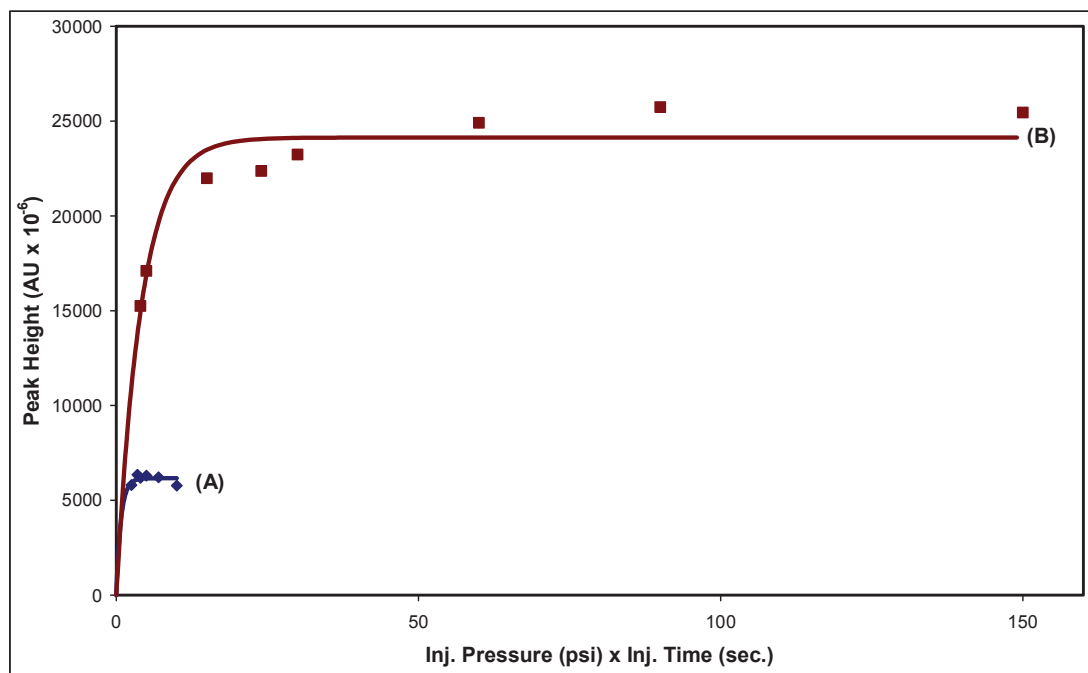


**Figure S4:** Peak height plotted against injected volume for **4-ethylaniline** under (A) conventional conditions, (B) sweeping conditions, using **50 mmol L<sup>-1</sup> SDS**, 10 mmol L<sup>-1</sup> borate buffer, pH 9.37 as a BGE. For experimental parameters refer to Figure S3.

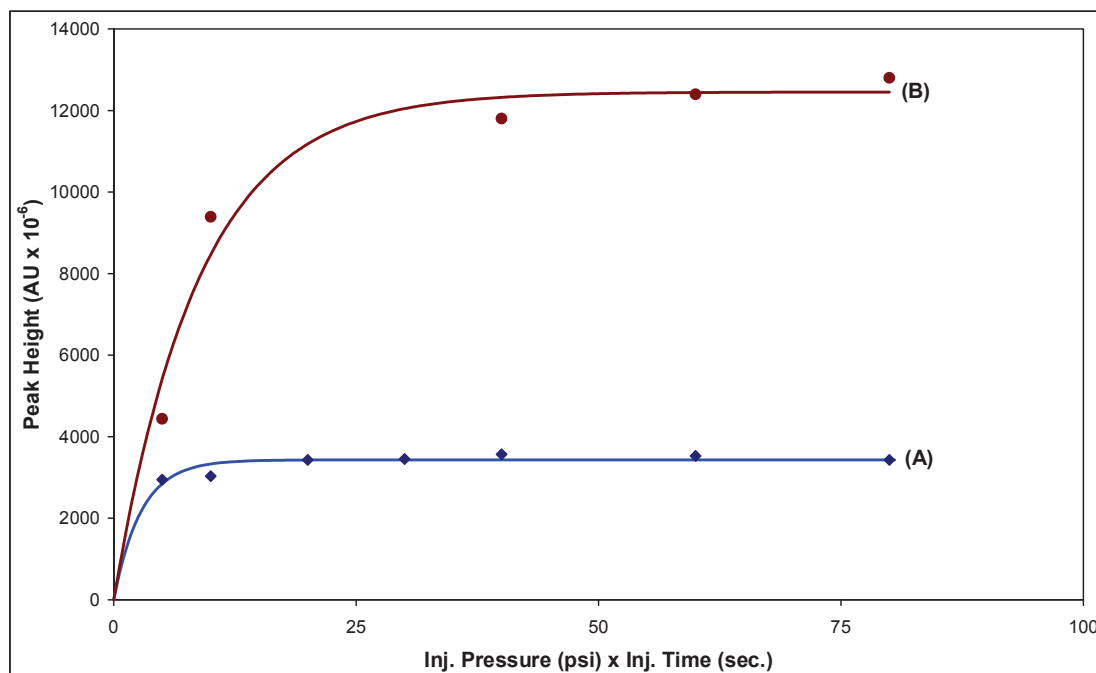


**Figure S5:** Peak height plotted against injected volume for **ethylparaben** in MEEKC under (A) conventional conditions, (B) sweeping conditions. BGE: 20 mmol L<sup>-1</sup> phosphate buffer, pH 7 containing 3.3% (w/w) SDS, 0.8% (w/w) octane and 6.6% (w/w) 1-butanol, sample: 20 mg L<sup>-1</sup> EP or PP in water, detection wavelength: 254 nm, voltage: +25 kV, capillary: fused silica-capillary (50  $\mu$ m I.D., 362  $\mu$ m O.D.) with a total length of 60.9 cm and a length to the detector of 50.7 cm, kept at 40°C.

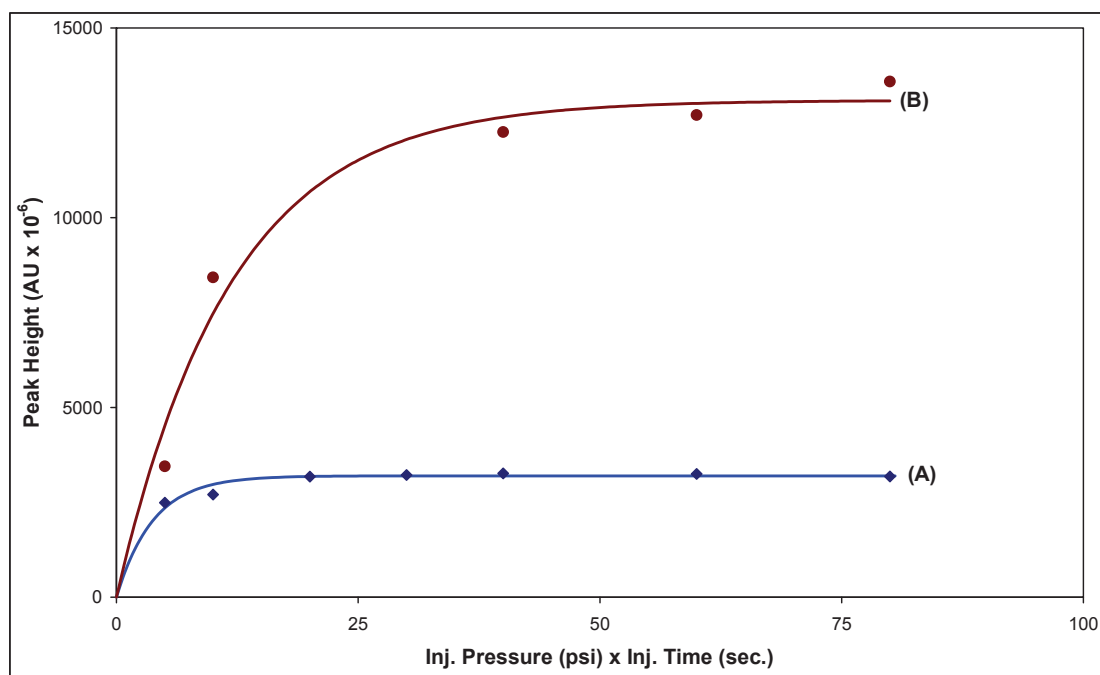


**Figure S6:** Peak height plotted against injected volume for **propylparaben** in MEEKC under (A) conventional conditions, (B) sweeping conditions. For experimental parameters refer to Figure S5.

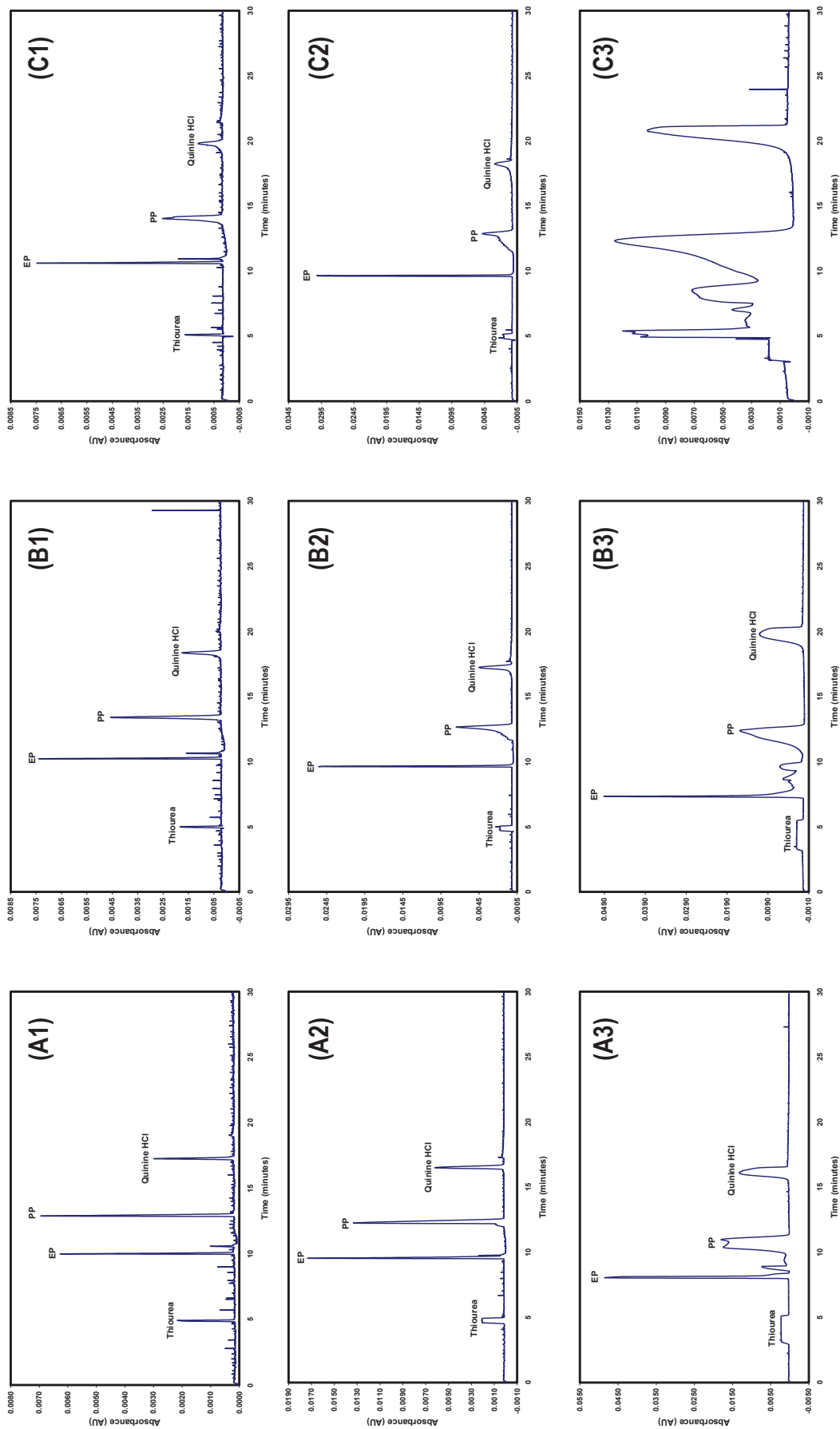


**Figure S7:** Another independent measurement series of the electropherograms obtained for different sample injection volumes with (A) 50 mmol L<sup>-1</sup>, (B) 100 mmol L<sup>-1</sup>, (C) 150 mmol L<sup>-1</sup> NaCl in the sample solution. Injection: hydrodynamic using pressure (A1,B1,C1) 1 psi for 10 s, (A2,B2,C2) 1 psi for 40 s, (A3,B3,C3) 5 psi for 40 s; BGE: 25 mmol L<sup>-1</sup> SDS, 20 mmol L<sup>-1</sup> phosphate buffer, pH 7. For other experimental parameters refer to Figure S1.

**Animation: Sweeping and separation of neutral analytes in MEKC employing negatively charged micelles.**

For simplification, following assumptions were made: The velocity of the EOF is assumed to be close to zero and can be neglected. The anionic surfactant SDS is used as PSP in the reversed direction mode (RM-MEKC). The micelles are negatively charged and migrate from the cathode to the anode. The analytes are dissolved in the same solution as the BGE, however, void of micelles. A large volume of the sample is injected.

After starting the run and application of voltage, the micelles enter the sample zone and the process of sweeping is started. In other words, the micelles “pick up” analyte molecules and accumulate them into a narrow concentrated band, while there is a micelle-free zone formed before the swept sample zone. The sweeping process is continued until the front of the micelles reaches the sample/BGE boundary (completely swept sample zone). After completion of the sweeping process, regular MEKC separation takes place leading finally to separated preconcentrated analyte zones.



---



---

This is a License Agreement between Mohamed El-Awady ("You") and Elsevier ("Elsevier") provided by Copyright Clearance Center ("CCC"). The license consists of your order details, the terms and conditions provided by Elsevier, and the payment terms and conditions.

**All payments must be made in full to CCC. For payment instructions, please see information listed at the bottom of this form.**

Supplier	Elsevier Limited The Boulevard, Langford Lane Kidlington, Oxford, OX5 1GB, UK
Registered Company Number	1982084
Customer name	Mohamed El-Awady
Customer address	University of Marburg, Marburg, Hesse 35032
License number	3163170179940
License date	Jun 06, 2013
Licensed content publisher	Elsevier
Licensed content publication	Journal of Chromatography A
Licensed content title	Processes involved in sweeping under inhomogeneous electric field conditions as sample enrichment procedure in micellar electrokinetic chromatography
Licensed content author	Mohamed El-Awady, Carolin Huhn, Ute Pyell
Licensed content date	16 November 2012
Licensed content volume number	1264
Licensed content issue number	
Number of pages	13
Start Page	124
End Page	136
Type of Use	reuse in a thesis/dissertation
Portion	full article
Format	both print and electronic
Are you the author of this Elsevier article?	Yes
Will you be translating?	No
Order reference number	
Title of your thesis/dissertation	Investigation of sweeping as sample enrichment method in micellar electrokinetic chromatography in the analysis of pharmaceutical preparations and biological fluids
Expected completion date	Jul 2013



## **5.2. Publication II**

**Sweeping as a multistep enrichment process in micellar electrokinetic chromatography: The retention factor gradient effect**

Mohamed El-Awady, Ute Pyell

*Journal of Chromatography A, 1297 (2013) 213-225*

*doi: 10.1016/j.chroma.2013.04.069*



## 5.2.1. Summary and discussion

In this publication, our new method developed for the assessment of sweeping efficiency is extended to the general case, in which the distribution coefficient of the analyte in the sample and BGE zones and the electric conductivity of the sample are varied. Parabens, benzamide and anilines are studied as model analytes under MEKC conditions with SDS as anionic surfactant. In contrast to the classical description of sweeping, we show experimentally and theoretically that focusing due to sweeping is not only affected by the retention factor of analyte in the sample zone, but also by the retention factor of analyte in the BGE. We introduce the term “retention factor gradient effect (RFGE)” to express the additional focusing or defocusing effect that arises if the distribution coefficient and hence the retention factor of the analyte is different in the sample and BGE compartments. A schematic illustration of this effect is presented in Figure 1.

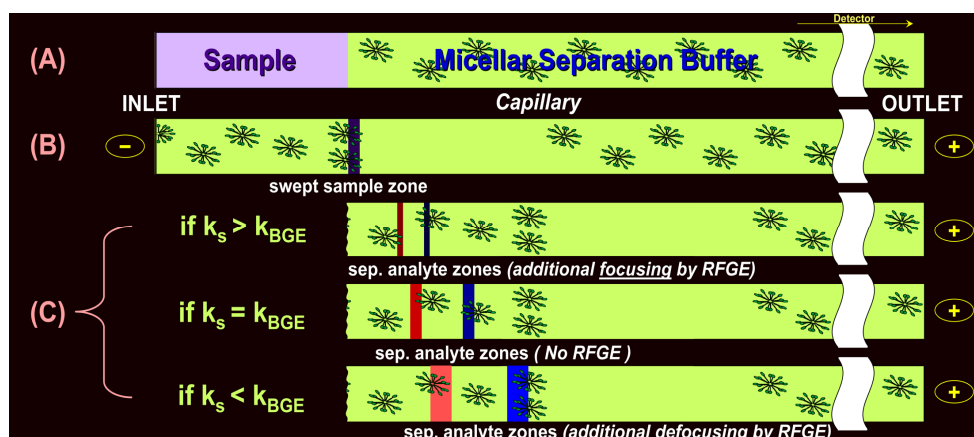


**Figure 1:** Schematic view of the RFGE: (A) Initial situation: sample injected in a capillary filled with BGE. (B) Application of voltage and start of sweeping process. (C) RFGE.

We propose the following final equation to account for the general case of sweeping in presence of RFGE:

$$l_{\text{grad}} = \frac{k_s k_{\text{BGE}} + k_{\text{BGE}}}{k_s k_{\text{BGE}} + k_s} \cdot \frac{1}{1 + k_s} l_{\text{inj}} = \frac{1}{f} \cdot \frac{1}{(1 + k_s)} l_{\text{inj}} \quad (1)$$

where  $l_{\text{grad}}$  is the final length of the sample zone after sweeping with RFGE,  $l_{\text{inj}}$  is the initial sample-plug length,  $k_{\text{BGE}}$  is the retention factor in the BGE,  $k_s$  is the retention factor obtained with a capillary filled with a solution identical to that of the sample matrix with surfactant in identical concentration as the “original” BGE and  $f$  is the additional focusing/defocusing factor due to RFGE.

The validity of this equation is confirmed under variation of the content or type of organic solvent (in the sample and/or the BGE), of the electric conductivity or pH (in the sample), and of the surfactant concentration (in the BGE). In the general case, the enrichment efficiency due to sweeping with RFGE is independent of the electric conductivity of the sample matrix. It is also shown that sweeping with RFGE can be favorably used in those cases where the solubility of the analyte in the sample solution is increased by variation of pH.

## **5.2.2. Author contribution**

All the experimental part of this publication was carried out by me. The draft of the manuscript was written by me and corrected by Prof. Ute Pyell. The final revision of the manuscript was conducted by me and Prof. Pyell before submission to the journal. Prof. Ute Pyell was responsible for the supervision of this work.



## Sweeping as a multistep enrichment process in micellar electrokinetic chromatography: The retention factor gradient effect



Mohamed El-Awady, Ute Pyell\*

University of Marburg, Department of Chemistry, Hans-Meerwein-Straße, D-35032 Marburg, Germany

### ARTICLE INFO

#### Article history:

Received 19 February 2013  
Received in revised form 18 April 2013  
Accepted 21 April 2013  
Available online 2 May 2013

#### Keywords:

Micellar electrokinetic chromatography  
Sweeping  
Assessment of enrichment factor  
Retention factor gradient effect

### ABSTRACT

The application of a new method developed for the assessment of sweeping efficiency in MEKC under homogeneous and inhomogeneous electric field conditions is extended to the general case, in which the distribution coefficient and the electric conductivity of the analyte in the sample zone and in the separation compartment are varied. As test analytes *p*-hydroxybenzoates (parabens), benzamide and some aromatic amines are studied under MEKC conditions with SDS as anionic surfactant. We show that in the general case – in contrast to the classical description – the obtainable enrichment factor is not only dependent on the retention factor of the analyte in the sample zone but also dependent on the retention factor in the background electrolyte (BGE). It is shown that in the general case sweeping is inherently a multistep focusing process. We describe an additional focusing/defocusing step (the retention factor gradient effect, RFGE) quantitatively by extending the classical equation employed for the description of the sweeping process with an additional focusing/defocusing factor. The validity of this equation is demonstrated experimentally (and theoretically) under variation of the organic solvent content (in the sample and/or the BGE), the type of organic solvent (in the sample and/or the BGE), the electric conductivity (in the sample), the pH (in the sample), and the concentration of surfactant (in the BGE). It is shown that very high enrichment factors can be obtained, if the pH in the sample zone makes possible to convert the analyte into a charged species that has a high distribution coefficient with respect to an oppositely charged micellar phase, while the pH in the BGE enables separation of the neutral species under moderate retention factor conditions.

© 2013 Elsevier B.V. All rights reserved.

### 1. Introduction

One disadvantage of capillary electromigration separation techniques is the low detection sensitivity. This disadvantage can be circumvented by on-line sample preconcentration techniques. Sweeping is one of the most important preconcentration techniques in MEKC. It is based on the accumulation of analyte molecules by the pseudostationary phase (PSP) that penetrates the sample zone being void of PSP [1].

In 1998 Quirino and Terabe [1] presented the concept of sweeping applied to neutral analytes and samples having the same electric conductivity as the BGE containing an anionic surfactant. Very soon, a more detailed discussion on sweeping under homogeneous and inhomogeneous electric field conditions was published by the same authors [2,3]. The applicability of sweeping was further extended to MEKC with cationic surfactant [4] and to sweeping combined with electrokinetic injection [5].

According to the concept, presented by Quirino and Terabe [1], the length of the sample zone after sweeping  $l_{\text{sweep}}$  depends only on the initial sample-plug length  $l_{\text{inj}}$  and on the retention factor in the sample zone  $k_S$  during sweeping. The enrichment factor ( $=l_{\text{inj}}/l_{\text{sweep}}$ ) is then directly proportional to  $k_S$ :

$$l_{\text{sweep}} = \frac{1}{1 + k_S} l_{\text{inj}} \quad (1)$$

There has been a debate on the impact of differences in the electric conductivity between the sample matrix and the BGE on the reachable enrichment factor (sweeping under inhomogeneous electric field conditions) [3,6–10]. In our previous publication on processes involved in sweeping under inhomogeneous electric field conditions [11], we were able to show experimentally and theoretically that the enrichment factor obtained by sweeping is independent of the electric conductivity of the sample matrix, provided that no micellar transient isotachopheresis takes place and that the distribution coefficient  $K_D$  of the analyte (regarding distribution between the PSP and the surrounding phase) in the sample matrix and in the BGE is identical.

There are, however, numerous cases in which sweeping takes place under conditions where  $K_D$  in the sample solution and in the

\* Corresponding author. Tel.: +49 6421 2822192; fax: +49 6421 2822124.  
E-mail address: [pyellu@staff.uni-marburg.de](mailto:pyellu@staff.uni-marburg.de) (U. Pyell).

BGE is not identical as in case of different organic solvent contents, different pH or different contents of a complex-forming agent. For example, Gilges [12] discovered that high focusing factors could be reached with samples being void of micelles and having a volume fraction of acetonitrile lower than that of the BGE. Shi and Palmer [13] observed for polymeric PSP very high enrichment factors (up to 10,000), if they inject a sample zone of low organic solvent content which is followed by a separation with a BGE containing a high volume fraction of organic modifier. Their first studies were done with neutral analytes in a sample matrix containing 25 mmol L<sup>-1</sup> phosphoric acid with 9% (v/v) acetone and a BGE containing 1.0% (w/v) poly(sodium 10-undecenyl sulfate) as PSP in 25 mmol L<sup>-1</sup> phosphoric acid with 13% (v/v) acetonitrile. A further increase of the enrichment factor was achieved by using a sample matrix containing 25 mmol L<sup>-1</sup> phosphoric acid with only 5% (v/v) methanol and a BGE containing 2.7% (w/v) poly(sodium 2-acrylamido-2-methyl-1-propane-sulfonate-co-stearyl acrylamide) as PSP in 42 mmol L<sup>-1</sup> phosphoric acid with 28% (v/v) methanol. Shi and Palmer [13] suggested the presence of an additional focusing mechanism (beside sweeping), which was not quantified.

Addition of an organic solvent to the separation buffer is a very important aspect in method optimization. Different authors investigated the effect of addition of an organic solvent on the separation and/or sensitivity in MEKC under sweeping conditions. Fang et al. [14] achieved an optimum separation and sensitivity for the analysis of three lysergic acid derivatives using a BGE consisting of 100 mmol L<sup>-1</sup> SDS, 3 mmol L<sup>-1</sup> Brij-30 and 50 mmol L<sup>-1</sup> H<sub>3</sub>PO<sub>4</sub> in a mixed acetonitrile–methanol–water solution (5:35:60, v/v) while the analytes were dissolved in the same solution but without SDS. Takeda et al. [15] used a micellar BGE containing 10% (v/v) methanol and 5 mmol L<sup>-1</sup> β-cyclodextrin for the development of a very sensitive method for the analysis of bisphenol A and three alkylphenols dissolved in a BGE being void of micelles. Similarly, Aranas et al. [16] achieved up to 305-fold sensitivity enhancement in the simultaneous analysis of several tricyclic antidepressants and β-blockers in wastewater by sweeping-MEKC using acetonitrile as an organic modifier and phosphoric acid as a sample solvent.

Beside the effect of addition of an organic solvent, in sweeping-MEKC also the effect of pH variation (difference in pH between sample solution and BGE) on the optimization of separation and sensitivity was investigated. For example, a combination of dynamic pH junction and sweeping with a sample having a pH different from the pH of the BGE and being void of the PSP was utilized by Britz-McKibbin et al. [17] for the analysis of flavin derivatives. A more than 4-fold enhancement in the band narrowing of solute zones was achieved by dynamic pH junction-sweeping compared to either sweeping or dynamic pH junction alone. Very soon, Britz-McKibbin et al. [18] extended their study to analyze trace amounts of flavins in different biological matrices. Yan et al. [19,20] intensively studied the relation between peak height and pH of the BGE for developing a sensitive method for the trace analysis of nateglinide in animal plasma and phenol pollutants in industrial wastewater, respectively. However, Yang et al. [21] showed that the presence of a pH gradient within the capillary might lead to the appearance of false peaks under sweeping conditions using a large injection volume of the sample and a high concentration of SDS.

In the present work, we extend our previous studies [11] to the general case, in which neither  $K_D$  nor the electric conductivity  $\kappa$  with regard to sample solution and BGE are kept constant. We show that in contrast to the classical description (see Eq. (1)), the enrichment factor is not only dependent on  $k_S$  but also dependent on the retention factor  $k_{BGE}$  in the BGE. This dependence can be understood by taking an effect into account, which had been completely neglected so far and is present in all cases when  $K_D$  differs between the sample zone and the BGE.

This new effect termed “retention factor gradient effect (RFGE)” can result in considerable additional focusing or defocusing of the sample zone after completion of the sweeping process. RFGE can be regarded to be similar to zone compression (or decompression) in gradient chromatography with stepwise gradient. RFGE is independent of the electric conductivity  $\kappa$  of the sample solution and the BGE. It is present under homogeneous and under inhomogeneous electric field conditions. It can be considered as an additional focusing (or defocusing) step beside the classical sweeping mechanism.

A mathematical description of this new effect is presented. Taking weakly acidic parabens, neutral benzamide, and weakly basic anilines (separated in SDS-containing buffer) as examples, the enrichment factors have been experimentally determined. The obtained values confirm the correctness of the derived equations. In accordance with our previous publication [11], determination of the enrichment factor is based on plotting the peak height against the injected sample volume. This method has been shown to be very precise and accurate. It eliminates those errors, which are due to varied migration times and hydrodynamic dispersion as a consequence of local EOF velocity differences [22–24]. In a further experimental study, we confirm that the obtainable enrichment factors for neutral analytes are independent of the electric conductivity of the sample matrix even in presence of RFGE. It will be shown that RFGE must be taken into account in all cases where  $K_D$  in the sample zone is not identical to that in the BGE for example, when an organic modifier is added to the sample solution whereas the BGE has a lower content of this modifier. It will be also shown that sweeping with RFGE can be favorably used in those cases where the solubility of the analyte in the sample solution is increased by variation of pH.

## 2. Theoretical considerations

### 2.1. Sweeping under homogeneous and inhomogeneous electric field conditions

In our previous publication [11], we described the sweeping process as a multistep enrichment process based on considerations made by Quirino and Terabe [1,3], Quirino et al. [6,25] and by Chien and Burgi [26]. This multistep enrichment process includes: (i) stacking or destacking of the micelles entering the sample zone at the boundary BGE/sample, (ii) sweeping of the analytes by the stacked or destacked micelles and (iii) destacking or stacking of the swept zone at the boundary sample/BGE. In this context, we have introduced the phase ratio shift factor  $\theta$  to quantitatively describe the retention factor  $k$  for an analyte in the sample zone assuming that  $K_D$  is constant in the two zones. This factor has been used in the derivation of equations that describe sweeping under homogeneous and inhomogeneous electric field conditions. In this special case, the final length of the focused sample zone  $l_{\text{focus}}$  after completion of the sweeping process can be calculated from the initial sample-plug length  $l_{\text{inj}}$  as follows:

$$l_{\text{focus}} = \frac{1}{\gamma \theta (1 + k_{\text{BGE}})} l_{\text{inj}} \quad (2)$$

where  $\gamma$  = field-strength enhancement factor [26] (=ratio of the electric field strengths in the sample zone and in the BGE ( $E_S/E_{\text{BGE}}$ )) or ratio of the electric conductivities of the BGE and the sample solution ( $\kappa_{\text{BGE}}/\kappa_S$ );  $\theta$  = phase ratio shift factor or quotient of phase ratios in the sample zone during sweeping and in the BGE ( $\varphi_S/\varphi_{\text{BGE}}$ ). In case of homogeneous electric field conditions, both  $\gamma$  and  $\theta$  equal 1 and Eq. (2) becomes equivalent to Eq. (1). We have also shown for inhomogeneous electric field conditions that, if  $K_D$  is identical in the sample zone and in the separation zone, the product  $\gamma \theta$  can be approximated with 1 [11].

However, if  $K_D$  differs for the sample zone and the separation zone (e.g., in case of different organic solvent contents, different contents of a complex-forming agent like cyclodextrin or borate, or different pH), additional effects must be taken into consideration and both Eqs. (1) and (2) are no longer valid.

### 2.2. Retention factor gradient effect

The retention factor gradient effect (RFGE) is an additional focusing/defocusing step complementing the sweeping process. It takes place in the BGE compartment next to the sample zone simultaneously together with the destacking or stacking of the micelles at the sample/BGE boundary. RFGE is related to micelle to solvent stacking (MSS) [27–30], whereas the difference lies in the fact that MSS works with a sample containing cationic or anionic micelles and a BGE being void of micelles.

For the sake of simplifying our considerations, we make the following assumptions: (i) the velocity of the EOF is negligible. (ii) The anionic surfactant SDS is used as PSP in the reversed direction mode. (iii) The analyte is neutral. (iv) The sample is injected hydrodynamically as a zone of the length  $l_{inj}$ . (v) The velocity of the micelles  $v_{mc}$  and the electric field strength are constant along the capillary.

A graphical illustration of the processes taking place under these conditions is presented in Fig. 1 (see also the animation file included in the Supplementary Data). Fig. 1A shows the initial situation where the sample solution (being void of micelles) is injected into a capillary filled with BGE. In Fig. 1B, the separation voltage is applied and sweeping takes place which results in a swept sample zone of the length  $l_{sweep}$ . After completion of this process, the analyte zone starts to enter the BGE compartment directly next to the sample zone (see Fig. 1C). If  $k_S = k_{BGE}$ , no additional focusing or defocusing takes place and the sample zone length  $l_{grad,1} = l_{sweep}$  (Fig. 1C1). If  $k_S > k_{BGE}$ , additional focusing due to RFGE takes place when the analyte zone enters the BGE compartment of lower  $k$  because at the boundary sample/BGE the observed velocity of the analyte zone is abruptly decreased. This sudden change in velocity means further focusing ( $l_{grad,2} < l_{sweep}$ , Fig. 1C2). However, if  $k_S < k_{BGE}$ , RFGE causes additional defocusing because of the abrupt increase in the observed velocity of the analyte zone which enters the BGE compartment. In this case,  $l_{grad,3} > l_{sweep}$  (Fig. 1C3). According to this scheme  $l_{grad,2} < l_{sweep} < l_{grad,3}$ .

The observed equilibrium velocities of the analyte in the sample zone  $v_{a,S}$  and in the BGE  $v_{a,BGE}$  can be calculated as follows [31]:

$$v_{a,S} = \frac{k_S}{k_S + 1} v_{mc} \quad (3)$$

$$v_{a,BGE} = \frac{k_{BGE}}{k_{BGE} + 1} v_{mc} \quad (4)$$

It should be noted here that we regard the retention factor in the sample zone  $k_S$  during sweeping in this discussion and in the following text to be the retention factor that would be obtained for the analyte in a buffer, which contains the PSP in a concentration identical to that of the “original” BGE however in a matrix identical to that of the “original” sample solution. According to Fig. 1C there are three possible cases: (i) if  $k_S = k_{BGE}$  (Fig. 1C1), the sweeping process is not accompanied by RFGE because there is no change in the observed velocity of the analyte zone when passing the boundary between the sample zone and the BGE compartment. (ii) If  $k_S > k_{BGE}$  (Fig. 1C2, e.g., in case of pure aqueous sample solvent and a BGE with  $\varphi(\text{methanol}) = 10\%$ ), there is a decrease in the observed velocity of the analyte zone entering the BGE compartment:

$$\frac{l_{grad}}{l_{sweep}} = \frac{v_{a,BGE}}{v_{a,S}} \quad (5)$$

By substitution from Eq. (3) and (4):

$$l_{grad} = \left( \frac{k_{BGE}}{k_{BGE} + 1} \right) \left( \frac{k_S + 1}{k_S} \right) l_{sweep} = \frac{k_S k_{BGE} + k_{BGE}}{k_S k_{BGE} + k_S} l_{sweep} \quad (6)$$

As in this case  $k_{BGE} < k_S$ , it follows  $l_{grad} < l_{sweep}$  corresponding to an improvement in the focusing efficiency. (iii) If  $k_S < k_{BGE}$  (Fig. 1C3, e.g., in case of pure aqueous BGE and a sample solvent with  $\varphi(\text{methanol}) = 10\%$ ), there is an increase in the observed velocity of the analyte zone entering the BGE compartment. In this case, the final length of the sample zone  $l_{grad}$  can be calculated as in the previous case. As in this case  $k_{BGE} > k_S$ , it follows  $l_{grad} > l_{sweep}$  corresponding to a decrease in the focusing efficiency.

We also define what we call “the additional focusing/defocusing factor  $f$ ” due to RFGE:

$$f = \frac{l_{sweep}}{l_{grad}} = \frac{k_S k_{BGE} + k_S}{k_S k_{BGE} + k_{BGE}} \quad (7)$$

According to this equation,  $f > 1$  when  $k_S > k_{BGE}$  indicating additional focusing while  $f < 1$  when  $k_S < k_{BGE}$  indicating additional defocusing. In MEKC, the value of  $k_{BGE}$  is recommended to be in the range between 0.5 and 10 [32,33] while  $k_S$  has no limitation. The maximum focusing factor can be achieved if  $k_S$  is very high and  $k_{BGE}$  is very small. If we assume that  $k_S = 1000$  and  $k_{BGE} = 0.5$  (for example), it follows that  $f$  is approximately equal to 3. On the other side, the maximum defocusing factor is obtained with very small  $k_S$  and very high  $k_{BGE}$  and if we assume that  $k_S = 0.1$  and  $k_{BGE} = 10$  (for example) then  $f$  is approximately equal to 0.1. In other words, we can say that the additional factor  $f$  is expected to be in the range of 1–3 (in case of focusing) and in the range of 0.1–1 (in case of defocusing). The above ranges are valid if the enriched analytes are to be separated by MEKC after the enrichment step and before detection. However, there are also possible applications in which the main purpose of the enrichment technique might be to pre-concentrate the sample as in case of MS analysis or in case of following the enrichment step by another separation approach. In this situation, the upper limit of  $f$  (in case of focusing,  $k_S = 1000$ ) can reach 11 if the value of  $k_{BGE}$  is reduced to an extremely small value (e.g., 0.1). By multiplying the factor  $f$  with the sweeping efficiency calculated via Eq. (1), the final enrichment factor due to sweeping with RFGE can be obtained.

Eqs. (1) and (6) can be combined to the following final equation which accounts for the general case of sweeping of neutral analytes:

$$l_{grad} = \frac{k_S k_{BGE} + k_{BGE}}{k_S k_{BGE} + k_S} \cdot \frac{1}{1 + k_S} l_{inj} = \frac{1}{f} \cdot \frac{1}{(1 + k_S)} l_{inj} \quad (8)$$

Again we emphasize that (in contrast to discussions in the literature) we regard  $k_S$  in this discussion and in the following text to be the retention factor that would be obtained for the analyte in a buffer containing an identical PSP concentration as in the BGE but in a matrix corresponding to the sample solution. Eq. (8) corresponds to that equation, which has been derived by Quirino and Terabe [1] in their pioneering paper expanded by the additional focusing/defocusing factor  $f$ . This additional factor takes into account that in case of sweeping under generalized conditions, the final focusing efficiency is not only dependent on the retention factor of the analyte in the sample zone but also the retention factor of the analyte in the BGE. To the best of our knowledge, this effect has not yet been quantitatively described in the literature.

## 3. Experimental

### 3.1. Apparatus

All measurements were done with a Beckman (Fullerton, CA, USA) P/ACE™ MDQ CE-system equipped with a UV-detector.

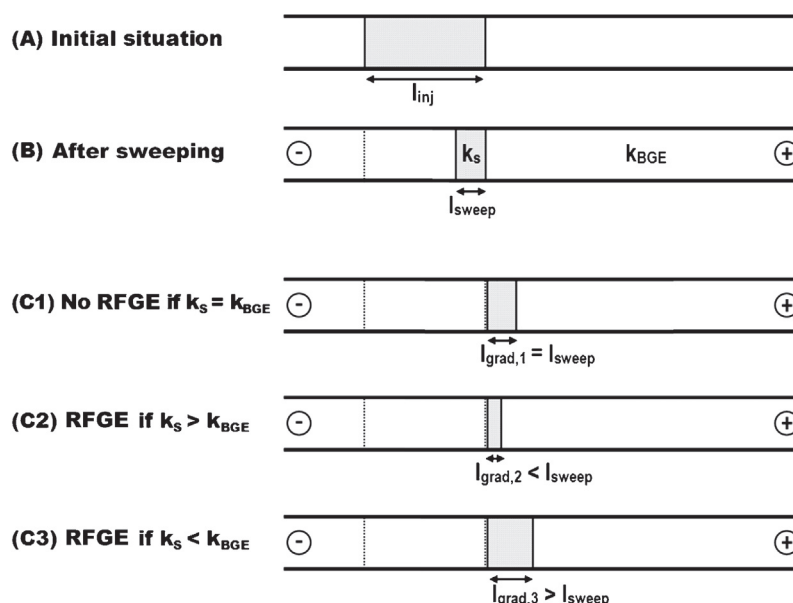


**Fig. 1.** Schematic view of the generalized sweeping processes under homogeneous electric field conditions: (A) initial situation: sample injected in a capillary filled with BGE, sample-zone length =  $l_{inj}$ . (B) Application of voltage and occurrence of sweeping process, sample-zone length =  $l_{sweep}$ . (C1) No RFGE when  $k_s = k_{BGE}$ , sample-zone length remains  $l_{sweep}$ . (C2) Additional focusing by RFGE when  $k_s > k_{BGE}$ , sample-zone length =  $l_{grad,2}$ . (C3) Additional defocusing by RFGE when  $k_s < k_{BGE}$ , sample-zone length =  $l_{grad,3}$ .

Temperature of the capillary was kept at 25 °C. The sample tray was kept at 25 °C or 15 °C (for samples containing organic solvents). Determination of enrichment factors for parabens, benzamide and anilines was carried out at a voltage of 20, 15, or 22 kV, respectively at a detection wavelength of 254 nm. Data were recorded with Beckman 32 Karat software (v. 5.0). Fused-silica capillaries (50- $\mu$ m I.D., 362- $\mu$ m O.D.) were from Polymicro Technologies (Phoenix, AZ, USA). New capillaries were conditioned by flushing them first with 0.2 mol L<sup>-1</sup> NaOH solution for 60 min, then with water for 30 min and then with BGE for 30 min. A rinsing step with BGE for 5 min was performed between runs. HI 8817 pH meter (Hanna Instruments, Kehl, Germany) was used for pH measurements, and LF 191 conductometer (WTW, Weinheim, Germany) was used to measure

the electric conductivity. Origin 8.5 software (OriginLab corporation, Northhampton, USA) (using BoxLucas1 function) or GraphPad Prism 4.03 software (GraphPad Software, Inc., San Diego, USA) (using Zero-to-Top function) were used for performing non-linear regression needed for the assessment of enrichment factors.

### 3.2. Chemicals and background electrolytes

Ethylparaben, quinine hydrochloride, SDS and disodium hydrogen phosphate were from Fluka, Buchs, Switzerland. Propylparaben, aniline, 4-ethylaniline, 4-butylaniline, acetophenone, propiophenone, butyrophenone, valerophenone and hexanophenone were from Sigma, St. Louis, USA. Benzamide was from

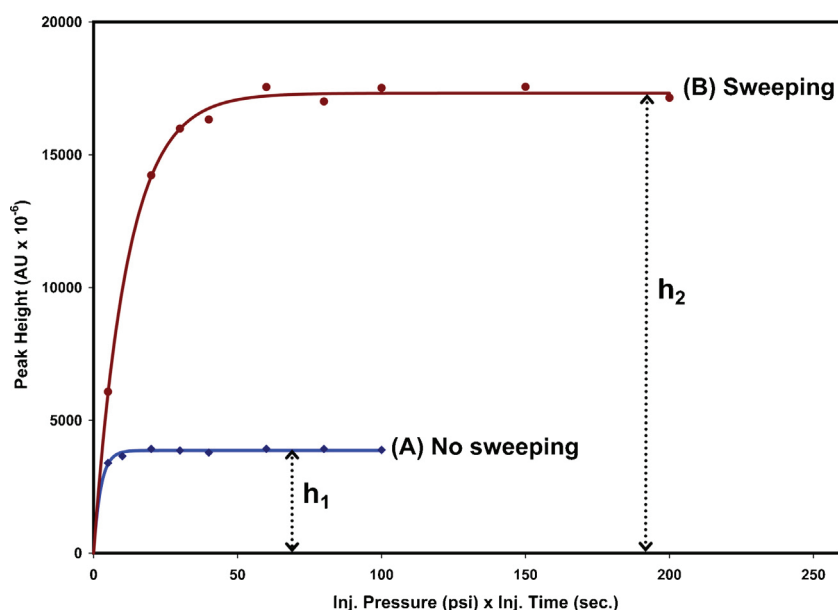


**Fig. 2.** Peak height plotted against injected volume for EP under (A) conventional conditions (analyte dissolved in BGE), (B) sweeping conditions (analyte dissolved in BGE without surfactant). BGE: 10% methanolic phosphate buffer (20 mmol L<sup>-1</sup>, pH 7.00) containing 50 mmol L<sup>-1</sup> SDS; sample solvent under sweeping conditions: 10% methanolic phosphate buffer (20 mmol L<sup>-1</sup>, pH 7.00); injection: hydrodynamic; capillary: fused-silica capillaries (50- $\mu$ m I.D., 362- $\mu$ m O.D.) with a total length of 60.9 cm and a length to the detector of 50.7 cm; temperature of the capillary: 25 °C and of the sample tray: 15 °C; voltage: +20 kV; detection wavelength: 254 nm.

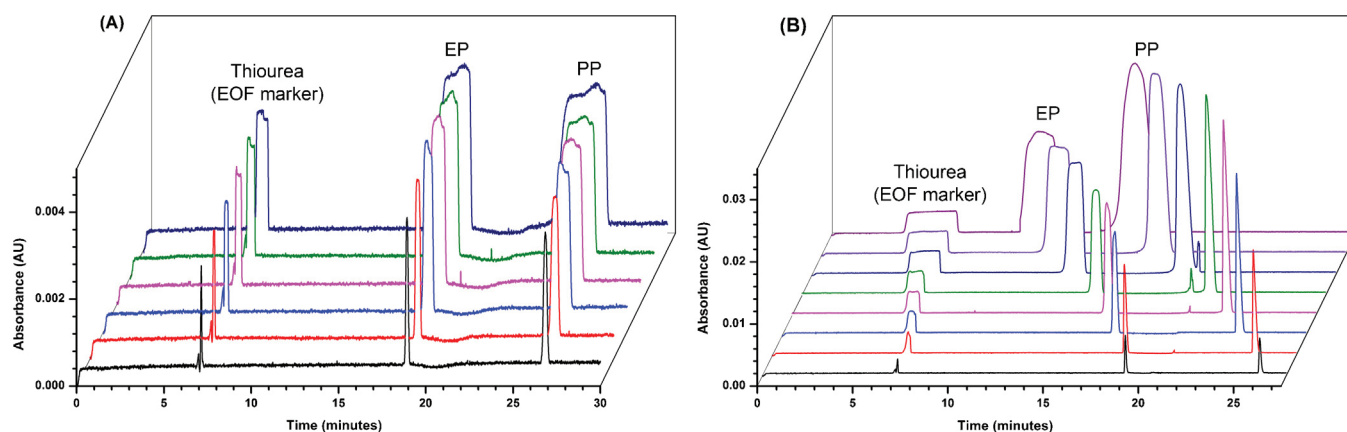


**Fig. 3.** Electropherograms for EP and PP obtained with varied injected sample volume under (A) conventional conditions, (B) sweeping conditions. BGE: 10% methanolic phosphate buffer (20 mmol L<sup>-1</sup>, pH 7) containing 50 mmol L<sup>-1</sup> SDS; sample solvent under sweeping conditions: 10% methanolic phosphate buffer (20 mmol L<sup>-1</sup>, pH 7); injection: hydrodynamic; capillary: fused silica-capillaries (50 μm I.D., 362 μm O.D.) with a total length of 60.9 cm and a length to the detector of 50.7 cm; temperatures of the capillary: 25 °C and of the sample tray: 15 °C; voltage: +20 kV; detection wavelength: 254 nm.

Acros Organics, Geel, Belgium. Boric acid, disodium tetraborate decahydrate and sodium dihydrogen phosphate were from Merck, Darmstadt, Germany. Thiourea was from Riedel-de Haën, Seelze, Germany. Methanol, ethanol, 1-propanol, 1-butanol and 1-propanol of HPLC grade were from VWR-BDH-Prolabo, Leuven, Belgium. All stock solutions of the analytes were prepared in water. The analyte concentrations in the final sample solution were 20, 40 and 50 mg L<sup>-1</sup> for parabens, benzamide and anilines, respectively.

Stock solutions of phosphate and borate buffers were prepared and further diluted for the preparation of background electrolytes. Stock phosphate buffer (40 mmol L<sup>-1</sup>, pH 7.00) was prepared by dissolving 2.760 g sodium dihydrogen phosphate and 3.560 g disodium hydrogen phosphate in 500 mL of water, adjusting the pH by sodium hydroxide or phosphoric acid if necessary and diluting to 1000 mL with water. Stock boric acid buffer (20 mmol L<sup>-1</sup>, pH 9.00) was prepared by dissolving 1.236 g boric acid in 500 mL of water, adjusting the pH with 1 mol L<sup>-1</sup> sodium hydroxide (about 10 mL) and then diluting to 1000 mL with water. Stock disodium tetraborate buffer (20 mmol L<sup>-1</sup>, pH 9.37) was prepared by dissolving 7.627 g disodium tetraborate decahydrate in 500 mL of water and diluting to 1000 mL with water.

The BGEs were 20 mmol L<sup>-1</sup> phosphate buffer, pH 7.00 containing 25 or 50 mmol L<sup>-1</sup> SDS for parabens, 10 mmol L<sup>-1</sup> borate buffer, pH 9.00 containing 75 or 100 mmol L<sup>-1</sup> SDS for benzamide and 10 mmol L<sup>-1</sup> borate buffer, pH 9.37 containing 50 mmol L<sup>-1</sup> SDS for anilines.

## 4. Results and discussion

### 4.1. Assessment of the enrichment factor

In the present work we extend the applicability of the method developed in our previous publication [11] for measuring the sweeping efficiency in the special case in absence of RFGE to measuring the overall enrichment factor in the general case in presence of RFGE. The principle of this method is illustrated in Fig. 2. It depends on measuring the ratio of peak heights in the volume overload region obtained under sweeping and non-sweeping conditions via recording the peak height vs. (injection pressure × injection time) plot. Non-linear regression is performed to achieve the best curve fitting for the function  $Y = a(1 - e^{-bX})$  where “a” and “b” are the fitted parameters. The parameter “a” represents the limiting peak height, which is used for further calculations:

$$\text{Enrichment factor} = a_2/a_1 = h_2/h_1 \quad (9)$$

where  $a_2$  and  $a_1$  are the fitted parameters, which correspond to  $h_2$  (limiting peak height under sweeping conditions) and  $h_1$  (limiting peak height under non-sweeping conditions), respectively. The principle is also demonstrated by selected electropherograms for EP and PP obtained with varied injection volumes under sweeping and non-sweeping conditions (Fig. 3). In case of highly hydrophobic analytes, it is not possible to reach the volume overload (plateau) region under sweeping conditions due to the limited capillary

**Table 1**

Application of the proposed method for the assessment of the enrichment factor in presence of organic modifier using different SDS concentrations.

Analyte	Sample matrix <sup>a</sup>	BGE <sup>a</sup>	Retention factor <sup>b</sup> ( $k_{BGE} = k_S$ )	Enrichment factor	
				Experimentally measured <sup>c</sup>	Theoretically predicted
EP	10% Methanolic buffer	10% Methanolic buffer/25 mmol L <sup>-1</sup> SDS	1.25 ± 0.01	2.54 ± 0.02	2.25 ± 0.01
	10% Methanolic buffer	10% Methanolic buffer/50 mmol L <sup>-1</sup> SDS	2.58 ± 0.03	4.47 ± 0.06	3.58 ± 0.03
	10% Ethanolic buffer	10% Ethanolic buffer/25 mmol L <sup>-1</sup> SDS	1.12 ± 0.01	2.42 ± 0.03	2.12 ± 0.01
	10% Ethanolic buffer	10% Ethanolic buffer/50 mmol L <sup>-1</sup> SDS	2.41 ± 0.02	4.00 ± 0.04	3.41 ± 0.02
PP	10% Methanolic buffer	10% Methanolic buffer/25 mmol L <sup>-1</sup> SDS	2.80 ± 0.03	5.28 ± 0.07	3.80 ± 0.03
	10% Methanolic buffer	10% Methanolic buffer/50 mmol L <sup>-1</sup> SDS	5.66 ± 0.13	10.25 ± 0.18	6.66 ± 0.13
	10% Ethanolic buffer	10% Ethanolic buffer/25 mmol L <sup>-1</sup> SDS	2.51 ± 0.04	4.65 ± 0.06	3.51 ± 0.04
	10% Ethanolic buffer	10% Ethanolic buffer/50 mmol L <sup>-1</sup> SDS	5.42 ± 0.07	9.34 ± 0.05	6.42 ± 0.07
BNZ	10% Methanolic buffer	10% Methanolic buffer/75 mmol L <sup>-1</sup> SDS	0.55 ± 0.00	1.84 ± 0.02	1.55 ± 0.00
	10% Methanolic buffer	10% Methanolic buffer/100 mmol L <sup>-1</sup> SDS	0.64 ± 0.01	2.04 ± 0.03	1.64 ± 0.01

<sup>a</sup> The buffers used were 20 mmol L<sup>-1</sup> phosphate buffer (pH 7.00) for EP and PP and 10 mmol L<sup>-1</sup> borate buffer (pH 9.00) for BNZ.

<sup>b</sup> Each value is the mean of at least three repetitions.

<sup>c</sup> Standard deviation is calculated from the corresponding standard errors estimated by non-linear regression applying the rules for error propagation [36].

volume. In this case, the highest possible peak height corresponding to the maximum allowed injection volume is taken as  $h_2$  (see Eq. (9)). Moreover, a simplified faster but slightly less precise procedure of the above method was also developed, which is based on measuring the peak height for only two or three pre-selected injection volumes that are known to be in the volume overload region (confirmed by the recorded broad and nearly rectangular peak shape) [11].

Following analytes were selected: ethylparaben (EP) and propylparaben (PP) as examples of weakly acidic analytes, benzamide (BNZ) as an example of a neutral analyte and aniline, 4-ethylaniline and 4-butylaniline as examples of weakly basic analytes. These analytes have moderate retention factors and adequate water solubility. In all cases, the analyte is dissolved in a solution without surfactant. In a first measurement series, both the sample and the BGE contain methanol or ethanol in the same concentration (10%, v/v) to avoid the presence of RFGE. As an example, the regression curves recorded for EP, in presence of 10% (v/v) methanol in the sample matrix and in the BGE, are shown in Fig. 2 (additional regression curves are included in the Supplementary Data). Table 1 summarizes the results obtained for the studied analytes using different SDS concentrations and different buffer types. Associated standard deviations were calculated from the corresponding standard errors estimated by non-linear regression (confidence range = standard error  $\times t(P, n - 1)$ ).

For confirming the accuracy of the measured enrichment factors, the experimental values are compared with those, which are calculated from Eq. (1) using experimentally measured retention factors [here: the enrichment factor =  $1 + k_S = 1 + k_{BGE}$ ] (details about the experimental measurement of retention factors are discussed in the Supplementary Data). As shown in Table 1, the experimentally measured enrichment factors are in good agreement (with regard to unavoidable measuring errors) with the predicted values despite the difficulty to measure the retention factor in the presence of an organic solvent. The correlation coefficient  $r$  for the data shown in Table 1 was found to be 0.9944 indicating good correlation between the experimentally measured and the theoretically calculated enrichment factors. Experimental values determined via the developed method have the tendency to be slightly higher than those calculated on the basis of Eq. (1). Small differences between measured and predicted values were also observed by Quirino and Terabe [2].

#### 4.2. Retention factor gradient effect

Regarding Eq. (8), the enrichment factor is not only dependent on  $k_S$  but also on  $k_{BGE}$ . First, methanol or ethanol was added at a volume fraction of 10% either to the sample solution or to the BGE or to both. According to the presence or absence of organic solvent in the sample matrix and/or in the BGE, we have four different experimental cases. For each case the enrichment factor was experimentally measured according to the method described previously [11] using the plateau curve procedure. Fig. 4 shows the electropherogram for EP recorded with fixed injection volume under the four different conditions. The highest peak is obtained with aqueous sample and 10% methanol in the BGE while the lowest peak and most distorted peak shape was obtained with 10% methanol in the sample and aqueous BGE. The results obtained for EP, PP and BNZ showing the effect of presence of methanol or ethanol on the enrichment factor are given in Tables 2 and 3, respectively (refer to Figs. S-2–S-37 at the Supplementary Data for the corresponding regression curves). The results clearly corroborate the presence of RFGE acting as an additional focusing effect when the retention factor of analyte in the sample solution is higher than in the BGE and vice versa. The obtained enrichment factors are not independent of the retention factor in the BGE.

**Table 2**  
Effect of the presence of methanol in the sample and/or the BGE on the enrichment factor for ethylparaben, propylparaben and benzamide.

Condition	Sample solvent	Aqueous phosphate/borate <sup>a</sup> buffer		10% Methanolic phosphate/borate <sup>a</sup> buffer + SDS		10% Methanolic phosphate/borate <sup>a</sup> buffer		10% Methanolic phosphate/borate <sup>a</sup> buffer + SDS	
		Aqueous phosphate/borate <sup>a</sup> buffer	Aqueous phosphate/borate <sup>a</sup> buffer + SDS	10% Methanolic phosphate/borate <sup>a</sup> buffer + SDS	10% Methanolic phosphate/borate <sup>a</sup> buffer + SDS	10% Methanolic phosphate/borate <sup>a</sup> buffer	10% Methanolic phosphate/borate <sup>a</sup> buffer + SDS	10% Methanolic phosphate/borate <sup>a</sup> buffer	10% Methanolic phosphate/borate <sup>a</sup> buffer + SDS
Enrichment factor <sup>c</sup>	For EP (using 25 mmol L <sup>-1</sup> SDS)	5.02 ± 0.04	4.16 ± 0.03 <sup>b</sup>	2.54 ± 0.02	2.16 ± 0.03	2.54 ± 0.02	2.16 ± 0.03	2.54 ± 0.02	2.16 ± 0.03
	For EP (using 50 mmol L <sup>-1</sup> SDS)	7.86 ± 0.06	7.08 ± 0.19 <sup>b</sup>	4.47 ± 0.06	3.99 ± 0.08	4.47 ± 0.06	3.99 ± 0.08	4.47 ± 0.06	3.99 ± 0.08
	For PP (using 25 mmol L <sup>-1</sup> SDS)	12.24 ± 0.24	10.11 ± 0.02 <sup>b</sup>	5.28 ± 0.07	4.69 ± 0.05	5.28 ± 0.07	4.69 ± 0.05	5.28 ± 0.07	4.69 ± 0.05
	For PP (using 50 mmol L <sup>-1</sup> SDS)	17.77 ± 0.31	15.08 ± 0.25 <sup>b</sup>	10.25 ± 0.18	9.98 ± 0.25	10.25 ± 0.18	9.98 ± 0.25	10.25 ± 0.18	9.98 ± 0.25
	For BNZ (using 75 mmol L <sup>-1</sup> SDS)	2.66 ± 0.02	2.05 ± 0.01 <sup>b</sup>	1.84 ± 0.02	1.36 ± 0.01	1.84 ± 0.02	1.36 ± 0.01	1.84 ± 0.02	1.36 ± 0.01
	For BNZ (using 100 mmol L <sup>-1</sup> SDS)	2.93 ± 0.03	2.40 ± 0.05 <sup>b</sup>	2.04 ± 0.03	1.58 ± 0.02	2.04 ± 0.03	1.58 ± 0.02	2.04 ± 0.03	1.58 ± 0.02

<sup>a</sup> The used buffers were 20 mmol L<sup>-1</sup> phosphate buffer (pH 7.00) for EP and PP and 10 mmol L<sup>-1</sup> borate buffer (pH 9.00) for BNZ.

<sup>b</sup> Data taken from our previous publication [11].

<sup>c</sup> Standard deviation is calculated from the corresponding standard errors estimated by non-linear regression applying the rules for error propagation [36].

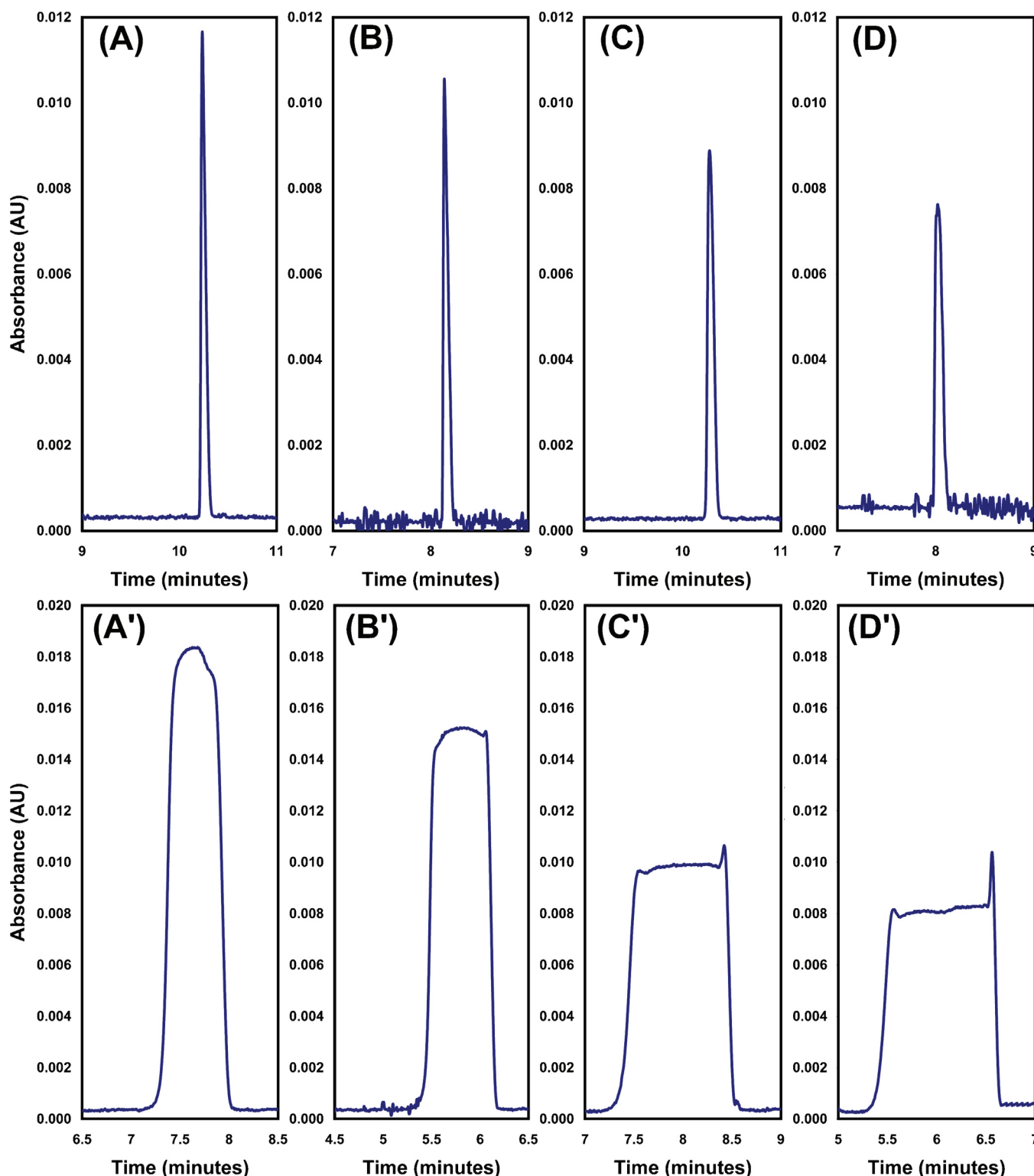


**Fig. 4.** Electropherograms of EP without and with organic solvent in the sample matrix and/or in the BGE: (A,A') sample solvent: aqueous phosphate buffer, BGE: 10% methanolic phosphate buffer +25 mmol L<sup>-1</sup> SDS. (B,B') Sample solvent: aqueous phosphate buffer, BGE: aqueous phosphate buffer +25 mmol L<sup>-1</sup> SDS. (C,C') Sample solvent: 10% methanolic phosphate buffer, BGE: 10% methanolic phosphate buffer +25 mmol L<sup>-1</sup> SDS. (D,D') Sample solvent: 10% methanolic phosphate buffer, BGE: aqueous phosphate buffer +25 mmol L<sup>-1</sup> SDS. (A,B,C,D) injection pressure 1 psi for 10 s, (A',B',C',D') injection pressure 4 psi for 40 s. In all cases, phosphate buffer is 20 mmol L<sup>-1</sup>, pH 7.00. For other experimental parameters, refer to Fig. 2.

In addition, presence of organic solvent in the BGE caused widening of the migration window because the organic solvent decreases the EOF velocity due to changes in the viscosity and the dielectric constant and modifies the velocity of the PSP via modification of the micellar structure [34].

In a further study, the enrichment factor for benzamide was experimentally determined at fixed composition of the sample solution under variation of the concentration of methanol in the BGE (0, 5, 10, 15 and 20%, v/v). The lowest enrichment factor was observed with aqueous BGE, whereas by increasing the content

**Table 3**  
Effect of the presence of ethanol in the sample and/or the BGE on the enrichment factor for ethyl- and propylparaben.

Condition	Sample solvent	Aqueous phosphate buffer	Aqueous phosphate buffer	10% Ethanolic phosphate buffer	10% Ethanolic phosphate buffer
	BGE	10% Ethanolic phosphate buffer + SDS	Aqueous phosphate buffer + SDS	10% Ethanolic phosphate buffer + SDS	Aqueous phosphate buffer + SDS
Enrichment factor <sup>b</sup>	For EP (using 25 mmol L <sup>-1</sup> SDS)	5.26 ± 0.03	4.16 ± 0.03 <sup>a</sup>	2.42 ± 0.03	1.88 ± 0.02
	For EP (using 50 mmol L <sup>-1</sup> SDS)	8.03 ± 0.12	7.08 ± 0.19 <sup>a</sup>	4.00 ± 0.04	3.35 ± 0.06
	For PP (using 25 mmol L <sup>-1</sup> SDS)	12.27 ± 0.15	10.11 ± 0.02 <sup>a</sup>	4.65 ± 0.06	3.76 ± 0.04
	For PP (using 50 mmol L <sup>-1</sup> SDS)	17.91 ± 0.33	15.08 ± 0.25 <sup>a</sup>	9.34 ± 0.05	7.65 ± 0.15

<sup>a</sup> Data taken from our previous publication [11].

<sup>b</sup> Standard deviation is calculated from the corresponding standard errors estimated by non-linear regression applying the rules for error propagation [36].

of methanol in the BGE, the enrichment factor is improved (see Fig. 5). In accordance with Eq. (8) the highest enrichment factor was achieved with the highest content of methanol in the BGE.

Confirmation of the validity of Eq. (8) requires both knowledge of the retention factor in the BGE and knowledge of the retention factor in a buffer containing the surfactant in a concentration identical to that of the BGE while the matrix corresponds to that of the sample solution. For measuring the retention factor, different approaches have been published in the literature [35]. A detailed description of the employed procedures in this study can be found in the Supplementary Data.

Knowledge of retention factors allows to compare the theoretically derived and the experimentally measured additional focusing/defocusing factor due to RFGE ( $f = l_{\text{sweep}}/l_{\text{grad}}$ ). Whereas the theoretical value  $f_{\text{theo}}$  is calculated from Eq. (7), the experimental value  $f_{\text{exp}}$  was determined from the ratio of two enrichment factors:

$$f_{\text{exp}} = \frac{\text{Enrichment factor (with RFGE)}}{\text{Enrichment factor (without RFGE)}} \quad (10)$$

In Tables 4–6,  $f_{\text{theo}}$  and  $f_{\text{exp}}$  (obtained in different independent measurement series) are compared for three different analytes; EP, PP and BNZ. The enrichment factor with RFGE refers to the value measured for the case in which the BGE and the sample solution have different organic solvent contents, whereas the enrichment

factor without RFGE refers to the value measured for a BGE with a content of organic solvent identical to that of the sample matrix. The parameter  $k_s$  is determined as the retention factor obtained with a capillary filled with a solution identical to that of the sample matrix with surfactant in identical concentration as the BGE. Experimental factors  $f_{\text{exp}}$  show excellent agreement with theoretically predicted factors  $f_{\text{theo}}$ . We applied a paired  $t$ -test [36] on all values of  $f_{\text{theo}}$  and  $f_{\text{exp}}$  listed in Tables 4–6. The calculated  $t$  was found to be 1.13 at  $df = 22$ , which is smaller than the tabulated  $t$  value (2.07 at  $df = 22$  and  $P = 0.05$ ). On the chosen significance level, there is no significant difference between  $f_{\text{theo}}$  and  $f_{\text{exp}}$ .

In our previous publication [11] we have demonstrated that the sweeping efficiency for neutral analytes is independent of the electric conductivity  $\kappa$  of the sample matrix, if  $K_D$  in the sample is identical to that in the BGE. Under the conditions of RFGE, however,  $K_D$  in the sample is no longer identical to that in the BGE. According to our model, sweeping (including stacking/destacking of the micelles entering the sample zone and destacking/stacking of the micelles leaving the sample zone) and RFGE are two independent processes. Consequently, we can expect that also sweeping with RFGE is independent of the electric conductivity of the sample matrix. To confirm the predicted independence of the enrichment factor on the field strength enhancement factor  $\gamma$  in presence of RFGE, the enrichment factor for BNZ was determined with varied electric conductivity of the sample solution at constant

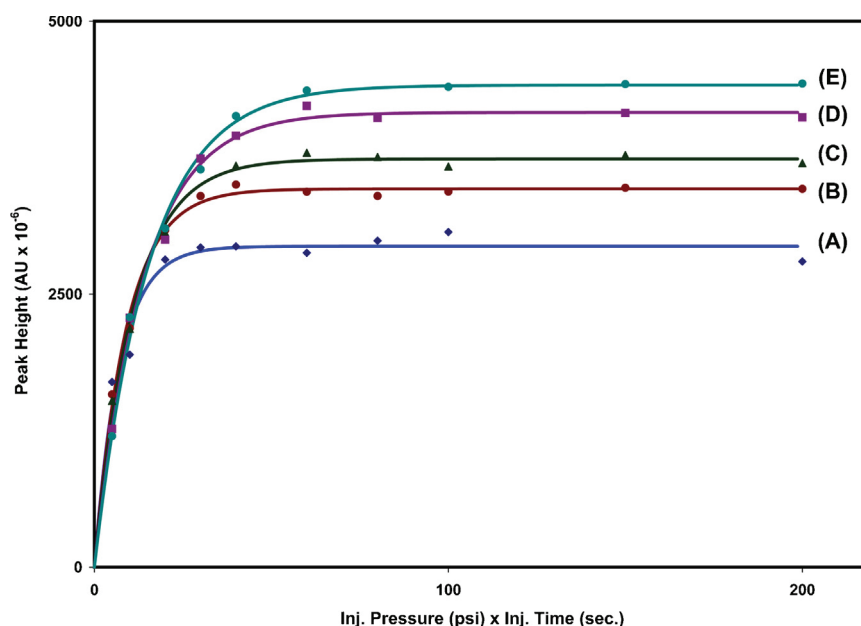


**Fig. 5.** Assessment of the enrichment factor for benzamide using different concentrations (A) 0%, (B) 5%, (C) 10%, (D) 15%, (E) 20% (v/v) of methanol in the BGE (10 mmol L<sup>-1</sup> borate buffer, pH 9.00 containing 100 mmol L<sup>-1</sup> SDS). Sample solvent: aqueous borate buffer (10 mmol L<sup>-1</sup>, pH 9.00); capillary: fused-silica capillaries (50- $\mu$ m I.D., 362- $\mu$ m O.D.) with a total length of 60.9 cm and a length to the detector of 50.7 cm; temperature of the capillary: 25 °C and of the sample tray: 15 °C; voltage: +15 kV; detection wavelength: 254 nm.

**Table 4**  
Comparison of theoretically predicted and experimentally measured additional focusing/defocusing factor due to RFGE<sup>a</sup> for ethylparaben.

SDS concentration (mmol L <sup>-1</sup> )	Sample matrix	$k_s$	Without RFGE		With RFGE		Additional focusing/defocusing factor			
			BGE	$k_{BGE} (=k_s)$	Enrichment factor <sup>b</sup>	BGE	$k_{BGE}$	Enrichment factor <sup>b</sup>	$f_{theo}$ (Eq. (7))	$f_{exp}$ (Eq. (10))
25 SDS	Aqueous	2.46	Aqueous	2.46	4.16 ± 0.03 <sup>c</sup>	10% Methanolic	1.25	5.02 ± 0.04	1.28	1.21
25 SDS	10% Methanolic	1.25	10% Methanolic	1.25	2.54 ± 0.02	Aqueous	2.46	2.16 ± 0.03	0.78	0.85
50 SDS	Aqueous	5.15	Aqueous	5.15	7.08 ± 0.19 <sup>c</sup>	10% Methanolic	2.58	7.86 ± 0.06	1.16	1.11
50 SDS	10% Methanolic	2.58	10% Methanolic	2.58	4.47 ± 0.06	Aqueous	5.15	3.99 ± 0.08	0.86	0.89
25 SDS	Aqueous	2.46	Aqueous	2.46	4.16 ± 0.03 <sup>c</sup>	10% Ethanolic	1.12	5.26 ± 0.03	1.34	1.26
25 SDS	10% Ethanolic	1.12	10% Ethanolic	1.12	2.42 ± 0.03	Aqueous	2.46	1.88 ± 0.02	0.74	0.78
50 SDS	Aqueous	5.15	Aqueous	5.15	7.08 ± 0.19 <sup>c</sup>	10% Ethanolic	2.41	8.03 ± 0.12	1.18	1.13
50 SDS	10% Ethanolic	2.41	10% Ethanolic	2.41	4.00 ± 0.04	Aqueous	5.15	3.35 ± 0.06	0.84	0.84

<sup>a</sup> RFGE = Retention factor gradient effect.

<sup>b</sup> Standard deviation is calculated from the corresponding standard errors estimated by non-linear regression applying the rules for error propagation [36].

<sup>c</sup> Data taken from our previous publication [11].

**Table 5**  
Comparison of theoretically predicted and experimentally measured additional focusing/defocusing factor due to RFGE<sup>a</sup> for propylparaben.

SDS concentration (mmol L <sup>-1</sup> )	Sample matrix	$k_s$	Without RFGE		With RFGE		Additional focusing/defocusing factor			
			BGE	$k_{BGE} (=k_s)$	Enrichment factor <sup>b</sup>	BGE	$k_{BGE}$	Enrichment factor <sup>b</sup>	$f_{theo}$ (Eq. (7))	$f_{exp}$ (Eq. (10))
25 SDS	Aqueous	6.53	Aqueous	6.53	10.11 ± 0.02 <sup>c</sup>	10% Methanolic	2.80	12.24 ± 0.24	1.18	1.21
25 SDS	10% Methanolic	2.80	10% Methanolic	2.80	5.28 ± 0.07	Aqueous	6.53	4.69 ± 0.05	0.85	0.89
50 SDS	Aqueous	13.99	Aqueous	13.99	15.08 ± 0.25 <sup>c</sup>	10% Methanolic	5.66	17.77 ± 0.31	1.10	1.18
50 SDS	10% Methanolic	5.66	10% Methanolic	5.66	10.25 ± 0.18	Aqueous	13.99	9.98 ± 0.25	0.91	0.97
25 SDS	Aqueous	6.53	Aqueous	6.53	10.11 ± 0.02 <sup>c</sup>	10% Ethanolic	2.51	12.27 ± 0.15	1.21	1.21
25 SDS	10% Ethanolic	2.51	10% Ethanolic	2.51	4.65 ± 0.06	Aqueous	6.53	3.76 ± 0.04	0.82	0.81
50 SDS	Aqueous	13.99	Aqueous	13.99	15.08 ± 0.25 <sup>c</sup>	10% Ethanolic	5.42	17.91 ± 0.33	1.11	1.19
50 SDS	10% Ethanolic	5.42	10% Ethanolic	5.42	9.34 ± 0.05	Aqueous	13.99	7.65 ± 0.15	0.90	0.82

<sup>a</sup> RFGE = Retention factor gradient effect.

<sup>b</sup> Standard deviation is calculated from the corresponding standard errors estimated by non-linear regression applying the rules for error propagation [36].

<sup>c</sup> Data taken from our previous publication [11].

**Table 6**  
Comparison of theoretically predicted and experimentally measured additional focusing/defocusing factor due to RFGE<sup>a</sup> for benzamide.

SDS concentration (mmol L <sup>-1</sup> )	Sample matrix	k <sub>s</sub>	Without RFGE			With RFGE			Additional focusing/defocusing factor	
			BGE	k <sub>BGE</sub> (=k <sub>s</sub> )	Enrichment factor <sup>b</sup>	BGE	k <sub>BGE</sub>	Enrichment factor <sup>b</sup>	f <sub>theo</sub> (Eq. (7))	f <sub>exp</sub> (Eq. (10))
75 SDS	Aqueous	0.83	Aqueous	0.83	2.05 ± 0.01 <sup>c</sup>	10% Methanolic	0.55	2.66 ± 0.02	1.28	1.30
75 SDS	10% Methanolic	0.55	10% Methanolic	0.55	1.84 ± 0.02	Aqueous	0.83	1.36 ± 0.01	0.78	0.74
100 SDS	Aqueous	1.09	Aqueous	1.09	2.40 ± 0.05 <sup>c</sup>	5% Methanolic	0.72	2.74 ± 0.02	1.24	1.14
100 SDS	Aqueous	1.09	Aqueous	1.09	2.40 ± 0.05 <sup>c</sup>	10% Methanolic	0.64	2.93 ± 0.03	1.34	1.22
100 SDS	Aqueous	1.09	Aqueous	1.09	2.40 ± 0.05 <sup>c</sup>	15% Methanolic	0.57	3.28 ± 0.04	1.45	1.37
100 SDS	Aqueous	1.09	Aqueous	1.09	2.40 ± 0.05 <sup>c</sup>	20% Methanolic	0.45	3.66 ± 0.03	1.69	1.53
100 SDS	10% Methanolic	0.64	10% Methanolic	0.64	2.40 ± 0.05 <sup>c</sup>	Aqueous	1.09	1.58 ± 0.02	0.75	0.77

<sup>a</sup> RFGE = Retention factor gradient effect.

<sup>b</sup> Standard deviation is calculated from the corresponding standard errors estimated by non-linear regression applying the rules for error propagation [36].

<sup>c</sup> Data taken from our previous publication [11].

composition of the BGE (20%, v/v methanol, 10 mmol L<sup>-1</sup> borate, 100 mmol L<sup>-1</sup> SDS, pH 9.00). This measurement series included several samples of different  $\gamma$  values ranging from 0.54 to 324. The data clearly show that the measured enrichment factors were not significantly changed by variation of  $\gamma$  (Table 7). The relative standard deviation RSD for the measured enrichment factors is 4.9%. These data indicate that also in the general case there is no dependence of the enrichment factor on  $\gamma$ .

#### 4.3. Variation of concentration and alkyl chain length of organic modifier

There are many cases, in which the analyte is not soluble in purely aqueous solutions. One possibility, to avoid solubility problems, is to dissolve the analyte in an aqueous/organic solvent. According to the classical description introduced by Quirino and Terabe [1,2] we expect (when adding an organic solvent to the sample solution) a decrease in the enrichment factor compared to that obtained with purely aqueous sample matrix due to a decrease in  $k_s$  (see Eq. (1)). According to our theoretical considerations, however, we would expect an additional defocusing effect because  $f < 1$  if  $k_s < k_{BGE}$  (see Eq. (7)), detectable as an additional decrease in the enrichment factor.

In Fig. 6 the enrichment factor is given for ethyl- and propylparaben dependent on the concentration of an *n*-alkanol (methanol, ethanol, 1-propanol, 1-butanol or 1-pentanol) in the sample. The maximum concentration for 1-pentanol was 2% (w/v) due to its limited solubility in water. In this case, the simplified “selected points” procedure [11] was employed for measuring the enrichment factor. In all cases, the enrichment factor was reduced. The higher the content of *n*-alkanol and the longer the alkyl chain, the more pronounced is the reduction. It is now possible to calculate the fraction of decrease in the enrichment factor due to RFGE using the following equation:

$$\% \text{Contribution of the RFGE} = \frac{EF_2 - EF_3}{EF_1 - EF_3} \times 100 \quad (11)$$

where  $EF_1$  is the enrichment factor with aqueous sample and aqueous BGE (No RFGE),  $EF_2$  is the enrichment factor with aqueous/organic sample and aqueous/organic BGE (No RFGE), and  $EF_3$  is the enrichment factor with aqueous/organic sample and aqueous BGE (RFGE with  $f < 1$ ). Retention factors were calculated from the experimentally obtained enrichment factors (Fig. 6) using Eq. (8). For all cases shown in Fig. 6A or B, the relative contribution of the RFGE to the total decrease in the enrichment factor is constant (see Tables S-1 and S-2 in the Supplementary Data). As shown in the Supplementary Data, this result can be attributed to the underlying equation:

$$\% \text{Contribution of the RFGE} = \frac{1}{k_{BGE} + 1} \times 100 \quad (12)$$

This equation shows that the contribution of RFGE to the total decrease in the enrichment factor depends only on the retention factor in the BGE. Since the value of  $k_{BGE}$  in MEKC is recommended to be in the range between 0.5 and 10 [32,33], it follows that the range of the percentage contribution of the RFGE to the observed decrease in the enrichment factor in case of addition of organic solvent to the sample matrix is expected to be between 9% and 67%.

As we have shown, for a given BGE the fraction of decrease in the enrichment factor due to RFGE remains constant. Consequently, the decrease in the enrichment factor shown in Fig. 6 directly reflects the decrease in  $k_s$ . With low concentration of medium-chain alcohols (1-butanol and 1-pentanol) in the sample matrix, the decrease in the enrichment factor follows a sharp trend. At higher concentration of the solvent, it reaches a constant plateau region with no further decrease in the enrichment factor. This behavior can

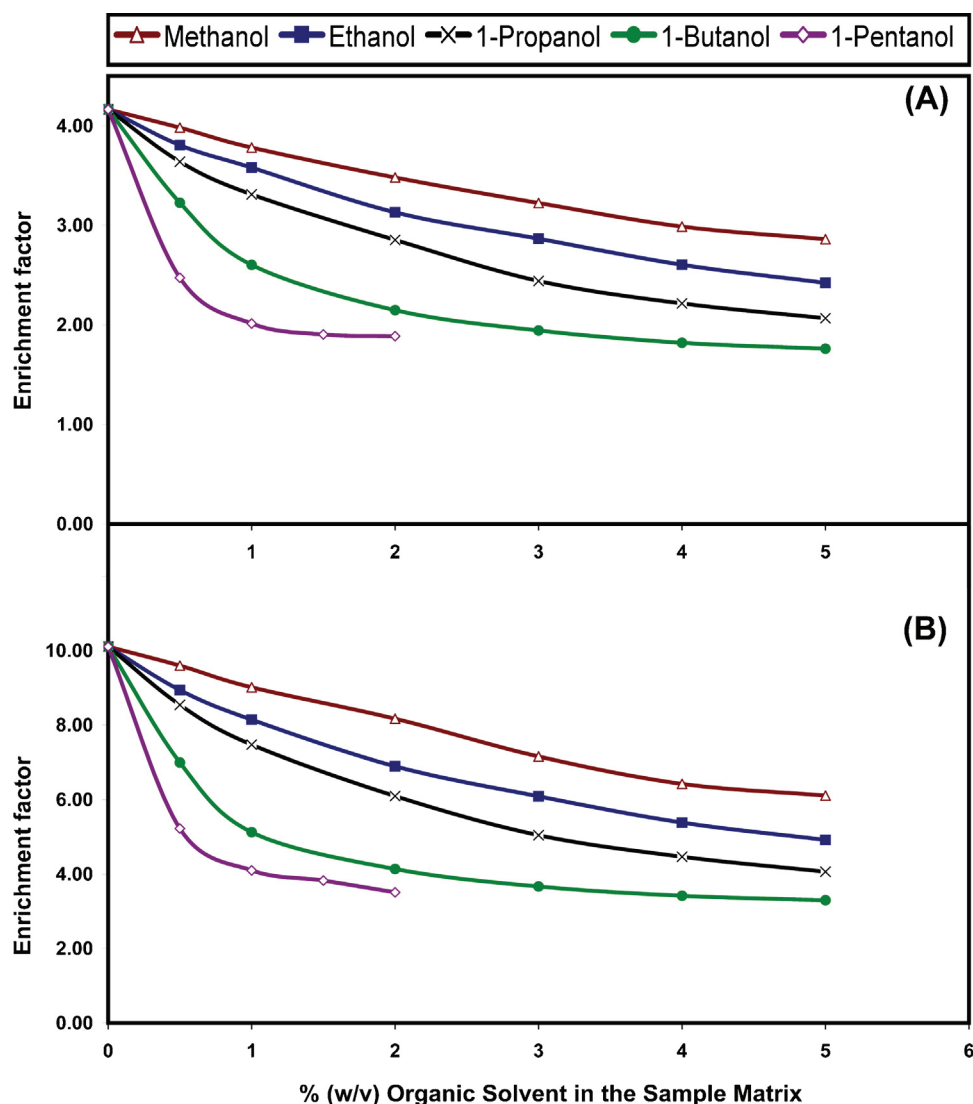


Fig. 6. Effect of concentration and chain length of the *n*-alkanol content in the sample matrix (20 mmol L<sup>-1</sup> phosphate buffer, pH 7.00) on the enrichment factor for (A) EP and (B) PP using 25 mmol L<sup>-1</sup> SDS in 20 mmol L<sup>-1</sup> phosphate buffer, pH 7.00 as BGE. For experimental parameters refer to Fig. 2.

be explained on the basis of: (i) distribution of *n*-alkanol between micellar and surrounding phase, (ii) modification of surrounding phase by dissolved *n*-alkanol, (iii) modification of micellar phase by incorporated *n*-alkanol, (iv) variation of phase ratio micellar phase/surrounding phase due to the influence of the dissolved *n*-alkanol on the CMC [37] and due to swelling of micelles by

incorporated *n*-alkanol (cosurfactant) [38]. It is interesting to note that the curves shown in Fig. 6 directly correspond to those which have been determined by Lopez-Grijo et al. [37] in micellar liquid chromatography for the dependence of the retention factor on the concentration of alcohol (1-propanol, 1-butanol and 1-pentanol) in the mobile phase.

Table 7

Enrichment factors for BNZ in sample matrices with varied electric conductivity using a buffer with 20% (v/v) methanol, 10 mmol L<sup>-1</sup> borate, 100 mmol L<sup>-1</sup> SDS (pH 9.00) as the BGE.

Sample matrix	Electric conductivity of the sample solution (mS/cm)	Field-strength enhancement factor ( $\gamma$ ) <sup>a</sup>	Enrichment factor <sup>b</sup>
Water	0.01	324	3.75 ± 0.05
2.5 mmol L <sup>-1</sup> borate buffer	0.07	46.3	3.78 ± 0.05
5 mmol L <sup>-1</sup> borate buffer	0.14	23.1	3.80 ± 0.02
10 mmol L <sup>-1</sup> borate buffer	0.28	11.6	3.66 ± 0.03
20 mmol L <sup>-1</sup> borate buffer	0.56	5.79	3.61 ± 0.04
40 mmol L <sup>-1</sup> borate buffer	1.10	2.95	3.59 ± 0.04
150 mmol L <sup>-1</sup> borate buffer	3.84	0.84	3.46 ± 0.03
200 mmol L <sup>-1</sup> borate buffer	4.96	0.65	3.38 ± 0.03
250 mmol L <sup>-1</sup> borate buffer	6.02	0.54	3.31 ± 0.02

<sup>a</sup> The electric conductivity of the BGE is 3.24 mS/cm.

<sup>b</sup> Standard deviation is calculated from the corresponding standard errors estimated by non-linear regression applying the rules for error propagation [36].

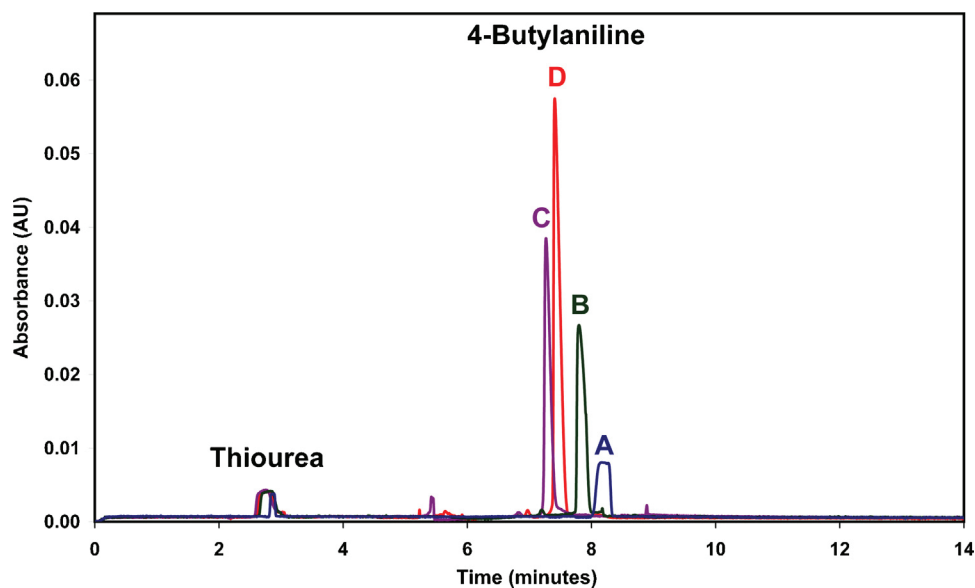


**Fig. 7.** Electropherograms at constant injection volumes of 4-butylaniline in different sample matrices (A) in BGE, (B) in 10 mmol L<sup>-1</sup> borate buffer, pH 9.37, (C) in 10 mmol L<sup>-1</sup> phosphoric acid, pH 3.50, (D) in 10 mmol L<sup>-1</sup> glutamic acid, pH 3.35. BGE: 10 mmol L<sup>-1</sup> borate buffer, pH 9.37 containing 50 mmol L<sup>-1</sup> SDS; injection: hydrodynamic, pressure 3 psi for 10 s; capillary: fused-silica capillaries (50- $\mu$ m I.D., 362- $\mu$ m O.D.) with a total length of 50.65 cm and a length to the detector of 40.25 cm; temperature of the capillary and the sample tray: 25 °C; voltage: +22 kV; detection wavelength: 254 nm.

#### 4.4. Variation of pH of the sample matrix

A promising approach to increase the enrichment factor and simultaneously overcome solubility problems for hydrophobic analytes is to modify the pH of the sample matrix so that the degree of ionization of the studied analyte is increased, which will consequently increase its polarity and solubility. As already outlined by Quirino and Terabe [2], electrostatic interaction of positively charged basic solutes (in low-pH sample matrix) with negatively charged SDS micelles causes high retention factors in the sample compartment. Orentaite et al. [39] observed for acidic solutes in MEKC with cationic surfactant about one order of magnitude higher retention factors for the charged species compared to those retention factors obtained for the neutral species. High retention factors for charged analytes in MEKC with oppositely charged surfactant are due to the simultaneous presence of electrostatic interaction with the oppositely charged micellar outer shell and hydrophobic interaction with the hydrophobic micellar core.

In this approach, the following points have to be taken into consideration: (i) changing the effective charge number of basic, acidic, or amphoteric solutes will change their distribution coefficients (with respect to the distribution between the PSP and the surrounding phase). If the effective charge number of the analyte is different in the sample matrix and in the BGE (i.e., different pH of the sample matrix and the BGE), RFGC is unavoidable. (ii) As

reported by Orentaite et al. [39], retention factors of charged species with respect to an oppositely charged PSP are highly dependent on the concentration of co-ions. Therefore, when employing a low-pH sample matrix with basic solutes in combination with an anionic surfactant or a high-pH sample matrix with acidic solutes in combination with a cationic surfactant, the reachable enrichment factor will depend also on the type and the concentration of co-ions.

As proof of principle, we determined the enrichment factor for several aromatic amines (aniline, 4-ethylaniline and 4-butylaniline) by dissolving them in matrices of different pH (10 mmol L<sup>-1</sup> borate buffer, pH 9.37; 10 mmol L<sup>-1</sup> phosphoric acid, pH 3.50; and 10 mmol L<sup>-1</sup> glutamic acid, pH 3.35). Whereas in low-pH matrix the solutes are protonated with an effective charge number of +1, in high-pH matrix their effective charge number is zero. Separation by MEKC was reached with a high-pH BGE: 50 mmol L<sup>-1</sup> SDS, 10 mmol L<sup>-1</sup> borate buffer, pH 9.37. Fig. 7 shows the electropherograms obtained for 4-butylaniline with different composition of the sample matrix and fixed injection parameters. The electric conductivities of the sample solutions were adjusted to the electric conductivity of the BGE by adding KCl. In accordance with the above outlined considerations, there is a marked increase in the peak height with the lowered pH of the sample matrix. Similar results were also obtained for aniline and 4-ethylaniline as shown in Table 8 (refer to Figs. S-38–S-40 at the Supplementary Data for the corresponding regression curves).

**Table 8**  
Sweeping efficiencies for aniline, 4-ethylaniline and 4-butylaniline in three different sample matrices using 10 mmol L<sup>-1</sup> borate buffer, pH 9.37 containing 50 mmol L<sup>-1</sup> SDS as the BGE.

	Analyte	Sample matrix		
		Borate buffer (pH 9.37)	Phosphoric acid (pH 3.50)	Glutamic acid (pH 3.35)
Enrichment factor <sup>c</sup>	Aniline	1.38 ± 0.01 <sup>a</sup>	1.44 ± 0.01	2.06 ± 0.05
	4-Ethylaniline	3.92 ± 0.11 <sup>a</sup>	11.3 <sup>b</sup>	16.7 <sup>b</sup>
	4-Butylaniline	6.33 ± 0.31	14.3 <sup>b</sup>	17.1 <sup>b</sup>

<sup>a</sup> Data taken from our previous publication [11].

<sup>b</sup> Estimated from the highest possible peak height corresponding to the maximum allowed injection volume used as  $h_2$  in Eq. (9).

<sup>c</sup> Standard deviation is calculated from the corresponding standard errors estimated by non-linear regression applying the rules for error propagation [36].

According to Eq. (8) an improvement in the enrichment factor must be accompanied with an increase in  $k_S$ . As an example we determined the retention factor of 4-ethylaniline in 10 mmol L<sup>-1</sup> glutamic acid solution pH 3.35, containing 50 mmol L<sup>-1</sup> SDS (the electric conductivity  $\kappa$  adjusted by addition of KCl). With this BGE  $k=40$ , whereas in 50 mmol L<sup>-1</sup> SDS, 10 mmol L<sup>-1</sup> borate buffer, pH 9.37  $k=2.90$  (details about the measurement of retention factors are discussed in the Supplementary Data).

According to Eq. (8) (with  $k_S=40$  and  $k_{BGE}=2.90$ ), the enrichment factor ( $=I_{inj}/I_{grad}$ ) is expected to be 53.8. Measured data for the enrichment factor are given in Table 8. The enrichment factor measured for 4-ethylaniline with glutamic acid solution, pH 3.35 as a sample matrix is 16.7. This value was calculated by taking the peak height corresponding to the maximum allowed injection volume as  $h_2$  in Eq. (9). It should be taken into consideration that with this hydrophobic analyte, it was not possible to reach the volume overload region under enrichment conditions. Therefore, the experimental value of the enrichment factor is lower than the theoretically predicted one. Small differences in the pH of the sample matrix between phosphoric and glutamic acids result in small differences in the degree of protonation, 0.975 at pH 3.50 and 0.983 at pH 3.35 for 4-ethylaniline ( $pK_a=5.1$ ) [40] and hence slightly different  $k_S$  and slightly different enrichment factors.

## 5. Conclusions

In the general case (different  $K_D$  in the sample and in the BGE), sweeping is accompanied by RFGE, which can account for a large part of the observed decrease or increase in the enrichment efficiency. Consequently, the focusing process is not only influenced by the retention factor of the analyte in the sample zone, but also by the retention factor of the analyte in the BGE. The equations derived allow calculating quantitatively the contribution of the RFGE to the final enrichment factor. Also in the general case, the enrichment efficiency due to sweeping with RFGE is in first approximation independent of the electric conductivity of the sample matrix.

## Acknowledgement

M. El-Awady thanks Yousef-Jameel Foundation for the financial support of this work.

## Appendix A. Supplementary data

Supplementary data associated with this article can be found, in the online version, at <http://dx.doi.org/10.1016/j.chroma.2013.04.069>.

## References

- [1] J.P. Quirino, S. Terabe, *Science* 282 (1998) 465.
- [2] J.P. Quirino, S. Terabe, *Anal. Chem.* 71 (1999) 1638.
- [3] J.P. Quirino, S. Terabe, *J. High Resolut. Chromatogr.* 22 (1999) 367.
- [4] J.B. Kim, J.P. Quirino, K. Otsuka, S. Terabe, *J. Chromatogr. A* 916 (2001) 123.
- [5] J. Palmer, D.S. Burgi, J.P. Landers, *Anal. Chem.* 74 (2002) 632.
- [6] J.P. Quirino, S. Terabe, P. Bocek, *Anal. Chem.* 72 (2000) 1934.
- [7] J. Palmer, N.J. Munro, J.P. Landers, *Anal. Chem.* 71 (1999) 1679.
- [8] J. Palmer, J.P. Landers, *Anal. Chem.* 72 (2000) 1941.
- [9] J.F. Palmer, *J. Chromatogr. A* 1036 (2004) 95.
- [10] B.C. Giordano, C.I.D. Newman, P.M. Federowicz, G.E. Collins, D.S. Burgi, *Anal. Chem.* 79 (2007) 6287.
- [11] M. El-Awady, C. Huhn, U. Pyell, *J. Chromatogr. A* 1264 (2012) 124.
- [12] M. Gilges, *Chromatographia* 44 (1997) 191.
- [13] W. Shi, C.P. Palmer, *J. Sep. Sci.* 25 (2002) 215.
- [14] C. Fang, J.T. Liu, C.H. Lin, *Talanta* 58 (2002) 691.
- [15] S. Takeda, A. Omura, K. Chayama, H. Tsuji, K. Fukushi, M. Yamane, S.i. Wakida, S. Tsubota, S. Terabe, *J. Chromatogr. A* 1014 (2003) 103.
- [16] A.T. Aranas, A.M. Guidote Jr., P.R. Haddad, J.P. Quirino, *Talanta* 85 (2011) 86.
- [17] P. Britz-McKibbin, K. Otsuka, S. Terabe, *Anal. Chem.* 74 (2002) 3736.
- [18] P. Britz-McKibbin, M.J. Markuszewski, T. Iyanagi, K. Matsuda, T. Nishioka, S. Terabe, *Anal. Biochem.* 313 (2003) 89.
- [19] H. Yan, G. Yang, F. Qiao, Y. Chen, *J. Pharm. Biomed. Anal.* 36 (2004) 169.
- [20] H. Yan, G. Yang, F. Qiao, H. Liu, C. Yi, *Chem. J. Internet* 6 (2004).
- [21] G.I. Yang, B.h. Li, D.X. Wang, Y. Chen, *Chin. J. Chem.* 20 (2002) 1579.
- [22] R.L. Chien, J.C. Helmer, *Anal. Chem.* 63 (1991) 1354.
- [23] D.S. Burgi, R.L. Chien, *Anal. Chem.* 63 (1991) 2042.
- [24] C. Huhn, U. Pyell, *J. Chromatogr. A* 1217 (2010) 4476.
- [25] J.P. Quirino, J.B. Kim, S. Terabe, *J. Chromatogr. A* 965 (2002) 357.
- [26] R.L. Chien, D.S. Burgi, *Anal. Chem.* 64 (1992) 489A.
- [27] A.M. Guidote Jr., J.P. Quirino, *J. Chromatogr. A* 1217 (2010) 6290.
- [28] J.P. Quirino, *J. Chromatogr. A* 1217 (2010) 7776.
- [29] J.P. Quirino, A.M. Guidote Jr., *J. Chromatogr. A* 1218 (2011) 1004.
- [30] J.P. Quirino, P. Anres, J. Sirieix-Plenet, N. Delaunay, P. Gareil, *J. Chromatogr. A* 1218 (2011) 5718.
- [31] J.P. Quirino, S. Terabe, *J. Chromatogr. A* 781 (1997) 119.
- [32] S. Terabe, K. Otsuka, T. Ando, *Anal. Chem.* 57 (1985) 834.
- [33] H. Waetzig, M. Degenhardt, A. Kunkel, *Electrophoresis* 19 (1998) 2695.
- [34] U. Pyell, *J. Chromatogr. A* 1037 (2004) 479.
- [35] S.K. Wiedmer, J. Lokajova, M.L. Riekkola, *J. Sep. Sci.* 33 (2010) 394.
- [36] J.C. Miller, J.N. Miller, *Statistics and Chemometrics for Analytical Chemistry*, 5th ed., Pearson Education Limited, Harlow, England, 2005.
- [37] S. Lopez-Grijo, J.J. Baeza-Baeza, M.C. Garcia-Alvarez-Coque, *Chromatographia* 48 (1998) 655.
- [38] H. Van, R. Szucs, P. Sandra, *J. High Resolut. Chromatogr.* 19 (1996) 674.
- [39] I. Orentaite, A. Maruska, U. Pyell, *Electrophoresis* 32 (2011) 604.
- [40] O. Jimenez, T.E. Mueller, W. Schwieger, J.A. Lercher, *J. Catal.* 239 (2006) 42.



**5.2.4. Sweeping as a multistep enrichment process in micellar electrokinetic chromatography:  
The retention factor gradient effect.**

Mohamed El-Awady, Ute Pyell\*

University of Marburg, Department of Chemistry, Hans-Meerwein-Straße, D-35032 Marburg, Germany

\* corresponding author

**Supplementary data**

- Measurement of retention factors.
- Calculation of the contribution of the retention factor gradient effect (RFGE) to the decrease in the enrichment factor due to addition of organic modifier to the sample solution.
- Plateau (regression) curves for the studied analytes under different experimental conditions.

**Measurement of retention factors:**

For measuring the retention factor for neutral solutes, different approaches have been published in the literature [1]. In aqueous BGE, the retention factor can be determined experimentally by using marker compounds; e.g. thiourea as an EOF marker and quinine hydrochloride as a micelle marker (for anionic surfactant). If all analytes can be regarded to be neutral under the conditions of enrichment, the following equation is valid:

$$k = \frac{t_s - t_0}{t_0(1 - t_s / t_{mc})} \quad (\text{S-1})$$

where  $t_0$  = migration time of the EOF marker,  $t_s$  = migration time of the solute,  $t_{mc}$  = migration time of the micelle marker.

In presence of organic solvent in the BGE, the direct measurement of retention factors using a single compound as a micelle marker is no longer reliable [2]. That is because the prerequisite that the micelle marker should have a retention factor of infinity is no longer fulfilled [2]. Therefore, in these cases we have to use the iterative procedure published by Bushey and Jorgenson [3,4] for the determination of the electrophoretic mobility of the micelles based on the Martin equation valid for the retention factors of the members of a homologous series of different hydrophobicities. In the present study, retention factors for the homologous series of alkyl phenyl ketones namely acetophenone, propiophenone, butyrophenone, valerophenone and hexanophenone were determined. The same homologous series was used by Chen *et al.* [2] for measuring  $t_{mc}$  values in BGEs containing methanol, acetonitrile, 1-propanol and tetrahydrofuran.

In this approach, hexanophenone is first assumed to be a micelle marker and the retention factor  $k$  for acetophenone, propiophenone, butyrophenone and valerophenone is calculated according to Eq. (S-1), where  $t_r$  is the migration time of the analyte and  $t_0$  is the migration time of the EOF marker (methanol used to solubilize the mixture of alkyl phenyl ketones). Then  $\log k$  is plotted against the carbon number  $N_C$  of the alkyl group. Using this plot, a temporary value of  $k$  for hexanophenone is obtained from  $\log k$  at  $N_C = 6$  from which a new  $t_{mc}$  is calculated using Eq. (S-1). Then the values of  $\log k$  are recalculated employing the improved estimation of  $t_{mc}$  and re-plotted against  $N_C$ . The iterative procedure is repeated until a constant value of  $t_{mc}$  is obtained with the lowest possible sum of squared errors (SSE) and the highest possible squared correlation coefficient  $R^2$ . This iterative procedure is performed with the help of a Microsoft Excel® data sheet (See Figure S-1). From the obtained  $t_{mc}$  value, the electrophoretic mobility of the micelles can be calculated which is then used for the determination of the retention factor of the studied analytes. Those retention factors measured by this iterative procedure are included in Tables 1, 4-6.

For measuring the retention factor for charged solutes (e.g. 4-ethylaniline in a BGE of 50 mmol L<sup>-1</sup> SDS and 10 mmol L<sup>-1</sup> glutamic acid, pH 3.35) in micellar BGE a completely different approach is needed. The calculation is based on following equation [5]:

$$k = \frac{\mu - \mu_{\text{eff}}}{\mu_{\text{mc}} - \mu} \tag{S-2}$$

where  $\mu$  = pseudoeffective electrophoretic mobility of the analyte in micellar BGE,  $\mu_{\text{eff}}$  = effective electrophoretic mobility of the analyte in micelle-free BGE (here: under CZE conditions with glutamic acid solution as BGE), and  $\mu_{\text{mc}}$  = electrophoretic mobility of the micelles in micellar BGE. These values were determined in separate measurements using thiourea as EOF marker and quinine hydrochloride as micelle marker. For measuring the electroosmotic mobility, the method developed by Sandoval and Chen [6] was used. The retention factor of 4-ethylaniline in 10 mmol L<sup>-1</sup> glutamic acid solution pH 3.35, containing 50 mmol L<sup>-1</sup> SDS ( $\kappa$  adjusted by addition of KCl), was found to be 40, whereas in 50 mmol L<sup>-1</sup> SDS, 10 mmol L<sup>-1</sup> borate buffer, pH 9.37 the retention factor was determined to be 2.90.

References

- [1] S.K. Wiedmer, J. Lokajova, M.L. Riekkola, J. Sep. Sci. 33 (2010) 394.
- [2] N. Chen, S. Terabe, T. Nakagawa, Electrophoresis 16 (1995) 1457.
- [3] M.M. Bushey, J.W. Jorgenson, J. Microcolumn Sep. 1 (1989) 125.
- [4] M.M. Bushey, J.W. Jorgenson, Anal. Chem. 61 (1989) 491.
- [5] K. Otsuka, S. Terabe, T. Ando, J. Chromatogr. 348 (1985) 39.
- [6] J.E. Sandoval, S.M. Chen, Anal. Chem. 68 (1996) 2771.

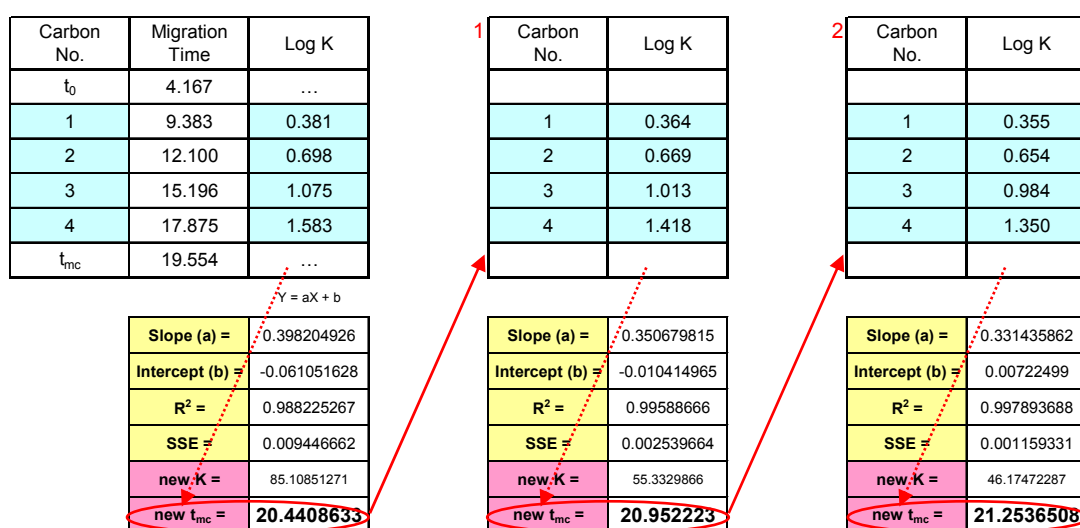


**Figure S-1:** Snapshot from the Microsoft Excel® file used for performing the iterative procedure used for measuring the retention factor.

**Calculation of the contribution of the retention factor gradient effect (RFGE) to the decrease in the enrichment factor due to addition of organic modifier to the sample solution:**

Our target is to calculate the fraction by which the RFGE contributes to the observed decrease in the enrichment factor due to the addition of organic solvent to the sample matrix compared to aqueous sample. It is possible to calculate the fraction of decrease in the enrichment factor due to RFGE using the following equation:

$$\% \text{ Contribution of the RFGE} = \frac{EF_2 - EF_3}{EF_1 - EF_3} \times 100 \quad (\text{S-3})$$

where  $EF_1$  is the enrichment factor using aqueous sample and aqueous BGE (No RFGE),  $EF_2$  is the enrichment factor using aqueous/organic sample and aqueous/organic BGE (No RFGE), and  $EF_3$  is the enrichment factor using aqueous/organic sample and aqueous BGE (RFGE with  $f < 1$ ). Within this section  $k_s$  is the retention factor of the analyte in the aqueous/organic sample matrix (having a PSP concentration corresponding to that of the BGE) and  $k_{BGE}$  is the retention factor of the analyte in the aqueous BGE, whereas the corresponding enrichment factor is  $EF_3$  (Case 3).

For Case 1 (aqueous sample and aqueous BGE) and Case 2 (aqueous/organic sample and aqueous/organic BGE), there is no RFGE. Based on the concepts presented in 1998 by Quirino and Terabe [Science 282 (1998) 465], in these two cases  $EF_1$  and  $EF_2$  can be expressed as follows:

$$EF_1 = k_{BGE} + 1 \quad (\text{S-4})$$

$$EF_2 = k_s + 1 \quad (\text{S-5})$$

For Case 3 (aqueous/organic sample with aqueous BGE),  $EF_3$  has to be calculated using Eq. (8):

$$EF_3 = \frac{k_s k_{BGE} + k_s}{k_s k_{BGE} + k_{BGE}} \frac{1 + k_s}{1} \quad (\text{S-6})$$

By substitution of Equations (S-4), (S-5) and (S-6) in Equation (S-3), the % contribution of the RFGE can be calculated as follows:

$$\% \text{ Contribution of the RFGE} = \frac{(k_s + 1) - \left[ \frac{k_s k_{BGE} + k_s}{k_s k_{BGE} + k_{BGE}} \frac{1 + k_s}{1} \right]}{(k_{BGE} + 1) - \left[ \frac{k_s k_{BGE} + k_s}{k_s k_{BGE} + k_{BGE}} \frac{1 + k_s}{1} \right]} \times 100 \quad (\text{S-7})$$

$$= \frac{(k_S + 1) - \left[ \frac{k_S}{k_{BGE}} \frac{(k_{BGE} + 1)}{(k_S + 1)} \frac{(1 + k_S)}{1} \right]}{(k_{BGE} + 1) - \left[ \frac{k_S}{k_{BGE}} \frac{(k_{BGE} + 1)}{(k_S + 1)} \frac{(1 + k_S)}{1} \right]} \times 100 \quad (S-8)$$

$$= \frac{(k_S + 1) - \left[ \frac{k_S}{k_{BGE}} (k_{BGE} + 1) \right]}{(k_{BGE} + 1) - \left[ \frac{k_S}{k_{BGE}} (k_{BGE} + 1) \right]} \times 100 \quad (S-9)$$

$$= \frac{k_S + 1 - k_S - \frac{k_S}{k_{BGE}}}{(k_{BGE} + 1) \left( 1 - \frac{k_S}{k_{BGE}} \right)} \times 100 \quad (S-10)$$

$$= \frac{\left( 1 - \frac{k_S}{k_{BGE}} \right)}{(k_{BGE} + 1) \left( 1 - \frac{k_S}{k_{BGE}} \right)} \times 100 \quad (S-11)$$

Finally, the % contribution of the RFGE can be calculated as follows:

$$\% \text{ Contribution of the RFGE} = \frac{1}{k_{BGE} + 1} \times 100 \quad (S-12)$$

**Table S-1:** % contribution of the RFGE to the decrease in the enrichment factor (EF) for ethylparaben<sup>a</sup>[EF<sub>1</sub> (aq. sample and aq. BGE) = 4.16, k<sub>BGE</sub> (calculated form EF<sub>1</sub>) = 3.16]

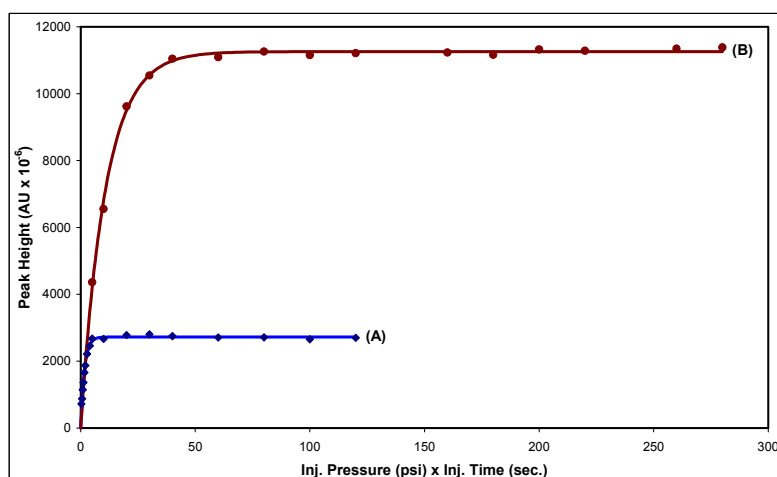
Alcohol	% alcohol in sample	EF <sub>3</sub> (alc. sample & aq. BGE)	k <sub>s</sub>	EF <sub>2</sub> (alc. sample & alc. BGE)	%RFGE <sup>b</sup>
Methanol	0.5	3.98	3.024	4.02	24%
	1	3.78	2.872	3.87	24%
	2	3.48	2.644	3.64	24%
	3	3.22	2.449	3.45	24%
	4	2.99	2.269	3.27	24%
	5	2.86	2.172	3.17	24%
Ethanol	0.5	3.81	2.891	3.89	24%
	1	3.58	2.719	3.72	24%
	2	3.13	2.377	3.38	24%
	3	2.86	2.176	3.18	24%
	4	2.60	1.978	2.98	24%
	5	2.42	1.839	2.84	24%
1-Propanol	0.5	3.64	2.764	3.76	24%
	1	3.31	2.514	3.51	24%
	2	2.85	2.167	3.17	24%
	3	2.44	1.854	2.85	24%
	4	2.21	1.682	2.68	24%
	5	2.07	1.57	2.57	24%
1-Butanol	0.5	3.23	2.451	3.45	24%
	1	2.60	1.976	2.98	24%
	2	2.15	1.631	2.63	24%
	3	1.94	1.476	2.48	24%
	4	1.82	1.382	2.38	24%
	5	1.76	1.337	2.34	24%
1-Pentanol	0.5	2.47	1.879	2.88	24%
	1	2.01	1.529	2.53	24%
	1.5	1.90	1.445	2.45	24%
	2	1.89	1.432	2.43	24%

<sup>a</sup> For experimental parameters refer to Figure 6.<sup>b</sup> %RFGE is calculated using Equation S-3.

**Table S-2:** % contribution of the RFGE to the decrease in the enrichment factor (EF) for propylparaben<sup>a</sup>[EF<sub>1</sub> (aq. sample and aq. BGE) = 10.32, k<sub>BGE</sub> (calculated form EF<sub>1</sub>) = 9.32]

Alcohol	% alcohol in sample	EF <sub>3</sub> (alc. sample & aq. BGE)	k <sub>s</sub>	EF <sub>2</sub> (alc. sample & alc. BGE)	%RFGE <sup>b</sup>
Methanol	0.5	9.80	8.846	9.85	10%
	1	9.20	8.307	9.31	10%
	2	8.34	7.53	8.53	10%
	3	7.30	6.597	7.60	10%
	4	6.56	5.921	6.92	10%
	5	6.23	5.63	6.63	10%
Ethanol	0.5	9.12	8.24	9.24	10%
	1	8.31	7.506	8.51	10%
	2	7.04	6.355	7.35	10%
	3	6.21	5.613	6.61	10%
	4	5.49	4.96	5.96	10%
	5	5.02	4.532	5.53	10%
1-Propanol	0.5	8.72	7.872	8.87	10%
	1	7.63	6.888	7.89	10%
	2	6.22	5.617	6.62	10%
	3	5.15	4.649	5.65	10%
	4	4.56	4.115	5.11	10%
	5	4.15	3.746	4.75	10%
1-Butanol	0.5	7.14	6.447	7.45	10%
	1	5.23	4.724	5.72	10%
	2	4.22	3.812	4.81	10%
	3	3.74	3.378	4.38	10%
	4	3.49	3.148	4.15	10%
	5	3.36	3.038	4.04	10%
1-Pentanol	0.5	5.33	4.815	5.81	10%
	1	4.18	3.777	4.78	10%
	1.5	3.90	3.525	4.53	10%
	2	3.58	3.233	4.23	10%

<sup>a</sup> For experimental parameters refer to Figure 6.<sup>b</sup> %RFGE is calculated using Equation S-3.

**Plateau (regression) curves for the studied analytes under different experimental conditions:**

**Figure S-2:** Peak height plotted against injected volume for **ethylparaben** under (A) conventional conditions (analyte dissolved in BGE), (B) sweeping conditions (analyte dissolved in phosphate buffer) . BGE: **aqueous** phosphate buffer (20 mmol L<sup>-1</sup>, pH 7) containing **25** mmol L<sup>-1</sup> SDS; sample solvent under sweeping conditions: **aqueous** phosphate buffer (20 mmol L<sup>-1</sup>, pH 7); injection: hydrodynamic; capillary: fused-silica capillary (50  $\mu$ m I.D., 362  $\mu$ m O.D.) with a total length of 60.9 cm and a length to the detector of 50.7 cm; temperatures of the capillary and the sample tray: 25°C; voltage: +20 kV; detection wavelength: 254 nm [Reprinted from M. El-Awady, C. Huhn, U. Pyell, J. Chromatogr. A 1264 (2012) 124, the online supplementary data, copyright 2012, with permission from Elsevier].

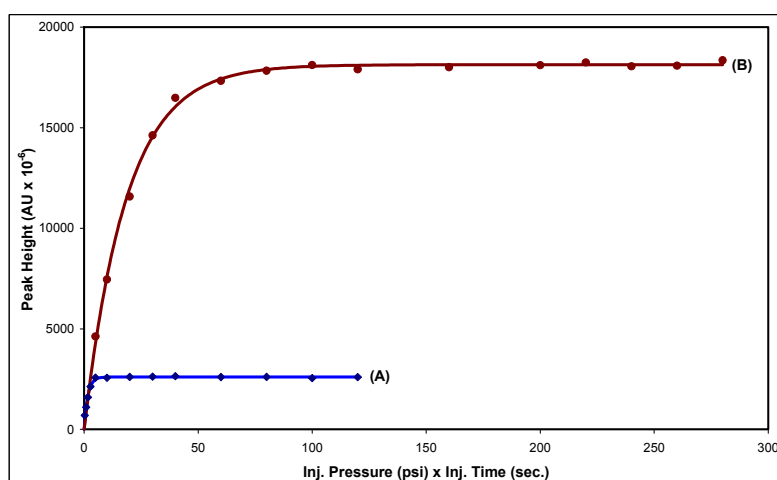


**Figure S-3:** Peak height plotted against injected volume for **ethylparaben** under (A) conventional conditions (analyte dissolved in BGE), (B) sweeping conditions (analyte dissolved in phosphate buffer) . BGE: **aqueous** phosphate buffer (20 mmol L<sup>-1</sup>, pH 7) containing **50** mmol L<sup>-1</sup> SDS; sample solvent under sweeping conditions: **aqueous** phosphate buffer (20 mmol L<sup>-1</sup>, pH 7); for other experimental parameters refer to Figure S-2. [Reprinted from M. El-Awady, C. Huhn, U. Pyell, J. Chromatogr. A 1264 (2012) 124, the online supplementary data, copyright 2012, with permission from Elsevier].

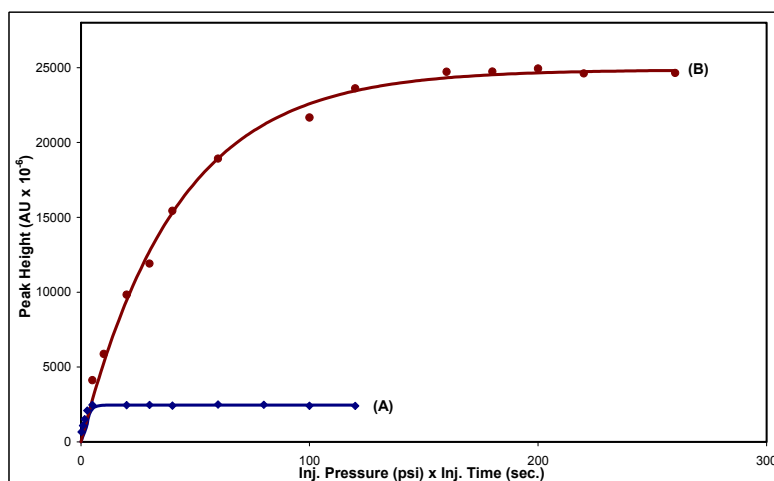


**Figure S-4:** Peak height plotted against injected volume for **Propylparaben** under (A) conventional conditions (analyte dissolved in BGE), (B) sweeping conditions (analyte dissolved in phosphate buffer) . BGE: **aqueous** phosphate buffer (20 mmol L<sup>-1</sup>, pH 7) containing **25** mmol L<sup>-1</sup> SDS; sample solvent under sweeping conditions: **aqueous** phosphate buffer (20 mmol L<sup>-1</sup>, pH 7); for other experimental parameters refer to Figure S-2. [Reprinted from M. El-Awady, C. Huhn, U. Pyell, J. Chromatogr. A 1264 (2012) 124, copyright 2012, with permission from Elsevier].

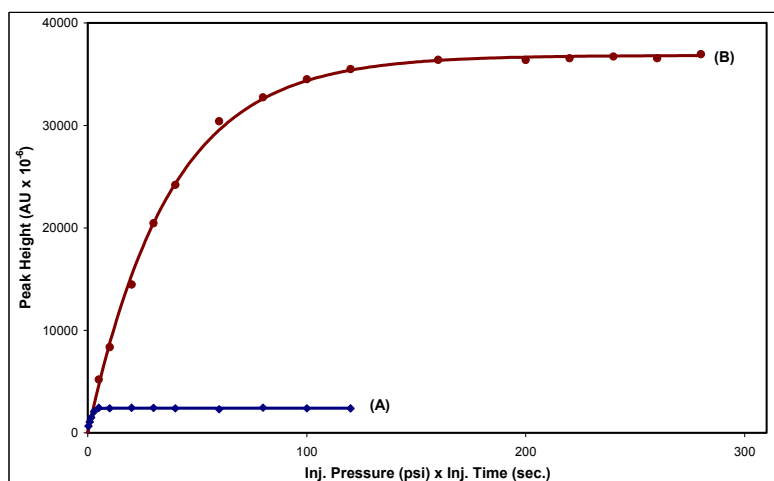


**Figure S-5** Peak height plotted against injected volume for **Propylparaben** under (A) conventional conditions (analyte dissolved in BGE), (B) sweeping conditions (analyte dissolved in phosphate buffer) . BGE: **aqueous** phosphate buffer (20 mmol L<sup>-1</sup>, pH 7) containing **50** mmol L<sup>-1</sup> SDS; sample solvent under sweeping conditions: **aqueous** phosphate buffer (20 mmol L<sup>-1</sup>, pH 7); for other experimental parameters refer to Figure S-2. [Reprinted from M. El-Awady, C. Huhn, U. Pyell, J. Chromatogr. A 1264 (2012) 124, copyright 2012, with permission from Elsevier].

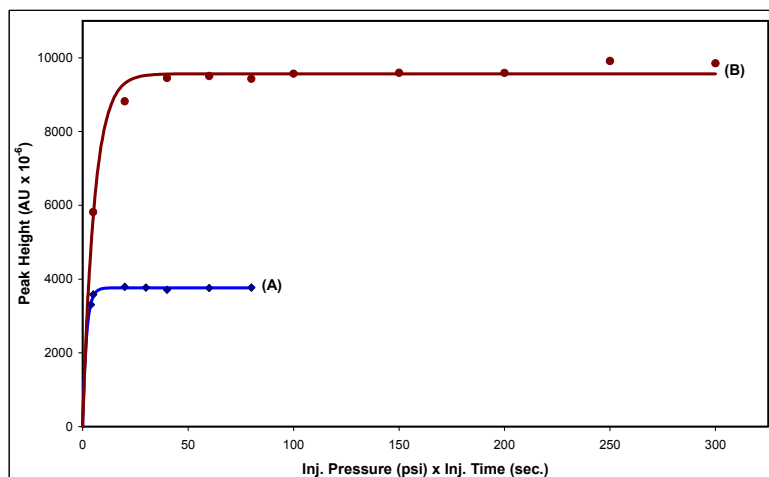


**Figure S-6:** Peak height plotted against injected volume for **ethylparaben** under (A) conventional conditions (analyte dissolved in BGE), (B) sweeping conditions (analyte dissolved in phosphate buffer) . BGE: **10% methanolic** phosphate buffer (20 mmol L<sup>-1</sup>, pH 7) containing **25** mmol L<sup>-1</sup> SDS; sample solvent under sweeping conditions: **10% methanolic** phosphate buffer (20 mmol L<sup>-1</sup>, pH 7); injection: hydrodynamic; capillary: fused-silica capillary (50  $\mu$ m I.D., 362  $\mu$ m O.D.) with a total length of 60.9 cm and a length to the detector of 50.7 cm; temperatures of the capillary: 25°C and of the sample tray: 15°C; voltage: +20 kV; detection wavelength: 254 nm.

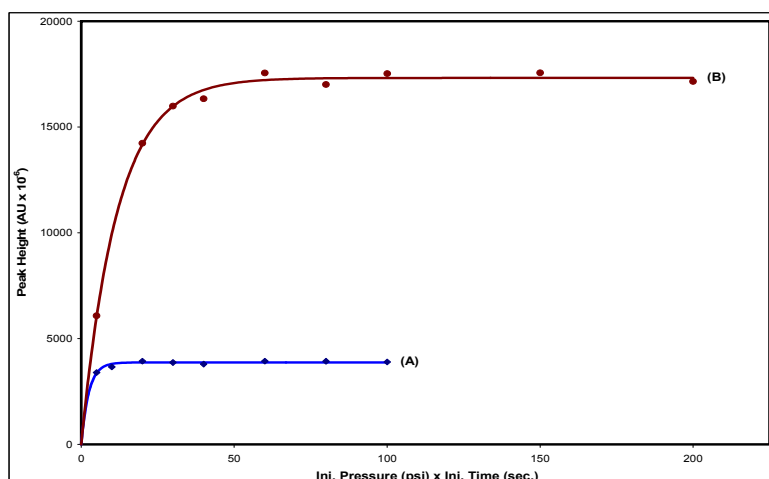


**Figure S-7:** Peak height plotted against injected volume for **ethylparaben** under (A) conventional conditions (analyte dissolved in BGE), (B) sweeping conditions (analyte dissolved in phosphate buffer) . BGE: **10% methanolic** phosphate buffer (20 mmol L<sup>-1</sup>, pH 7) containing **50** mmol L<sup>-1</sup> SDS; sample solvent under sweeping conditions: **10% methanolic** phosphate buffer (20 mmol L<sup>-1</sup>, pH 7); for other experimental parameters refer to Figure S-6.

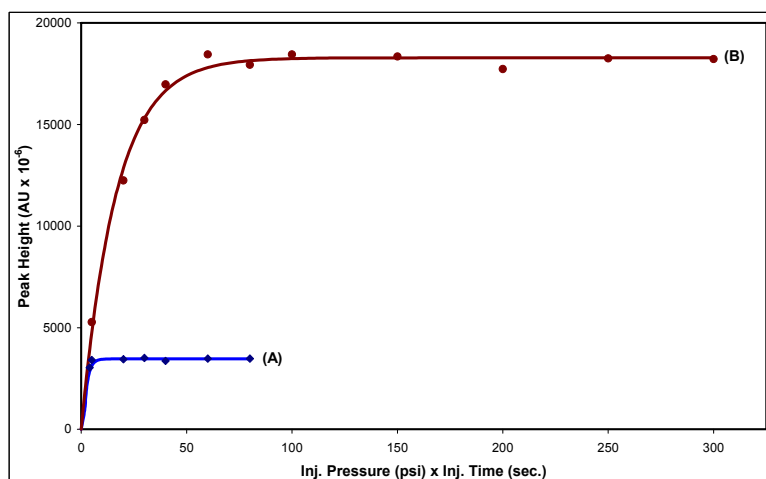


**Figure S-8:** Peak height plotted against injected volume for **propylparaben** under (A) conventional conditions (analyte dissolved in BGE), (B) sweeping conditions (analyte dissolved in phosphate buffer) . BGE: **10% methanolic** phosphate buffer (20 mmol L<sup>-1</sup>, pH 7) containing **25** mmol L<sup>-1</sup> SDS; sample solvent under sweeping conditions: **10% methanolic** phosphate buffer (20 mmol L<sup>-1</sup>, pH 7); for other experimental parameters refer to Figure S-6.

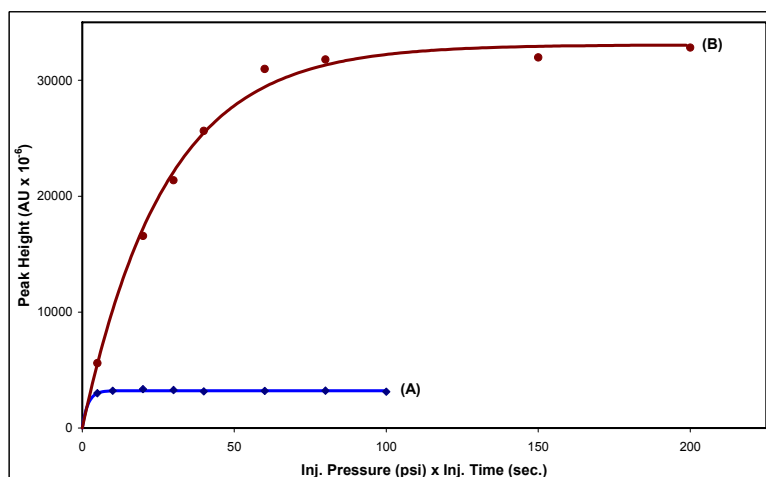


**Figure S-9:** Peak height plotted against injected volume for **propylparaben** under (A) conventional conditions (analyte dissolved in BGE), (B) sweeping conditions (analyte dissolved in phosphate buffer) . BGE: **10% methanolic** phosphate buffer (20 mmol L<sup>-1</sup>, pH 7) containing **50** mmol L<sup>-1</sup> SDS; sample solvent under sweeping conditions: **10% methanolic** phosphate buffer (20 mmol L<sup>-1</sup>, pH 7); for other experimental parameters refer to Figure S-6.

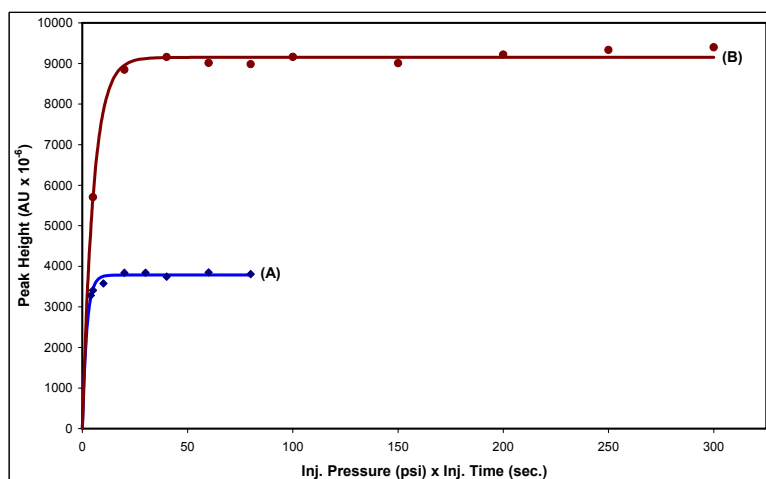


**Figure S-10:** Peak height plotted against injected volume for **ethylparaben** under (A) conventional conditions (analyte dissolved in BGE), (B) sweeping conditions (analyte dissolved in phosphate buffer). BGE: **10% ethanolic** phosphate buffer (20 mmol L<sup>-1</sup>, pH 7) containing **25** mmol L<sup>-1</sup> SDS; sample solvent under sweeping conditions: **10% ethanolic** phosphate buffer (20 mmol L<sup>-1</sup>, pH 7); for other experimental parameters refer to Figure S-6.

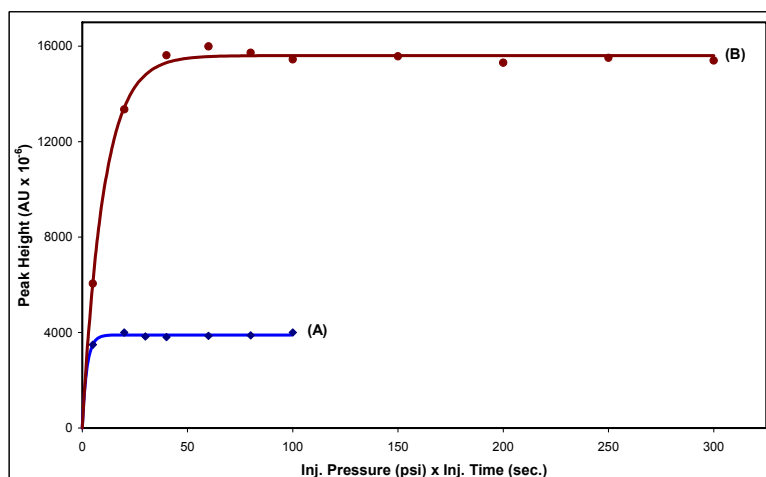


**Figure S-11:** Peak height plotted against injected volume for **ethylparaben** under (A) conventional conditions (analyte dissolved in BGE), (B) sweeping conditions (analyte dissolved in phosphate buffer). BGE: **10% ethanolic** phosphate buffer (20 mmol L<sup>-1</sup>, pH 7) containing **50** mmol L<sup>-1</sup> SDS; sample solvent under sweeping conditions: **10% ethanolic** phosphate buffer (20 mmol L<sup>-1</sup>, pH 7); for other experimental parameters refer to Figure S-6.

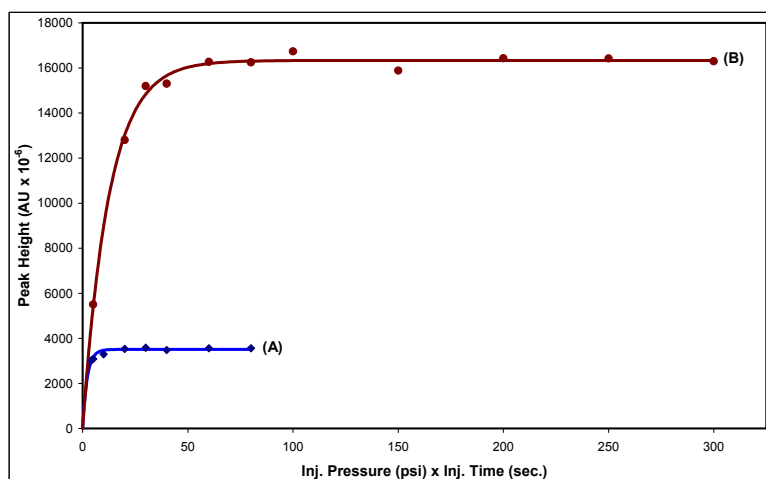


**Figure S-12:** Peak height plotted against injected volume for **propylparaben** under (A) conventional conditions (analyte dissolved in BGE), (B) sweeping conditions (analyte dissolved in phosphate buffer) . BGE: **10% ethanolic** phosphate buffer (20 mmol L<sup>-1</sup>, pH 7) containing **25** mmol L<sup>-1</sup> SDS; sample solvent under sweeping conditions: **10% ethanolic** phosphate buffer (20 mmol L<sup>-1</sup>, pH 7); for other experimental parameters refer to Figure S-6.

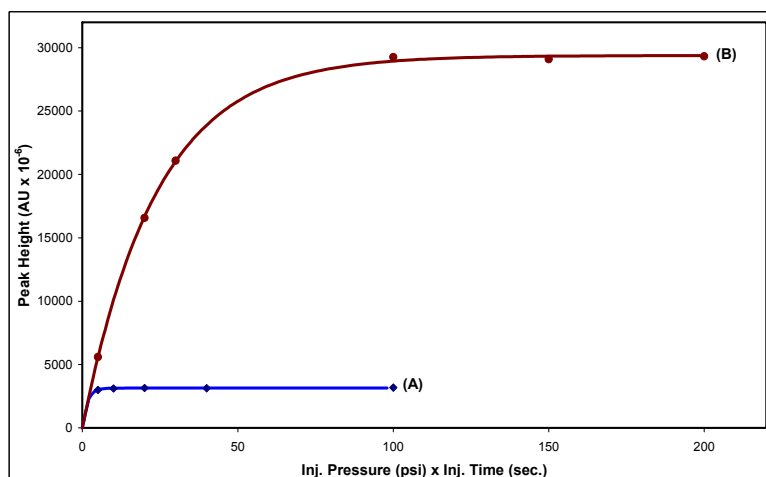


**Figure S-13:** Peak height plotted against injected volume for **propylparaben** under (A) conventional conditions (analyte dissolved in BGE), (B) sweeping conditions (analyte dissolved in phosphate buffer) . BGE: **10% ethanolic** phosphate buffer (20 mmol L<sup>-1</sup>, pH 7) containing **50** mmol L<sup>-1</sup> SDS; sample solvent under sweeping conditions: **10% ethanolic** phosphate buffer (20 mmol L<sup>-1</sup>, pH 7); for other experimental parameters refer to Figure S-6.

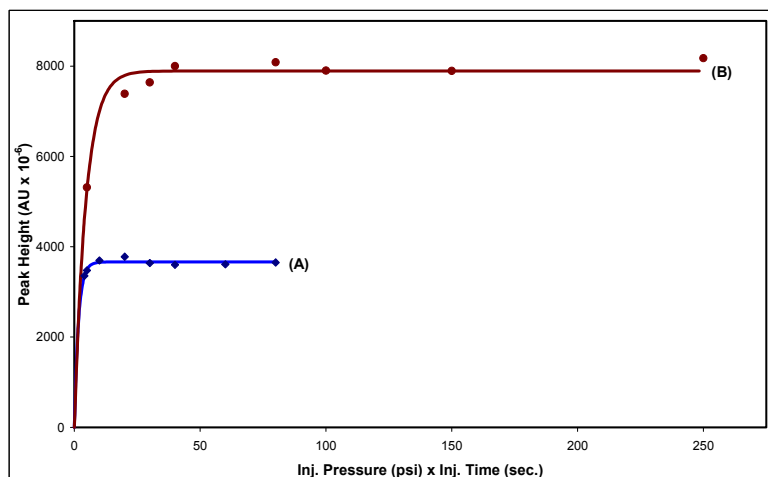


**Figure S-14:** Peak height plotted against injected volume for **ethylparaben** under (A) conventional conditions (analyte dissolved in BGE), (B) sweeping conditions (analyte dissolved in phosphate buffer) . BGE: **aqueous** phosphate buffer (20 mmol L<sup>-1</sup>, pH 7) containing **25** mmol L<sup>-1</sup> SDS; sample solvent under sweeping conditions: **10% methanolic** phosphate buffer (20 mmol L<sup>-1</sup>, pH 7); for other experimental parameters refer to Figure S-6.

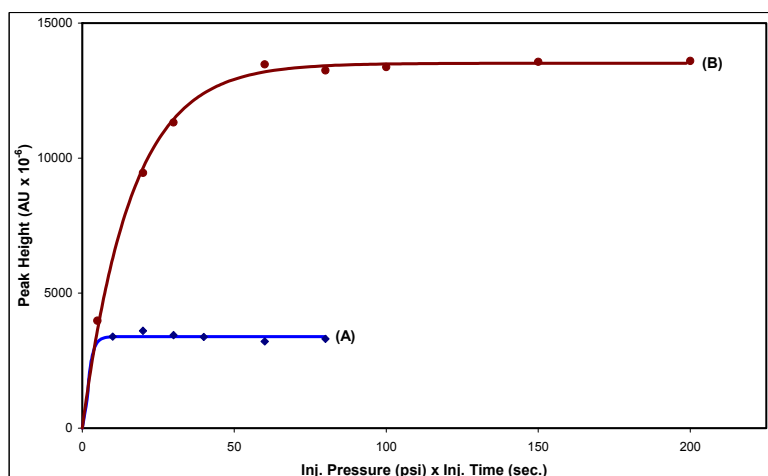


**Figure S-15:** Peak height plotted against injected volume for **ethylparaben** under (A) conventional conditions (analyte dissolved in BGE), (B) sweeping conditions (analyte dissolved in phosphate buffer) . BGE: **aqueous** phosphate buffer (20 mmol L<sup>-1</sup>, pH 7) containing **50** mmol L<sup>-1</sup> SDS; sample solvent under sweeping conditions: **10% methanolic** phosphate buffer (20 mmol L<sup>-1</sup>, pH 7); for other experimental parameters refer to Figure S-6.

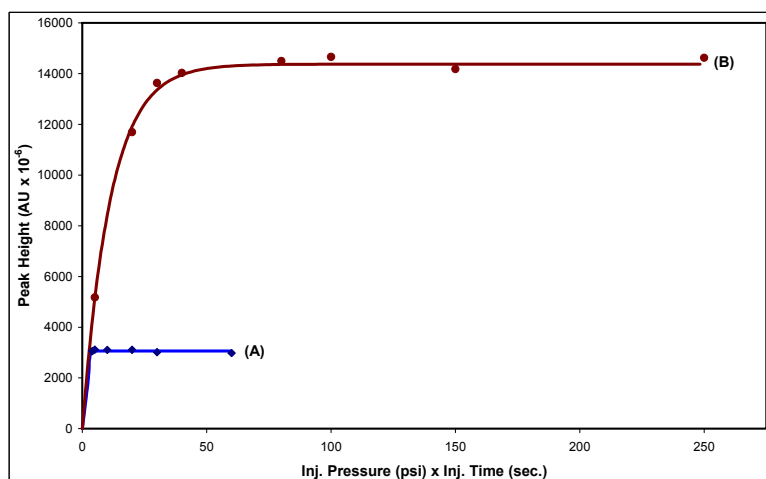


**Figure S-16:** Peak height plotted against injected volume for **propylparaben** under (A) conventional conditions (analyte dissolved in BGE), (B) sweeping conditions (analyte dissolved in phosphate buffer) . BGE: **aqueous** phosphate buffer (20 mmol L<sup>-1</sup>, pH 7) containing **25** mmol L<sup>-1</sup> SDS; sample solvent under sweeping conditions: **10% methanolic** phosphate buffer (20 mmol L<sup>-1</sup>, pH 7); for other experimental parameters refer to Figure S-6.

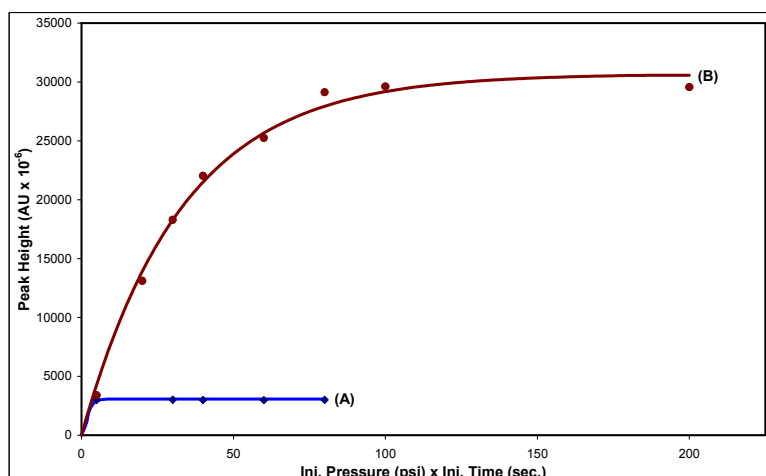


**Figure S-17:** Peak height plotted against injected volume for **propylparaben** under (A) conventional conditions (analyte dissolved in BGE), (B) sweeping conditions (analyte dissolved in phosphate buffer) . BGE: **aqueous** phosphate buffer (20 mmol L<sup>-1</sup>, pH 7) containing **50** mmol L<sup>-1</sup> SDS; sample solvent under sweeping conditions: **10% methanolic** phosphate buffer (20 mmol L<sup>-1</sup>, pH 7); for other experimental parameters refer to Figure S-6.

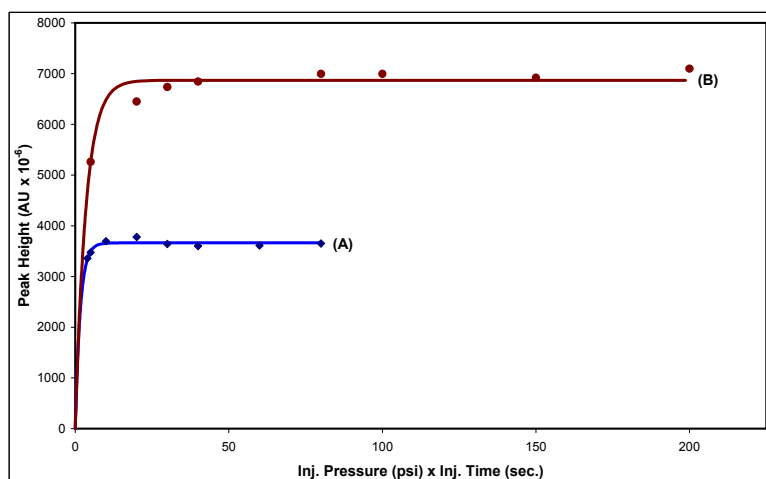


**Figure S-18:** Peak height plotted against injected volume for **ethylparaben** under (A) conventional conditions (analyte dissolved in BGE), (B) sweeping conditions (analyte dissolved in phosphate buffer) . BGE: **aqueous** phosphate buffer (20 mmol L<sup>-1</sup>, pH 7) containing **25** mmol L<sup>-1</sup> SDS; sample solvent under sweeping conditions: **10% ethanolic** phosphate buffer (20 mmol L<sup>-1</sup>, pH 7); for other experimental parameters refer to Figure S-6.

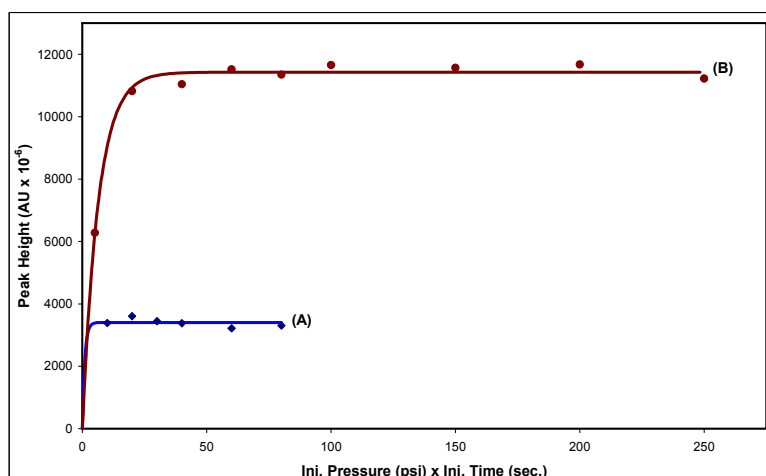


**Figure S-19:** Peak height plotted against injected volume for **ethylparaben** under (A) conventional conditions (analyte dissolved in BGE), (B) sweeping conditions (analyte dissolved in phosphate buffer) . BGE: **aqueous** phosphate buffer (20 mmol L<sup>-1</sup>, pH 7) containing **50** mmol L<sup>-1</sup> SDS; sample solvent under sweeping conditions: **10% ethanolic** phosphate buffer (20 mmol L<sup>-1</sup>, pH 7); for other experimental parameters refer to Figure S-6.

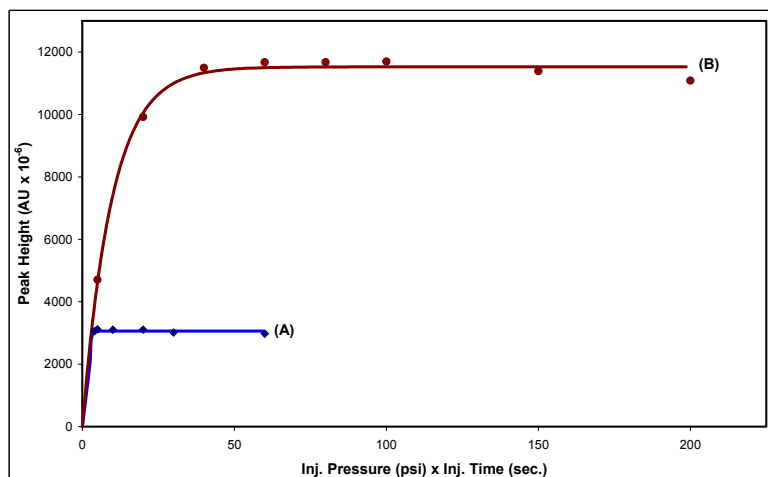


**Figure S-20:** Peak height plotted against injected volume for **propylparaben** under (A) conventional conditions (analyte dissolved in BGE), (B) sweeping conditions (analyte dissolved in phosphate buffer) . BGE: **aqueous** phosphate buffer (20 mmol L<sup>-1</sup>, pH 7) containing **25** mmol L<sup>-1</sup> SDS; sample solvent under sweeping conditions: **10% ethanolic** phosphate buffer (20 mmol L<sup>-1</sup>, pH 7); for other experimental parameters refer to Figure S-6.

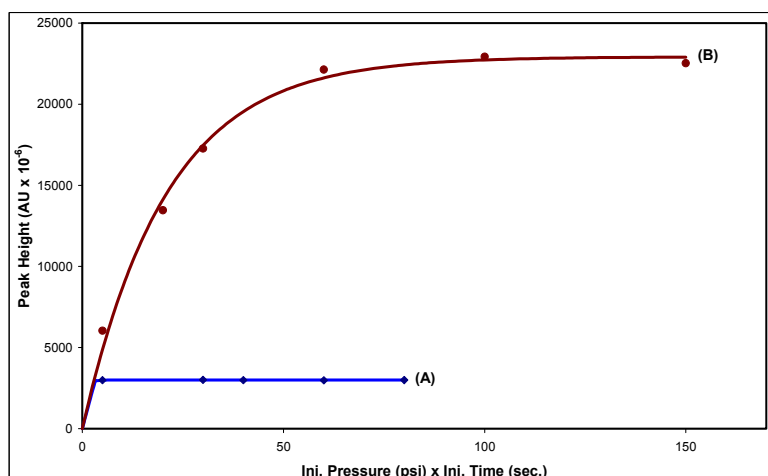


**Figure S-21:** Peak height plotted against injected volume for **propylparaben** under (A) conventional conditions (analyte dissolved in BGE), (B) sweeping conditions (analyte dissolved in phosphate buffer) . BGE: **aqueous** phosphate buffer (20 mmol L<sup>-1</sup>, pH 7) containing **50** mmol L<sup>-1</sup> SDS; sample solvent under sweeping conditions: **10% ethanolic** phosphate buffer (20 mmol L<sup>-1</sup>, pH 7); for other experimental parameters refer to Figure S-6.

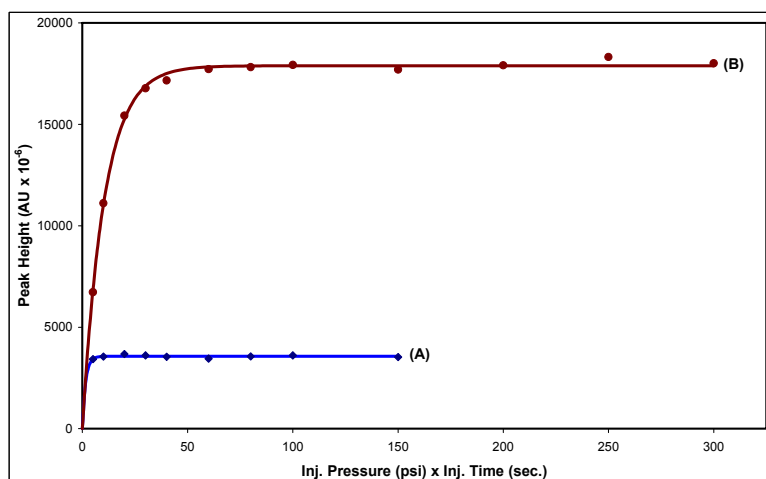


**Figure S-22:** Peak height plotted against injected volume for **ethylparaben** under (A) conventional conditions (analyte dissolved in BGE), (B) sweeping conditions (analyte dissolved in phosphate buffer) . BGE: **10% methanolic** phosphate buffer (20 mmol L<sup>-1</sup>, pH 7) containing **25** mmol L<sup>-1</sup> SDS; sample solvent under sweeping conditions: **aqueous** phosphate buffer (20 mmol L<sup>-1</sup>, pH 7); for other experimental parameters refer to Figure S-6.

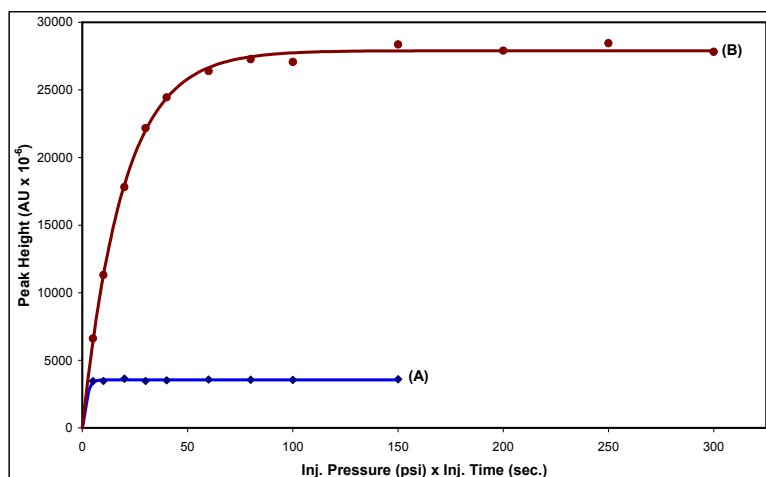


**Figure S-23:** Peak height plotted against injected volume for **ethylparaben** under (A) conventional conditions (analyte dissolved in BGE), (B) sweeping conditions (analyte dissolved in phosphate buffer) . BGE: **10% methanolic** phosphate buffer (20 mmol L<sup>-1</sup>, pH 7) containing **50** mmol L<sup>-1</sup> SDS; sample solvent under sweeping conditions: **aqueous** phosphate buffer (20 mmol L<sup>-1</sup>, pH 7); for other experimental parameters refer to Figure S-6.

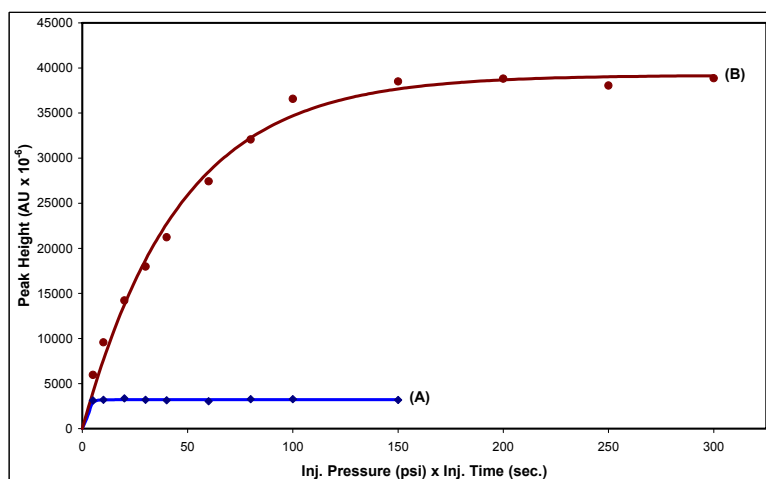


**Figure S-24:** Peak height plotted against injected volume for **propylparaben** under (A) conventional conditions (analyte dissolved in BGE), (B) sweeping conditions (analyte dissolved in phosphate buffer) . BGE: **10% methanolic** phosphate buffer (20 mmol L<sup>-1</sup>, pH 7) containing **25** mmol L<sup>-1</sup> SDS; sample solvent under sweeping conditions: **aqueous** phosphate buffer (20 mmol L<sup>-1</sup>, pH 7); for other experimental parameters refer to Figure S-6.

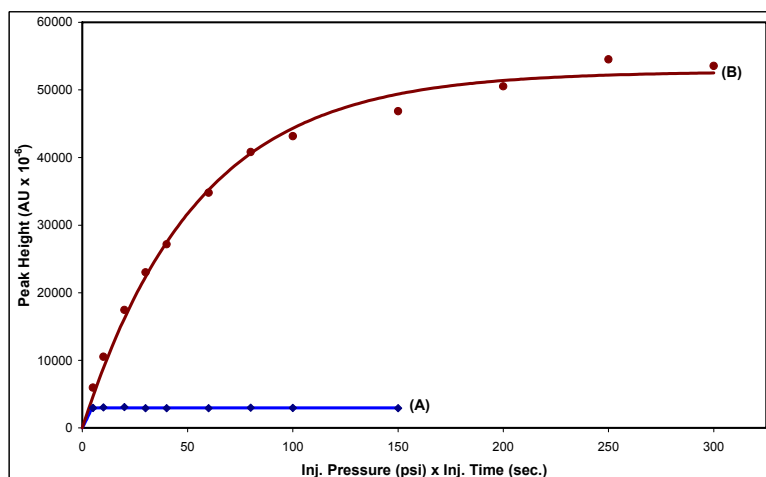


**Figure S-25:** Peak height plotted against injected volume for **propylparaben** under (A) conventional conditions (analyte dissolved in BGE), (B) sweeping conditions (analyte dissolved in phosphate buffer) . BGE: **10% methanolic** phosphate buffer (20 mmol L<sup>-1</sup>, pH 7) containing **50** mmol L<sup>-1</sup> SDS; sample solvent under sweeping conditions: **aqueous** phosphate buffer (20 mmol L<sup>-1</sup>, pH 7); for other experimental parameters refer to Figure S-6.

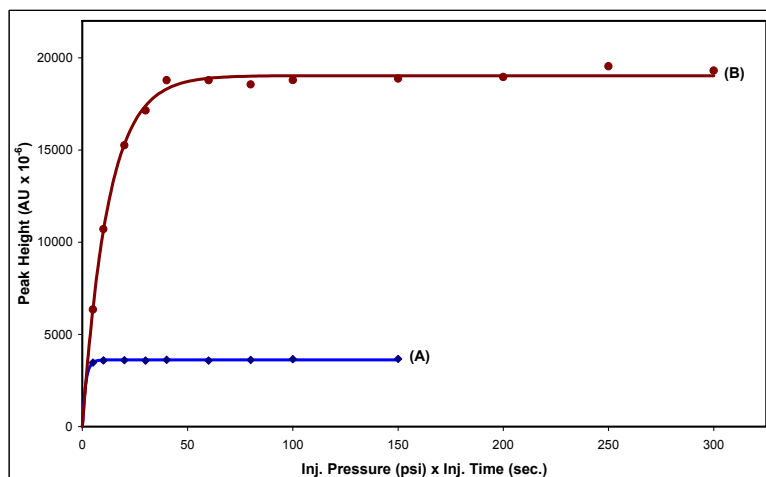


**Figure S-26:** Peak height plotted against injected volume for **ethylparaben** under (A) conventional conditions (analyte dissolved in BGE), (B) sweeping conditions (analyte dissolved in phosphate buffer) . BGE: **10% ethanolic** phosphate buffer (20 mmol L<sup>-1</sup>, pH 7) containing **25** mmol L<sup>-1</sup> SDS; sample solvent under sweeping conditions: **aqueous** phosphate buffer (20 mmol L<sup>-1</sup>, pH 7); for other experimental parameters refer to Figure S-6.

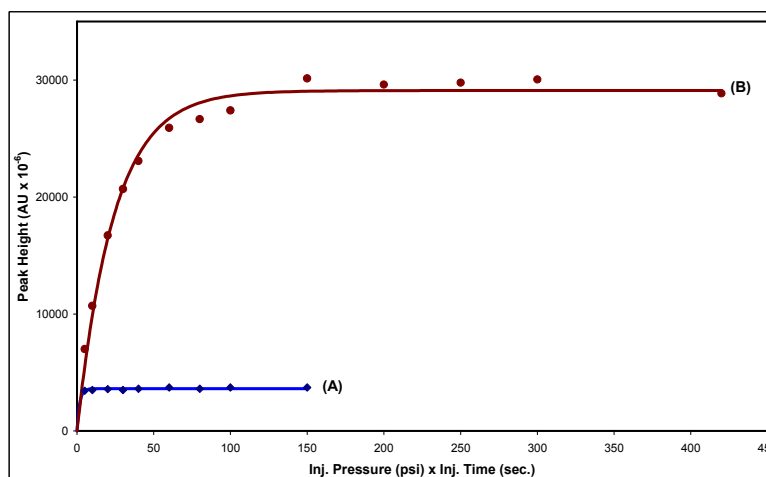


**Figure S-27:** Peak height plotted against injected volume for **ethylparaben** under (A) conventional conditions (analyte dissolved in BGE), (B) sweeping conditions (analyte dissolved in phosphate buffer) . BGE: **10% ethanolic** phosphate buffer (20 mmol L<sup>-1</sup>, pH 7) containing **50** mmol L<sup>-1</sup> SDS; sample solvent under sweeping conditions: **aqueous** phosphate buffer (20 mmol L<sup>-1</sup>, pH 7); for other experimental parameters refer to Figure S-6.

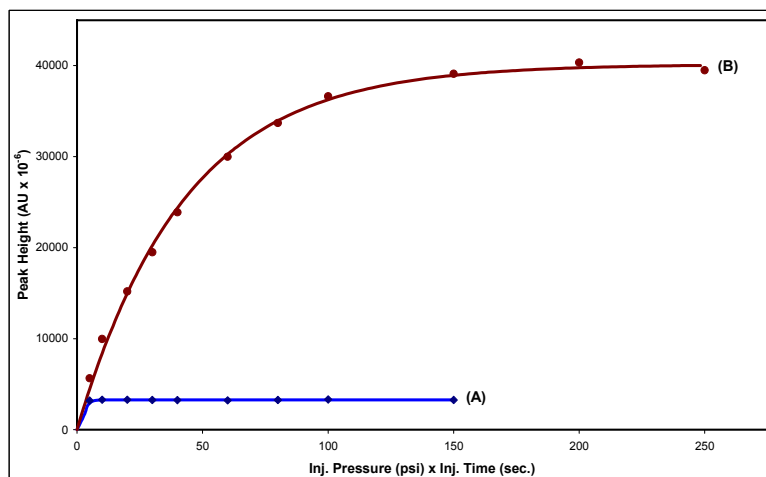


**Figure S-28:** Peak height plotted against injected volume for **propylparaben** under (A) conventional conditions (analyte dissolved in BGE), (B) sweeping conditions (analyte dissolved in phosphate buffer) . BGE: **10% ethanolic** phosphate buffer (20 mmol L<sup>-1</sup>, pH 7) containing **25** mmol L<sup>-1</sup> SDS; sample solvent under sweeping conditions: **aqueous** phosphate buffer (20 mmol L<sup>-1</sup>, pH 7); for other experimental parameters refer to Figure S-6.

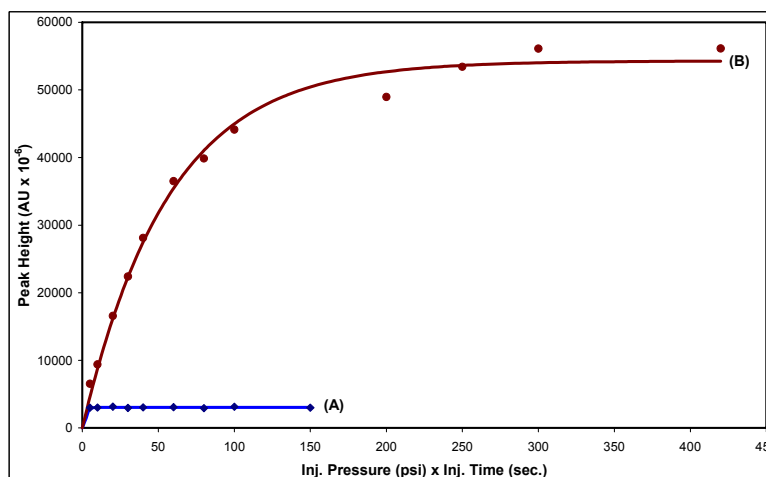


**Figure S-29:** Peak height plotted against injected volume for **propylparaben** under (A) conventional conditions (analyte dissolved in BGE), (B) sweeping conditions (analyte dissolved in phosphate buffer) . BGE: **10% ethanolic** phosphate buffer (20 mmol L<sup>-1</sup>, pH 7) containing **50** mmol L<sup>-1</sup> SDS; sample solvent under sweeping conditions: **aqueous** phosphate buffer (20 mmol L<sup>-1</sup>, pH 7); for other experimental parameters refer to Figure S-6.

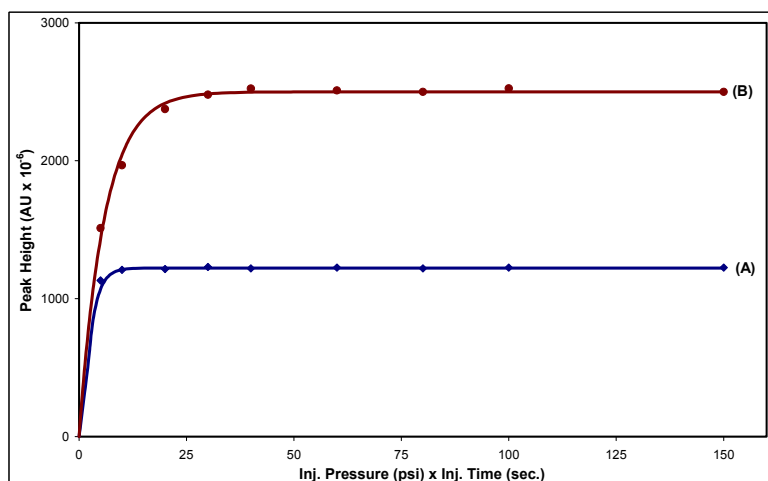


**Figure S-30:** Peak height plotted against injected volume for **benzamide** under (A) conventional conditions (analyte dissolved in BGE), (B) sweeping conditions (analyte dissolved in borate buffer). BGE: **aqueous** borate buffer (10 mmol L<sup>-1</sup>, pH 9.00) containing **75** mmol L<sup>-1</sup> SDS; sample solvent under sweeping conditions: **aqueous** borate buffer (10 mmol L<sup>-1</sup>, pH 9.00); injection: hydrodynamic; capillary: fused-silica capillary (50  $\mu$ m I.D., 362  $\mu$ m O.D.) with a total length of 60.9 cm and a length to the detector of 50.7 cm; temperatures of the capillary and the sample tray: 25°C; voltage: +15 kV; detection wavelength: 254 nm [Reprinted from M. El-Awady, C. Huhn, U. Pyell, J. Chromatogr. A 1264 (2012) 124, copyright 2012, with permission from Elsevier].

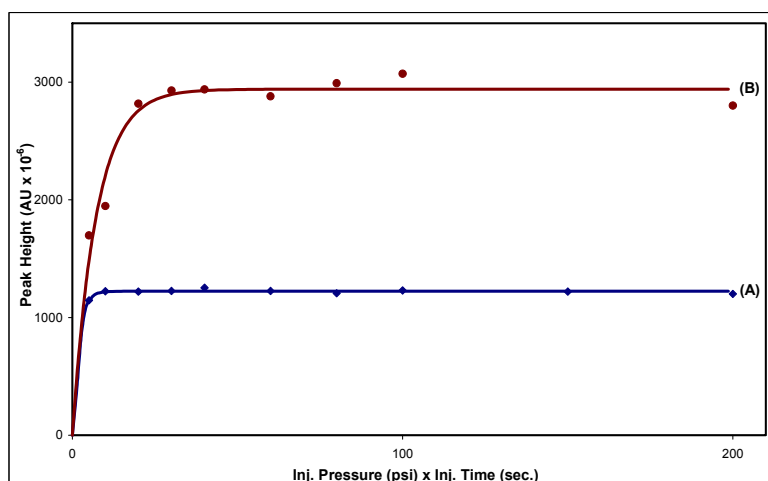


**Figure S-31:** Peak height plotted against injected volume for **benzamide** under (A) conventional conditions (analyte dissolved in BGE), (B) sweeping conditions (analyte dissolved in borate buffer). BGE: **aqueous** borate buffer (10 mmol L<sup>-1</sup>, pH 9.00) containing **100** mmol L<sup>-1</sup> SDS; sample solvent under sweeping conditions: **aqueous** borate buffer (10 mmol L<sup>-1</sup>, pH 9.00); for other experimental parameters refer to Figure S-30. [Reprinted from M. El-Awady, C. Huhn, U. Pyell, J. Chromatogr. A 1264 (2012) 124, copyright 2012, with permission from Elsevier].

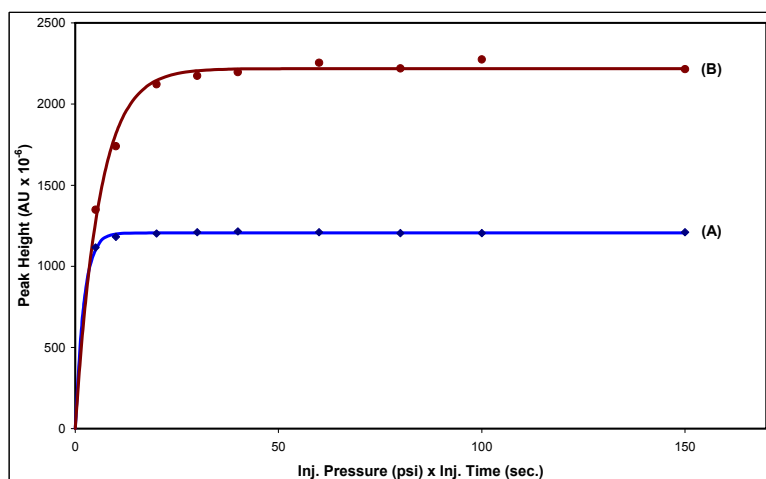


**Figure S-32:** Peak height plotted against injected volume for **benzamide** under (A) conventional conditions (analyte dissolved in BGE), (B) sweeping conditions (analyte dissolved in borate buffer). BGE: **10% methanolic** borate buffer (10 mmol L<sup>-1</sup>, pH 9.00) containing **75 mmol L<sup>-1</sup> SDS**; sample solvent under sweeping conditions: **10% methanolic** borate buffer (10 mmol L<sup>-1</sup>, pH 9.00); injection: hydrodynamic; capillary: fused-silica capillary (50  $\mu$ m I.D., 362  $\mu$ m O.D.) with a total length of 60.9 cm and a length to the detector of 50.7 cm; temperatures of the capillary: 25°C and of the sample tray: 15°C; voltage: +15 kV; detection wavelength: 254 nm.

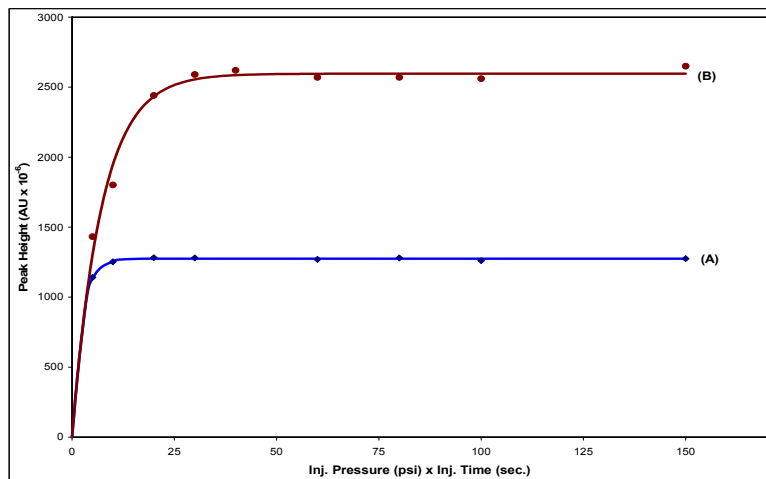


**Figure S-33:** Peak height plotted against injected volume for **benzamide** under (A) conventional conditions (analyte dissolved in BGE), (B) sweeping conditions (analyte dissolved in borate buffer). BGE: **10% methanolic** borate buffer (10 mmol L<sup>-1</sup>, pH 9.00) containing **100 mmol L<sup>-1</sup> SDS**; sample solvent under sweeping conditions: **10% methanolic** borate buffer (10 mmol L<sup>-1</sup>, pH 9.00 for other experimental parameters refer to Figure S-32.

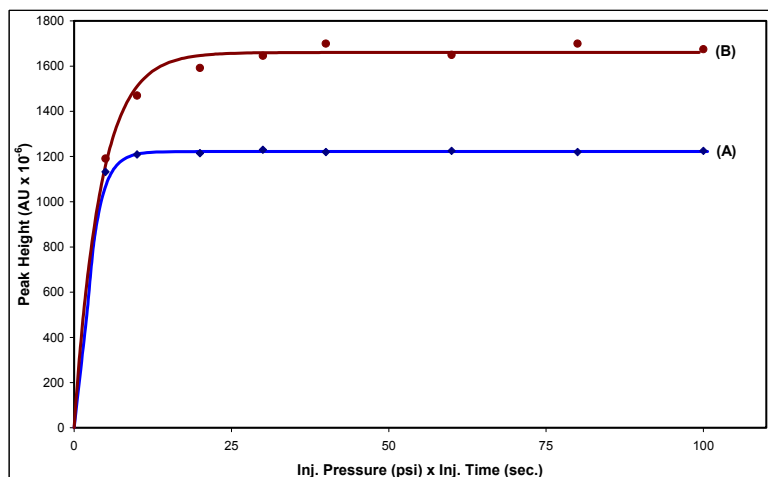


**Figure S-34:** Peak height plotted against injected volume for **benzamide** under (A) conventional conditions (analyte dissolved in BGE), (B) sweeping conditions (analyte dissolved in borate buffer). BGE: **aqueous** borate buffer (10 mmol L<sup>-1</sup>, pH 9.00) containing **75** mmol L<sup>-1</sup> SDS; sample solvent under sweeping conditions: **10% methanolic** borate buffer (10 mmol L<sup>-1</sup>, pH 9.00); for other experimental parameters refer to Figure S-32.

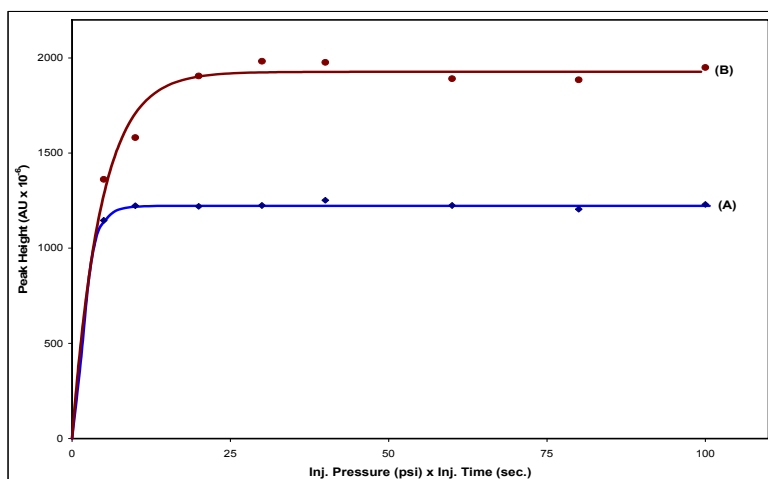


**Figure S-35:** Peak height plotted against injected volume for **benzamide** under (A) conventional conditions (analyte dissolved in BGE), (B) sweeping conditions (analyte dissolved in borate buffer). BGE: **aqueous** borate buffer (10 mmol L<sup>-1</sup>, pH 9.00) containing **100** mmol L<sup>-1</sup> SDS; sample solvent under sweeping conditions: **10% methanolic** borate buffer (10 mmol L<sup>-1</sup>, pH 9.00); for other experimental parameters refer to Figure S-32.

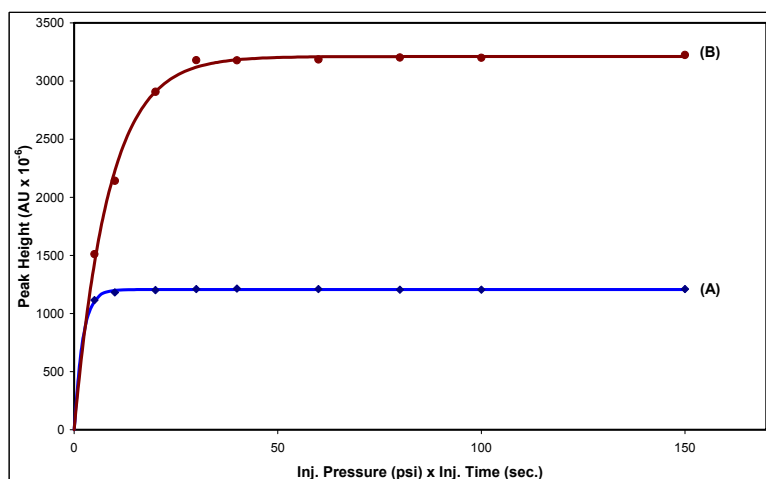


**Figure S-36:** Peak height plotted against injected volume for **benzamide** under (A) conventional conditions (analyte dissolved in BGE), (B) sweeping conditions (analyte dissolved in borate buffer). BGE: **10% methanolic** borate buffer (10 mmol L<sup>-1</sup>, pH 9.00) containing **75** mmol L<sup>-1</sup> SDS; sample solvent under sweeping conditions: **aqueous** borate buffer (10 mmol L<sup>-1</sup>, pH 9.00); for other experimental parameters refer to Figure S-32.

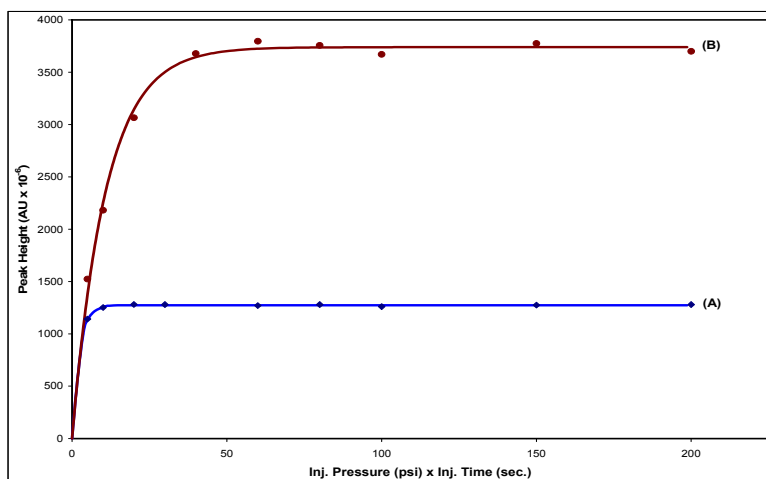


**Figure S-37:** Peak height plotted against injected volume for **benzamide** under (A) conventional conditions (analyte dissolved in BGE), (B) sweeping conditions (analyte dissolved in borate buffer). BGE: **10% methanolic** borate buffer (10 mmol L<sup>-1</sup>, pH 9.00) containing **100** mmol L<sup>-1</sup> SDS; sample solvent under sweeping conditions: **aqueous** borate buffer (10 mmol L<sup>-1</sup>, pH 9.00); for other experimental parameters refer to Figure S-32.

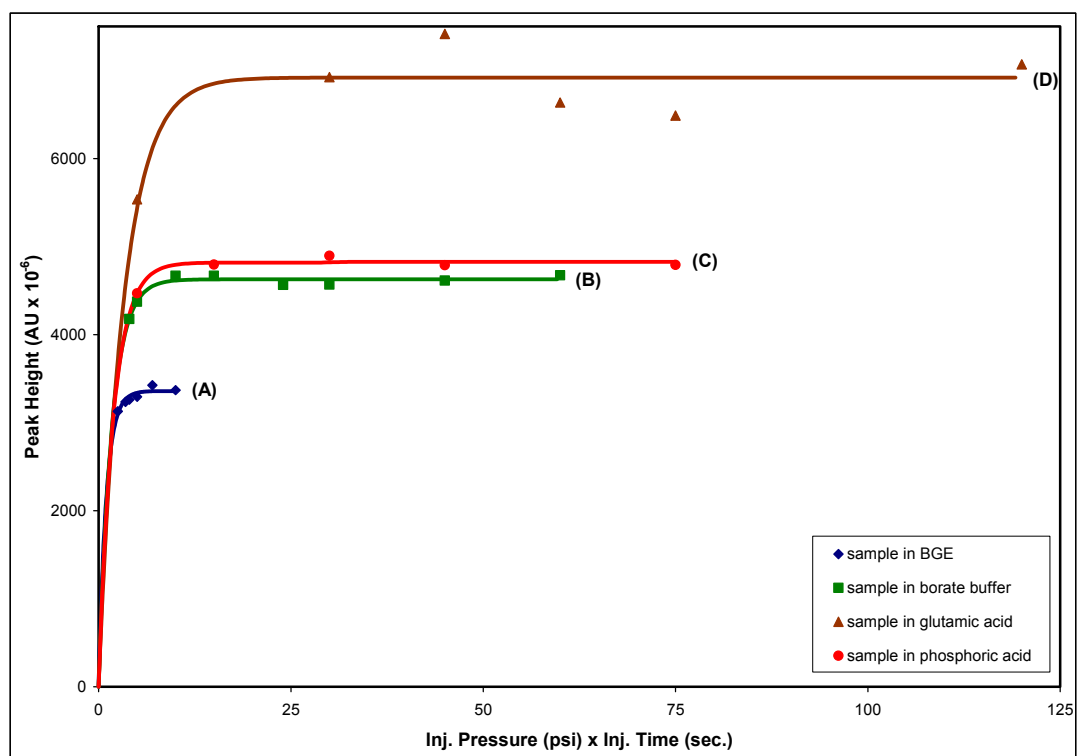


**Figure S-38:** Peak height plotted against injected volume for **aniline** under (A) conventional conditions (analyte dissolved in BGE), (B) sweeping conditions with analyte dissolved in 10 mmol L<sup>-1</sup> borate buffer, pH 9.37, (C) sweeping conditions with analyte dissolved in 10 mmol L<sup>-1</sup> phosphoric acid, pH 3.5, (D) sweeping conditions with analyte dissolved in 10 mmol L<sup>-1</sup> glutamic acid, pH 3.35. BGE: 10 mmol L<sup>-1</sup> borate buffer, pH 9.37 containing 50 mmol L<sup>-1</sup> SDS; injection: hydrodynamic; capillary: fused silica-capillaries (50  $\mu$ m I.D., 362  $\mu$ m O.D.) with a total length of 50.65 cm and a length to the detector of 40.25 cm; temperatures of the capillary and the sample tray: 25°C; voltage: +22 kV; detection wavelength: 254 nm.

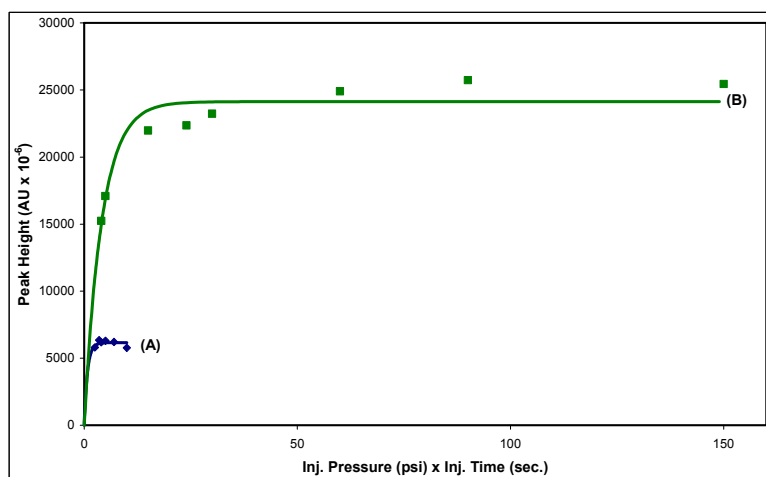


**Figure S-39:** Peak height plotted against injected volume for **4-ethylaniline** under (A) conventional conditions (analyte dissolved in BGE), (B) sweeping conditions (analyte dissolved in 10 mmol L<sup>-1</sup> borate buffer, pH 9.37). BGE: 10 mmol L<sup>-1</sup> borate buffer, pH 9.37 containing 50 mmol L<sup>-1</sup> SDS; for other experimental parameters refer to Figure S-38. [Reprinted from M. El-Awady, C. Huhn, U. Pyell, J. Chromatogr. A 1264 (2012) 124, the online supplementary data, copyright 2012, with permission from Elsevier].

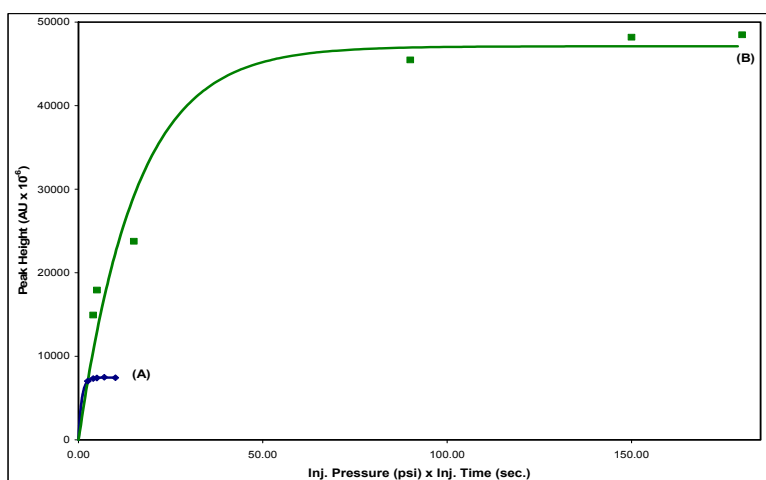


**Figure S-40:** Peak height plotted against injected volume for **4-butylaniline** under (A) conventional conditions (analyte dissolved in BGE), (B) sweeping conditions (analyte dissolved in 10 mmol L<sup>-1</sup> borate buffer, pH 9.37). BGE: 10 mmol L<sup>-1</sup> borate buffer, pH 9.37 containing 50 mmol L<sup>-1</sup> SDS; for other experimental parameters refer to Figure S-38.



---

---

This is a License Agreement between Mohamed El-Awady ("You") and Elsevier ("Elsevier") provided by Copyright Clearance Center ("CCC"). The license consists of your order details, the terms and conditions provided by Elsevier, and the payment terms and conditions.

**All payments must be made in full to CCC. For payment instructions, please see information listed at the bottom of this form.**

Supplier	Elsevier Limited The Boulevard,Langford Lane Kidlington,Oxford,OX5 1GB,UK
Registered Company Number	1982084
Customer name	Mohamed El-Awady
Customer address	University of Marburg, Marburg, Hesse 35032
License number	3167350967090
License date	Jun 13, 2013
Licensed content publisher	Elsevier
Licensed content publication	Journal of Chromatography A
Licensed content title	Sweeping as a multistep enrichment process in micellar electrokinetic chromatography: The retention factor gradient effect
Licensed content author	Mohamed El-Awady,Ute Pyell
Licensed content date	5 July 2013
Licensed content volume number	1297
Licensed content issue number	
Number of pages	13
Start Page	213
End Page	225
Type of Use	reuse in a thesis/dissertation
Intended publisher of new work	other
Portion	full article
Format	both print and electronic
Are you the author of this Elsevier article?	Yes
Will you be translating?	No
Order reference number	
Title of your thesis/dissertation	Investigation of sweeping as sample enrichment method in micellar electrokinetic chromatography in the analysis of pharmaceutical preparations and biological fluids
Expected completion date	Jul 2013



### **5.3. Publication III**

**Processes involved in sweeping as sample enrichment method in cyclodextrin-modified micellar electrokinetic chromatography of hydrophobic basic analytes**

Mohamed El-Awady, Ute Pyell

*Submitted to: Electrophoresis*



### **5.3.1. Summary and discussion**

In this publication, we first theoretically discuss possible underlying processes involved in the sweeping mechanism with a special focus on the retention factor gradient effect (RFGE), the combination of sweeping with dynamic pH junction and the effect of adsorption onto the capillary wall especially for hydrophobic basic analytes. The applicability of our developed method for the assessment of sweeping efficiency in cyclodextrin-modified MEKC (CD-MEKC) is confirmed taking ethylparaben (pharmaceutical preservative) as an example of acidic analytes and desloratadine (antihistaminic drug) as an example of basic analytes. Different types of  $\beta$ -cyclodextrins are investigated in the present study using SDS-containing borate buffer (pH = 9.30) as the the background electrolyte (BGE). Those considerations made in the second publication of this dissertation regarding the RFGE as an additional step affecting the reachable sweeping efficiency are also confirmed in sweeping-CD-MEKC using ethylparaben as a studied analyte. In this case, the apparent distribution coefficient differs for the sample and the BGE due to different content of CD as a complex-forming agent. Moreover, the RFGE is confirmed for the more general case in which the difference in the apparent distribution coefficient is also due to different pH in the sample and in the BGE (dynamic pH junction).

Although desloratadine is significantly more hydrophobic than ethylparaben, it shows an unexpectedly low enrichment factor using a basic BGE and an acidic sample matrix. In contrast to our expectation, the enrichment factor for desloratadine is nearly unaffected by the addition of different types and concentrations of cyclodextrin to the BGE. Moreover, the obtained enrichment factors for desloratadine are significantly lower than those obtained with the less hydrophobic anilines studied in the second publication of this dissertation. This unexpected behavior is attributed to the strong adsorption of this protonated hydrophobic basic analyte onto the inner wall of the capillary only in the sample zone. Adsorption onto the inner capillary wall exclusively within the sample zone can reduce the focusing efficiency dramatically without impairing resolution and efficiency in the subsequent separation step. This effect is confirmed by the improvement in the enrichment factor achieved by the addition of triethylamine (dynamic coating agent) to the sample solution.

It can be concluded from the obtained results that in case of CD-MEKC with a sample solution having a pH different from that of the BGE (i.e. dynamic pH junction-sweeping-CD-MEKC), different effects are simultaneously contributing to the final overall enrichment factor including the RFGE, focusing by dynamic pH junction and adsorption onto the inner capillary wall within the sample zone. The addition of a dynamic coating agent exclusively to the sample matrix is a promising approach to improve the focusing efficiency without having a negative impact on the separation.

## **5.3.2. Author contribution**

The design of experiments and all the practical steps of this study were carried out by me. The draft of the manuscript was written by me and corrected by Prof. Ute Pyell. The final revision of the manuscript was conducted by me and Prof. Pyell before submission to the journal. Prof. Ute Pyell was responsible for the supervision of this work.

**5.3.3. Processes involved in sweeping as sample enrichment method in cyclodextrin-modified micellar electrokinetic chromatography of hydrophobic basic analytes**

Mohamed El-Awady, Ute Pyell\*

University of Marburg, Department of Chemistry, Hans-Meerwein-Straße, D-35032 Marburg, Germany

\* corresponding author

**Tel.: +49 6421 2822192**

**Fax: +49 6421 2822124**

**e-mail: [pyellu@staff.uni-marburg.de](mailto:pyellu@staff.uni-marburg.de)**

**Keywords**

Cyclodextrin-modified micellar electrokinetic chromatography; Sweeping; Retention factor gradient effect; Dynamic pH junction; Adsorption; Dynamic coating.

## Abstract

Sweeping has been described as a multistep enrichment method in MEKC including stacking/destacking of the micelles, sweeping of analytes by the stacked/destacked micelles, destacking/stacking of the swept analyte zone and retention factor gradient effect (RFGE). In this study we additionally focus on dynamic pH junction and adsorption of the analyte onto the capillary wall (especially with hydrophobic basic analytes). Our new method for the assessment of sweeping efficiency is further extended to cyclodextrin-modified MEKC (CD-MEKC) taking ethylparaben (pharmaceutical preservative) as an example of acidic analytes and desloratadine (antihistaminic drug) as an example of basic analytes using different types of  $\beta$ -cyclodextrins. Our previous study of RFGE as an additional focusing/defocusing effect in sweeping-MEKC is confirmed for the case that the apparent distribution coefficient differs for the sample and the background electrolyte (BGE) due to different content of a complex-forming agent like cyclodextrin and due to a pH difference between the sample and the BGE (dynamic pH junction). Despite being significantly more hydrophobic than ethylparaben, desloratadine shows an unexpectedly low enrichment factor. Moreover, this enrichment factor is nearly unaffected by the addition of cyclodextrin to the BGE. This unexpected behavior is attributed to the strong adsorption of the protonated hydrophobic basic analyte onto the inner wall of the capillary in the sample zone that significantly counteracts the sweeping process, which is confirmed by the improvement in the enrichment factor achieved by the addition of a dynamic coating agent to the sample solution.

## 1. Introduction

It is well-known that capillary electromigration separation techniques suffer from poor sensitivity due to the limited injection volume of the sample as well as the short optical path length caused by using on-line detection. Therefore, on-line preconcentration techniques are very necessary for overcoming this problem. Sweeping is one of the most important sample preconcentration techniques in MEKC. It is based on the accumulation of analyte molecules by the pseudostationary phase (PSP) that penetrates the sample zone being void of PSP [1]. Investigations related to sweeping have been early described by some authors but under different names [2, 3]. In 1998, the concept of sweeping was introduced by Quirino and Terabe [1]. They investigated neutral analytes dissolved in matrices having the same electric conductivity as the BGE using sodium dodecyl sulfate (SDS) as anionic surfactant. In 1999, more investigations on the sweeping phenomenon and the role of analyte charge and electroosmotic flow were performed by the same authors including sweeping under homogeneous and inhomogeneous electric field conditions [4, 5]. Very soon, sweeping was further applied by Kim *et al.* [6] using cationic surfactants. In a similar approach, Palmer *et al.* [7] used electokinetic injection of a sample containing neutral analytes dissolved in BGE void of micelles.

Sweeping is most efficient for analytes with high distribution coefficients regarding distribution between the micellar phase (or another PSP) and the aqueous phase. As reported by Quirino and Terabe [1], the length of the sample zone after sweeping  $l_{\text{sweep}}$  depends on the initial sample plug length  $l_{\text{inj}}$  and on the retention factor in the sample zone during sweeping  $k_s$ . Hence, the enrichment factor ( $= l_{\text{inj}}/l_{\text{sweep}}$ ) is directly proportional to  $k_s$  as shown in the following equation:

$$l_{\text{sweep}} = \frac{1}{1 + k_s} l_{\text{inj}} \quad (1)$$

However, we showed experimentally and theoretically in our previous publication [8] that the focusing process due to sweeping is not only influenced by the retention factor of the analyte in the sample zone, but also by the retention factor of the analyte in the BGE.

A debate on the effect of different electric conductivities between the sample and BGE on the reachable enrichment factor can be found in the literature [5, 9-13]. In our publication [14] on processes involved in sweeping under inhomogeneous electric field conditions, we were able to show experimentally and theoretically that the enrichment factor obtained by sweeping is - within the experimental range - independent of the electric conductivity of the sample matrix, provided that no micellar transient isotachopheresis takes place and that the distribution coefficient  $K_D$  of the analyte (regarding distribution between the PSP and the surrounding phase) in the sample and in the BGE is identical. Very soon, we confirmed that even in the general case (different  $K_D$  in the sample and the BGE as in case of different

organic solvent contents, different contents of a complex-forming agent like CD or borate, or different pH), the enrichment efficiency due to sweeping is in first approximation independent of the electric conductivity of the sample matrix [8].

The analysis of highly hydrophobic analytes by MEKC is usually problematic because these compounds tend to be totally incorporated into the micelles and therefore co-migrate at the velocity of micelles rendering their separation very difficult [15]. To overcome this problem, different approaches have been investigated like the use of bile salt surfactants instead of long alkyl chain surfactants [16, 17] or the use of different modifiers added to the BGE like organic solvents [18-23], organic silanating reagents to modify the inner surface of the capillary [24], urea [21, 23, 25, 26] and cyclodextrin (CD-MEKC) [27-30]. CDs can form inclusion complexes with a variety of hydrophobic and hydrophilic analytes [31-33]. These inclusion complexes are usually characterized by a 1:1 stoichiometry, although a 2:1 stoichiometry is occasionally reported [34]. In CD-MEKC, the analyte is formally distributed among three pseudophases; the micellar phase, CD (complexed analyte) and the aqueous phase although CD is dissolved in the aqueous phase. The separation in CD-MEKC depends on the presence of coupled equilibria, a distribution equilibrium regarding the distribution of analyte between the aqueous phase and the micelles as well as a complexation equilibrium between the analyte and CD. The interaction between the analyte molecules and the micelles is based on hydrophobic and/or ionic interactions while the interaction with CD is a host-guest (inclusion) complexation that is mainly influenced by steric parameters, hydrophobic interactions, and by the possibility of hydrogen bond formation based on the fitting of the analyte molecule with the CD cavity. If the analyte molecule is included in the CD cavity, it is transported with the electroosmotic velocity because CD itself is electrically neutral while it migrates with the micellar velocity if it is incorporated into the micelle. Therefore, the optimum separation can be achieved by compromising between these two possibilities [15, 27]. The applications of CD-MEKC have been reviewed in several articles [35-39].

In the present work, we first theoretically discuss possible underlying processes involved in the sweeping mechanism with a special focus on the RFGE, the combination of sweeping with dynamic pH junction and the effect of adsorption onto the capillary wall especially for hydrophobic basic analytes. Then our previous study of the RFGE [8] is further extended to CD-MEKC where the apparent distribution coefficient differs for the sample and the background electrolyte (BGE) due to different content of CD as a complex-forming agent. Weakly acidic ethylparaben and weakly basic desloratadine are investigated during this study using SDS-containing borate buffer (pH = 9.30) as BGE. Ethylparaben is a well-known pharmaceutical preservative while desloratadine is a non-sedating antihistaminic drug and it is also the major active metabolite of loratadine as well as one of its impurities [40, 41]. Different

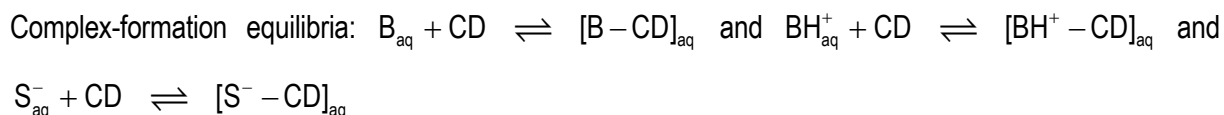
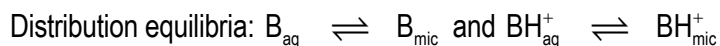
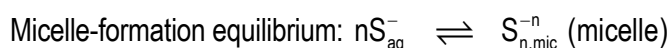
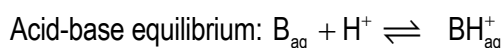
types of  $\beta$ -CD are studied. The effect of pH variation between the sample and the BGE (dynamic pH junction) is discussed. Moreover, the negative impact on the sweeping efficiency due to adsorption of the analyte onto the capillary wall in the sample compartment and the positive effect of addition of dynamic coating reagents to the sample matrix to minimize this problem are demonstrated. Throughout the study the enrichment factors are measured by using the method described in the first part of this series [14] which eliminates errors due to varied migration times and hydrodynamic dispersion as a consequence of local EOF velocity differences [42-44]. To the best of our knowledge, this is the first study describing the impact of wall adsorption exclusively in the sample zone with regard to sweeping efficiency and peak distortion.

## 2. Theoretical considerations

It should be noted here that we define CD in this discussion and in the following text to be a native or a derivatized neutral cyclodextrin.

### 2.1. Equilibria involved in CD-MEKC

For better understanding of the processes employed in CD-MEKC, different equilibria should be taken into consideration. These include the simple acid-base equilibrium of weak acids or weak bases, the micelle-formation equilibrium, the distribution equilibria and the complex-formation equilibria. The distribution equilibria refer to the distribution of both the ionized and non-ionized forms of the analyte between the aqueous phase and the micellar phase. The complex-formation equilibria refer to the formation of inclusion complexes between CD and both the ionized and non-ionized forms of the analyte as well as the surfactant monomers. For a basic analyte B and an anionic surfactant S (where S is the surfactant monomer), the involved equilibria under CD-MEKC conditions can be summarized as follows:



By addition of CD to the BGE the apparent distribution coefficient  $K_{D,\text{app}}$  is altered which can be defined as the ratio of the sum of the concentrations of all forms of the analyte (ionized and non-ionized) in the micellar phase and the sum of the concentrations of all forms of the analyte (ionized and non-ionized in the free and complexed forms) in the aqueous phase.  $K_{D,\text{app}}$  can be calculated by as follows:

$$K_{D,\text{app}} = \frac{c(B_{\text{mic}}) + c(BH_{\text{mic}}^+)}{c(B_{\text{aq}}) + c(BH_{\text{aq}}^+) + c([B - CD]_{\text{aq}}) + c([BH^+ - CD]_{\text{aq}})} \quad (2)$$

whereas the apparent retention factor  $k_{\text{app}}$  is defined as:

$$k_{\text{app}} = K_{D,\text{app}} \cdot \frac{V_{\text{mic}}}{V_{\text{aq}}} \quad (3)$$

where  $V_{\text{mic}}/V_{\text{aq}}$  is the phase ratio (= volume of micellar phase/volume of aqueous phase).

## 2.2. Processes involved in sweeping as a multistep enrichment method

Sweeping in MEKC can be described as a multistep enrichment method because several processes should be considered upon investigation of this technique. These processes include: (i) stacking or destacking of the micelles entering the sample zone at the boundary BGE/sample, (ii) sweeping of the analytes by the stacked or destacked micelles, (iii) destacking or stacking of the swept zone at the boundary sample/BGE, (iv) retention factor gradient effect (RFGE), (v) dynamic pH junction and (vi) adsorption (especially in case of hydrophobic basic analytes).

The first three processes were discussed in detail in our previous publication [14] based on the considerations made by Quirino and Terabe [1, 5], Quirino *et al.* [10, 45] and by Chien and Burgi [46]. In that publication [14], we introduced the phase ratio shift factor  $\theta$  to quantitatively describe the retention factor  $k$  for an analyte in the sample zone assuming that the distribution coefficient  $K_D$  is constant in the the sample and separation zones. In addition, equations that describe sweeping under homogeneous and inhomogeneous electric field conditions were derived and the final length of the focused sample zone  $l_{\text{focus}}$  after completion of the sweeping process could be calculated from the initial sample-plug length  $l_{\text{inj}}$  using the following equation [14]:

$$l_{\text{focus}} = \frac{1}{\gamma \theta (1 + k_{\text{BGE}})} l_{\text{inj}} \quad (4)$$

where  $\gamma$  = field-strength enhancement factor [46] (= ratio of the electric field strengths in the sample zone and in the BGE ( $E_S/E_{\text{BGE}}$ ) or ratio of the electric conductivities of the BGE and the sample solution ( $\kappa_{\text{BGE}}/\kappa_S$ ));  $\theta$  = phase ratio shift factor or quotient of phase ratios in the sample zone during sweeping and in the BGE ( $\varphi_S/\varphi_{\text{BGE}}$ ). In case of homogeneous electric field conditions, both  $\gamma$  and  $\theta$  equal 1 and Eq. (4) becomes equivalent to Eq. (1), while under inhomogeneous electric field conditions, the product of  $\gamma$  and  $\theta$ , in first approximation, equals 1 and  $l_{\text{focus}}$  becomes independent of the electric conductivity  $\kappa_S$  of the sample matrix.

### 2.2.1. Retention factor gradient effect

In our previous publication [8], we have introduced the term “retention factor gradient effect (RFGE)” to express the additional focusing or defocusing effect that arises if  $k_s$  is different from  $k_{\text{BGE}}$ . RFGE takes place in the BGE compartment next to the sample zone. RFGE can have a significant effect on the reachable sweeping efficiency. The percentage contribution of RFGE to the observed change in the final enrichment factor ranges between 9% and 67% [8]. We have shown that RFGE must be taken into account in all cases where  $K_D$  in the sample zone is not identical to that in the BGE as in case of

different organic solvent contents, different contents of a complex-forming agent like CD or borate, or different pH in the sample and the BGE associated with different degree of ionization of the analyte. According to our investigations, we have defined “the additional focusing/defocusing factor  $f$ ” due to RFGE as the ratio of the final enrichment factor with RFGE and the enrichment factor without RFGE. This factor is related to the retention factor of the solute in the sample solution and in the BGE:

$$f = \frac{l_{\text{sweep}}}{l_{\text{grad}}} = \frac{k_S k_{\text{BGE}} + k_S}{k_S k_{\text{BGE}} + k_{\text{BGE}}} \quad (5)$$

where  $l_{\text{sweep}}$  is the length of the sample zone after sweeping (without RFGE),  $l_{\text{grad}}$  is the final length of the sample zone after sweeping including RFGE,  $k_{\text{BGE}}$  is the retention factor in the BGE and  $k_S$  is the retention factor obtained with a capillary filled with a solution identical to that of the sample matrix with surfactant in identical concentration as the “original” BGE.

By multiplying the factor  $f$  with the sweeping efficiency calculated via Eq. (1) the final enrichment factor due to sweeping with RFGE is accessible [8]:

$$l_{\text{grad}} = \frac{k_S k_{\text{BGE}} + k_{\text{BGE}}}{k_S k_{\text{BGE}} + k_S} \cdot \frac{1}{1 + k_S} l_{\text{inj}} \quad (6)$$

Accordingly, the focusing process is not only affected by the retention factor  $k_S$  of the analyte in the sample zone, but also by the retention factor  $k_{\text{BGE}}$  of the analyte in the BGE. The final enrichment efficiency will be improved with increasing  $k_S$  and decreasing  $k_{\text{BGE}}$ , while it will be decreased with decreasing  $k_S$  and increasing  $k_{\text{BGE}}$ . In [8], we studied the cases in which  $k_S$  is different from  $k_{\text{BGE}}$  due to different organic solvent contents or due to different pH in the sample and the BGE (different degree of protonation or deprotonation of basic or acidic solutes, respectively).

However, RFGE can also be observed with cases in which the retention factor is different between the sample and BGE due to different content of a complex-forming agent like CD. Because of its capacity to form inclusion complexes with a considerable number of analytes (host-guest interaction), CD can significantly alter the apparent retention factor of several analytes by introducing additional complex-formation equilibria as discussed in Section 2.1. CD added to the BGE reduces the apparent distribution coefficient of the analyte between the micellar phase and the aqueous pseudophase by increasing the fraction of analyte in the non-micellar phase resulting in a significant decrease in the apparent retention factor  $k_{\text{BGE, app}}$  [15, 27]. In addition, CD forms an inclusion complex with SDS monomers and that significantly affects the micellization of SDS molecules because the micelle-formation equilibrium is

shifted in favor of the formation of inclusion complexes between SDS monomers and CD. Consequently, the apparent critical micelle concentration ( $CMC_{app}$ ) of SDS increases and that is another reason for the significant decrease of  $k_{BGE, app}$  upon addition of CD to the BGE [47-50]. Therefore and according to Eq. (5) and Eq. (6), the addition of CD to the BGE is expected to lead to an additional focusing effect due to RFGE and consequently enhancing the enrichment efficiency.

### 2.2.2. Dynamic pH junction combined with sweeping

The mechanism of dynamic pH junction is based on the presence of a difference in pH between the sample and the BGE that is associated with a considerable difference in mobility of the analyte at these different pH segments such that when the analyte moves from one pH segment to the other there is a significant change in its mobility. Therefore, the analyte must be a weakly acidic, a weakly basic or an amphoteric compound so that it will be present in two different species differing in their effective charge number. Dynamic pH junction has been used to concentrate several amphoteric, acidic and basic analytes using both low-pH sample/high-pH BGE and high-pH sample/low-pH BGE systems [51]. For example, the preconcentration of epinephrine was achieved by Britz-McKibbin *et al.* [52] based on the presence of a dynamic pH junction between an acidic sample zone and a basic BGE compartment. Epinephrine is an amphoteric compound that has opposing mobilities under acidic and basic conditions. Upon application of the voltage, the hydroxide ions in the BGE migrate through the sample plug and start to raise the pH of the plug where epinephrine acquires a negative charge associated with a significant reduction of its velocity as it migrates at this pH against the EOF leading to focusing of the sample zone. This process is continued until the hydroxide ions reach the rear end of the sample zone. After completion of this process the negatively charged analytes are transported to the detector under the effect of the EOF [52]. Several weakly acidic or basic analytes can acquire different local effective electrophoretic mobilities within the two segments of different pH inside the capillary through a change in their effective charge number dependent on their  $pK_a$  [51]. The first use of dynamic pH junction as a method for improving sensitivity in capillary electromigration techniques was done by Aebersold and Morrison [53] in 1990, although a similar approach was utilized in gels before this date. They were able to achieve five to ten fold improvement in sensitivity for the analysis of a mixture of dilute peptide samples. Between 1998 and 2000, Britz-McKibbin *et al.* [52, 54, 55] and Britz-McKibbin and Chen [56] published a series of papers describing and investigating this focusing method and introduced the term "dynamic pH junction" by which it has been known in the literature. A comprehensive review of the use of dynamic pH junction for online sample preconcentration in capillary electromigration separation techniques was reported by Kazarian *et al.* [51] showing a large variety of sample/BGE combinations (low-pH sample/high-pH BGE and high-pH sample/low-pH BGE) with which the focusing by dynamic pH

junction was possible with several acidic, basic and amphoteric analytes. Kazarian *et al.* [51] stated that both types of sample/BGE combination can be used for both weak acids and weak bases although their literature review revealed that the low-pH sample/high-pH BGE system was most frequently used, with an emphasize that these conditions are strongly dependent on the investigated analytes and their  $pK_a$ .

Generally, the precise description of the mechanism of focusing by a dynamic pH junction is difficult. Those parameters which have to be taken into consideration are: (i) the  $pK_a$  of the analyte, (ii) the pH of the sample matrix and the BGE, (iii) the buffering capacity of the sample matrix and the BGE, and (iv) the exact composition of the sample and the BGE [51]. Determining the direction in which the boundary will move relies on the concentrations of all acidic and basic components in the sample and the BGE, their  $pK_a$  and their ionic mobilities [57].

For the sake of simplicity, a graphical illustration of the changes in the length of an injected sample plug in presence of a dynamic pH junction within an open fused-silica capillary upon application of voltage is presented in Figure 1 based on the discussion made by Kazarian *et al.* [51]. This figure summarizes different possibilities for focusing the analyte zone by using the dynamic pH junction mechanism. It is important here to re-emphasize that the possibility of online sample enrichment by dynamic pH junction is not possible with all analytes because additional parameters must be taken into consideration as described above. The focusing process can be described as follows: a basic analyte is positively charged in acidic pH (relative to the  $pK_a$ ) having a positive effective electrophoretic mobility while in basic pH (relative to the  $pK_a$ ) the analyte is present as a neutral species. In contrary, an acidic analyte is negatively charged in basic pH (relative to the  $pK_a$ ) having a negative effective electrophoretic mobility while in acidic pH (relative to the  $pK_a$ ) it is present as a neutral species. When the voltage is applied, excess  $OH^-$  or  $H^+$  ions migrate through the sample zone [58], forming a moving reaction boundary. This titration of the sample zone is associated with an electrokinetic zone focusing mechanism due to differences in the effective electrophoretic mobility of the analyte in different pH segments of the capillary.

The combination of dynamic pH junction and sweeping can be utilized to simultaneously focus neutral (hydrophobic) and ionic analytes. It can improve the focusing efficiency for certain analytes if compared to that of either dynamic pH junction or sweeping alone [59]. This combination was first investigated by Britz–McKibbin *et al.* [59] for the analysis of flavin derivatives. The authors used a sample having a pH different from that of the BGE (dynamic pH junction condition) and being void of SDS (sweeping condition). A more than 4-fold enhancement in the focusing of solute zones was achieved by dynamic pH junction-sweeping compared to either sweeping or dynamic pH junction alone. The work published by Britz–McKibbin *et al.* [59] is related to the method reported by Zhu *et al.* [60] except that in the latter, the sample was electrokinetically injected by field amplified sample stacking into a water plug while in

the former study, sample stacking was not amenable because of the high salt content of the sample matrix. Very soon, Britz–McKibbin *et al.* [61, 62] extended their study to the analysis of trace concentrations of flavins in different biological matrices using laser-induced fluorescence detection. Later, dynamic pH junction combined with sweeping found a wide range of applications by several authors [63-68]. However, Yang *et al.* [69] showed that the presence of a pH gradient within the capillary might lead to the appearance of false peaks under sweeping conditions using a large injection volume of the sample and a high concentration of SDS in the BGE.

The impact of a pH variation (between sample solution and BGE) on the focusing efficiency involving sweeping affects a multitude of phenomena including sweeping, RFGE and enrichment by those processes described above for a dynamic pH junction. The impact of a pH variation on the RFGE is related to the effect of the pH on the degree of dissociation/protonation and hence the distribution coefficient of analyte in the sample and the BGE. The retention factor is significantly dependent on the pH because the degree of dissociation/protonation controls the strength of ionic interaction between micelle and analyte. The retention behaviour of ionizable analytes in MEKC was intensively investigated by Khaledi *et al.* [70]. For example, a weakly basic analyte has stronger ionic interactions with anionic micelles in lower pH buffer than in higher pH buffer (with regard to the  $pK_a$  of the analyte). Based on our discussion of RFGE in Section 2.2.1 and in our previous publication [8], in case of a pH variation between sample solution and BGE, the difference in retention factor between the sample and BGE compartments will influence the final enrichment factor.

The second effect, which should be considered, is the effect of pH on the degree of ionization and hence the effective electrophoretic mobility of the analyte (focusing by dynamic pH junction). The final enrichment factor obtained by the combination of dynamic pH junction and sweeping depends on the degree by which each of the three effects discussed above contributes in the overall enrichment process, e.g. the overall observable enrichment efficiency will depend on the ratio of the electrophoretic mobility of the micelles to the electrophoretic mobility of the (dissociated/protonated) analyte in the sample compartment.

### **2.2.3. Adsorption**

Adsorption of analytes onto the wall of the fused-silica capillary is a very common phenomenon especially in the case of hydrophobic basic analytes [71]. Adsorption of proteins is a very clear example of this problem [72]. Generally, adsorption of solutes onto the capillary wall can lead to a number of perturbations in capillary electromigration techniques such as alteration of the EOF velocity, peak deformation, sample loss, deterioration of efficiency and irreproducible migration time [73]. The main

driving forces for the adsorption of analytes onto the capillary wall are hydrophobic and/or electrostatic interactions [74-79].

As will be shown in the present work, in MEKC an important consequence of the wall adsorption of some analytes is the impairment of sweeping efficiency even if the adsorption is restricted only to the sample zone compartment of the capillary. Adsorption of analytes on the capillary wall counteracts the sweeping process. In their pioneering paper about sweeping, Quirino and Terabe [1] attributed the deviation of the measured sweeping enhancement factor from the predicted values to the adsorption of the analytes onto the capillary wall. Adsorption phenomena were also suggested by the same authors to explain the unexpectedly low enhancement factors and poor reproducibility obtained during their study on sweeping-MEKC analysis of polycyclic aromatic hydrocarbons [4]. Moreover, Quirino *et al.* [10] rationalized the gradual decrease of the corrected peak area or the disappearance of the peak of hexanophenone with the increase in sweeping enhancement factor to the adsorption of this analyte onto the capillary wall or onto the wall of containers.

Several approaches have been proposed to overcome the problems encountered with adsorption of analytes onto the capillary wall such as adjusting the pH of the BGE to extreme values, manipulating the ionic strength of the BGE, covalently modifying the silanol functionalities and dynamically coating the inner capillary surface with organic molecules [80-85]. Dynamic coating is generally simpler than covalent coating. Several compounds can be utilized for dynamic coating in capillary electromigration separation techniques such as ethylamine, triethylamine, triethanolamine, glucosamine, galactosamine, putrescine, cadaverine, hexamethonium bromide, spermidine, spermine and tetraethylenepentamine [85]. In the present work, it will be investigated whether or not the addition of a dynamic coating agent exclusively to the sample solution has a positive impact on the sweeping efficiency in case of hydrophobic basic analytes which are very prone to adsorption problems.

### 3. Materials and methods

#### 3.1 Apparatus

All measurements were done with a Beckman (Fullerton, CA, USA) P/ACE™ MDQ CE-system equipped with a UV-detector. The temperature of the capillary was kept at 25°C or 30°C and that of the sample tray was kept at 25°C or 30°C, respectively. Analysis was carried out at a voltage of 25 kV at a detection wavelength of 200 nm. Data were recorded with Beckman 32 Karat software (v. 5.0). Fused-silica capillaries (50- $\mu\text{m}$  I.D., 363- $\mu\text{m}$  O.D.) were from Polymicro Technologies (Phoenix, AZ, USA) with a total length of 50.3 cm and a length to the detector of 40.1 cm. New capillaries were conditioned by flushing them first with 1 mol L<sup>-1</sup> NaOH solution for 60 min, then with water for 30 min and then with BGE for 30 min. A rinsing step with BGE for 5 min was performed between runs. Inolab pH 720 (WTW, Weilheim, Germany) was used for pH measurements, and LF 191 conductometer (WTW, Weilheim, Germany) was used to measure the electric conductivity. Origin 8.5 software (OriginLab corporation, Northampton, USA) (using BoxLucas1 function) or GraphPad Prism 4.03 software (GraphPad Software, Inc., San Diego, USA) (using Zero-to-Top function) were used for performing non-linear regression needed for the assessment of enrichment factors.

#### 3.2 Chemicals and background electrolytes

Ethylparaben, quinine hydrochloride, SDS and triethylamine were from Fluka, Buchs, Switzerland. Desloratadine (certified to have a purity of 99.6%) was kindly provided by Schering–Plough Corporation, USA. Acetophenone, propiophenone, butyrophenone, valerophenone, hexanophenone,  $\beta$ -cyclodextrin and methyl- $\beta$ -cyclodextrin were from Sigma, St. Louis, USA. Hydroxypropyl- $\beta$ -cyclodextrin, 97% was from Acros Organics, Geel, Belgium. Sodium borate decahydrate ( $\text{Na}_2\text{B}_4\text{O}_7 \cdot 10\text{H}_2\text{O}$ ) and orthophosphoric acid were from Merck, Darmstadt, Germany. Thiourea was from Riedel-de Haën, Seelze, Germany. The analyte concentrations in the final sample solution were 10 and 20 mg L<sup>-1</sup> for desloratadine and ethylparaben, respectively.

Stock sodium borate buffer (50 mmol L<sup>-1</sup>, pH 9.30) was prepared by dissolving 19.068 g disodium tetraborate ( $\text{Na}_2\text{B}_4\text{O}_7 \cdot 10\text{H}_2\text{O}$ ) in 500 mL of water and diluting to 1000 mL with water. This stock solution was further diluted for the preparation of background electrolytes.

The BGEs were 10 mmol L<sup>-1</sup> sodium borate buffer (10 mmol L<sup>-1</sup>  $\text{Na}_2\text{B}_4\text{O}_7 \cdot 10\text{H}_2\text{O}$ ), pH 9.30 containing variable concentrations of SDS and of different types of  $\beta$ -cyclodextrin (as indicated in the Section of Results and discussion).

## 4. Results and discussion

### 4.1. Assessment of the enrichment factor.

The enrichment factors were measured with the method presented in [14]. Figure 2 illustrates an example for the application of this method. This method is based on the measurement of the ratio of peak heights in the volume overload region obtained under sweeping and under non-sweeping conditions via plotting the peak height vs. (injection pressure  $\times$  injection time) for one sample with different injection parameters. Non-linear regression is performed to achieve the best curve fitting for the function  $Y = a(1 - e^{-bX})$  where "a" and "b" are the fitted parameters. The parameter "a" represents the limiting peak height, which is used for further calculations:

$$\text{Enrichment factor} = a_2/a_1 = h_2/h_1 \quad (7)$$

where  $a_2$  and  $a_1$  are the fitted parameters, which correspond to  $h_2$  (limiting peak height under sweeping conditions) and  $h_1$  (limiting peak height under non-sweeping conditions), respectively. In case of highly hydrophobic analytes (i.e. high retention factor), it is not possible to reach the volume overload (plateau) region under sweeping conditions due to the limited capillary volume. In this case, the highest possible peak height corresponding to the maximum allowed injection volume is taken as  $h_2$  in Eq. (7) [14].

Two analytes were studied in the present work; ethylparaben and desloratadine as examples of weakly acidic and weakly basic analytes, respectively. As it will be discussed in the following sections, online enrichment by sweeping was achieved by dissolving the analyte in sodium borate buffer of the same concentration as the BGE, however, without micelles or CD and without modification of the electric conductivity of the sample solution. In addition, other studies were performed by dissolving the analyte in phosphoric acid solution being void of micelles to investigate the sweeping process in the presence of a pH junction. The results obtained for measuring the enrichment factor of the studied analytes under different experimental conditions are shown in Tables 1 and 2 (the corresponding regression curves are shown in Figure 2 and Figures S1 – S18 in the Supporting Information). Associated standard deviations were calculated from the corresponding standard errors estimated by non-linear regression (confidence range = standard error  $\times$   $t(P, n-1)$ ).

### 4.2. Measurement of retention factors.

The retention factor is a crucial parameter in studying the fundamentals of sweeping. Therefore, it is necessary to measure the retention factor of the studied analytes in each of the investigated BGEs. For measuring the retention factor for neutral analytes, different approaches have been published in the

literature [86]. In the present study, the retention factors in BGEs void of CDs were experimentally measured by using marker compounds; thiourea as an EOF marker and quinine hydrochloride as a micelle marker (for anionic surfactant). If the analytes are regarded to be neutral under the conditions of enrichment, the following equation is valid:

$$k = \frac{t_s - t_0}{t_0(1 - t_s / t_{mc})} \quad (8)$$

where  $t_0$  = migration time of the EOF marker,  $t_s$  = migration time of the analyte,  $t_{mc}$  = migration time of the micelle marker.

In presence of CDs in the BGE, the direct measurement of retention factors using a single compound as a micelle marker is no longer reliable. That is because the prerequisite that the micelle marker should have a retention factor of infinity is no longer fulfilled. The difficulty of a direct measurement of the retention factors in the presence of CDs is similar to that observed by Chen *et al.* [87] during their study of the effect of organic modifier concentrations on the electrophoretic mobility of micelles in MEKC. Therefore, in these cases we have to use the iterative approach published by Bushey and Jorgenson [88, 89] for the determination of the electrophoretic mobility of the micelles which is based on the Martin equation (valid for the retention factors of the members of a homologous series). In the present study, the homologous series of alkyl phenyl ketones namely acetophenone, propiophenone, butyrophenone, valerophenone and hexanophenone were used. The same homologous series was used by Chen *et al.* [87] for measuring the  $t_{mc}$  values in BGEs containing different organic modifiers.

In this iterative approach, hexanophenone is first assumed to be a micelle marker and the retention factor  $k$  for acetophenone, propiophenone, butyrophenone and valerophenone is calculated according to Eq. (8), where  $t_r$  is the migration time of the analyte and  $t_0$  is the migration time of the EOF marker (methanol used to solubilize the mixture of alkyl phenyl ketones). Then  $\log k$  is plotted against the carbon number  $N_C$  of the alkyl group. Using this plot, a temporary value of  $k$  for hexanophenone is obtained from  $\log k$  at  $N_C = 6$  from which a new  $t_{mc}$  is calculated using Eq. (8). Then the values of  $\log k$  are re-calculated employing the improved estimation of  $t_{mc}$  and re-plotted against  $N_C$ . The iterative procedure is then repeated until a constant value of  $t_{mc}$  is obtained with the lowest possible sum of squared errors (SSE) and the highest possible squared correlation coefficient  $R^2$ . In all cases the convergence criterion was reached. Retention factors measured by this iterative approach are included in Tables 1 and 2.

For measuring the retention factor of charged solute (as in the case of ethylparaben in a BGE of 40 mmol L<sup>-1</sup> SDS and 10 mmol L<sup>-1</sup> sodium borate buffer, pH 9.30), a completely different approach should be used. The calculation is then based on following equation [90]:

$$k = \frac{\mu - \mu_{\text{eff}}}{\mu_{\text{mc}} - \mu} \quad (9)$$

where  $\mu$  = pseudoeffective electrophoretic mobility of the analyte in micellar BGE,  $\mu_{\text{eff}}$  = effective electrophoretic mobility of the analyte in micelle-free BGE (here: under CZE conditions with 10 mmol L<sup>-1</sup> sodium borate buffer, pH 9.30 as a BGE), and  $\mu_{\text{mc}}$  = electrophoretic mobility of the micelles in micellar BGE. These values were determined in separate measurements using thiourea as EOF marker and quinine hydrochloride as micelle marker in absence of CD or using the iterative procedure in presence of CD. Retention factors of ethylparaben in a BGE of 40 mmol L<sup>-1</sup> SDS and 10 mmol L<sup>-1</sup> sodium borate buffer, pH 9.30 in the presence of a variable concentration of hydroxypropyl- $\beta$ -CD are included in Table 1.

#### 4.3. Retention factor gradient effect in CD-MEKC.

In this measurement series, we extend our previous investigation of the RFGE [8] to CD-MEKC where the apparent distribution coefficient differs for the sample solution and the background electrolyte (BGE) due to different contents of CD. According to the RFGE, the enrichment factor is not only dependent on  $k_S$  but also on  $k_{\text{BGE}}$ . Ethylparaben dissolved in 10 mmol L<sup>-1</sup> sodium borate buffer, pH 9.30 was used as the studied sample in this section. Three BGEs consisting of 40 mmol L<sup>-1</sup> SDS in 10 mmol L<sup>-1</sup> sodium borate buffer, pH 9.30 and containing 0, 10 and 20 mmol L<sup>-1</sup> hydroxypropyl- $\beta$ -CD were investigated. For each of the three cases, the enrichment factor was experimentally measured using the plateau curve procedure [8, 14]. The measured enrichment factors as well as the corresponding  $k_{\text{BGE}}$  are included in Table 1 (the corresponding regression curves are shown in Figure 2 and Figures S1 – S5 in the Supporting Information). As an example, the peaks recorded for EP in the volume overload region, in presence of different concentrations of hydroxypropyl- $\beta$ -CD in the BGE, are shown in Figure 3. A marked decrease in  $k_{\text{BGE}}$  was achieved by addition of hydroxypropyl- $\beta$ -CD to the BGE and that decrease is associated with a significant increase in the measured enrichment factor. The lowest enrichment factor can be observed with the BGE void of CD, whereas by increasing the concentration of CD in the BGE, the enrichment factor is improved. These results are in accord with the presence of RFGE acting as an additional focusing effect in the case of  $k_S > k_{\text{BGE}}$ .

#### 4.4. Dynamic pH junction.

We were interested in studying the effect of the combination of sweeping with a dynamic pH junction. Therefore, other measurement conditions were investigated using a sample of ethylparaben dissolved in 10 mmol L<sup>-1</sup> phosphoric acid, pH 2.15 while the BGE consists of 40 mmol L<sup>-1</sup> SDS in 10 mmol L<sup>-1</sup> sodium borate buffer, pH 9.30 and containing 0, 10 or 20 mmol L<sup>-1</sup> hydroxypropyl- $\beta$ -CD. The results of this measurement series are summarized in Table 1 showing that the obtained enrichment factors are significantly higher with a sample solution of pH 2.15 (low-pH sample/high-pH BGE) compared to those obtained with a continuous electrolyte system (high-pH sample/high-pH BGE).

Ethylparaben (Figure 4) is a weakly acidic analyte with a pK<sub>a</sub> of 8.3 at 25°C [91]. At pH 2.15, ethylparaben is completely protonated and neutral while at pH 9.30, ethylparaben is negatively charged with a degree of dissociation = 0.91. Consequently, at pH 2.15, ethylparaben will have a much higher  $k_s$  than at pH 9.30 [70]. We therefore expect an increase in the enrichment factor due to the impact of the sample pH on  $k_s$ . Based on the principles of the dynamic pH junction discussed in Section 2.2.2 (see Figure 1), the difference in the effective electrophoretic mobility of ethylparaben in the low pH sample solution and the high pH BGE can result in an additional focusing effect. Beside these effects, the RFGE has to be taken into account because in this measurement series  $k_s$  is higher than  $k_{BGE}$ . Simultaneously, different concentration and reaction boundaries will develop. The simultaneous presence of these boundaries can produce peak splitting and peak distortion, which is clearly visible in the recorded electropherograms (results not shown). This gives an explanation for the low enrichment factor obtained with the BGE containing 40 mmol L<sup>-1</sup> SDS and 10 mmol L<sup>-1</sup> hydroxypropyl- $\beta$ -CD compared to that containing 40 mmol L<sup>-1</sup> SDS only (see Table 1).

A second measurement series was performed using desloratadine as the studied analyte. In this series, desloratadine was dissolved in four different sample matrices while the BGE was kept constant in all cases. The BGE used was 40 mmol L<sup>-1</sup> SDS and 20 mmol L<sup>-1</sup> hydroxypropyl- $\beta$ -CD in 10 mmol L<sup>-1</sup> sodium borate buffer (pH 9.30), while the four sample matrices included 10 mmol L<sup>-1</sup> phosphoric acid (pH 2.15), 10% v/v methanolic solution of 10 mmol L<sup>-1</sup> phosphoric acid (pH 2.15), 10% v/v methanolic solution of 10 mmol L<sup>-1</sup> sodium borate buffer (pH 9.30) and the same solution as the BGE (non-sweeping condition). In all cases, the peak height for desloratadine was recorded using three different injection volumes. The obtained electropherograms are shown in Figure 5. The results revealed that the highest sensitivity was reached with the aqueous phosphoric acid matrix (dynamic pH junction + RFGE with the highest  $k_s$ ) followed by the solution of phosphoric acid/10% methanol (dynamic pH junction + RFGE with lower  $k_s$ ) and then by borate buffer/10% methanol (no dynamic pH junction, RFGE with the lowest  $k_s$ ). The sample with the analyte dissolved in BGE (no dynamic pH junction, non-sweeping conditions) resulted in the lowest sensitivity.

These results are in accord with Eq. (1). There is no peak distortion due to the presence of different concentration and reaction boundaries, which are expected to develop in case of sweeping with RFGE under dynamic pH junction conditions.

#### 4.5. Effect of adsorption.

In the first two papers of this series [8, 14], we observed a good agreement of the experimentally measured enrichment factors with those factors calculated from the measured retention factors. With the intention to confirm the equations derived in [8, 14] for CD-modified MEKC we studied the enrichment factors obtained for desloratadine employing sweeping with RFGE under dynamic pH junction conditions.

Desloratadine (Figure 4) is a weak base having two  $pK_a$  values, 4.41 and 9.97 at 25°C [92]. Omar *et al.* [93] studied the inclusion complexation of loratadine with different types of CDs through the inclusion of the chlorophenyl moiety and/or the pyridine moiety in the CD cavity. Due to the high structural similarity to loratadine, we expect desloratadine to behave similarly and to form stable inclusion complexes with CD. The highest complex formation constant can be achieved with  $\beta$ -CDs compared to that of  $\gamma$ - and  $\alpha$ -CDs because of the better cavity fitting [93].

The enrichment factors obtainable for desloratadine were measured with different BGEs. In one measurement series, BGEs consisting of 25 mmol L<sup>-1</sup> SDS in 10 mmol L<sup>-1</sup> sodium borate buffer, pH 9.30 and containing variable concentrations of different types of cyclodextrins namely  $\beta$ -CD, methyl- $\beta$ -CD and hydroxypropyl- $\beta$ -CD were investigated. In the second measurement series, BGEs consisting of 40 mmol L<sup>-1</sup> SDS in 10 mmol L<sup>-1</sup> sodium borate buffer, pH 9.30 and containing 0, 10 or 20 mmol L<sup>-1</sup> hydroxypropyl- $\beta$ -CD (same conditions as those employed for the enrichment of ethylparaben) were tested. The enrichment factors were experimentally measured in all cases using the plateau curve procedure [8, 14] (refer to Figures S-6 to S-18 at the Supporting Information for the corresponding regression curves). In all cases, desloratadine was dissolved in 10 mmol L<sup>-1</sup> phosphoric acid, pH 2.15. In this sample matrix, desloratadine, which has a large hydrophobic moiety, is protonated at two positions and has an effective charge number of +2. It can be expected to have a very high retention factor [4] due to the simultaneous strong hydrophobic and electrostatic interaction with the negatively charged outer shell and the hydrophobic micellar core. Orentaite *et al.* [94] observed about one order of magnitude higher retention factors for the charged species compared to those retention factors obtained for the neutral species during their study of weakly acidic analytes by MEKC with cationic surfactant. Since  $k_s$  is much higher than  $k_{BGE}$ , a marked additional focusing effect because of the RFGE is expected. In addition, dynamic pH junction conditions are given. Therefore, we expected that desloratadine would have a very high enrichment factor.

In contrast to our expectations and despite being significantly more hydrophobic than ethylparaben, desloratadine showed in all cases unexpectedly very low enrichment factors (Tables 1 and 2). Moreover, the enrichment factor was nearly unaffected by the addition of CD to the BGE, which is in contradiction to the expected improvement due to RFGE. The obtained enrichment factors for desloratadine were significantly lower than those obtained with the less hydrophobic anilines studied before [8] (See Table S-1 in the Supporting Information). We attribute this unexpected deterioration of the enrichment efficiency to the strong adsorption of this hydrophobic basic analyte onto the inner wall of the capillary in the sample compartment where desloratadine has an effective charge number of +2. E.g. divalent metal cations are reported to strongly interact with the negatively charged silanol groups of the capillary wall [95-97]. Adsorption of the analyte onto the capillary wall within the sample zone will significantly counteract on-line zone focusing by sweeping and/or dynamic pH junction.

A promising approach to minimize this problem and to increase the final enrichment factor was the use of a dynamic coating agent to be added to the sample solution. The dynamic coating agent will preferentially interact with the inner capillary wall reducing considerably the fraction of analyte adsorbed onto the wall.

Triethylamine is one of the well-known dynamic coating agents [84, 85]. Different concentrations of triethylamine were added to the sample solution of desloratadine and the electropherograms were recorded for four different injection volumes. Figure 6 shows the electropherograms of desloratadine with and without addition of triethylamine. It is obvious that the addition of triethylamine had a positive effect indicating better sweeping efficiency in the presence of a dynamic coating agent in the sample solution although the addition of triethylamine elevates the pH of the sample solution and hence reduces  $k_s$ . Highest peak heights, using moderate injection volumes, were reached when 0.2% v/v of triethylamine was added to the sample and the pH is adjusted back to pH 2.15 by 1 mol L<sup>-1</sup> phosphoric acid. The broad distorted peaks with very high injection volumes shown in Figure 6 are attributed to the marked effect of adsorption at low pH in the sample zone associated with extraordinary injection conditions. It is important to compromise between the effect of the dynamic coating agent with regard to adsorption and the elevation of pH caused by this addition. This elevation of pH reduces the degree of protonation of this basic analyte and consequently  $k_s$  with considerable effect on the reachable enrichment efficiency (refer to Eq. (6)). However, the lower effective charge number will reduce the adsorption coefficient with the capillary wall and therefore can have a positive impact on the sensitivity.

These results support our conclusion that adsorption onto the inner capillary wall has a significant role in the unexpected reduction of the sweeping efficiency associated with protonated hydrophobic basic analytes (here effective charge number > 1) even if the adsorption is restricted to the sample zone.

## 5. Concluding remarks

Those considerations made in our previous publications regarding the retention factor gradient effect (RFGE) on the reachable sweeping efficiency are also valid in sweeping-CD-MEKC. In the special case of a sample solution having a pH different from that of the BGE (dynamic pH junction-sweeping-CD-MEKC), the retention factor gradient effect, focusing by dynamic pH junction and adsorption onto the inner capillary wall within the sample zone are simultaneously contributing to the final overall enrichment factor. Adsorption onto the inner capillary wall exclusively within the sample zone can reduce the focusing efficiency dramatically without impairing resolution and efficiency in the subsequent separation step, e.g. in the case of the hydrophobic basic analyte desloratadine, which is present in the low pH sample zone as the diprotonated species and in the separation compartment as the neutral species. First experiments with triethylamine as additive to the sample solution show that for this analyte the addition of a dynamic coating agent exclusively to the sample solution can increase the final overall enrichment factor, also if the retention factor of the analyte in the sample zone is reduced. We conclude that for dynamic pH junction-sweeping-CD-MEKC of analytes that are strongly adsorbed within the sample zone onto the inner capillary wall, the addition of a dynamic coating agent exclusively to the sample matrix is a promising approach to improve the focusing efficiency without having a negative impact on the separation.

## Acknowledgements

M. El-Awady thanks Yousef-Jameel Foundation for the financial support of this work.

*The authors have declared no conflict of interest.*

## References

- [1] Quirino, J. P., Terabe, S., *Science* 1998, 282, 465-468.
- [2] Liu, Z., Sam, P., Sirimanne, S. R., McClure, P. C., et al., *J. Chromatogr. A* 1994, 673, 125-132.
- [3] Gilges, M., *Chromatographia* 1997, 44, 191-196.
- [4] Quirino, J. P., Terabe, S., *Anal. Chem.* 1999, 71, 1638-1644.
- [5] Quirino, J. P., Terabe, S., *J. High Resolut. Chromatogr.* 1999, 22, 367-372.
- [6] Kim, J. B., Quirino, J. P., Otsuka, K., Terabe, S., *J. Chromatogr. A* 2001, 916, 123-130.
- [7] Palmer, J., Burgi, D. S., Landers, J. P., *Anal. Chem.* 2002, 74, 632-638.
- [8] El-Awady, M., Pyell, U., *J. Chromatogr. A* 2013, 1297, 213-225.
- [9] Palmer, J., Munro, N. J., Landers, J. P., *Anal. Chem.* 1999, 71, 1679-1687.
- [10] Quirino, J. P., Terabe, S., Bocek, P., *Anal. Chem.* 2000, 72, 1934-1940.
- [11] Palmer, J., Landers, J. P., *Anal. Chem.* 2000, 72, 1941-1943.
- [12] Palmer, J. F., *J. Chromatogr. A* 2004, 1036, 95-100.
- [13] Giordano, B. C., Newman, C. I. D., Federowicz, P. M., Collins, G. E., Burgi, D. S., *Anal. Chem.* 2007, 79, 6287-6294.
- [14] El-Awady, M., Huhn, C., Pyell, U., *J. Chromatogr. A* 2012, 1264, 124-136.
- [15] Terabe, S., Miyashita, Y., Ishihama, Y., Shibata, O., *J. Chromatogr.* 1993, 636, 47-55.
- [16] Nishi, H., Fukuyama, T., Matsuo, M., Terabe, S., *J. Chromatogr.* 1990, 513, 279-295.
- [17] Cole, R. O., Sepaniak, M. J., Hinze, W. L., Gorse, J., Oldiges, K., *J. Chromatogr.* 1991, 557, 113-123.
- [18] Gorse, J., Balchunas, A. T., Swaile, D. F., Sepaniak, M. J., *HRC CC, J. High Resolut. Chromatogr. Chromatogr. Commun.* 1988, 11, 554-559.
- [19] Otsuka, K., Higashimori, M., Koike, R., Karuhaka, K., et al., *Electrophoresis* 1994, 15, 1280-1283.
- [20] Muijselaar, P. G. H. M., Claessens, H. A., Cramers, C. A., *J. Chromatogr. A* 1995, 696, 273-284.
- [21] Butehorn, U., Pyell, U., *J. Chromatogr. A* 1997, 792, 157-163.
- [22] Butehorn, U., Pyell, U., *J. Chromatogr. A* 1997, 772, 27-38.
- [23] Liu, Z., Zou, H., Ye, M., Ni, J., Zhang, Y., *Electrophoresis* 1999, 20, 2898-2908.
- [24] Balchunas, A. T., Sepaniak, M. J., *Anal. Chem.* 1987, 59, 1466-1470.

Publication III: Main manuscript

- [25] Terabe, S., Ishihama, Y., Nishi, H., Fukuyama, T., Otsuka, K., *J. Chromatogr.* 1991, 545, 359-368.
- [26] Pyell, U., Buetehorn, U., *J. Chromatogr. A* 1995, 716, 81-95.
- [27] Terabe, S., Miyashita, Y., Shibata, O., Barnhart, E. R., et al., *J. Chromatogr.* 1990, 516, 23-31.
- [28] Gotti, R., Fiori, J., Hudaib, M., Cavrini, V., *Electrophoresis* 2002, 23, 3084-3092.
- [29] Takeda, S., Omura, A., Chayama, K., Tsuji, H., et al., *J. Chromatogr. A* 2002, 979, 425-429.
- [30] Takeda, S., Omura, A., Chayama, K., Tsuji, H., et al., *J. Chromatogr. A* 2003, 1014, 103-107.
- [31] Bender, M. L., Komiyama, M., *Cyclodextrin Chemistry*, Springer-Verlag, Berlin 1978.
- [32] Saenger, W., in: Atwood, J. L., Davies, J. E. D., MacNicol, D. D. (Eds.), *Inclusion Compounds, Vol. 2: Structural Aspects of Inclusion Compounds formed by Organic Host Lattices*, Academic Press, London 1984, pp. 231-259.
- [33] Saenger, W., in: Huber, O., Szejtli, J. (Eds.), *Proceedings of the Fourth International Symposium on Cyclodextrins*, Kluwer Academic Publishers, Munich 1988, pp. 159-164.
- [34] Armstrong, D. W., Nome, F., Spino, L. A., Golden, T. D., *J. Am. Chem. Soc.* 1986, 108, 1418-1421.
- [35] Otsuka, K., Terabe, S., *Chromatogr. Sci. Ser.* 1993, 64, 617-629.
- [36] Otsuka, K., Terabe, S., *Trends Anal. Chem.* 1993, 12, 125-130.
- [37] Schneiderman, E., Stalcup, A. M., *J. Chromatogr. , B: Biomed. Sci. Appl.* 2000, 745, 83-102.
- [38] Otsuka, K., Terabe, S., *Methods Mol. Biol.* 2004, 243, 355-363.
- [39] Cserhati, T., *Biomed. Chromatogr.* 2008, 22, 563-571.
- [40] *Martindale: The Complete Drug Reference, Electronic version*, Pharmaceutical Press, London 2013.
- [41] *European Pharmacopoeia 7th Edition (7.8), Online Version*, European directorate for the quality of medicines & healthcare (EDQM), Strasbourg 2013.
- [42] Chien, R. L., Helmer, J. C., *Anal. Chem.* 1991, 63, 1354-1361.
- [43] Burgi, D. S., Chien, R. L., *Anal. Chem.* 1991, 63, 2042-2047.
- [44] Huhn, C., Pyell, U., *J. Chromatogr. A* 2010, 1217, 4476-4486.
- [45] Quirino, J. P., Kim, J. B., Terabe, S., *J. Chromatogr. A* 2002, 965, 357-373.
- [46] Chien, R. L., Burgi, D. S., *Anal. Chem.* 1992, 64, 489A-496A.
- [47] Palepu, R., Reinsborough, V. C., *Can. J. Chem.* 1988, 66, 325-328.

Publication III: Main manuscript

- [48] Junquera, E., Tardajos, G., Aicart, E., *Langmuir* 1993, 9, 1213-1219.
- [49] Cifuentes, A., Bernal, J. L., Diez-Masa, J. C., *Anal. Chem.* 1997, 69, 4271-4274.
- [50] Lin, C. E., Huang, H. C., Chen, H. W., *J. Chromatogr. , A* 2001, 917, 297-310.
- [51] Kazarian, A. A., Hilder, E. F., Breadmore, M. C., *J. Sep. Sci.* 2011, 34, 2800-2821.
- [52] Britz-McKibbin, P., Kranack, A. R., Paprica, A., Chen, D. D. Y., *Analyst* 1998, 123, 1461-1463.
- [53] Aebersold, R., Morrison, H. D., *J. Chromatogr.* 1990, 516, 79-88.
- [54] Britz-McKibbin, P., Wong, J., Chen, D. D. Y., *J. Chromatogr. A* 1999, 853, 535-540.
- [55] Britz-McKibbin, P., Bebault, G. M., Chen, D. D. Y., *Anal. Chem.* 2000, 72, 1729-1735.
- [56] Britz-McKibbin, P., Chen, D. D. Y., *Anal. Chem.* 2000, 72, 1242-1252.
- [57] Cao, C. X., Zhou, S. L., Qian, Y. T., He, Y. Z., et al., *J. Chromatogr. A* 2002, 952, 29-38.
- [58] Duso, A. B., Chen, D. D. Y., *Anal. Chem.* 2002, 74, 2938-2942.
- [59] Britz-McKibbin, P., Otsuka, K., Terabe, S., *Anal. Chem.* 2002, 74, 3736-3743.
- [60] Zhu, L., Tu, C., Lee, H. K., *Anal. Chem.* 2002, 74, 5820-5825.
- [61] Britz-McKibbin, P., Terabe, S., *Chem. Rec.* 2002, 2, 397-404.
- [62] Britz-McKibbin, P., Markuszewski, M. J., Iyanagi, T., Matsuda, K., et al., *Anal. Biochem.* 2003, 313, 89-96.
- [63] Britz-McKibbin, P., Ichihashi, T., Tsubota, K., Chen, D. D. Y., Terabe, S., *J. Chromatogr. A* 2003, 1013, 65-76.
- [64] Su, A. K., Chang, Y. S., Lin, C. H., *Talanta* 2004, 64, 970-974.
- [65] Yu, L., Li, S. F. Y., *Electrophoresis* 2005, 26, 4360-4367.
- [66] Cheng, H. L., Liao, Y. M., Chiou, S. S., Wu, S. M., *Electrophoresis* 2008, 29, 3665-3673.
- [67] Petr, J., Vitkova, K., Ranc, V., Znaleziona, J., et al., *J. Agric. Food Chem.* 2008, 56, 3940-3944.
- [68] Chen, Y., Zhang, L., Cai, Z., Chen, G., *Analyst (Cambridge, U. K. )* 2011, 136, 1852-1858.
- [69] Yang, G. I., Li, B. h., Wang, D. X., Chen, Y., *Chin. J. Chem.* 2002, 20, 1579-1583.
- [70] Khaledi, M. G., Smith, S. C., Strasters, J. K., *Anal. Chem.* 1991, 63, 1820-1830.
- [71] Towns, J. K., Regnier, F. E., *Anal. Chem.* 1992, 64, 2473-2478.
- [72] Graf, M., Garcia, R. G., Waetzig, H., *Electrophoresis* 2005, 26, 2409-2417.
- [73] Beale, S. C., *Anal. Chem.* 1998, 70, 279R-300R.

Publication III: Main manuscript

- [74] Schure, M. R., Lenhoff, A. M., *Anal. Chem.* 1993, 65, 3024-3037.
- [75] Gas, B., Stedry, M., Rizzi, A., Kenndler, E., *Electrophoresis* 1995, 16, 958-967.
- [76] Stedry, M., Gas, B., Kenndler, E., *Electrophoresis* 1995, 16, 2027-2033.
- [77] Minarik, M., Gas, B., Rizzi, A., Kenndler, E., *J. Capillary Electrophor.* 1995, 2, 89-96.
- [78] Ermakov, S. V., Zhukov, M. Y., Capelli, L., Righetti, P. G., *J. Chromatogr. A* 1995, 699, 297-313.
- [79] Zhukov, M. Y., Ermakov, S. V., Righetti, P. G., *J. Chromatogr. A* 1997, 766, 171-185.
- [80] Bullock, J. A., Yuan, L. C., *J. Microcolumn Sep.* 1991, 3, 241-248.
- [81] Song, L., Ou, Q., Yu, W., *J. Chromatogr. , A* 1993, 657, 175-183.
- [82] Corradini, D., Rhomberg, A., Corradini, C., *J. Chromatogr. , A* 1994, 661, 305-313.
- [83] Corradini, D., Cannarsa, G., *Electrophoresis* 1995, 16, 630-635.
- [84] Qiu, Y. H., Huang, A. J., Sun, Y. L., *Chin. Chem. Lett.* 1999, 10, 227-230.
- [85] Righetti, P. G., Gelfi, C., Verzola, B., Castelletti, L., *Electrophoresis* 2001, 22, 603-611.
- [86] Wiedmer, S. K., Lokajova, J., Riekkola, M. L., *J. Sep. Sci.* 2010, 33, 394-409.
- [87] Chen, N., Terabe, S., Nakagawa, T., *Electrophoresis* 1995, 16, 1457-1462.
- [88] Bushey, M. M., Jorgenson, J. W., *J. Microcolumn Sep.* 1989, 1, 125-130.
- [89] Bushey, M. M., Jorgenson, J. W., *Anal. Chem.* 1989, 61, 491-493.
- [90] Otsuka, K., Terabe, S., Ando, T., *J. Chromatogr.* 1985, 348, 39-47.
- [91] Moffat, A. C., Osselton, M. D., Widdop, B., Editors., *Clarke's Analysis of Drugs and Poisons in Pharmaceuticals, Body Fluids and Postmortem Material, Fourth Edition*, Pharmaceutical Press, London 2011.
- [92] Popovic, G., Cakar, M., Agbaba, D., *J. Pharm. Biomed. Anal.* 2009, 49, 42-47.
- [93] Omar, L., El-Barghouthi, M. I., Masoud, N. A., Abdoh, A. A., et al., *J. Solution Chem.* 2007, 36, 605-616.
- [94] Orentaite, I., Maruska, A., Pyell, U., *Electrophoresis* 2011, 32, 604-613.
- [95] Fuerstenau, D. W., *J. Phys. Chem.* 1956, 60, 981-985.
- [96] Brechtel, R., Hohmann, W., Ruediger, H., Waetzig, H., *J. Chromatogr. A* 1995, 716, 97-105.
- [97] Pietrzyk, D. J., Chen, S., Chanthawat, B., *J. Chromatogr. A* 1997, 775, 327-338.
- [98] Miller, J. C., Miller, J. N., *Statistics and Chemometrics for Analytical Chemistry, 5th Edition*, Pearson Education Limited, Harlow, England 2005.

## Figure Legends

**Figure 1.** Scheme of different possibilities for focusing the analyte zone by using a dynamic pH junction.

**Figure 2.** Peak height plotted against injected volume for ethylparaben under (A) conventional conditions (analyte dissolved in BGE), (B) sweeping conditions (analyte dissolved in 10 mmol L<sup>-1</sup> sodium borate buffer, pH 9.30). BGE: 10 mmol L<sup>-1</sup> sodium borate buffer, pH 9.30 containing 40 mmol L<sup>-1</sup> SDS and 10 mmol L<sup>-1</sup> hydroxypropyl- $\beta$ -CD; injection: hydrodynamic; capillary: fused-silica capillaries (50  $\mu$ m I.D., 363  $\mu$ m O.D.) with a total length of 50.3 cm and a length to the detector of 40.1 cm; temperature of the capillary and the sample tray: 30°C; voltage: +25 kV; detection wavelength: 200 nm.

**Figure 3.** Electropherograms for ethylparaben under sweeping conditions using injection volume (5 psi for 20 s) in the volume overload region in presence of (A) 0, (B) 10 and (C) 20 mmol L<sup>-1</sup> hydroxypropyl- $\beta$ -CD in the BGE. For other experimental parameters, refer to Figure 2.

**Figure 4.** Chemical structures of the studied analytes.

**Figure 5.** Electropherograms obtained with three injection volumes of desloratadine dissolved in four different sample matrices including (A) 10 mmol L<sup>-1</sup> phosphoric acid, pH 2.15, (B) 10% v/v methanolic solution of 10 mmol L<sup>-1</sup> phosphoric acid, pH 2.15, (C) 10% v/v methanolic solution of 10 mmol L<sup>-1</sup> sodium borate buffer, pH 9.30 and (D) BGE (non-sweeping condition). BGE: 10 mmol L<sup>-1</sup> sodium borate buffer, pH 9.30 containing 40 mmol L<sup>-1</sup> SDS and 20 mmol L<sup>-1</sup> hydroxypropyl- $\beta$ -CD. Injection: hydrodynamic using pressure (A1,B1,C1,D1) 0.5 psi for 5 s, (A2,B2,C2,D2) 0.5 psi for 10 s, (A3,B3,C3,D3) 0.5 psi for 15 s. For other experimental parameters refer to Figure 2.

**Figure 6.** Electropherograms obtained with four injection volumes of desloratadine showing the effect of addition of triethylamine to the sample matrix: (A) 10 mmol L<sup>-1</sup> phosphoric acid, pH 2.15, (B) 0.1% v/v triethylamine in 10 mmol L<sup>-1</sup> phosphoric acid, final pH 3.5, (C) 0.2% v/v triethylamine in 10 mmol L<sup>-1</sup> phosphoric acid, final pH 6.0, and (D) 0.2% v/v triethylamine in 10 mmol L<sup>-1</sup> phosphoric acid, final pH is adjusted to approximately pH 2.15 by 1 mmol L<sup>-1</sup> phosphoric acid. BGE: 10 mmol L<sup>-1</sup> sodium borate buffer, pH 9.30 containing 40 mmol L<sup>-1</sup> SDS and 20 mmol L<sup>-1</sup> hydroxypropyl- $\beta$ -CD. Injection: hydrodynamic using pressure (A1,B1,C1,D1) 1 psi for 10 s, (A2,B2,C2,D2) 1 psi for 20 s, (A3,B3,C3,D3) 1 psi for 50 s, (A4,B4,C4,D4) 1 psi for 75 s. For other experimental parameters refer to Figure 2.

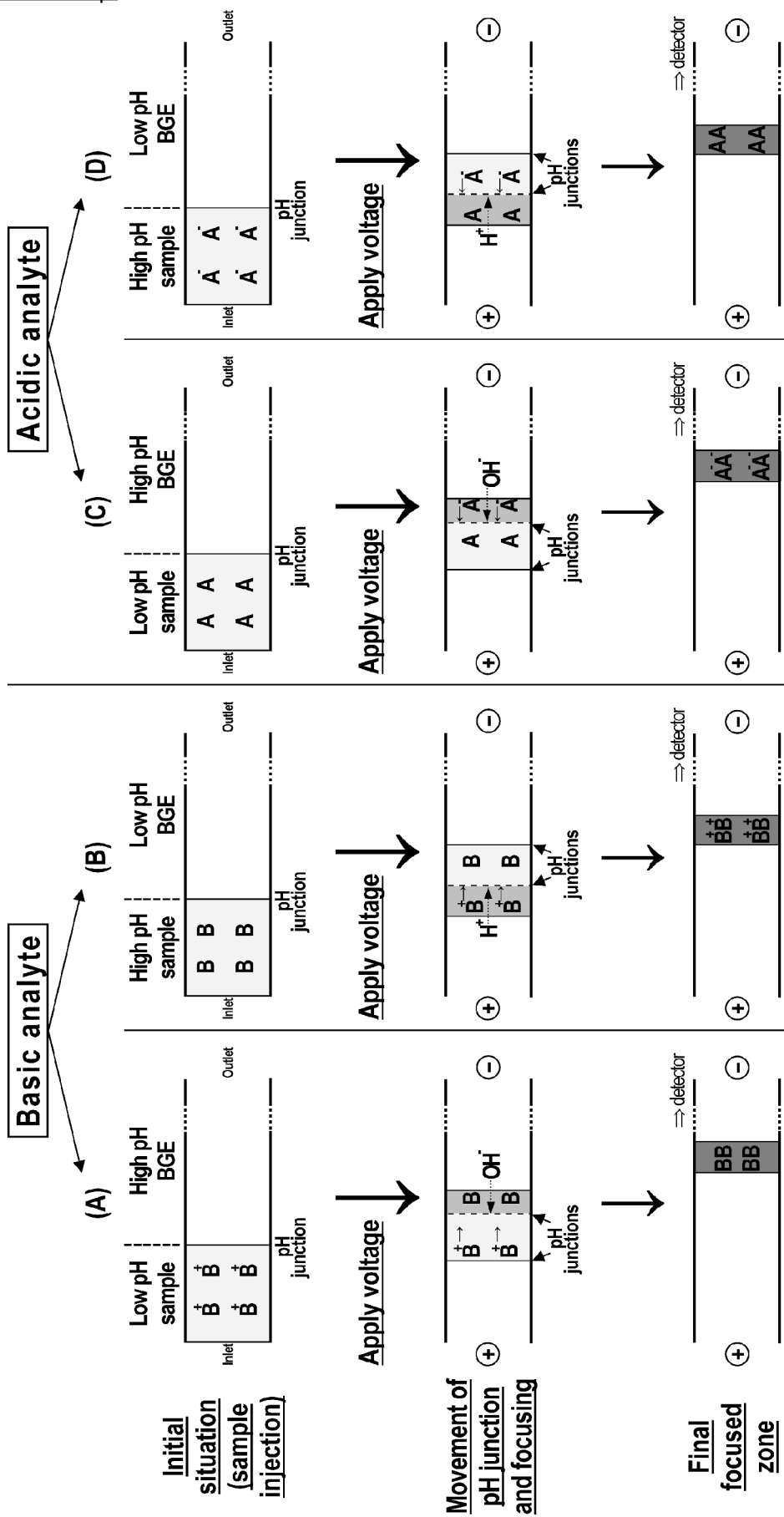


Figure 1

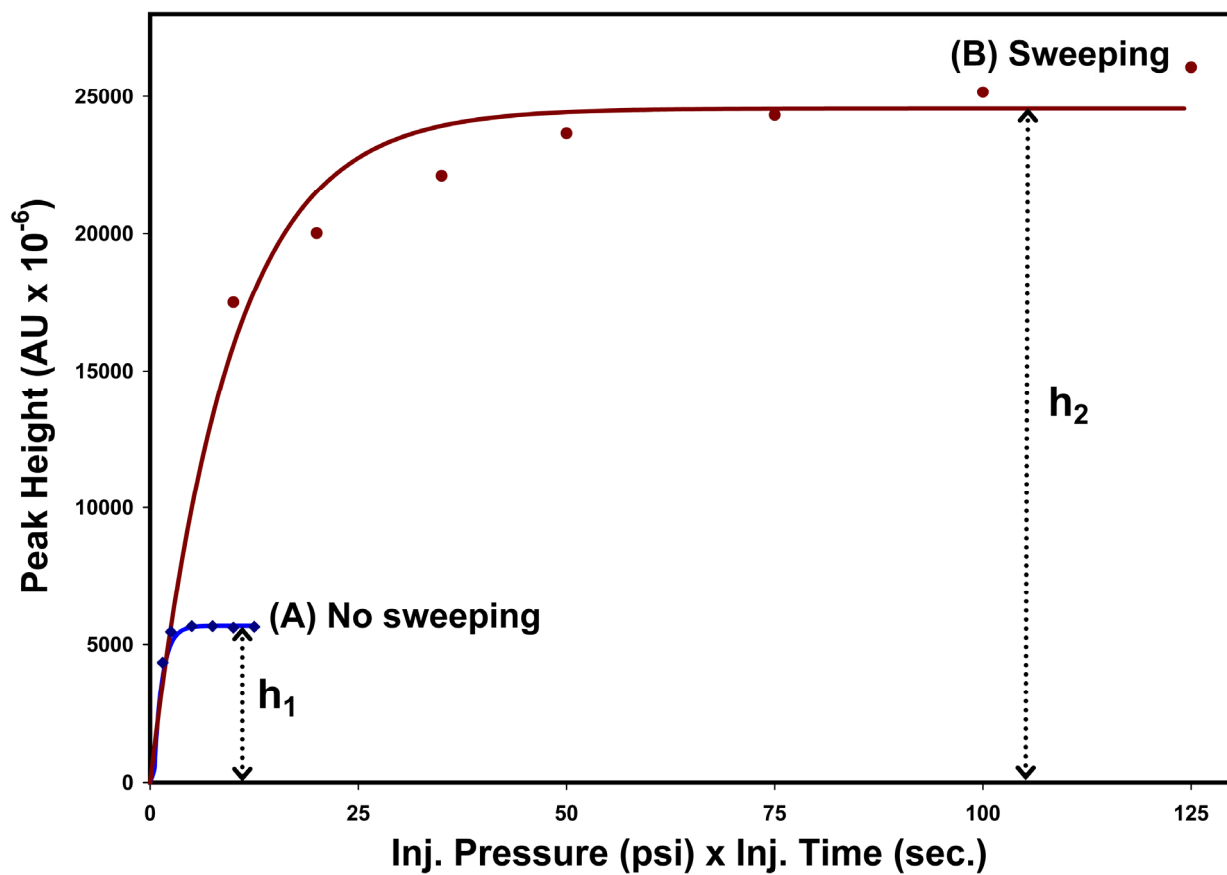


Figure 2

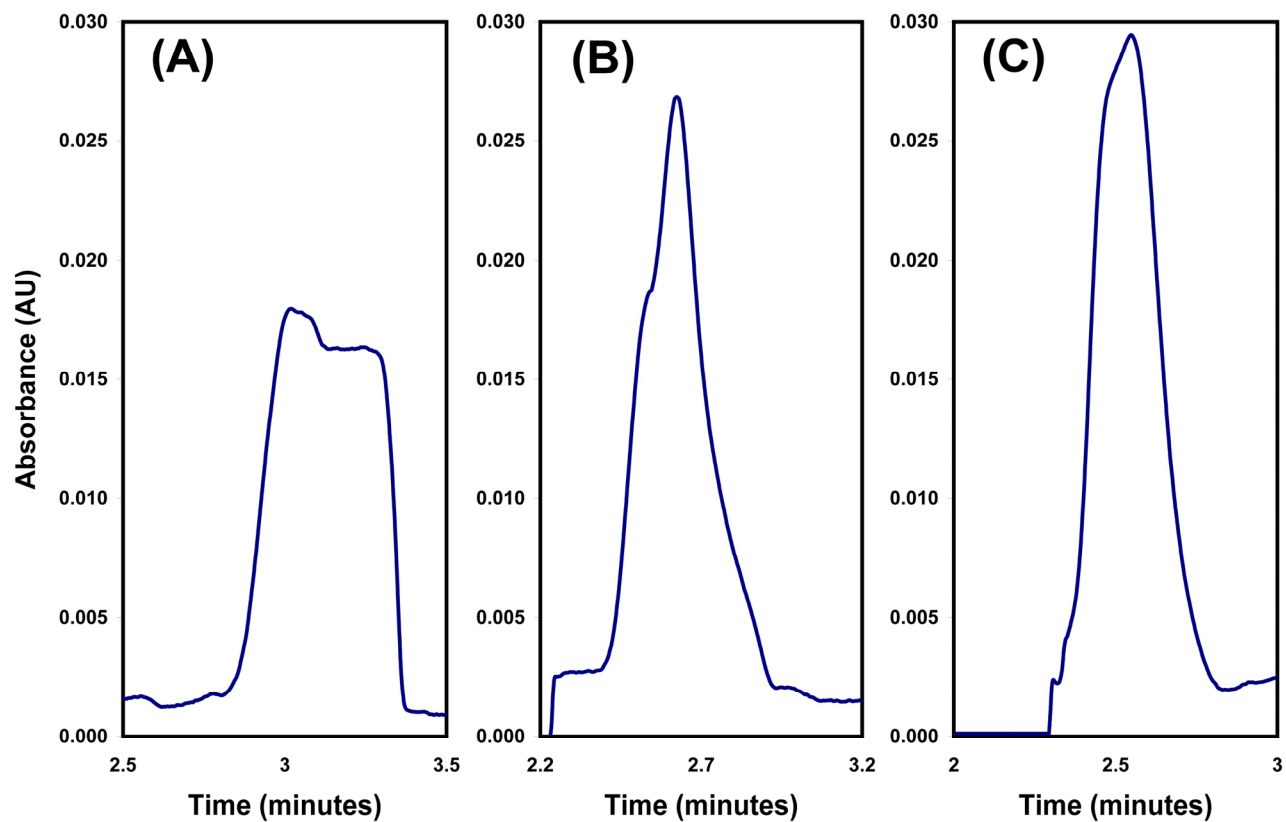
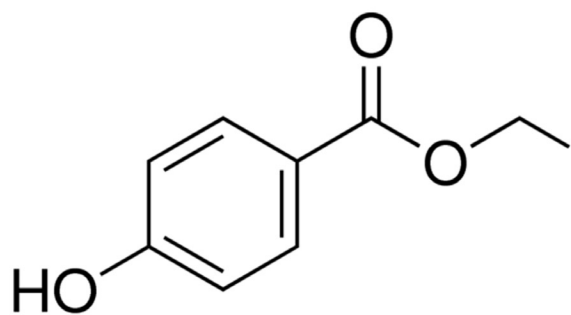
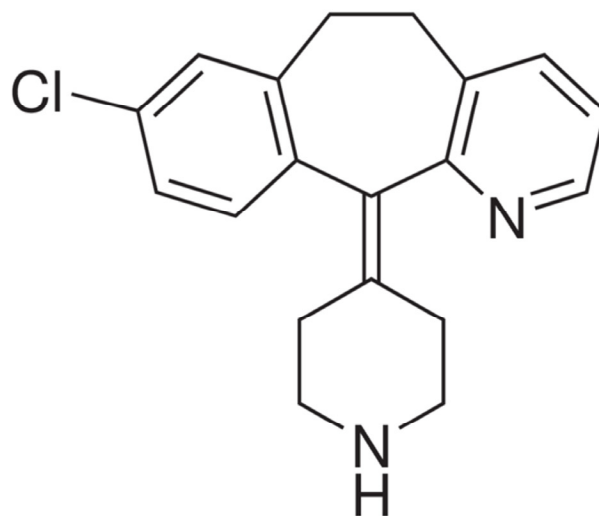


Figure 3



**Ethylparaben**



**Desloratadine**

Figure 4

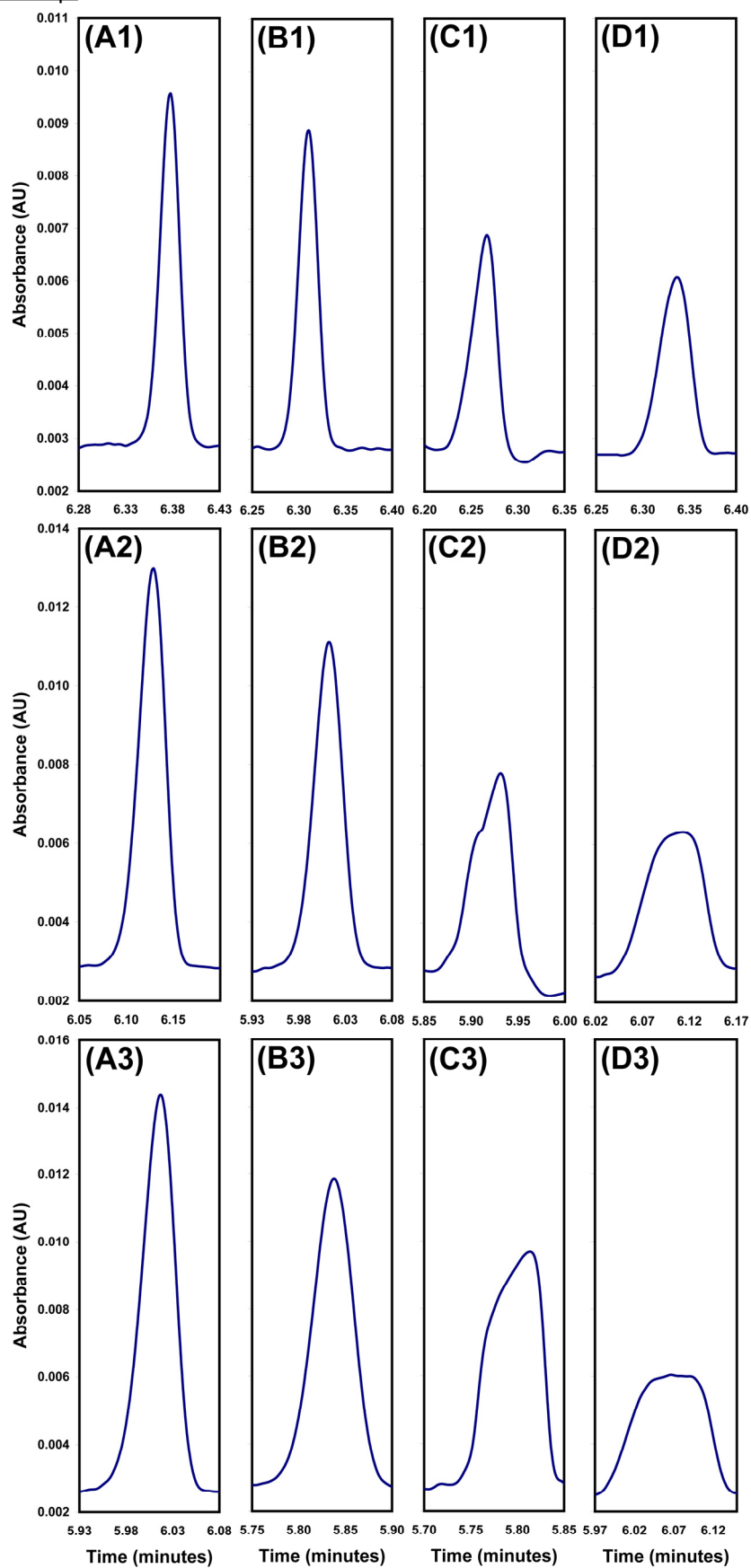


**Figure 5**

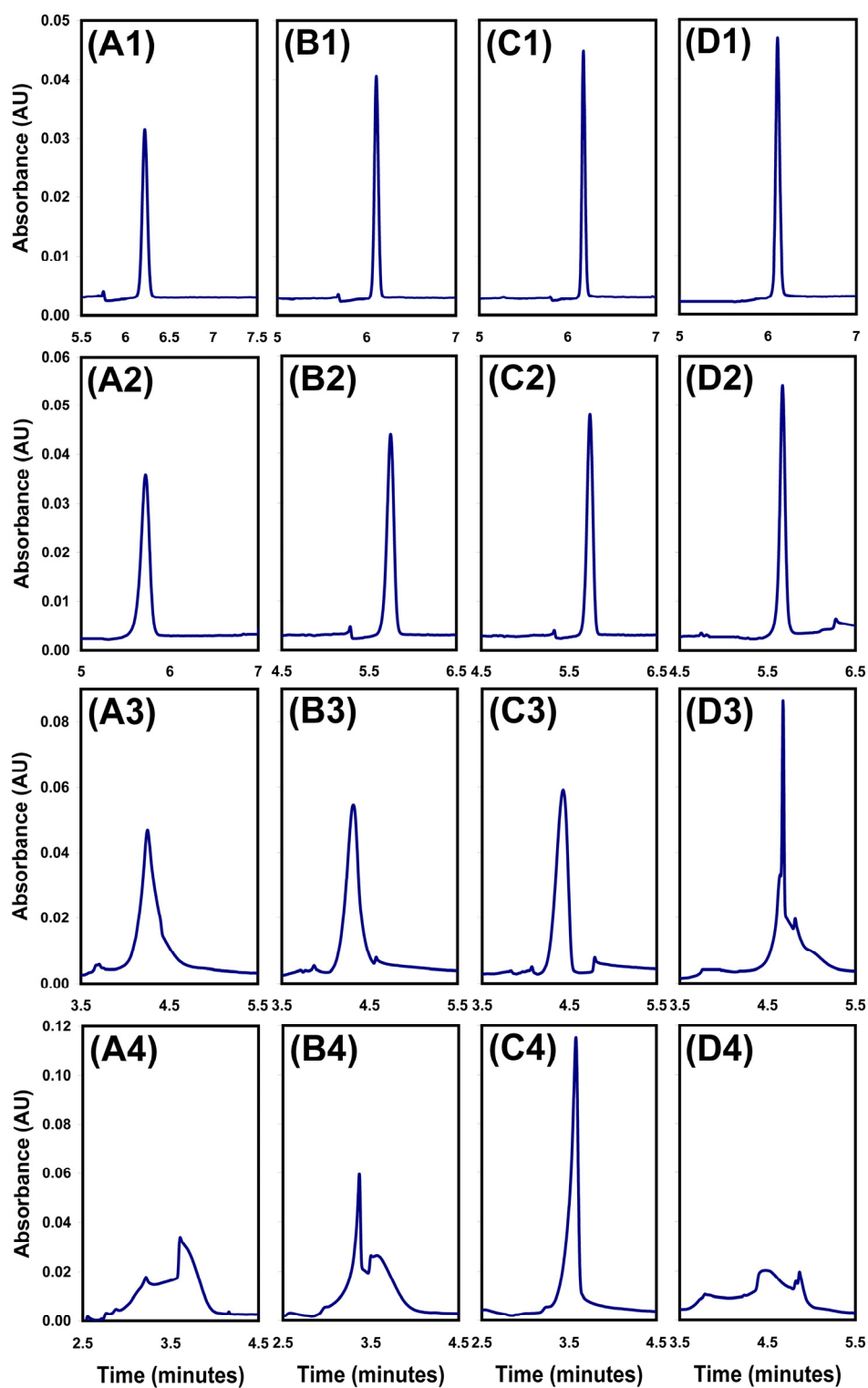


**Figure 6**

**Table 1.** Assessment of the enrichment factor for ethylparaben dissolved in two different sample matrices in presence of different concentrations of hydroxypropyl- $\beta$ -CD in the BGE.

BGE <sup>a</sup>	Retention factor <sup>b</sup> ( $k_{BGE}$ )	Enrichment factor <sup>c</sup>	
		Analyte dissolved in 10 mmol L <sup>-1</sup> sod. borate buffer, pH 9.30	Analyte dissolved in 10 mmol L <sup>-1</sup> phosphoric acid, pH 2.15
40 mmol L <sup>-1</sup> SDS	$0.67 \pm 0.0009$	$2.33 \pm 0.03$	$6.88 \pm 0.59$
40 mmol L <sup>-1</sup> SDS + 10 mmol L <sup>-1</sup> hydroxypropyl- $\beta$ -CD	$0.04 \pm 0.0002$	$4.32 \pm 0.14$	$5.32 \pm 0.17^d$
40 mmol L <sup>-1</sup> SDS + 20 mmol L <sup>-1</sup> hydroxypropyl- $\beta$ -CD	$(-0.24) \pm 0.0006$	$7.08 \pm 0.63$	$12.5 \pm 0.76$

<sup>a</sup> In all cases, SDS and hydroxypropyl- $\beta$ -CD were dissolved in 10 mmol L<sup>-1</sup> sodium borate buffer, pH 9.30.

<sup>b</sup> Each value is the mean of at least three repetitions. The negative value is due to the unavoidable measuring error of the iterative procedure.

<sup>c</sup> Standard deviation is calculated from the corresponding standard errors estimated by non-linear regression applying the rules for error propagation [98].

<sup>d</sup> This case is associated with peak splitting and peak distortion.

**Table 2.** Assessment of the enrichment factor for desloratadine in presence of different concentrations of CDs in the BGE.

BGE <sup>a</sup>		Retention factor <sup>b</sup> ( $k_{BGE}$ )	Enrichment factor <sup>c</sup>
SDS	Cyclodextrin		
25 mmol L <sup>-1</sup> SDS	none	$\infty$	2.84 ± 0.20
	5 mmol L <sup>-1</sup> $\beta$ -CD	33.3 ± 1.29	2.90 ± 0.13
	10 mmol L <sup>-1</sup> $\beta$ -CD	19.7 ± 0.42	1.90 ± 0.16
	15 mmol L <sup>-1</sup> $\beta$ -CD	13.5 ± 0.30	2.03 ± 0.17
	5 mmol L <sup>-1</sup> methyl- $\beta$ -CD	25.1 ± 0.70	2.92 ± 0.12
	10 mmol L <sup>-1</sup> methyl- $\beta$ -CD	13.9 ± 0.30	2.56 ± 0.08
	15 mmol L <sup>-1</sup> methyl- $\beta$ -CD	7.75 ± 0.33	2.82 ± 0.52
	5 mmol L <sup>-1</sup> hydroxypropyl- $\beta$ -CD	28.6 ± 1.29	2.86 ± 0.20
	10 mmol L <sup>-1</sup> hydroxypropyl- $\beta$ -CD	15.9 ± 0.34	2.31 ± 0.14
15 mmol L <sup>-1</sup> hydroxypropyl- $\beta$ -CD	13.1 ± 0.25	3.10 ± 0.11	
40 mmol L <sup>-1</sup> SDS	none	$\infty$	3.08 ± 0.25
	10 mmol L <sup>-1</sup> hydroxypropyl- $\beta$ -CD	25.0 ± 0.48	2.42 ± 0.14
	20 mmol L <sup>-1</sup> hydroxypropyl- $\beta$ -CD	9.78 ± 0.10	2.23 ± 0.08

<sup>a</sup> In all cases, SDS and hydroxypropyl- $\beta$ -CD were dissolved in 10 mmol L<sup>-1</sup> sodium borate buffer, pH 9.30 and desloratadine was dissolved in 10 mmol L<sup>-1</sup> phosphoric acid, pH 2.15.

<sup>b</sup> Each value is the mean of at least three repetitions. The negative value is due to the unavoidable measuring error of the iterative procedure.

<sup>c</sup> Standard deviation is calculated from the corresponding standard errors estimated by non-linear regression applying the rules for error propagation [98].



**5.3.4. Processes involved in sweeping as sample enrichment method in cyclodextrin-modified micellar electrokinetic chromatography of hydrophobic basic analytes**

Mohamed El-Awady, Ute Pyell\*

University of Marburg, Department of Chemistry, Hans-Meerwein-Straße, D-35032 Marburg, Germany

\* corresponding author

**Supporting information**

**Table S-1.** Sweeping efficiencies for aniline, 4-ethylaniline and 4-butylaniline in three different sample matrices using 10 mmol L<sup>-1</sup> borate buffer, pH 9.37 containing 50 mmol L<sup>-1</sup> SDS as the BGE.

	Analyte	Sample matrix		
		Borate buffer (pH 9.37)	Phosphoric acid (pH 3.50)	Glutamic acid (pH 3.35)
Enrichment factor <sup>a</sup>	Aniline	1.38 <sup>a</sup>	1.44	2.06
	4-Ethylaniline	3.92 <sup>a</sup>	11.3 <sup>b</sup>	16.7 <sup>b</sup>
	4-Butylaniline	6.33	14.3 <sup>b</sup>	17.1 <sup>b</sup>

<sup>a</sup> Data taken from our previous publication [El-Awady, M., Huhn, C., Pyell, U., J. Chromatogr. A 2012, 1264, 124-136].

<sup>b</sup> Estimated from the highest possible peak height corresponding to the maximum allowed injection volume used as  $h_2$  in Eq. (5).

[Reprinted from El-Awady, M., Pyell, U., J. Chromatogr. A 2013, 1297, 213-225, the online supplementary data, copyright 2013, with permission from Elsevier].

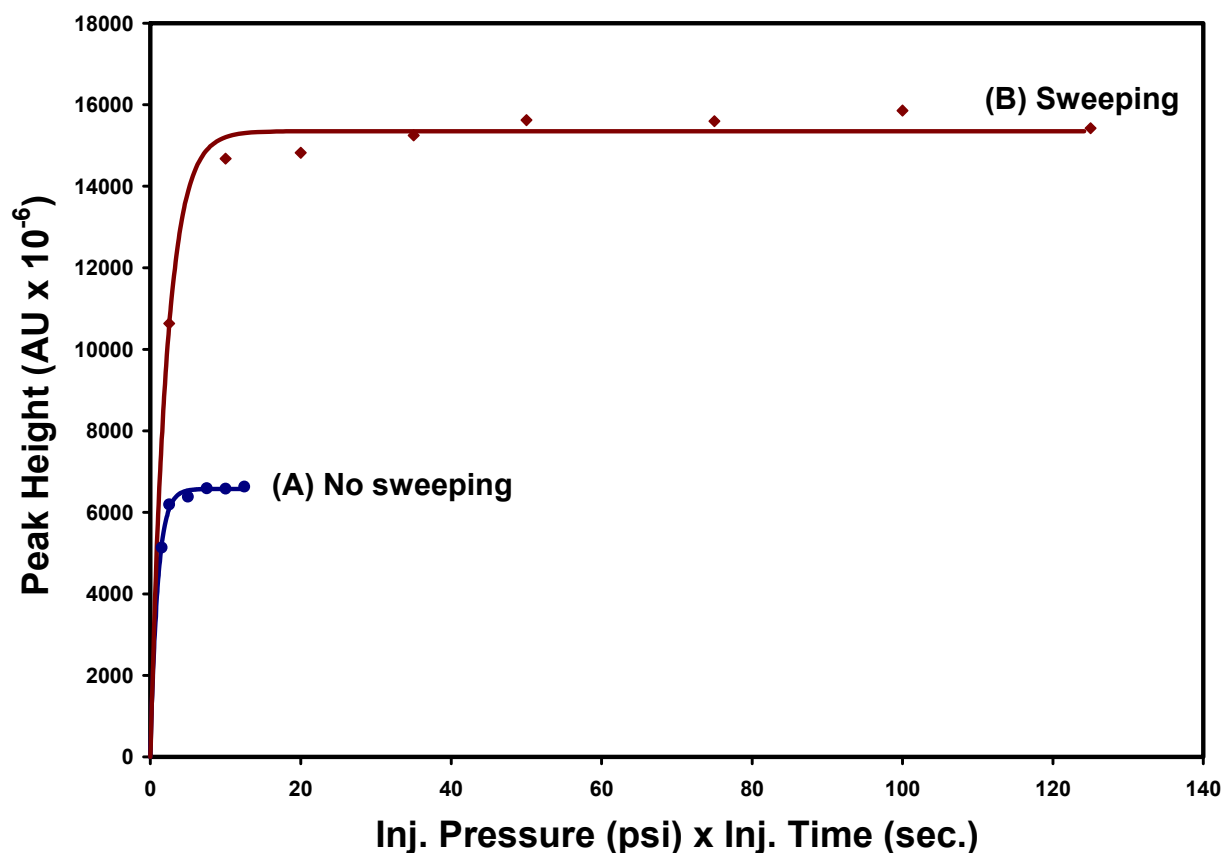


**Figure S-1.** Peak height plotted against injected volume for **ethylparaben** under (A) conventional conditions (analyte dissolved in BGE), (B) sweeping conditions (analyte dissolved in **10 mmol L<sup>-1</sup> sodium borate buffer, pH 9.3**). BGE: 10 mmol L<sup>-1</sup> sodium borate buffer, pH 9.3 containing **40 mmol L<sup>-1</sup> SDS**; injection: hydrodynamic; capillary: fused-silica capillaries (50- $\mu\text{m}$  I.D., 363- $\mu\text{m}$  O.D.) with a total length of 50.3 cm and a length to the detector of 40.1 cm; temperature of the capillary and the sample tray: 30°C; voltage: +25 kV; detection wavelength: 200 nm.

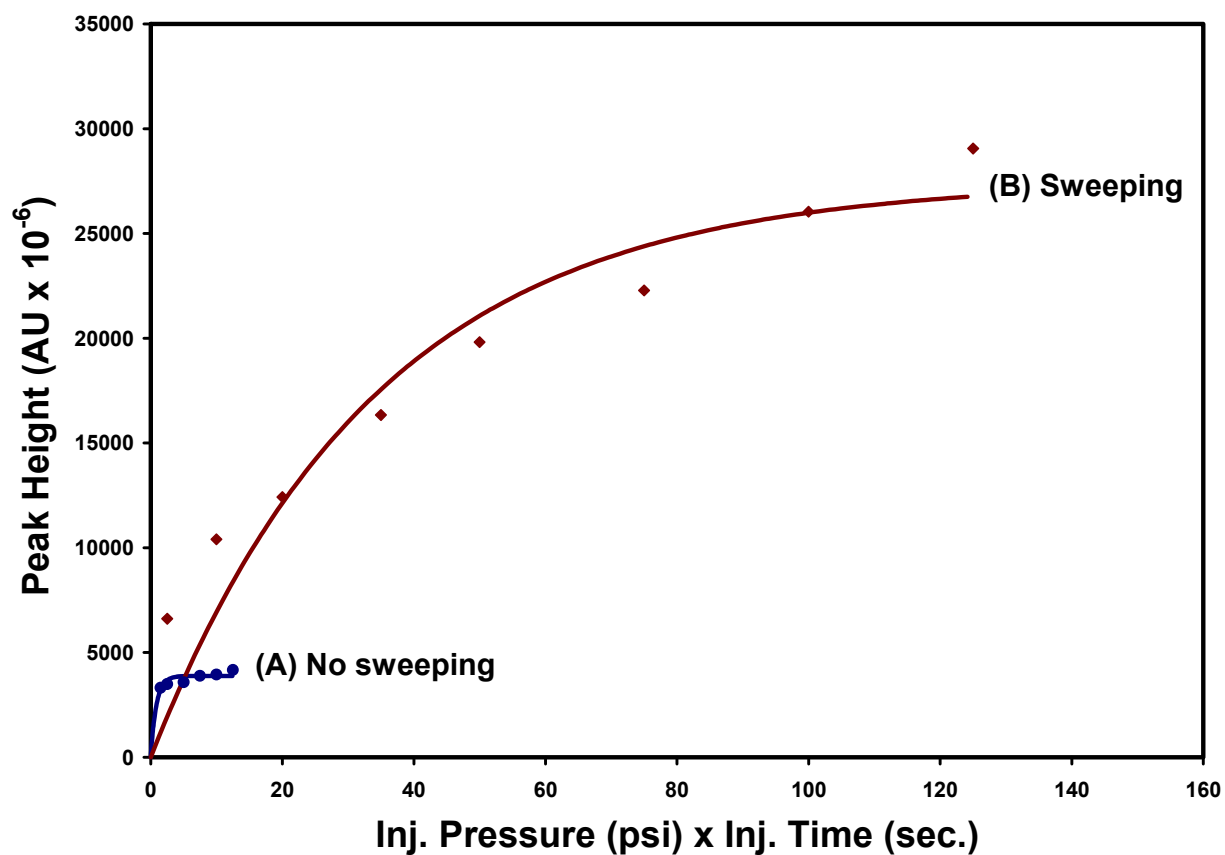


**Figure S-2.** Peak height plotted against injected volume for **ethylparaben** under (A) conventional conditions (analyte dissolved in BGE), (B) sweeping conditions (analyte dissolved in **10 mmol L<sup>-1</sup> sodium borate buffer, pH 9.3**). BGE: 10 mmol L<sup>-1</sup> sodium borate buffer, pH 9.3 containing **40 mmol L<sup>-1</sup> SDS and 20 mmol L<sup>-1</sup> hydroxypropyl- $\beta$ -CD**; injection: hydrodynamic; capillary: fused-silica capillaries (50- $\mu$ m I.D., 363- $\mu$ m O.D.) with a total length of 50.3 cm and a length to the detector of 40.1 cm; temperature of the capillary and the sample tray: 30°C; voltage: +25 kV; detection wavelength: 200 nm.

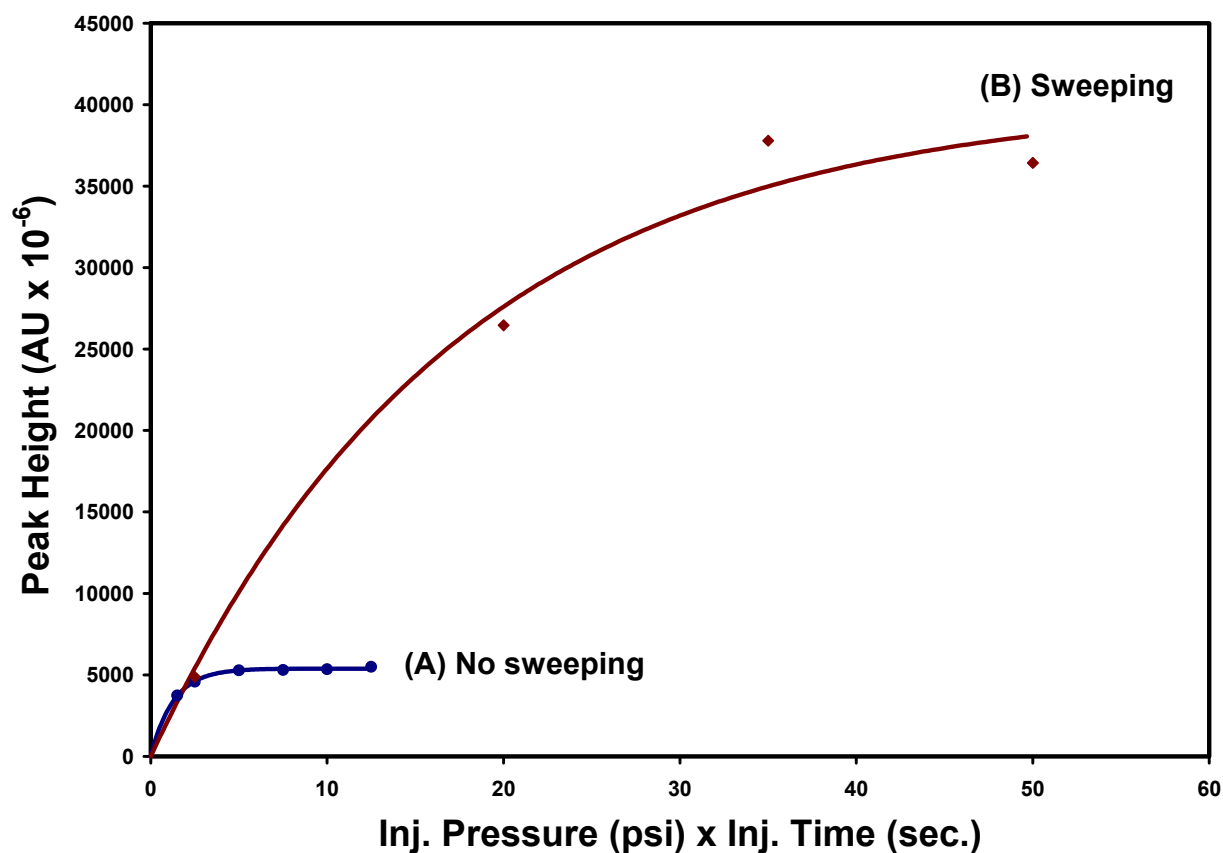


**Figure S-3.** Peak height plotted against injected volume for **ethylparaben** under (A) conventional conditions (analyte dissolved in BGE), (B) sweeping conditions (analyte dissolved in **10 mmol L<sup>-1</sup> phosphoric acid, pH 2.15**). BGE: 10 mmol L<sup>-1</sup> sodium borate buffer, pH 9.3 containing **40 mmol L<sup>-1</sup> SDS**; injection: hydrodynamic; capillary: fused-silica capillaries (50- $\mu$ m I.D., 363- $\mu$ m O.D.) with a total length of 50.3 cm and a length to the detector of 40.1 cm; temperature of the capillary and the sample tray: 30°C; voltage: +25 kV; detection wavelength: 200 nm.

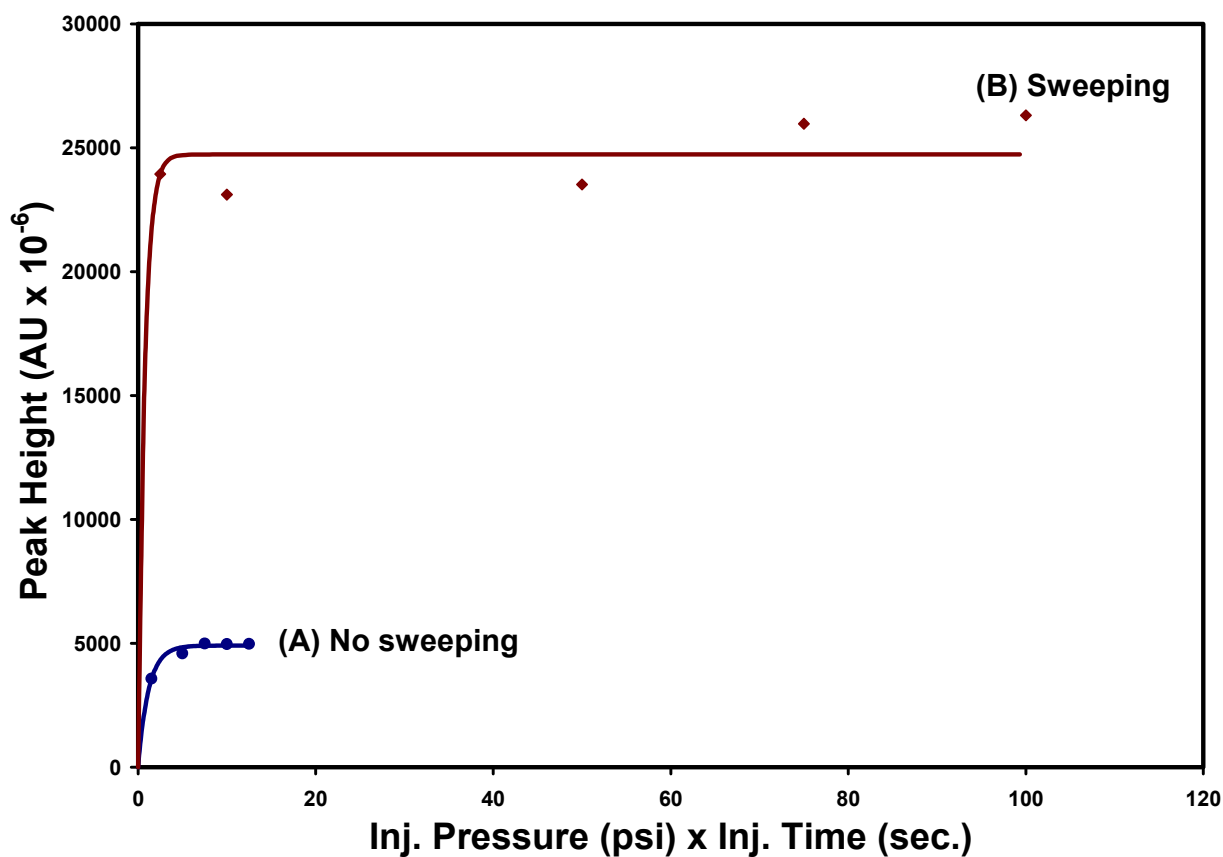


**Figure S-4.** Peak height plotted against injected volume for **ethylparaben** under (A) conventional conditions (analyte dissolved in BGE), (B) sweeping conditions (analyte dissolved in **10 mmol L<sup>-1</sup> phosphoric acid, pH 2.15**). BGE: 10 mmol L<sup>-1</sup> sodium borate buffer, pH 9.3 containing **40 mmol L<sup>-1</sup> SDS** and **10 mmol L<sup>-1</sup> hydroxypropyl- $\beta$ -CD**; injection: hydrodynamic; capillary: fused-silica capillaries (50- $\mu$ m I.D., 363- $\mu$ m O.D.) with a total length of 50.3 cm and a length to the detector of 40.1 cm; temperature of the capillary and the sample tray: 30°C; voltage: +25 kV; detection wavelength: 200 nm.

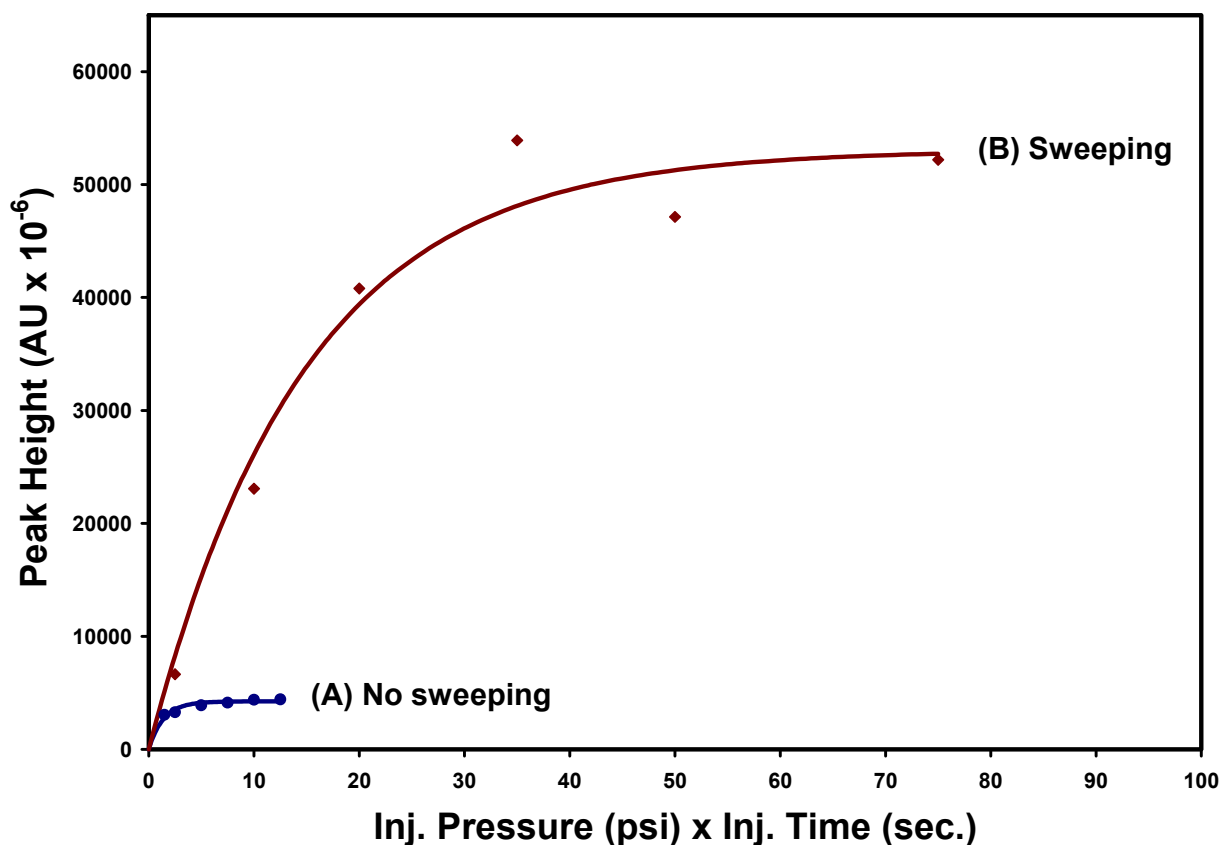


**Figure S-5.** Peak height plotted against injected volume for **ethylparaben** under (A) conventional conditions (analyte dissolved in BGE), (B) sweeping conditions (analyte dissolved in **10 mmol L<sup>-1</sup> phosphoric acid, pH 2.15**). BGE: 10 mmol L<sup>-1</sup> sodium borate buffer, pH 9.3 containing **40 mmol L<sup>-1</sup> SDS and 20 mmol L<sup>-1</sup> hydroxypropyl- $\beta$ -CD**; injection: hydrodynamic; capillary: fused-silica capillaries (50- $\mu$ m I.D., 363- $\mu$ m O.D.) with a total length of 50.3 cm and a length to the detector of 40.1 cm; temperature of the capillary and the sample tray: 30°C; voltage: +25 kV; detection wavelength: 200 nm.

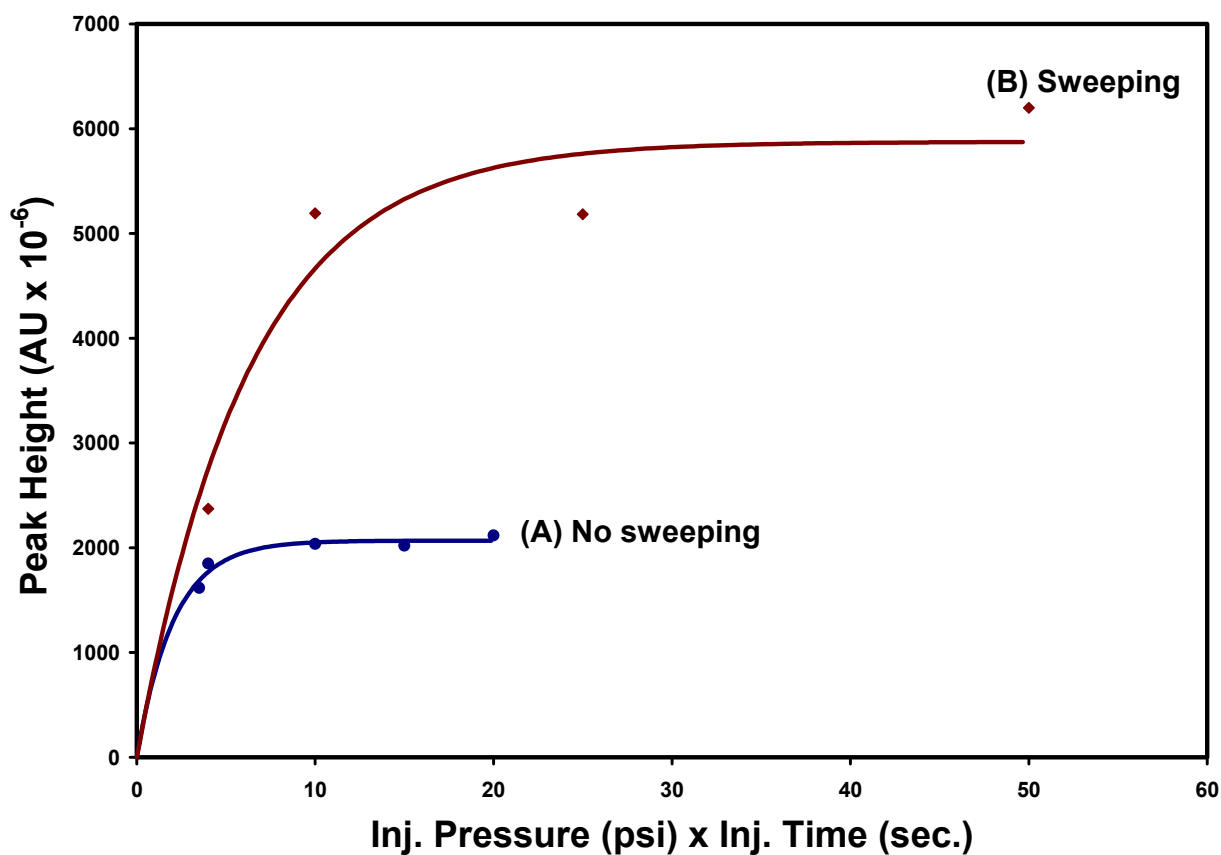


**Figure S-6.** Peak height plotted against injected volume for **desloratadine** under (A) conventional conditions (analyte dissolved in BGE), (B) sweeping conditions (analyte dissolved in **10 mmol L<sup>-1</sup> phosphoric acid, pH 2.15**). BGE: 10 mmol L<sup>-1</sup> sodium borate buffer, pH 9.3 containing **25 mmol L<sup>-1</sup> SDS**; injection: hydrodynamic; capillary: fused-silica capillaries (50- $\mu$ m I.D., 363- $\mu$ m O.D.) with a total length of 50.3 cm and a length to the detector of 40.1 cm; temperature of the capillary and the sample tray: 30°C; voltage: +25 kV; detection wavelength: 200 nm.

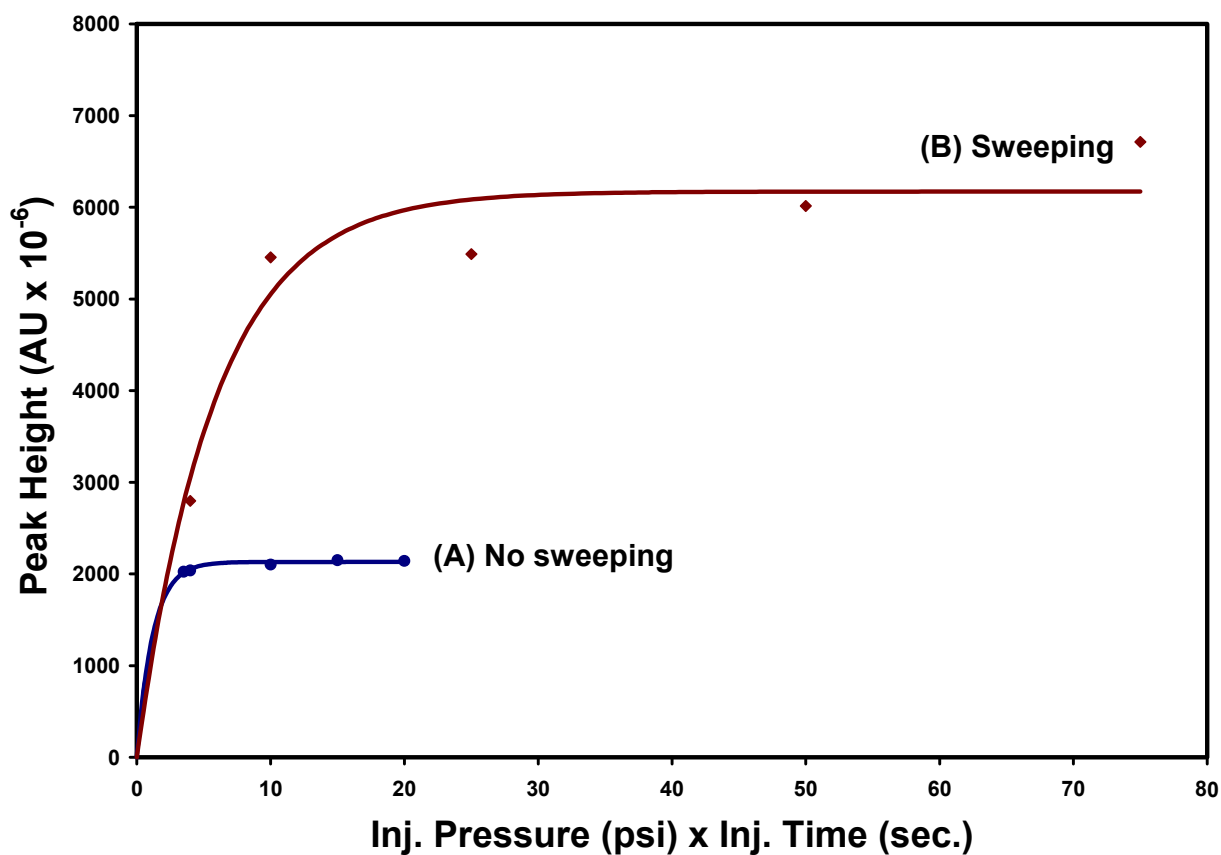


**Figure S-7.** Peak height plotted against injected volume for **desloratadine** under (A) conventional conditions (analyte dissolved in BGE), (B) sweeping conditions (analyte dissolved in **10 mmol L<sup>-1</sup> phosphoric acid, pH 2.15**). BGE: 10 mmol L<sup>-1</sup> sodium borate buffer, pH 9.3 containing **25 mmol L<sup>-1</sup> SDS** and **5 mmol L<sup>-1</sup>  $\beta$ -CD**; injection: hydrodynamic; capillary: fused-silica capillaries (50- $\mu$ m I.D., 363- $\mu$ m O.D.) with a total length of 50.3 cm and a length to the detector of 40.1 cm; temperature of the capillary and the sample tray: 30°C; voltage: +25 kV; detection wavelength: 200 nm.

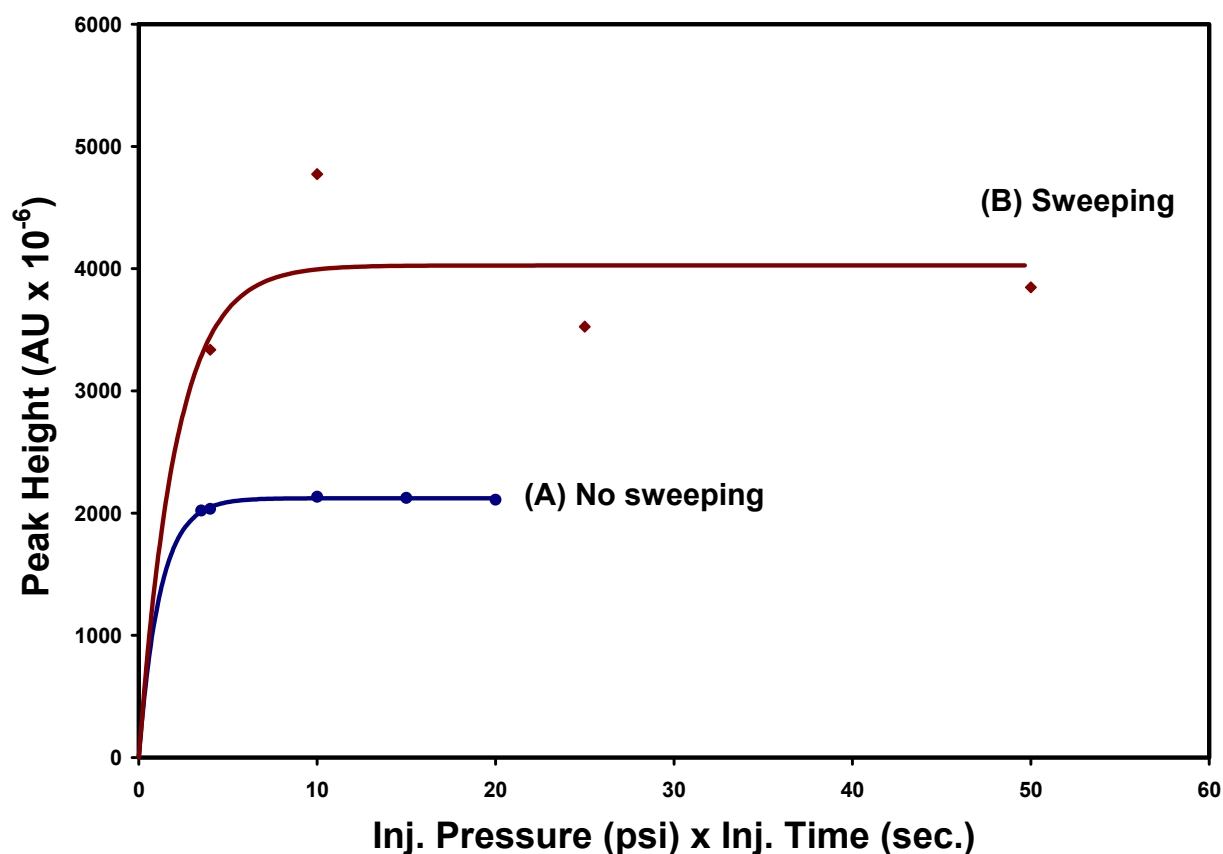


**Figure S-8.** Peak height plotted against injected volume for **desloratadine** under (A) conventional conditions (analyte dissolved in BGE), (B) sweeping conditions (analyte dissolved in **10 mmol L<sup>-1</sup> phosphoric acid, pH 2.15**). BGE: 10 mmol L<sup>-1</sup> sodium borate buffer, pH 9.3 containing **25 mmol L<sup>-1</sup> SDS** and **10 mmol L<sup>-1</sup>  $\beta$ -CD**; injection: hydrodynamic; capillary: fused-silica capillaries (50- $\mu$ m I.D., 363- $\mu$ m O.D.) with a total length of 50.3 cm and a length to the detector of 40.1 cm; temperature of the capillary and the sample tray: 30°C; voltage: +25 kV; detection wavelength: 200 nm.

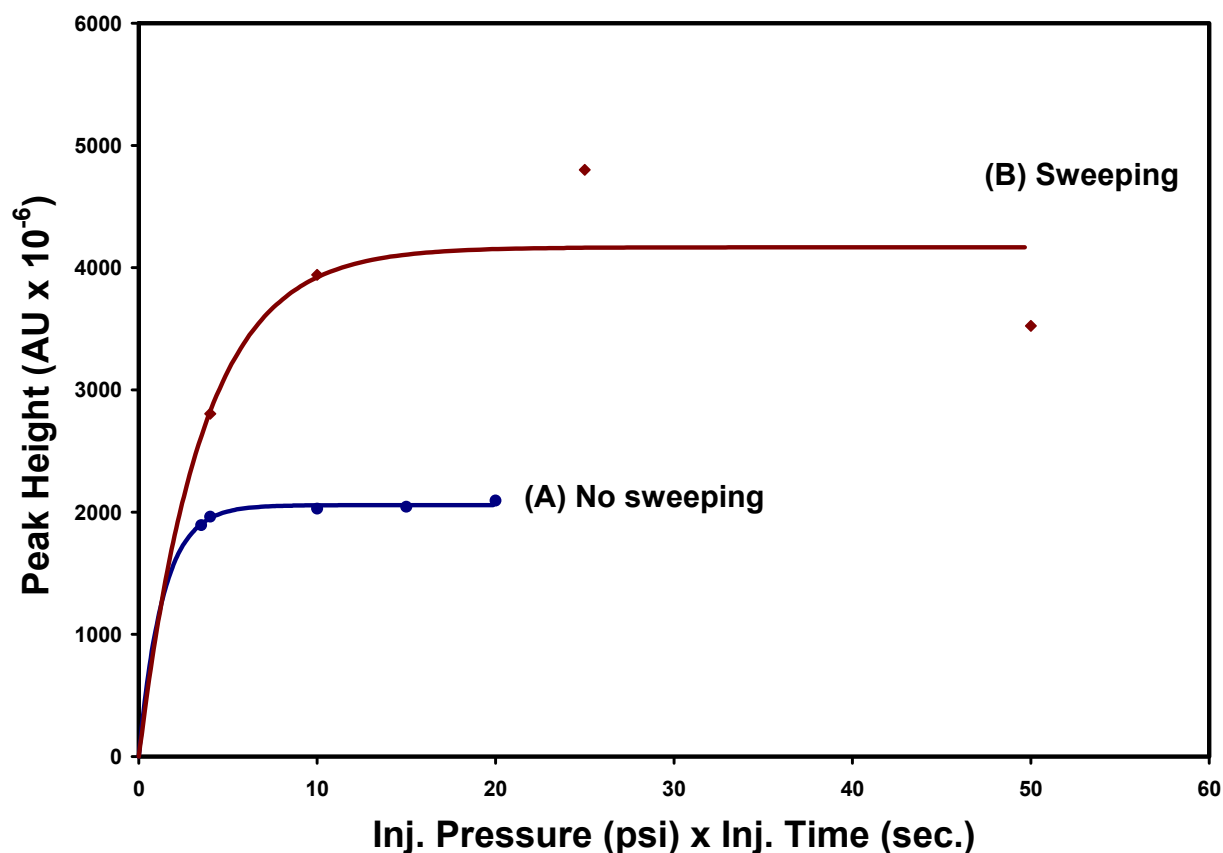


**Figure S-9.** Peak height plotted against injected volume for **desloratadine** under (A) conventional conditions (analyte dissolved in BGE), (B) sweeping conditions (analyte dissolved in **10 mmol L<sup>-1</sup> phosphoric acid, pH 2.15**). BGE: 10 mmol L<sup>-1</sup> sodium borate buffer, pH 9.3 containing **25 mmol L<sup>-1</sup> SDS** and **15 mmol L<sup>-1</sup>  $\beta$ -CD**; injection: hydrodynamic; capillary: fused-silica capillaries (50- $\mu$ m I.D., 363- $\mu$ m O.D.) with a total length of 50.3 cm and a length to the detector of 40.1 cm; temperature of the capillary and the sample tray: 30°C; voltage: +25 kV; detection wavelength: 200 nm.

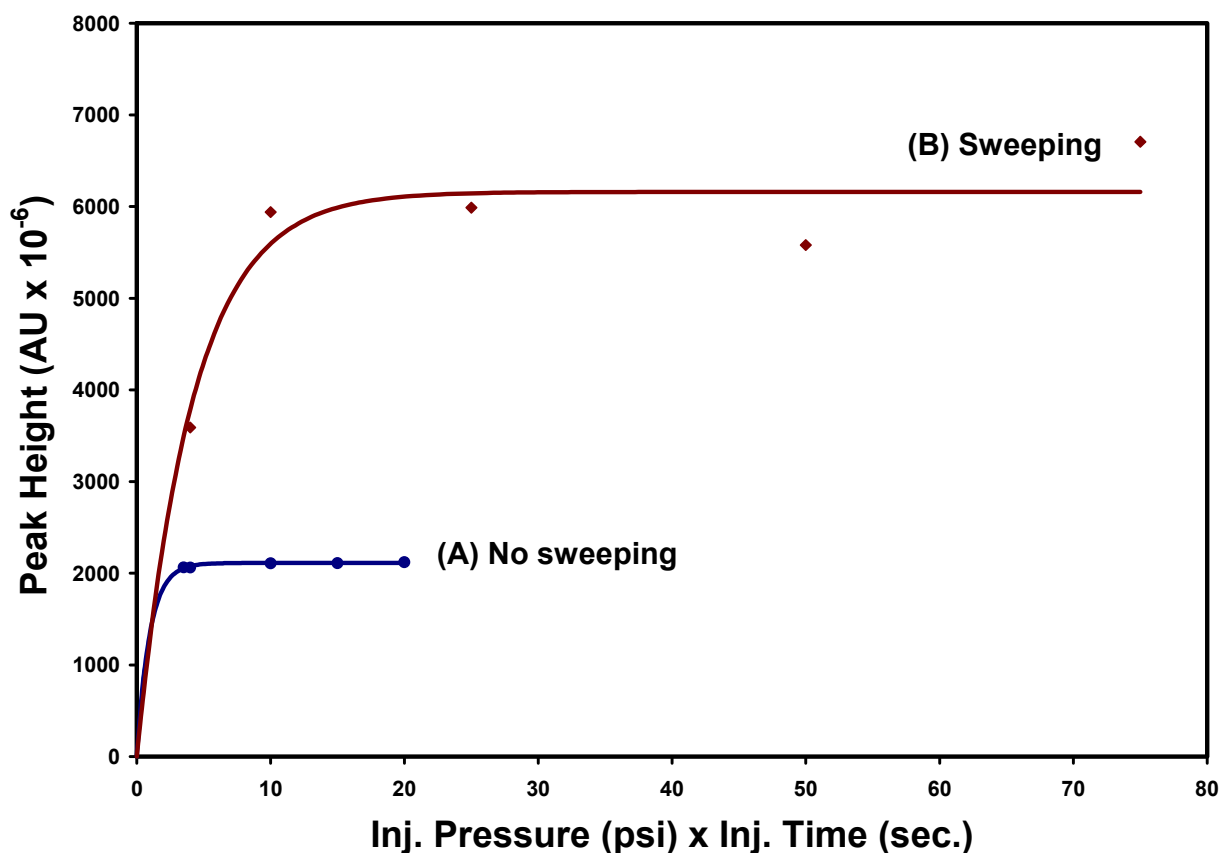


**Figure S-10.** Peak height plotted against injected volume for **desloratadine** under (A) conventional conditions (analyte dissolved in BGE), (B) sweeping conditions (analyte dissolved in **10 mmol L<sup>-1</sup> phosphoric acid, pH 2.15**). BGE: 10 mmol L<sup>-1</sup> sodium borate buffer, pH 9.3 containing **25 mmol L<sup>-1</sup> SDS and 5 mmol L<sup>-1</sup> methyl- $\beta$ -CD**; injection: hydrodynamic; capillary: fused-silica capillaries (50- $\mu$ m I.D., 363- $\mu$ m O.D.) with a total length of 50.3 cm and a length to the detector of 40.1 cm; temperature of the capillary and the sample tray: 30°C; voltage: +25 kV; detection wavelength: 200 nm.

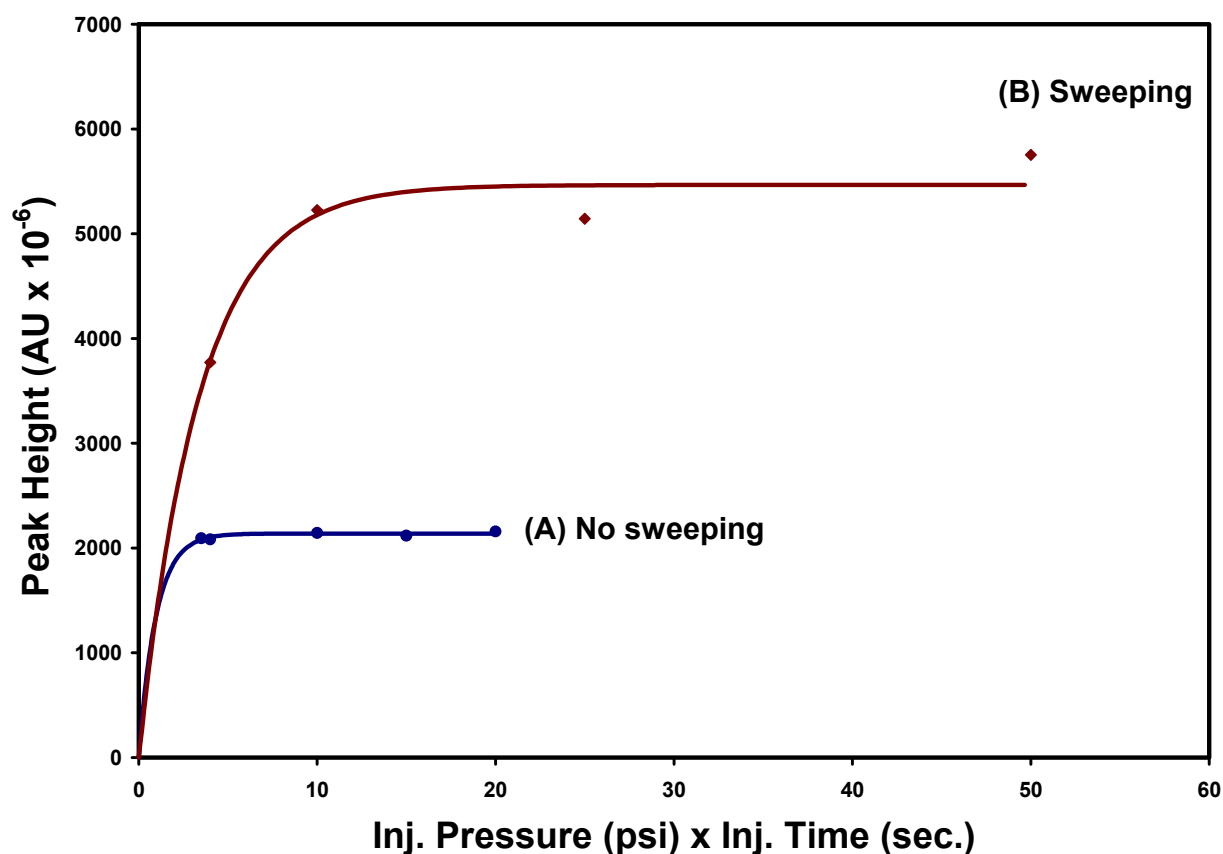


**Figure S-11.** Peak height plotted against injected volume for **desloratadine** under (A) conventional conditions (analyte dissolved in BGE), (B) sweeping conditions (analyte dissolved in **10 mmol L<sup>-1</sup> phosphoric acid, pH 2.15**). BGE: 10 mmol L<sup>-1</sup> sodium borate buffer, pH 9.3 containing **25 mmol L<sup>-1</sup> SDS** and **10 mmol L<sup>-1</sup> methyl- $\beta$ -CD**; injection: hydrodynamic; capillary: fused-silica capillaries (50- $\mu$ m I.D., 363- $\mu$ m O.D.) with a total length of 50.3 cm and a length to the detector of 40.1 cm; temperature of the capillary and the sample tray: 30°C; voltage: +25 kV; detection wavelength: 200 nm.

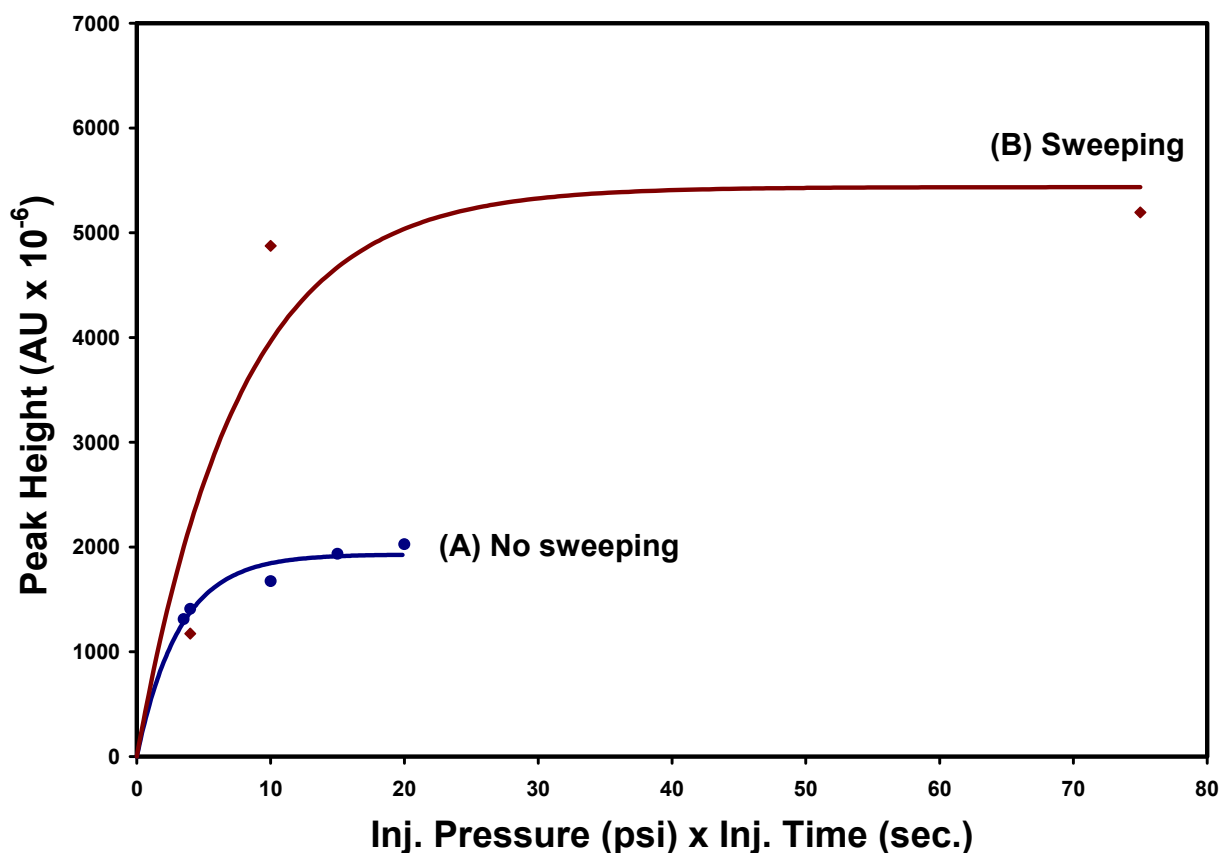


**Figure S-12.** Peak height plotted against injected volume for **desloratadine** under (A) conventional conditions (analyte dissolved in BGE), (B) sweeping conditions (analyte dissolved in **10 mmol L<sup>-1</sup> phosphoric acid, pH 2.15**). BGE: 10 mmol L<sup>-1</sup> sodium borate buffer, pH 9.3 containing **25 mmol L<sup>-1</sup> SDS and 15 mmol L<sup>-1</sup> methyl- $\beta$ -CD**; injection: hydrodynamic; capillary: fused-silica capillaries (50- $\mu$ m I.D., 363- $\mu$ m O.D.) with a total length of 50.3 cm and a length to the detector of 40.1 cm; temperature of the capillary and the sample tray: 30°C; voltage: +25 kV; detection wavelength: 200 nm.

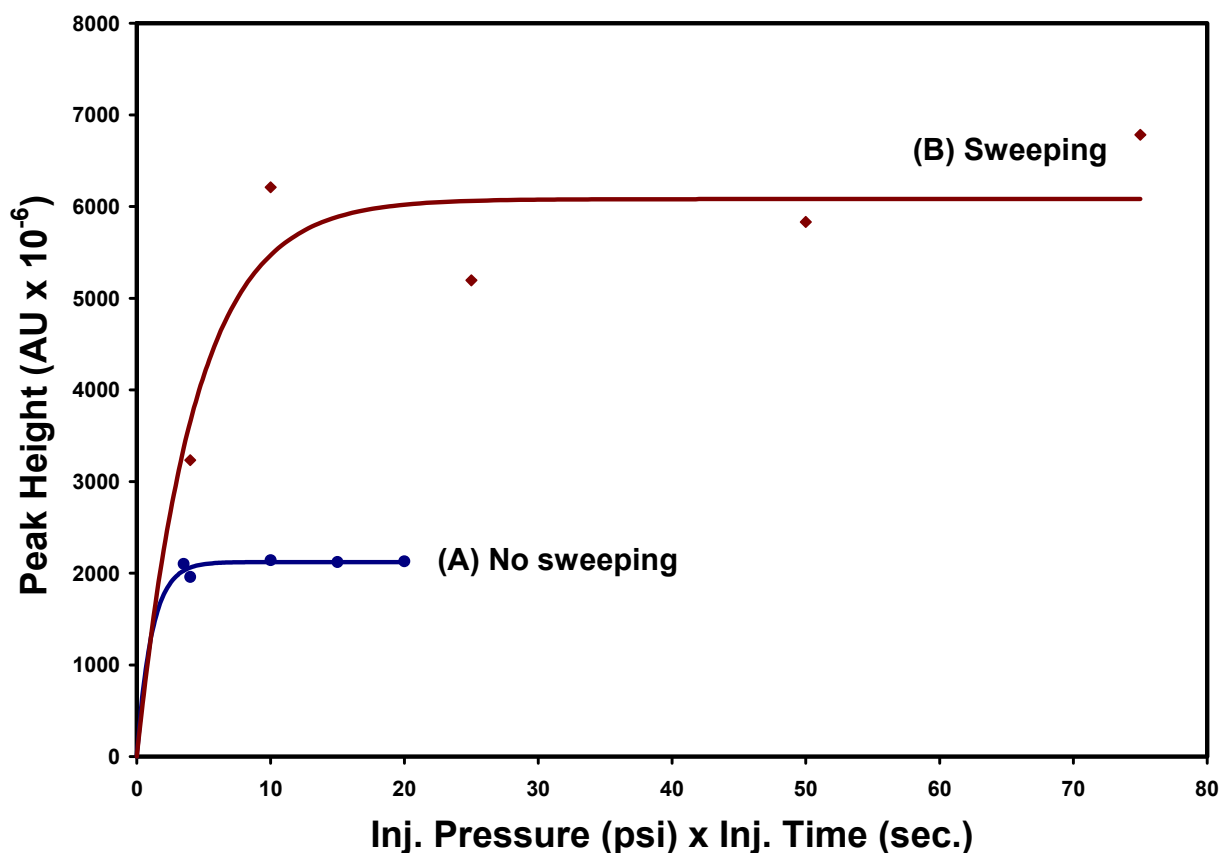


**Figure S-13.** Peak height plotted against injected volume for **desloratadine** under (A) conventional conditions (analyte dissolved in BGE), (B) sweeping conditions (analyte dissolved in **10 mmol L<sup>-1</sup> phosphoric acid, pH 2.15**). BGE: 10 mmol L<sup>-1</sup> sodium borate buffer, pH 9.3 containing **25 mmol L<sup>-1</sup> SDS and 5 mmol L<sup>-1</sup> hydroxypropyl- $\beta$ -CD**; injection: hydrodynamic; capillary: fused-silica capillaries (50- $\mu$ m I.D., 363- $\mu$ m O.D.) with a total length of 50.3 cm and a length to the detector of 40.1 cm; temperature of the capillary and the sample tray: 30°C; voltage: +25 kV; detection wavelength: 200 nm.

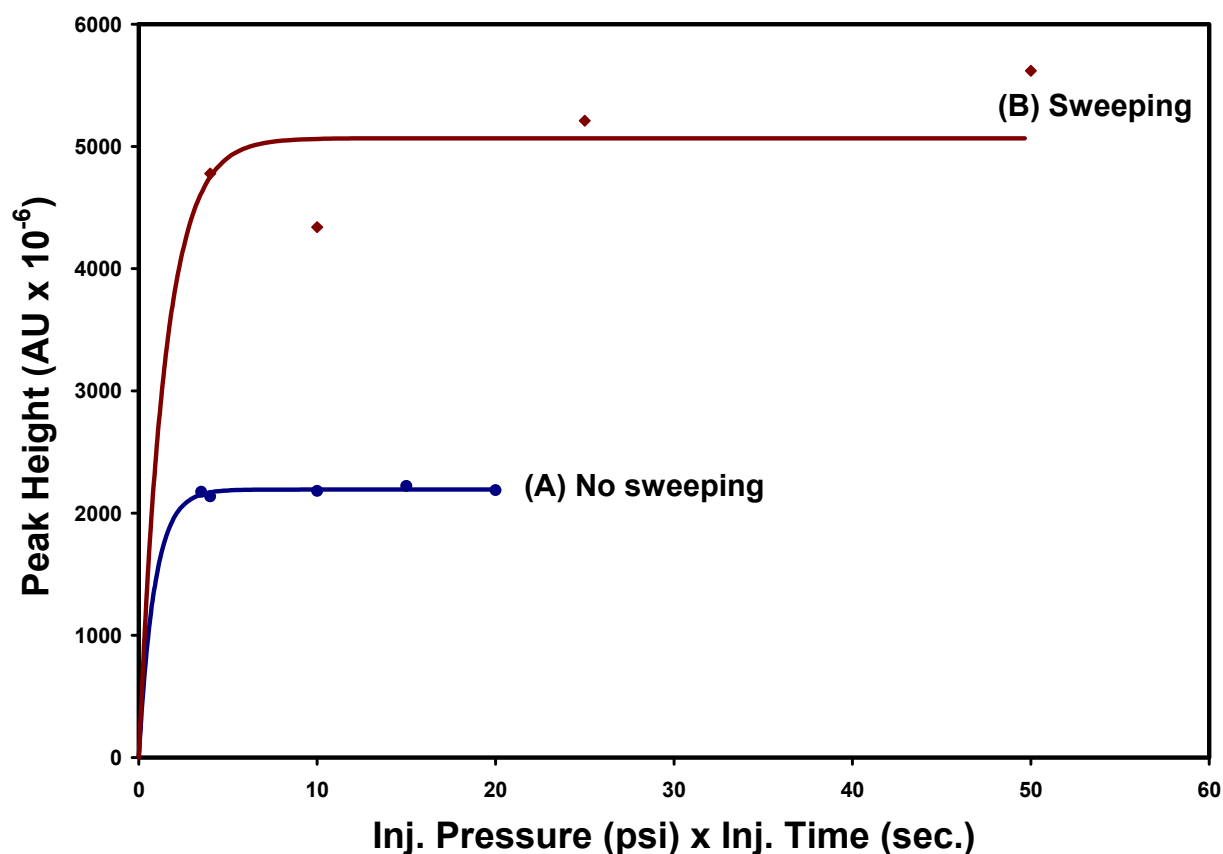


**Figure S-14.** Peak height plotted against injected volume for **desloratadine** under (A) conventional conditions (analyte dissolved in BGE), (B) sweeping conditions (analyte dissolved in **10 mmol L<sup>-1</sup> phosphoric acid, pH 2.15**). BGE: 10 mmol L<sup>-1</sup> sodium borate buffer, pH 9.3 containing **25 mmol L<sup>-1</sup> SDS and 10 mmol L<sup>-1</sup> hydroxypropyl- $\beta$ -CD**; injection: hydrodynamic; capillary: fused-silica capillaries (50- $\mu$ m I.D., 363- $\mu$ m O.D.) with a total length of 50.3 cm and a length to the detector of 40.1 cm; temperature of the capillary and the sample tray: 30°C; voltage: +25 kV; detection wavelength: 200 nm.

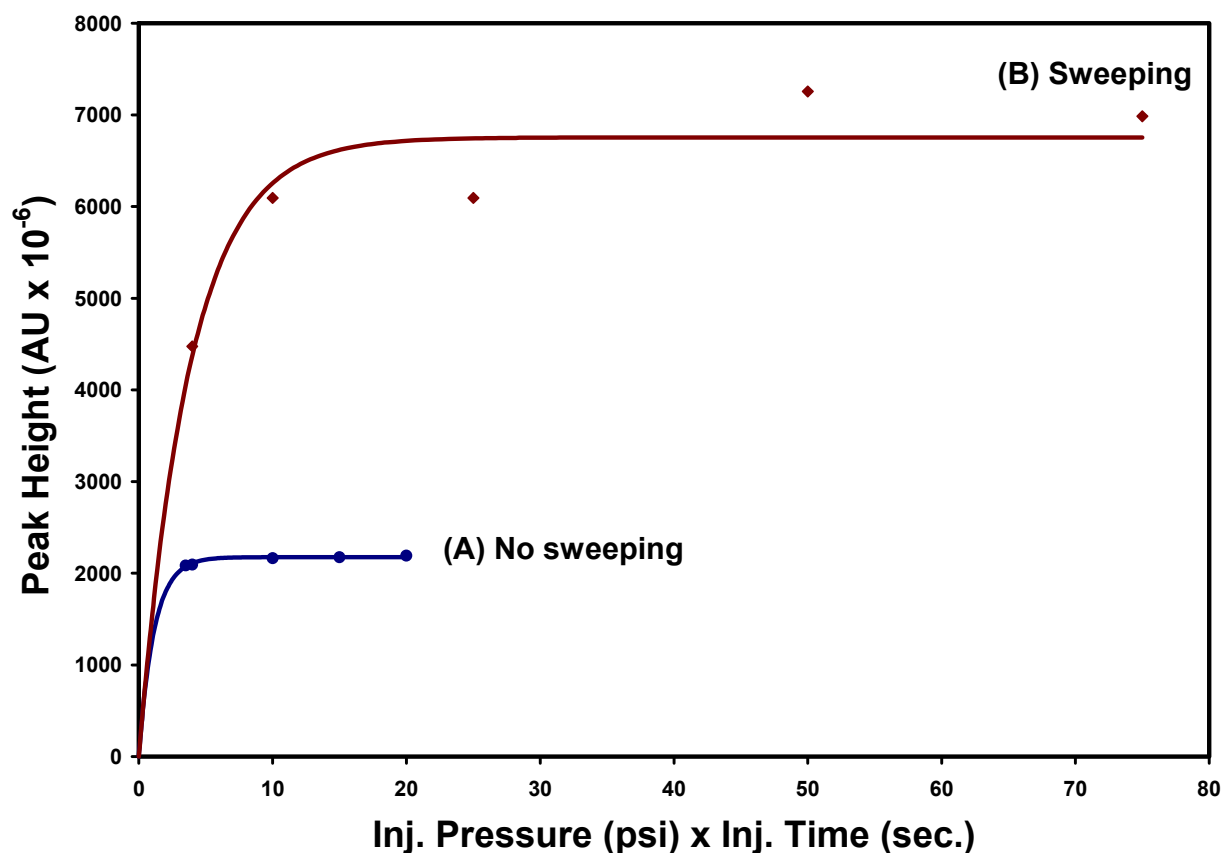


**Figure S-15.** Peak height plotted against injected volume for **desloratadine** under (A) conventional conditions (analyte dissolved in BGE), (B) sweeping conditions (analyte dissolved in **10 mmol L<sup>-1</sup> phosphoric acid, pH 2.15**). BGE: 10 mmol L<sup>-1</sup> sodium borate buffer, pH 9.3 containing **25 mmol L<sup>-1</sup> SDS and 15 mmol L<sup>-1</sup> hydroxypropyl- $\beta$ -CD**; injection: hydrodynamic; capillary: fused-silica capillaries (50- $\mu$ m I.D., 363- $\mu$ m O.D.) with a total length of 50.3 cm and a length to the detector of 40.1 cm; temperature of the capillary and the sample tray: 30°C; voltage: +25 kV; detection wavelength: 200 nm.

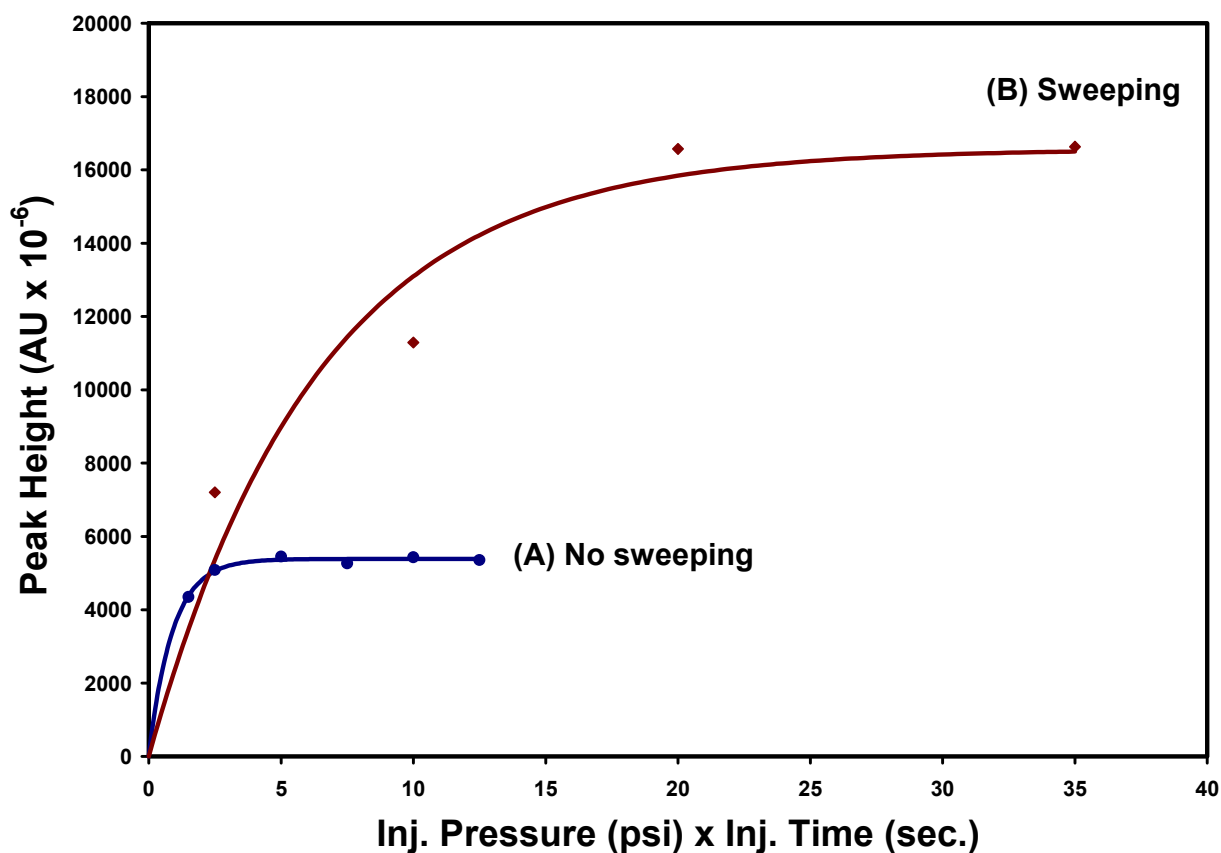


**Figure S-16.** Peak height plotted against injected volume for **desloratadine** under (A) conventional conditions (analyte dissolved in BGE), (B) sweeping conditions (analyte dissolved in **10 mmol L<sup>-1</sup> phosphoric acid, pH 2.15**). BGE: 10 mmol L<sup>-1</sup> sodium borate buffer, pH 9.3 containing **40 mmol L<sup>-1</sup> SDS**; injection: hydrodynamic; capillary: fused-silica capillaries (50- $\mu$ m I.D., 363- $\mu$ m O.D.) with a total length of 50.3 cm and a length to the detector of 40.1 cm; temperature of the capillary and the sample tray: 30°C; voltage: +25 kV; detection wavelength: 200 nm.

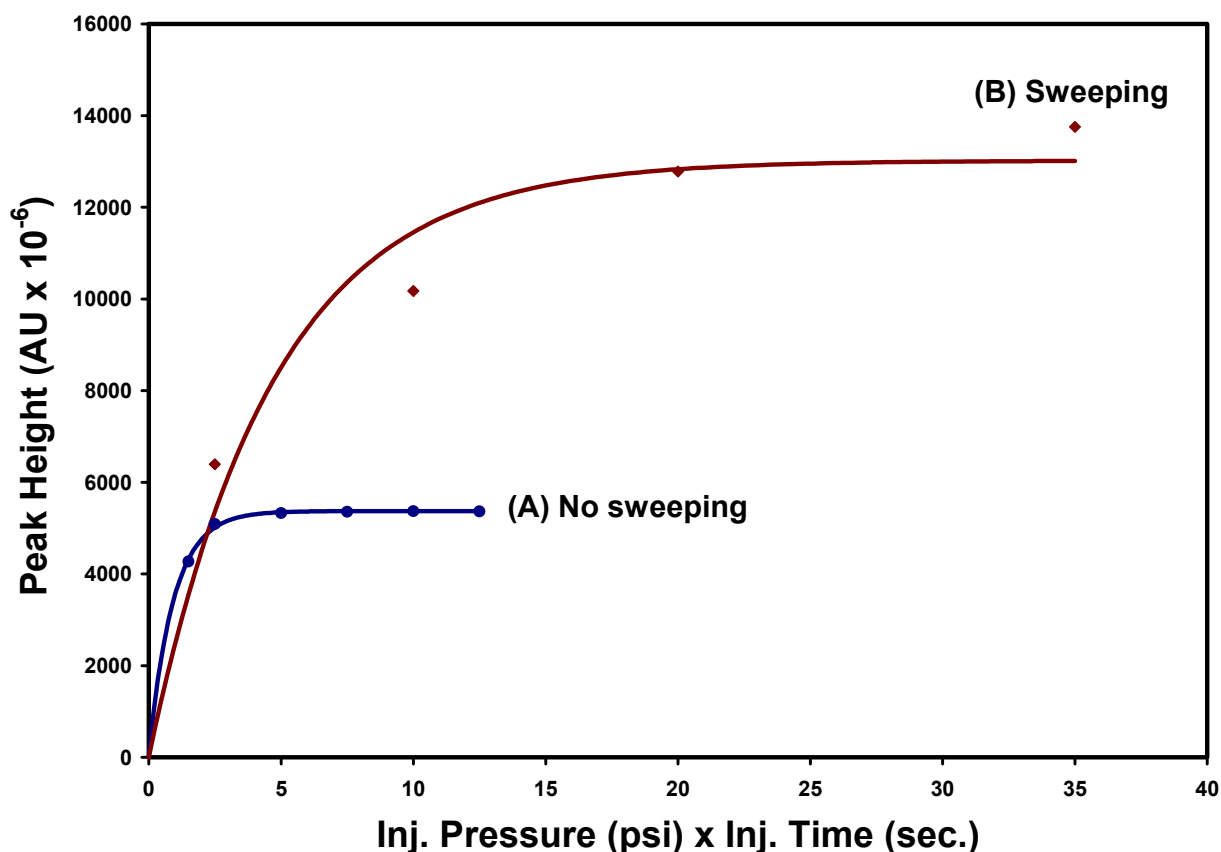


**Figure S-17.** Peak height plotted against injected volume for **desloratadine** under (A) conventional conditions (analyte dissolved in BGE), (B) sweeping conditions (analyte dissolved in **10 mmol L<sup>-1</sup> phosphoric acid, pH 2.15**). BGE: 10 mmol L<sup>-1</sup> sodium borate buffer, pH 9.3 containing **40 mmol L<sup>-1</sup> SDS and 10 mmol L<sup>-1</sup> hydroxypropyl- $\beta$ -CD**; injection: hydrodynamic; capillary: fused-silica capillaries (50- $\mu$ m I.D., 363- $\mu$ m O.D.) with a total length of 50.3 cm and a length to the detector of 40.1 cm; temperature of the capillary and the sample tray: 30°C; voltage: +25 kV; detection wavelength: 200 nm.

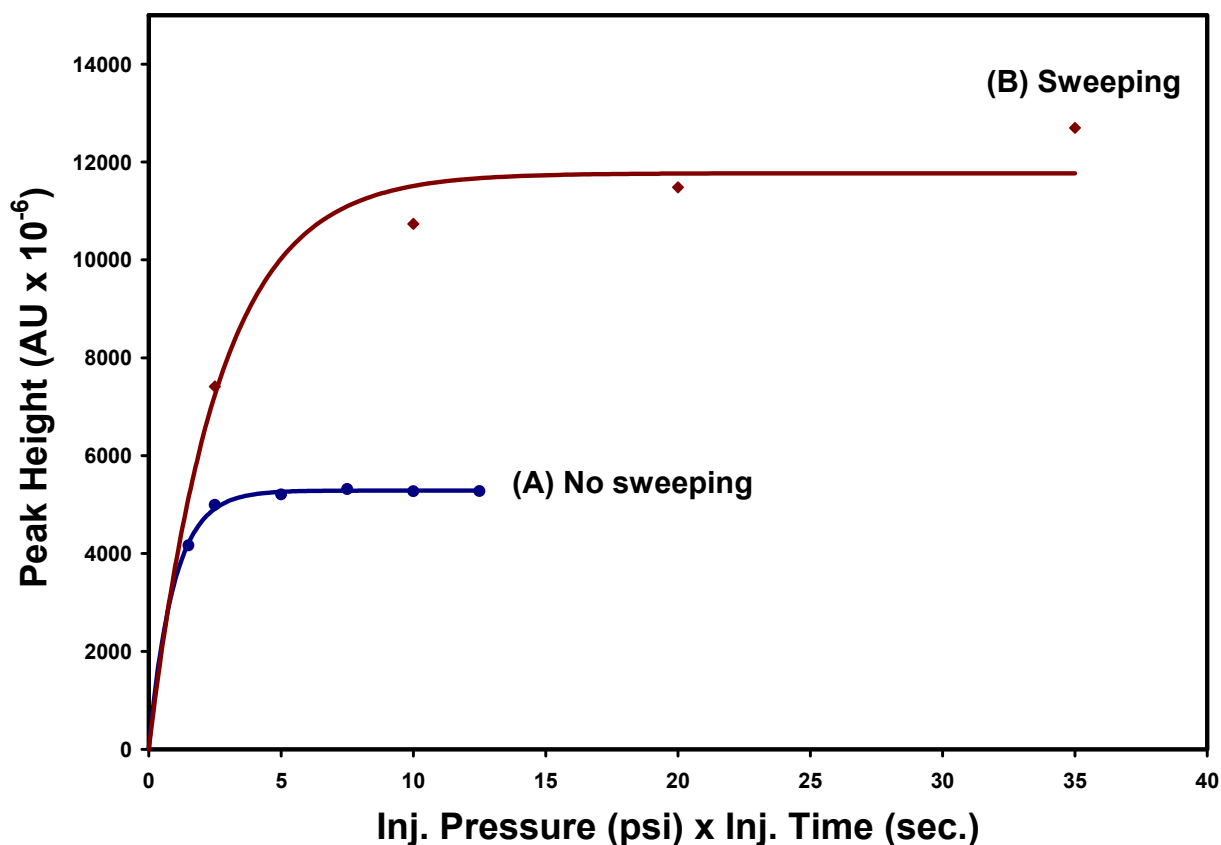


**Figure S-18.** Peak height plotted against injected volume for **desloratadine** under (A) conventional conditions (analyte dissolved in BGE), (B) sweeping conditions (analyte dissolved in **10 mmol L<sup>-1</sup> phosphoric acid, pH 2.15**). BGE: 10 mmol L<sup>-1</sup> sodium borate buffer, pH 9.3 containing **40 mmol L<sup>-1</sup> SDS** and **20 mmol L<sup>-1</sup> hydroxypropyl- $\beta$ -CD**; injection: hydrodynamic; capillary: fused-silica capillaries (50- $\mu$ m I.D., 363- $\mu$ m O.D.) with a total length of 50.3 cm and a length to the detector of 40.1 cm; temperature of the capillary and the sample tray: 30°C; voltage: +25 kV; detection wavelength: 200 nm.

## **5.4. Publication IV**

**Robust analysis of hydrophobic basic analytes in pharmaceutical preparations and biological fluids by sweeping-micellar electrokinetic chromatography with retention factor gradient effect and dynamic pH junction**

Mohamed El-Awady, Fathalla Belal, Ute Pyell

*Submitted to: Journal of Chromatography A*



## **5.4.1. Summary and discussion**

In this publication, a robust and reliable method is developed for the simultaneous determination of the two antihistaminic drugs loratadine (LOR) and its major metabolite desloratadine (DSL) which is also one of the potential impurities in LOR bulk powder. As hydrophobic basic analytes, LOR and DSL are difficult to be analyzed by MEKC because of their tendency to be adsorbed onto the inner capillary wall in addition to their extremely high retention factors that render their separation challenging. The developed method for the analysis of this mixture is based on cyclodextrin-modified micellar electrokinetic chromatography (CD-MEKC) with acidic sample matrix and basic background electrolyte (BGE). The use of a low-pH sample solution diminishes problems associated with the low solubility of these hydrophobic basic analytes in aqueous solution while having advantages with regard to online focusing. At the same time, the solubility of these analytes is significantly improved by the presence of hydroxypropyl- $\beta$ -CD (HP- $\beta$ -CD) and SDS in the BGE. In addition, the use of a basic BGE reduces considerably the observed problems due to solute-wall interactions and overcomes the problem of adsorption of LOR and DSL in the separation compartment as they are non-ionized at this pH and hence the ionic interaction with the negative silanol groups of the capillary wall is minimized. Moreover, the presence of HP- $\beta$ -CD in the BGE plays an additional role in reducing adsorption problems while improving the efficiency and reproducibility of the developed method.

Different experimental parameters are investigated in order to achieve the highest resolution within a short analysis time. The separation of LOR and DSL is achieved in less than 7 minutes using a BGE consisting of 10 mmol L<sup>-1</sup> sodium borate buffer, pH 9.30 containing 40 mmol L<sup>-1</sup> SDS and 20 mmol L<sup>-1</sup> HP- $\beta$ -CD while the sample matrix is composed of 10 mmol L<sup>-1</sup> phosphoric acid, pH 2.15. The validation criteria of the developed method are thoroughly studied adopting the official ICH guidelines. The developed method is successfully applied to analyze the studied drugs in tablets. The results are statistically evaluated and compared with those obtained by the pharmacopeial method and are found to be in a good agreement. The selectivity regarding potential interferences from tablet additives or from the co-formulated drug pseudoephedrine is verified. Pseudoephedrine is successfully separated from LOR and DSL. Therefore, our method can be also utilized for the analysis of a ternary mixture of these drugs. The developed method is applied to the analysis of DSL as an impurity in LOR bulk powder at the stated pharmacopeial limit (0.1%). Moreover, the analysis of LOR and DSL in spiked human urine is successfully conducted. To the best of our knowledge, the developed method is the first validated capillary electromigration separation method for the simultaneous determination of LOR and DSL. The strategies used in the development of this method are applicable to other hydrophobic basic analytes to develop robust and precise capillary electromigration separation methods for their qualitative and quantitative analysis.

## **5.4.2. Author contribution**

All the experimental part of this study was carried out by me except the official pharmacopeial method which was conducted by M.Sc. Heba Elmansi (Faculty of Pharmacy, Mansoura University). The studied analytes were suggested and supplied by Prof. Fathalla Belal (Faculty of Pharmacy, Mansoura University). The draft of the manuscript was written by me and corrected by Prof. Fathalla Belal and Prof. Ute Pyell. The final revision of the manuscript was conducted by me and Prof. Pyell before submission to the journal. Prof. Ute Pyell was responsible for the supervision of this work.

**5.4.3. Robust analysis of hydrophobic basic analytes in pharmaceutical preparations and biological fluids by sweeping-micellar electrokinetic chromatography with retention factor gradient effect and dynamic pH junction.**

Mohamed El-Awady<sup>1</sup>, Fathalla Belal<sup>2</sup>, Ute Pyell<sup>1\*</sup>

<sup>1</sup> University of Marburg, Department of Chemistry, Hans-Meerwein-Straße, D-35032 Marburg, Germany

<sup>2</sup> Mansoura University, Faculty of Pharmacy, Analytical Chemistry Department, 35516 Mansoura, Egypt

\* corresponding author

**Tel.: +49 6421 2822192**

**Fax: +49 6421 2822124**

**e-mail: [pyellu@staff.uni-marburg.de](mailto:pyellu@staff.uni-marburg.de)**

**Keywords**

Loratadine; Desloratadine; Cyclodextrin-modified micellar electrokinetic chromatography; Sweeping; Retention factor gradient effect; Spiked urine.

## Abstract

The analysis of hydrophobic basic analytes by micellar electrokinetic chromatography (MEKC) is usually challenging because of the tendency of these analytes to be adsorbed onto the inner capillary wall in addition to the difficulty to separate these compounds as they exhibit extremely high retention factors. A robust and reliable method for the simultaneous determination of loratadine (LOR) and its major metabolite desloratadine (DSL) is developed based on cyclodextrin-modified micellar electrokinetic chromatography (CD-MEKC) with acidic sample matrix and basic background electrolyte (BGE). The influence of the sample matrix on the reachable focusing efficiency is studied. It is shown that the application of a low pH sample solution mitigates problems associated with the low solubility of the hydrophobic basic analytes in aqueous solution while having advantages with regard to on-line focusing. Moreover, the use of a basic BGE reduces the adsorption of these analytes in the separation compartment. The separation of the studied analytes is achieved in less than 7 minutes using a BGE consisting of 10 mmol L<sup>-1</sup> sodium borate buffer, pH 9.30 containing 40 mmol L<sup>-1</sup> SDS and 20 mmol L<sup>-1</sup> hydroxypropyl- $\beta$ -CD while the sample solution is composed of 10 mmol L<sup>-1</sup> phosphoric acid, pH 2.15. A full validation study of the developed method based on the pharmacopeial guidelines is performed. The method is successfully applied to the analysis of the studied drugs in tablets without interference of tablet additives as well as the analysis of spiked human urine without any sample pretreatment. Furthermore, DSL can be detected as an impurity in LOR bulk powder at the stated pharmacopeial limit (0.1% w/w). The selectivity of the developed method allows the analysis of LOR and DSL in combination with the co-formulated drug pseudoephedrine. It is shown that in CD-MEKC with basic BGE, solute-wall interactions are effectively suppressed allowing the development of efficient and precise methods for the determination of hydrophobic basic analytes, whereas the use of a low pH sample solution has a positive impact on the attainable sweeping efficiency without compromising peak shape and resolution.

## 1. Introduction

Capillary electromigration separation techniques are characterized by their high versatility, short run times, selectivity, extremely high efficiency and minimum solvent consumption. The use of capillary electrophoretic methods for the analysis of hydrophobic basic analytes suffers some difficulties. One of these difficulties is the adsorption of these analytes onto the inner capillary wall, which can lead to a number of disturbances such as instability of the electroosmotic flow (EOF) velocity, poor figures-of-merit, peak deformation, sample loss, deterioration of separation efficiency and irreproducible migration times. The main driving forces for the adsorption of analytes onto the capillary wall are hydrophobic and/or electrostatic interactions [1]. Analysis of hydrophobic basic analytes by capillary zone electrophoresis is usually performed at acidic pH to get the analytes charged with positive electrophoretic mobility as well as to bring them dissolved in solution. The electrostatic interaction of these positively charged solutes with the inner capillary wall makes the adsorption problem more severe. Several approaches have been utilized to overcome this problem such as the use of extreme pH rinsing, manipulation of the ionic strength of the BGE, dynamic coating of the inner capillary surface with organic molecules or use of a permanently coated fused-silica capillary [2-5].

Another problem that is usually encountered with the analysis of highly hydrophobic analytes by MEKC is their high retention factors and the tendency to be totally incorporated into the micelles rendering their separation very difficult [6]. To overcome this problem, different approaches have been investigated [7-11]. Among these approaches is the use of CD-MEKC. CDs form stable inclusion complexes with a wide variety of analytes by host-guest interaction [12-14]. These inclusion complexes have usually a 1:1 stoichiometry, although a 2:1 stoichiometry is sometimes reported [15]. The addition of a CD to the BGE can significantly alter the apparent retention factor of several analytes by introducing an additional complex-formation equilibrium to the system. To understand the processes involved upon addition of CD to the BGE in CD-MEKC, different equilibria should be taken into account including the acid-base equilibrium of the weak base, the micelle-formation equilibrium, the distribution equilibria and the complex-formation equilibria. The distribution equilibria involve the distribution of both the ionized and non-ionized forms of the analyte between the aqueous phase and the micellar phase. The complex-formation equilibria involve the formation of inclusion complexes between CD and both the ionized and non-ionized forms of the analyte as well as the surfactant monomers. For a basic analyte B and an anionic surfactant S (where S is the surfactant monomer), the involved equilibria under CD-MEKC conditions can be summarized as follows [16]:

Acid-base equilibrium:



Micelle-formation equilibrium:



Distribution equilibria:



Complex-formation equilibria:



By addition of CD to the BGE, the apparent distribution coefficient  $K_{D,\text{app}}$  of the analyte between the micellar phase and the aqueous pseudophase is reduced by increasing the fraction of analyte in the non-micellar phase resulting in a significant decrease in the apparent retention factor  $k_{\text{BGE,app}}$  [6,9,16]. Moreover, CD can form an inclusion complex with SDS monomers and hence the micellization of SDS molecules is affected resulting in an increase of the apparent critical micelle concentration ( $\text{CMC}_{\text{app}}$ ) of SDS, which is another reason for the significant decrease of  $k_{\text{BGE,app}}$  upon addition of CD to the BGE [17-20].

Whereas reducing the retention factor and avoiding the adsorption of hydrophobic analytes onto the capillary wall can be achieved by addition of an organic solvent to the BGE [21], CDs being added to the BGE similarly do not only reduce the apparent retention factor but also effectively suppress the adsorption of analytes onto the inner capillary wall and hence are reported to improve the efficiency and reproducibility of the separation method [22]. Applications of CD-MEKC have been reviewed in several articles [23-25].

Sweeping is one of the most important sample preconcentration techniques in MEKC. It is based on the concentration enrichment of analyte by the pseudostationary phase (PSP) that penetrates the sample zone being void of PSP [26]. Early reports of Quirino and Terabe [26-28] assumed that the enrichment factor due to sweeping is directly proportional to the retention factor of analytes in the sample zone during sweeping. However, we showed experimentally and theoretically in a previous publication [29] that the focusing process due to sweeping is not only affected by the retention factor of the analyte in

the sample zone, but also by the retention factor of the analyte in the BGE. We introduced the term “retention factor gradient effect (RFGE)” to express the additional focusing or defocusing effect that arises if the distribution coefficient and hence the retention factor of analyte is different in the sample and BGE compartments [29]. Sweeping can also be combined with dynamic pH junction to improve the focusing efficiency for certain analytes if compared with either dynamic pH junction or sweeping alone [30]. This combination was first investigated by Britz–McKibbin *et al.* [30] for the analysis of flavin derivatives. The authors used a sample having a pH different from the pH of the BGE (dynamic pH junction condition) and being void of SDS (sweeping condition). Later, the combination of sweeping with dynamic pH junction has found a wide range of applications in the literature [31].

Loratadine (Figure 1) or ethyl 4-(8-chloro-5,6-dihydro-11*H*-benzo[5,6]cyclohepta[1,2-*b*]pyridin-11-ylidene)piperidine-1-carboxylate is a long-acting non-sedating antihistaminic drug used for the symptomatic relief of allergic conditions including rhinitis and chronic urticaria. LOR is also co-formulated with the decongestant drug pseudoephedrine. LOR is rapidly absorbed from the gastrointestinal tract after oral administration and then it is metabolized to its major metabolite desloratadine (DSL) that has a potent antihistaminic activity. The reported mean elimination half-lives for LOR and DSL are 8.4 and 28 hours, respectively. Most of the LOR dose is excreted equally in the urine and faeces, mainly in the form of metabolites [32]. Chemically, LOR is a weak base with a  $pK_a$  of 5.25 at 25°C [33] and an octanol/water partition coefficient  $\log P$  of 5 [34]. LOR is insoluble in water and soluble in acids and alcohol [35].

Desloratadine (Figure 1) or 8-Chloro-6,11-dihydro-11-(4-piperidylidene)-5*H*-benzo[5,6]cyclohepta[1,2-*b*]pyridine is also a long-acting non-sedating antihistaminic drug. Its oral dose is half of the LOR dose. DSL has the same medicinal uses as LOR and is also co-formulated with pseudoephedrine [32]. Beside being an antihistaminic drug and the active metabolite of LOR, DSL is also a potential impurity in LOR powder and it is reported by the European Pharmacopeia [36] and the United States Pharmacopeia [37] as one of the related substances of LOR that must pass a liquid chromatographic limit test. The maximum allowed limit of DSL as an impurity in LOR powder is 0.1% (w/w) [36,37]. Chemically, DSL is a weak base having two  $pK_a$  values, 4.41 and 9.97 at 25°C [33] and an octanol/water partition coefficient  $\log P$  of 3.2 [38]. DSL is slightly soluble in water and well soluble in acids, ethanol and propylene glycol [35]. DSL is synthesized by decarboxylation of LOR [39-43]. Therefore, LOR may be contained as an impurity in DSL powder due to incomplete reaction or purification steps.

The high structural and physicochemical similarities between LOR and DSL render the simultaneous analysis of both drugs very difficult. Different analytical methods for the simultaneous determination of LOR and DSL have been published in the literature. These include UPLC [44], HPLC [45-61], HPTLC

[62], TLC [63], GC [64] and spectrophotometric [65] methods. Most of the chromatographic methods reported for the simultaneous determination of LOR and DSL depend on mass spectrometric detectors which are expensive and not readily accessible in many laboratories.

Regarding capillary electromigration separation techniques, Fernandez *et al.* [66] developed a method for the determination of loratadine and its related impurities including desloratadine based on capillary zone electrophoresis (CZE) using an uncoated fused-silica capillary and a BGE consisting of 100 mmol L<sup>-1</sup> phosphoric acid made up to pH 2.5 with NaOH and containing 10% (v/v) acetonitrile. Fernandez *et al.* [66] reported that their developed method suffered from poor figures-of merit especially regarding the precision. They also reported that the variations in the results provided some validation parameters, which did not comply with the expected values. They attributed the reason of this problem to the analyte-wall interaction (adsorption of analytes onto the inner capillary wall). Different strategies to solve this problem were developed by the authors, however, with insignificant improvement. The final conclusion drawn by Fernandez *et al.* [66] was that the developed CZE method is suitable as a complementary tool for the impurity profiling of LOR during stability tests. Moreover, they stated that the validation parameters of this method are poorer than those described for an HPLC method for the same compounds and therefore HPLC would be more preferable to CZE for quantitation purposes.

In the present study, we intend to develop a robust, precise and reliable capillary electromigration separation method for the simultaneous determination of LOR and DSL based on CD-MEKC with acidic sample matrix and basic BGE (pH 9.30) that reduces considerably the observed problems due to solute-wall interactions. The basic pH of the BGE minimizes the adsorption of LOR and DSL on the inner capillary wall as they are non-ionized at this pH and hence the ionic interaction with the negative silanol groups of the capillary wall is minimized. At the same time, the solubility of these hydrophobic basic analytes is significantly improved by the presence of hydroxypropyl- $\beta$ -CD (HP- $\beta$ -CD) and SDS in the BGE [67]. Different experimental parameters are investigated in order to achieve the highest resolution within a short analysis time. The validation criteria of the developed method are thoroughly studied adopting the official ICH guidelines [68]. The method is successfully applied to the analysis of the studied drugs in pharmaceutical preparations and in urine. The selectivity regarding potential interferences from tablet additives or from the co-formulated drug pseudoephedrine is verified. Moreover, the developed method is shown to be applicable to the analysis of DSL as an impurity in LOR bulk powder at the stated pharmacopeial limit (0.1% w/w). The results are statistically evaluated and compared with those obtained by official methods and are found to be in a good agreement. To the best of our knowledge, the developed MEKC method is the first validated capillary electromigration separation method for the simultaneous determination of LOR and DSL.

### 3. Experimental

#### 3.1 Apparatus

All measurements were done with a Beckman (Fullerton, CA, USA) P/ACE™ MDQ CE-system equipped with a UV-detector. Data were recorded with Beckman 32 Karat software (v. 5.0). Under the optimized conditions, the temperature of the capillary and the sample tray was kept at 30°C and the separation was performed using an applied voltage of +25 kV with UV-detection at 200 nm. Hydrodynamic injection was utilized and the optimum injection pressure was 0.5 psi for 5 s. Fused-silica capillaries (50- $\mu\text{m}$  I.D., 363- $\mu\text{m}$  O.D.) were from Polymicro Technologies (Phoenix, AZ, USA) with a total length of 50.3 cm and a length to the detector of 40.1 cm. Under the optimized conditions, the resulting electric current was about 40  $\mu\text{A}$ . Inolab 720 pH meter (WTW, Weilheim, Germany) was used for pH measurements.

#### 3.2 Chemicals and materials

Loratadine (certified to have a purity of 99.7%) and desloratadine (certified to have a purity of 99.6%) were kindly provided by Schering–Plough Corporation, USA. Pseudoephedrine hydrochloride containing capsules were kindly donated by Amoun Pharmaceutical Co., El-Obour City, Egypt. Disodium tetraborate decahydrate and orthophosphoric acid were from Merck, Darmstadt, Germany. SDS and 2-phenylethylamine were from Fluka, Buchs, Switzerland.  $\beta$ -cyclodextrin and 4-ethylaniline were from Sigma, St. Louis, USA. Hydroxypropyl- $\beta$ -cyclodextrin, 97% was from Acros Organics, Geel, Belgium. Thiourea was from Riedel-de Haën, Seelze, Germany. All buffers were prepared in deionized water.

For application on pharmaceutical preparations, the following products were purchased from the German market: Lora-ADGC® tablets labeled to contain 10 mg loratadine, produced by KSK-Pharma AG, Berghausen, Germany and Aerius® film-coated tablets labeled to contain 5 mg desloratadine, produced by MSD SHARP & DOHME GmbH, Haar, Germany. For the study of spiked urine, a blank urine sample was obtained from a male 35-years old healthy volunteer.

#### 3.3. Preparation of background electrolyte

Stock sodium borate buffer (50 mmol L<sup>-1</sup>, pH 9.30) was prepared by dissolving 19.068 g disodium tetraborate (Na<sub>2</sub>B<sub>4</sub>O<sub>7</sub>·10H<sub>2</sub>O) in 1000 mL of deionized water and the final pH was 9.30 without any adjustment. This stock was very stable for at least one month when stored in the refrigerator. Stock SDS solution (200 mmol L<sup>-1</sup>) was prepared by dissolving 5.768 g SDS in 100 mL deionized water and the solution is stored in the refrigerator and used for maximum one week. The above stock solutions were used for the preparation of the final optimized BGE that consists of 10 mmol L<sup>-1</sup> sodium borate buffer,

pH 9.30 containing 40 mmol L<sup>-1</sup> SDS and 20 mmol L<sup>-1</sup> hydroxypropyl-β-CD. The BGE was filtered through a 0.45-μm membrane filter (Wicom GmbH, Germany) and degassed in an ultrasonic bath for 10 minutes

### **3.4. Sample preparation and procedures**

Standard solutions 200 μg mL<sup>-1</sup> of each of LOR and DSL in 10 mmol L<sup>-1</sup> phosphoric acid, pH 2.15 were prepared and used for maximum one week when stored in the refrigerator. Standard solutions 250 μg mL<sup>-1</sup> of 4-ethylaniline (I.S.) and 2000 μg mL<sup>-1</sup> of 2-phenylethylamine (another I.S. for urine analysis) in 10 mmol L<sup>-1</sup> phosphoric acid, pH 2.15 were freshly prepared daily.

#### **3.4.1. Rinsing procedure**

New capillaries were conditioned by flushing them first with 1 mol L<sup>-1</sup> NaOH solution for 60 min, then with water for 30 min and then with BGE for 30 min. A rinsing step with BGE for 5 min was performed between runs. A water-dipping step was performed before and after injection to avoid cross contamination of the acidic sample matrix and the basic BGE.

#### **3.4.2. General procedure and construction of the calibration curve**

Aliquots of the standard solutions of LOR and DSL were transferred into a series of 10-mL volumetric flasks so that the final concentration was in the range of 3-60 and 2-60 μg mL<sup>-1</sup>, respectively. To each flask, 1.0 mL of the standard solution of 4-ethylaniline (I.S.) was added so that its final concentration was 25 μg mL<sup>-1</sup> and the flasks were completed to volume with 10 mmol L<sup>-1</sup> phosphoric acid, pH 2.15.

The samples were then analyzed using the following experimental conditions: BGE: 10 mmol L<sup>-1</sup> sodium borate buffer, pH 9.30 containing 40 mmol L<sup>-1</sup> SDS and 20 mmol L<sup>-1</sup> hydroxypropyl-β-CD; capillary: fused silica-capillaries (50-μm I.D., 363-μm O.D.) with a total length of 50.3 cm and a length to the detector of 40.1 cm; temperature of the capillary and the sample tray: 30°C; applied voltage: +25 kV; injection: hydrodynamic injection using pressure 0.5 psi for 5 s, and detection wavelength: 200 nm.

The calibration curves were constructed by plotting the average peak area ratio (analyte/I.S.) versus the analyte concentration in μg mL<sup>-1</sup> followed by linear regression analysis of the obtained data.

#### **3.4.3. Analysis of pharmaceutical preparations**

For LOR, twenty Lora-ADGC® tablets were weighed and then finely powdered. An accurately weighed amount of the powder equivalent to 10.0 mg of LOR was transferred into a 100-mL volumetric flask and diluted to the mark with 10 mmol L<sup>-1</sup> phosphoric acid, pH 2.15. The flask was sonicated for 30 min,

filtered through a 0.45- $\mu\text{m}$  membrane filter and the resulting solution was analyzed as described under Section 3.4.2. The recovered concentration of LOR was determined from the corresponding regression equation. For DSL, Aeries<sup>®</sup> film-coated tablets were analyzed by the same procedure without needing to remove the colored film coating. There is no official monograph for DSL in the European Pharmacopeia [36] or the United States Pharmacopeia [37], therefore the liquid chromatographic method described in the European Pharmacopeia for the determination of DSL as a related substance of LOR was utilized for the simultaneous assay of LOR and DSL as a reference comparison method for our results (experimental details of the reference pharmacopeial method are included in the Supplementary Data).

#### **3.4.4. Analysis of spiked urine samples**

New calibration curves were constructed using spiked human urine samples as follows: 1.5 ml aliquots of urine were transferred into a series of 2-mL volumetric flasks and spiked with increasing volumes of the standard solutions of both LOR and DSL so that the final concentration of both drugs was in the range of 3-20  $\mu\text{g mL}^{-1}$ . To each flask, 0.05 mL of the standard solution of 2-phenylethylamine (I.S.) was added so that its final concentration was 50  $\mu\text{g mL}^{-1}$  and the flasks were completed to volume with 10 mmol L<sup>-1</sup> phosphoric acid, pH 2.15. Then the samples were well mixed and directly analyzed as described under Section 3.4.2 without sample pretreatment. The new calibration curves were obtained by plotting the average peak area ratio (analyte/I.S.) versus the analyte concentration in  $\mu\text{g mL}^{-1}$ .

Samples of spiked human urine with different concentrations of LOR and DSL in the working concentration range (3-20  $\mu\text{g mL}^{-1}$ ) were treated in the same manner and the recovered concentrations of both drugs were determined from the corresponding calibration line.

## 4. Results and discussion

### 4.1. Method development

A preliminary investigation regarding the separation of the studied analytes by MEKC using generic experimental conditions (5 mmol L<sup>-1</sup> sodium borate buffer, pH 9.30 containing 50 mmol L<sup>-1</sup> SDS) revealed that both LOR and DSL have very high retention factors. Both analytes were co-eluted with commonly used micelle marker compounds like quinine hydrochloride. In a first attempt to reduce the retention factors of the analytes, acetonitrile, methanol and urea were added as organic modifiers. An excellent separation was achieved using 30% v/v acetonitrile in the BGE with 25 mmol L<sup>-1</sup> SDS but the repeatability of the results under these conditions was very poor including the repeatability of the EOF velocity as well as the repeatability of the retention factor data. The results were not improved by burning-off few millimeters of the polyimide coating at both ends of the capillary to overcome the problem of swelling of the polyimide coating associated with acetonitrile containing buffer as recommended by Baeuml and Welsch [69]. We attribute the reasons for the observed bad repeatability of the results obtained with this acetonitrile-containing BGE to the instability of the EOF caused by the adsorption of the analyte onto the capillary wall and the volatility of acetonitrile at this high concentration [70] as well as the significant increase of the CMC of SDS so that SDS micelles are not present in the BGE, which will aggravate problems due to solute-wall interactions [71].

Therefore, we shifted to CD-modified MEKC. According to the study of inclusion complexation of LOR with different types of CDs done by Omar *et al.* [67], LOR can form stable inclusion complexes with CDs through the inclusion of the chlorophenyl moiety and/or the pyridine moiety in the CD cavity. The complex formation constant is reported to follow the order  $\beta$ -CD > HP- $\beta$ -CD >  $\gamma$ -CD >  $\alpha$ -CD. In addition, the study revealed that the aqueous solubility of LOR is significantly improved in presence of  $\beta$ -CD and HP- $\beta$ -CD by factors of 1011 and 571 fold, respectively [67]. Therefore, we selected  $\beta$ -CD and HP- $\beta$ -CD as potential modifiers to be included into our study. DSL is expected to undergo similar reactions because it has the same complexing moieties.

Sodium borate buffer, pH 9.30 was selected for this study because at this pH both LOR and DSL are completely non-ionized, which reduces their retention factors and minimizes their adsorption onto the inner capillary wall. Different experimental parameters were investigated in order to achieve the highest resolution and sensitivity of the developed method. Method optimization by multi-factorial design was not helpful because the problem of peak deformation or splitting could not be described adequately by the employed mathematical models. Therefore, an empirical optimization of the method parameters was preferred as shown in the following sections. As starting conditions, the following experimental parameters

were utilized: buffer: 5 mmol L<sup>-1</sup> sodium borate buffer (pH 9.30), sample solvent: 10 mmol L<sup>-1</sup> phosphoric acid (pH 2.15), applied voltage: 25 kV, temperature of the capillary and the sample tray: +25°C, detection wavelength: 200 nm, injection: hydrodynamic using pressure 0.5 psi for 4 s.

#### 4.1.1. Variation of the concentration of SDS and $\beta$ -CD/HP- $\beta$ -CD

In this measurement series, different concentrations of SDS in combination with  $\beta$ -CD or HP- $\beta$ -CD dissolved in 5 mmol L<sup>-1</sup> sodium borate buffer, pH 9.30 were investigated. With increasing concentration of CD, the peak resolution was improved, however, having a negative impact on the peak shape of LOR. Whereas increasing the concentration of SDS significantly improved the peak shape and prevented peak splitting or deformation, the resolution was negatively affected because of an increase in the retention factors. Acceptable separation conditions required the simultaneous optimization of the SDS concentration and the concentration of  $\beta$ -CD or HP- $\beta$ -CD. Three different concentrations of SDS (30, 40 and 50 mmol L<sup>-1</sup>) were combined each with three different concentrations (20, 25 and 30 mmol L<sup>-1</sup>) of  $\beta$ -CD or HP- $\beta$ -CD. The resolution  $R_s$  and the difference in migration time between the peaks of LOR and DSL were calculated and the results are shown in Table 1. Generally, electric current problems were very frequent with  $\beta$ -CD, which might be due to its poor aqueous solubility. The optimum separation was achieved by using 40 mmol L<sup>-1</sup> SDS and 20 mmol L<sup>-1</sup> HP- $\beta$ -CD. Under these conditions, the highest resolution was reached while a good peak shape was maintained for both analytes within a short run time.

To illustrate the effect of addition of HP- $\beta$ -CD to the BGE on the retention behavior of both LOR and DSL, the (apparent) retention factors for the two analytes were measured with a BGE containing 40 mmol L<sup>-1</sup> SDS and 20 mmol L<sup>-1</sup> HP- $\beta$ -CD dissolved in 5 mmol L<sup>-1</sup> sodium borate buffer, pH 9.30 and compared with those in the same BGE but without HP- $\beta$ -CD. Whereas the retention factors in the BGE void of HP- $\beta$ -CD were found to be quasi-infinity because the analytes co-migrated with quinine hydrochloride used as micelle marker, the apparent retention factors in presence of 20 mmol L<sup>-1</sup> HP- $\beta$ -CD were found to be  $4.28 \pm 0.07$  and  $5.17 \pm 0.09$  for LOR and DSL, respectively, indicating the significant effect of HP- $\beta$ -CD in reducing the apparent retention factors of the studied analytes (details regarding the experimental measurement of retention factors are discussed in the Supplementary Data).

#### 4.1.2. Variation of borate buffer concentration and applied voltage

Both the buffer concentration and the applied voltage affect the pseudoeffective electrophoretic mobility of the analytes, the electroosmotic mobility, the efficiency and consequently the resolution [72]. Table 2 shows the effect of sodium borate buffer concentration and applied voltage on resolution and total run

time. Based on these parameters, both 5 and 10 mmol L<sup>-1</sup> sodium borate buffer gave excellent resolution within a short analysis time (less than 7 min) at a voltage of 25 kV.

#### 4.1.2. Variation of sample matrix

The effect of the sample matrix is usually underestimated in the literature although it can significantly affect the sweeping efficiency and hence the sensitivity of the developed method. The sample matrix has an important impact on the retention factors of the analytes in the sample zone which is a crucial parameter for sweeping [26]. The difference in pH between the sample and the BGE induces an increase in the retention factor within the sample compartment due to coulomb interactions between analyte and charged micelle. In addition differences in the apparent distribution coefficient cause RFGE [29] and the pH difference enables zone focusing due to a dynamic pH junction [30].

In this measurement series, LOR and DSL were dissolved in four different sample matrices while the BGE (40 mmol L<sup>-1</sup> SDS and 20 mmol L<sup>-1</sup> HP- $\beta$ -CD in 10 mmol L<sup>-1</sup> sodium borate buffer, pH 9.30) is kept constant. The four sample matrices included 10 mmol L<sup>-1</sup> phosphoric acid (pH 2.15), 10% v/v methanol in 10 mmol L<sup>-1</sup> phosphoric acid (pH 2.15), 10% v/v methanol in 10 mmol L<sup>-1</sup> sodium borate buffer (pH 9.30) and the same solution as the BGE (non-sweeping condition). In all cases, the electropherograms were recorded using three different injection volumes (Figure 2). The results clearly reveal that the highest sensitivity is achieved with the aqueous phosphoric acid matrix (dynamic pH junction + RFGE with the highest  $k_s$ ) followed by the 10% methanolic solution of phosphoric acid (dynamic pH junction + RFGE with lower  $k_s$ ) and then the 10% methanolic solution of borate buffer (only RFGE with the lowest  $k_s$ ), while the run with the analytes dissolved in the BGE (non-sweeping condition) has the lowest sensitivity. Therefore, 10 mmol L<sup>-1</sup> phosphoric acid, pH 2.15 was used as the preferred sample matrix throughout the subsequent investigations. In this sample matrix, LOR and DSL, which have large hydrophobic moieties, are protonated with an effective charge number of +2. It can be expected that they will have a very high retention factor [27] due to the simultaneous strong hydrophobic and electrostatic interaction with the negatively charged SDS micelle outer shell and the hydrophobic micellar core. Orentaite *et al.* [73] observed about one order of magnitude higher retention factors for the charged species compared to those retention factors obtained for the neutral species during their study of weakly acidic analytes by MEKC with cationic surfactant. In addition, since  $k_s$  is much higher than  $k_{BGE}$ , a marked additional focusing effect because of the RFGE is expected. Moreover, conditions for additional focusing by dynamic pH junction are fulfilled. Therefore, we expected that LOR and DSL would have very high enrichment factors.

However, in contrast to our expectations, the observed increase in the enrichment factor by using acidic sample matrix was relatively low. The obtained enrichment factors for LOR and DSL were significantly lower than those obtained with the less hydrophobic anilines studied before [29]. These findings can be attributed to the strong adsorption of the protonated hydrophobic basic analytes on the inner capillary wall, which occurs only in the sample zone where LOR and DSL have an effective charge number of +2 (divalent metal cations are reported to strongly interact with the negatively charged silanol groups of the capillary wall [74-76]). Adsorption significantly counteracts zone focusing by sweeping as it hinders the picking up of analyte molecules by the micelles penetrating the sample zone. In accordance with the results presented in [16] we expect the addition of dynamic coating agents to reduce the degree of adsorption of the analytes onto the capillary wall and to improve the efficiency of the focusing step.

Because of the wide variation in pH between the strongly acidic sample matrix and the strongly basic BGE, a water-dipping step of the capillary and electrodes was performed before and after injection to avoid cross contaminations. The introduction of this step had a significant effect on the precision of the developed method (data not shown).

#### **4.1.3. Variation of temperature**

Although different physicochemical properties are affected by the temperature, this parameter is rarely used in systematic method development because the temperature can only be varied within a relatively small range [77]. Three different capillary temperatures (20, 25 and 30°C) were tested using two concentrations of sodium borate buffer (5 and 10 mmol L<sup>-1</sup>) and an applied voltage of 25 kV. The results were evaluated in terms of resolution obtained and total run time (see Table 3). With the two buffers the optimum temperature was 30°C regarding the peak resolution and the peak shape as decision criteria. Although the total run time is slightly longer with 10 mmol L<sup>-1</sup> sodium borate buffer, this concentration was selected as the optimum because of its higher buffer capacity which minimizes negative effects due to buffer depletion after several runs and hence improves the robustness of the method.

#### **4.1.4. Selection of the optimum injection volume, detection wavelength and internal standard**

The optimum injection volume for the developed method was selected so that it achieves the highest possible sensitivity without negative impact on the separation efficiency. In addition to the gain in sensitivity, a larger injection volume improves the signal-to-noise ratio which minimizes errors in integration and increases the precision of the method [78]. For selection of the optimum injection volume, the peak height is recorded for different injection volumes and a plot of the peak height vs. (injection pressure x injection time) is constructed (Figure S1 and S2 in the Supplementary Data). The optimum injection parameters

were 0.5 psi for 5 s which correspond to the highest possible peak height before reaching the volume overload region.

Three different detection wavelengths were tested 200, 214 and 254 nm. Both LOR and DSL exhibit the highest absorbance with 200 nm as detection wavelength which is usually difficult to use with liquid chromatographic methods because several organic solvents that are used as a mobile phase component in HPLC can absorb UV light at this low wavelength and hence strongly interfere with the detection [79]. This wavelength was also employed for the application of the developed method in the analysis of LOR and DSL in tablets and in spiked human urine.

Internal standards (I.S.) can significantly improve the precision of the method especially if the injection error is the predominant error source [80]. Different compounds were tested to be used as I.S. including aniline, 4-ethylaniline, 4-propylaniline and 4-butyraniline. All these compounds eluted between the EOF marker and the studied analytes. Based on the best peak shape, 4-ethylaniline was selected as the I.S. during the present study. For the analysis of spiked human urine, none of the above-mentioned anilines could be used as I.S. because of the marked overlap with the peaks of the urine matrix components. Therefore, in this case 2-phenylethylamine was employed as I.S. Generally, it is recommended to use a high concentration of the I.S. (avoiding any influence on resolution and peak shape). A minimum signal-to-noise ratio of 30 is required to avoid major integration errors [77]. Based on these considerations, the concentrations of 4-ethylaniline and 2-phenylethylamine were fixed to 25 and 50  $\mu\text{g mL}^{-1}$ , respectively.

#### **4.1.5. Optimization of the rinsing procedure between runs**

Three different strategies for rinsing the capillary between runs were pursued. The first one was rinsing for 5 min with the BGE. The second approach was rinsing 1 min with 0.2 mol L<sup>-1</sup> NaOH, 1 min with water and then 5 min with the BGE. The third method included rinsing 1 min with 10 mmol L<sup>-1</sup> phosphoric acid, 1 min with water, 1 min with 0.2 mol L<sup>-1</sup> NaOH, 1 min with water and then 5 min with the BGE. For each of the three strategies, the electropherograms were recorded for subsequent 10 runs and the relative standard deviations (RSD) of the migration time and the peak area of the last migrating peak (DSL peak) were determined. For all rinsing procedures, the RSD for the migration time of DSL was less than 0.5% while for the peak area the RSD values were 4.98%, 5.86% and 5.14%, respectively. It is interesting to note that the RSD of the measured peak area was significantly improved during the calibration by using the internal standard indicating that the major source of error was due to the injection process itself (variation in the injected volume). Based on these results the first rinsing procedure (5 min with the BGE) was utilized which was increased to 10 min in case of the analysis of spiked human urine. Figure 3 shows the electropherograms obtained for 10 subsequent runs using the

optimized experimental conditions indicating the precision of the developed method. After the tenth run, a delay in the migration time started to occur with an associated increase in the electric current indicating buffer depletion and the necessity to refill the buffer vials with fresh BGE solutions.

The final optimized conditions were as follows: BGE: 10 mmol L<sup>-1</sup> sodium borate buffer, pH 9.30 containing 40 mmol L<sup>-1</sup> SDS and 20 mmol L<sup>-1</sup> hydroxypropyl- $\beta$ -CD; temperature of the capillary and the sample tray: 30°C; applied voltage: +25 kV; injection: hydrodynamic injection using pressure 0.5 psi for 5 s, and detection wavelength: 200 nm. Under these conditions the resolution  $R_s$  for the peaks of LOR and DSL was found to be 3.9 and the total run time is less than 7 min.

## 4.2. Method validation

Various validation characteristics were investigated adopting the official ICH guidelines [68].

### 4.2.1. Linearity and range

The linearity of an analytical method is defined as the ability of the method (within a given range) to obtain test results that are directly proportional to the concentration of analyte in the sample, while the range is the interval between the upper and lower analyte concentrations (including these values) for which the method has a suitable level of precision, accuracy and linearity [68].

Four calibration graphs for the determination of each of LOR and DSL were constructed by plotting the peak height ratio (peak height of analyte/peak height of I.S.), the corrected peak area (peak area of analyte/migration time), the peak area ratio (peak area of analyte/peak area of I.S.) or the corrected peak area ratio (corrected peak area of analyte/corrected peak area of I.S.). For each case, the response was plotted against the concentration of analyte. The results of the statistical analysis [81] of the data are summarized in Table 4 showing the range of the developed method for each analyte (corresponding calibration graphs are shown in Figures S3-S10 included in the Supplementary Data). A high value of the correlation coefficient  $r$  of the regression line, small values of the standard deviation of residuals  $S_{y/x}$ , of intercept  $S_a$ , and of slope  $S_b$ , and a small value of the relative standard deviation and the relative error indicate the linearity of the calibration graphs. Moreover, the linearity of the calibration graphs was also confirmed by applying Mandel's fitting test [82] using DINTTEST program [83]. The best results were obtained when the peak area ratio is the response parameter indicating the importance of using an I.S. to overcome the variance due to the injection process (variation in injected volume).

#### **4.2.2. Accuracy**

Accuracy is the closeness of agreement between the value which is accepted either as a conventional true value or an accepted reference value and the value found [68]. The accuracy of the developed method was confirmed by measuring the recovery of known added amounts of each analyte into a blank matrix and comparing the results with those obtained by the reference liquid chromatographic pharmacopeial method [36]. Application of Student's *t*-test and variance ratio *F*-test [81] did not indicate a significant difference in the recoveries between the developed method and the reference pharmacopeial method which confirms the equivalence of the two methods regarding accuracy and precision, respectively. The results are summarized in Table 5.

#### **4.2.3. Precision**

The precision of an analytical method is the closeness of agreement (degree of scatter) between a series of measurements obtained from multiple sampling of the same homogeneous sample under the prescribed conditions [68]. Intraday and interday precisions were assessed using three concentrations and three replicates of each concentration. For each set of results, the RSD was calculated for the migration time and the peak area ratio. The obtained results confirm a good precision of the developed method as shown in Table 6.

#### **4.2.4. Specificity**

The specificity of the method was assessed by observing any interference encountered from the tablet additives cited in the information pamphlet of the studied pharmaceutical preparations (Lora-ADGC® tablets and Aerius® film-coated tablets). The following tablet additives were obtained from the Department of Chemistry, University of Marburg: magnesium stearate, lactose monohydrate, maize starch, povidone k 25 (polyvinylpyrrolidone), calcium hydrogen phosphate dihydrate, talc, titanium dioxide and macrogol 400 (polyethylene glycol). About 0.1 g, which approximately equals the weight of one tablet, of each additive was analyzed using the same procedure as described for the analysis of tablets (Section 3.4.3). In addition, an analysis of the extract of these additives after spiking with a known amount of LOR and DSL was performed. No interference was encountered from any tablet additive, which confirms an adequate specificity of the developed method.

Moreover, the interference introduced from pseudoephedrine, which is co-formulated with either LOR or DSL, was also tested. As shown in Figure 4, pseudoephedrine was successfully separated from the analytes to be determined. Therefore, our developed method can be also utilized for the analysis of a ternary mixture of LOR, DSL and pseudoephedrine.

#### **4.2.5. Detection limit and quantitation limit**

The detection limit (DL) was determined by establishing the minimum level at which the analyte can reliably be detected (signal-to-noise ratio is 3:1) while the quantitation limit (QL) was determined by establishing the lowest concentration of analyte that can be determined with acceptable precision and accuracy (signal-to-noise ratio is 10:1). As shown in Table 4, the DL was found to be 1 and 0.6  $\mu\text{g mL}^{-1}$  for LOR and DSL while the QL was found to be 3 and 2  $\mu\text{g mL}^{-1}$ , respectively.

#### **4.2.6. Robustness**

The robustness of an analytical procedure is a measure of its capacity to remain unaffected by small, but deliberate variations in method parameters and provides an indication of its reliability during normal usage [68]. The following parameters were varied in order to test the robustness: applied voltage, temperature, SDS concentration, HP- $\beta$ -CD concentration, borate buffer concentration and borate buffer pH. Each parameter is varied on three levels while keeping all other parameters constant. For each measurement set, the values of %RSD of migration times, resolution and peak area ratio were calculated using duplicate measurements for each level. The obtained results are summarized in Table 7 proving the robustness of the developed method. The most critical parameter (inducing the largest variation) is the HP- $\beta$ -CD concentration.

### **4.3. Applications**

#### **4.3.1. Application to pharmaceutical preparations**

The applicability of the developed method was tested by the determination of LOR and DSL in their tablet preparations. The content of each analyte in the pharmaceutical product was determined by triplicate injections of three different concentrations of the tablet extract. As shown in Table 8, the percentage recoveries obtained for both drugs were in all cases close to 100%. Moreover, the results obtained were in good agreement with those obtained with the official liquid chromatographic method as indicated by the significance tests performed. Figure 5 shows the electropherograms obtained for the analysis of Lora-ADGC<sup>®</sup> tablets and Aerius<sup>®</sup> film-coated tablets.

#### **4.3.2. Application to spiked human urine**

The developed method was successfully applied to the analysis of spiked human urine using direct injection without any sample pretreatment (Figure 6). New calibration curves were constructed for each analyte using 2-phenylethylamine as I.S. as described in Section 3.4.4 employing the peak area ratio

(analyte/I.S.) as the response variable (the calibration curves are shown in Figures S11 and S12 included in the Supplementary Data). For LOR, the slope, the y-intercept and the correlation coefficient  $r$  of this regression line were 0.0236, - 0.0394 and 0.9936 while for DSL these parameters were 0.0305, - 0.0569 and 0.9894, respectively. The linearity of the calibration graphs was also confirmed by applying Mandel's fitting test [82] using DINTEST program [83] which indicates that the linear regression is justifiable for the obtained results. Samples of human urine spiked with different concentrations of LOR and DSL within the working range (3-20  $\mu\text{g mL}^{-1}$ ) were analysed (Table 9). These results confirm the applicability of the developed method for the analysis of the studied analytes in urine matrix by direct injection of the sample.

#### **4.3.3. Application to impurity testing of LOR bulk powder**

The specificity of the developed method allowed the determination of DSL as an impurity in LOR bulk powder. A synthetic mixture of LOR and DSL in a ratio of 1000:1 (the pharmacopeial limit of DSL in LOR powder is 0.1% [36,37]) was analysed using the procedure described in Section 3.4.2. One of the obtained electropherograms is shown in Figure 7. The average percentage recovery of DSL for six replicate determinations was  $99.79 \pm 4.52$ . The obtained results indicate the suitability of our developed method to be an alternative to the pharmacopeial liquid chromatographic method for the detection of DSL as an impurity in LOR bulk powder.

### **5. Conclusion**

CD-MEKC with acidic sample matrix and basic BGE minimizes problems associated with the adsorption of hydrophobic basic analytes onto the inner capillary wall. The presence of a cyclodextrin in the BGE plays an additional role in reducing adsorption on the capillary wall while improving the efficiency and the reproducibility of the developed method. In addition, the difference in pH between the sample solution and the BGE provides an adequate solubility of the hydrophobic basic analytes in the sample solution without compromising sweeping efficiency and resolution.

CD-MEKC allows the development of a reliable method for the simultaneous determination of LOR and DSL in the drug compound as well as in pharmaceutical preparations. The method is also applicable for the determination of the studied compounds in spiked human urine. In addition, it can be utilised as an alternative to the pharmacopeial HPLC method for the impurity testing of DSL in LOR powder. The good validation criteria of the proposed method allow its use in quality control laboratories. The strategies used in the development of this method are applicable to other hydrophobic basic analytes in the development of robust and precise capillary electromigration separation methods for their qualitative and quantitative analysis.

### **Acknowledgements**

M. El-Awady thanks Yousef-Jameel Foundation for the financial support of this work. F. Belal thanks Alexander von Humboldt foundation, Bonn, Germany for supporting his research visit to Germany. We are very grateful to H. Elmansi (Mansoura University, Faculty of Pharmacy) for performing the pharmacopeial HPLC method.

## References

- [1] S.C. Beale, *Anal. Chem.* 70 (1998) 279R.
- [2] J.A. Bullock, L.C. Yuan, *J. Microcolumn Sep.* 3 (1991) 241.
- [3] L. Song, Q. Ou, W. Yu, *J. Chromatogr. , A* 657 (1993) 175.
- [4] D. Corradini, A. Rhomberg, C. Corradini, *J. Chromatogr. , A* 661 (1994) 305.
- [5] P.G. Righetti, C. Gelfi, B. Verzola, L. Castelletti, *Electrophoresis* 22 (2001) 603.
- [6] S. Terabe, Y. Miyashita, Y. Ishihama, O. Shibata, *J. Chromatogr.* 636 (1993) 47.
- [7] A.T. Balchunas, M.J. Sepaniak, *Anal. Chem.* 59 (1987) 1466.
- [8] H. Nishi, T. Fukuyama, M. Matsuo, S. Terabe, *J Chromatogr* 513 (1990) 279.
- [9] S. Terabe, Y. Miyashita, O. Shibata, E.R. Barnhart, L.R. Alexander, D.G. Patterson, B.L. Karger, K. Hosoya, N. Tanaka, *J. Chromatogr.* 516 (1990) 23.
- [10] K. Otsuka, M. Higashimori, R. Koike, K. Karuhaka, Y. Okada, S. Terabe, *Electrophoresis* 15 (1994) 1280.
- [11] U. Butehorn, U. Pyell, *J. Chromatogr. A* 792 (1997) 157.
- [12] M.L. Bender, M. Komiyama, *Cyclodextrin Chemistry*, Springer-Verlag, Berlin, 1978.
- [13] W. Saenger, in J.L. Atwood, J.E.D. Davies, D.D. MacNicol (Editors), *Inclusion Compounds, Vol. 2: Structural Aspects of Inclusion Compounds formed by Organic Host Lattices*, Academic Press, London, 1984, p. 231.
- [14] W. Saenger, in O. Huber, J. Szejtli (Editors), *Proceedings of the Fourth International Symposium on Cyclodextrins*, Kluwer Academic Publishers, Munich, 1988, p. 159.
- [15] D.W. Armstrong, F. Nome, L.A. Spino, T.D. Golden, *J. Am. Chem. Soc.* 108 (1986) 1418.
- [16] M. El-Awady, U. Pyell, *Electrophoresis* (2013) Submitted.
- [17] R. Palepu, V.C. Reinsborough, *Can. J. Chem.* 66 (1988) 325.
- [18] E. Junquera, G. Tardajos, E. Aicart, *Langmuir* 9 (1993) 1213.
- [19] A. Cifuentes, J.L. Bernal, J.C. Diez-Masa, *Anal. Chem.* 69 (1997) 4271.
- [20] C.E. Lin, H.C. Huang, H.W. Chen, *J. Chromatogr. , A* 917 (2001) 297.
- [21] A. Staub, S. Comte, S. Rudaz, J.L. Veuthey, J. Schappler, *Electrophoresis* 31 (2010) 3326.
- [22] A.S. Rathore, C. Horvath, *Electrophoresis* 19 (1998) 2285.
- [23] E. Schneiderman, A.M. Stalcup, *J. Chromatogr. , B: Biomed. Sci. Appl.* 745 (2000) 83.
- [24] K. Otsuka, S. Terabe, *Methods Mol. Biol.* 243 (2004) 355.

Publication IV: Main manuscript

- [25] T. Cserhati, *Biomed. Chromatogr.* 22 (2008) 563.
- [26] J.P. Quirino, S. Terabe, *Science* 282 (1998) 465.
- [27] J.P. Quirino, S. Terabe, *Anal. Chem.* 71 (1999) 1638.
- [28] J.P. Quirino, S. Terabe, *J. High Resolut. Chromatogr.* 22 (1999) 367.
- [29] M. El-Awady, U. Pyell, *J. Chromatogr. A* 1297 (2013) 213.
- [30] P. Britz-McKibbin, K. Otsuka, S. Terabe, *Anal. Chem.* 74 (2002) 3736.
- [31] A.A. Kazarian, E.F. Hilder, M.C. Breadmore, *J. Sep. Sci.* 34 (2011) 2800.
- [32] Martindale: The Complete Drug Reference, Electronic version, Pharmaceutical Press, London, 2013.
- [33] G. Popovic, M. Cakar, D. Agbaba, *J. Pharm. Biomed. Anal.* 49 (2009) 42.
- [34] C. Dagenais, A. Avdeef, O. Tsinman, A. Dudley, R. Beliveau, *Eur. J. Pharm. Sci.* 38 (2009) 121.
- [35] A.C. Moffat, M.D. Osselton, B. Widdop, Editors., *Clarke's Analysis of Drugs and Poisons in Pharmaceuticals, Body Fluids and Postmortem Material, Fourth Edition*, Pharmaceutical Press, London, 2011.
- [36] *European Pharmacopoeia 7th Edition (7.8)*, Online Version, European directorate for the quality of medicines & healthcare (EDQM), Strasbourg, 2013.
- [37] *The United States Pharmacopeia 32, the National Formulary 27*, Electronic Version, US Pharmacopoeial Convention, Rockville, 2009.
- [38] D.S. Wishart, C. Knox, A.C. Guo, S. Shrivastava, M. Hassanali, P. Stothard, Z. Chang, J. Woolsey, *Nucleic Acids Res.* 34 (2006) D668-D672.
- [39] B. Murugesan, S. Sathyanarayana, M. Prasad, Ranbaxy Laboratories Limited, India ., 2010, p. 11pp.
- [40] V. Vijayabaskar, S.M. Rao, P.V. Kannan, D.S.D. Prabhu, Orchid Chemicals and Pharmaceuticals Limited, India ., 2008, p. 9pp.
- [41] D. Murpani, M. Rafeeq, P. Raheja, S. Sathyanarayana, M. Prasad, Ranbaxy Laboratories Limited, India ., 2007, p. 10pp.
- [42] B.V.S. Kumar, S.A. Kale, R.B. Choudhari, N.S.C. Pradhan, Glenmark Pharmaceuticals Limited, India ., 2007, p. 10pp.
- [43] V. Vijayabaskar, S.M. Rao, P.V. Kannan, D.S.D. Prabu, Orchid Chemicals & Pharmaceuticals Ltd., India ., 2006, p. 9pp.
- [44] D.D. Rao, N.V. Satyanarayana, R. Malleswara, S.S. Sait, D. Chakole, K. Mukkanti, *J. Pharm. Biomed. Anal.* 51 (2010) 736.
- [45] D. Zhong, H. Blume, *Pharmazie* 49 (1994) 736.

Publication IV: Main manuscript

- [46] L. Yang, T.D. Mann, D. Little, N. Wu, R.P. Clement, P.J. Rudewicz, *Anal. Chem.* 73 (2001) 1740.
- [47] F.C.W. Sutherland, J. de, D. Badenhorst, T. Scanes, H.K.L. Hundt, K.J. Swart, A.F. Hundt, *J. Chromatogr. A* 914 (2001) 37.
- [48] F.J. Ruperez, H. Fernandez, C. Barbas, *J. Pharm. Biomed. Anal.* 29 (2002) 35.
- [49] L. Yang, M. Amad, W.M. Winnik, A.E. Schoen, H. Schweingruber, I. Mylchreest, P.J. Rudewicz, *Rapid Commun. Mass Spectrom.* 16 (2002) 2060.
- [50] W. Naidong, T. Addison, T. Schneider, X. Jiang, T.D.J. Halls, *J. Pharm. Biomed. Anal.* 32 (2003) 609.
- [51] O.Q.P. Yin, X. Shi, M.S.S. Chow, *J. Chromatogr. B: Anal. Technol. Biomed. Life Sci.* 796 (2003) 165.
- [52] M. Qi, P. Wang, Y. Geng, *J. Pharm. Biomed. Anal.* 38 (2005) 355.
- [53] D.T. El-Sherbiny, N. El-Enany, F.F. Belal, S.H. Hansen, *J. Pharm. Biomed. Anal.* 43 (2007) 1236.
- [54] S. Emara, A. El-Gindy, M.K. Mesbah, G.M. Hadad, *J. AOAC Int.* 90 (2007) 384.
- [55] L. Vlase, S. Imre, D. Muntean, S.E. Leucuta, *J. Pharm. Biomed. Anal.* 44 (2007) 652.
- [56] D.I. Sora, S. Udrescu, V. David, A. Medvedovici, *Biomed. Chromatogr.* 21 (2007) 1023.
- [57] G. Srinubabu, R.S. Patel, V.P. Shedbalkar, A.A. Rao, M.N. Rao, V.V.R. Bandaru, *J. Chromatogr. B: Anal. Technol. Biomed. Life Sci.* 860 (2007) 202.
- [58] B.N. Patel, N. Sharma, M. Sanyal, P.S. Shrivastav, *J. Chromatogr. Sci.* 48 (2010) 35.
- [59] J. Lu, Y.C. Wei, R.J. Markovich, A.M. Rustum, *J. Liq. Chromatogr. Relat. Technol.* 33 (2010) 603.
- [60] J. Lu, Y.C. Wei, R.J. Markovich, A.M. Rustum, *J. AOAC Int.* 93 (2010) 891.
- [61] G. Ramulu, Y.R. Kumar, K. Vyas, M.V. Suryanarayana, K. Mukkanti, *Sci. Pharm.* 79 (2011) 277.
- [62] R.M. Youssef, E.F. Khamis, M.A. El-Sayed, M.M. Abdel Moneim, *J. Planar Chromatogr. -- Mod. TLC* 25 (2012) 456.
- [63] N. Issa, M. Mlynarova, *Ceska Slov. Farm.* 53 (2004) 192.
- [64] R. Johnson, J. Christensen, C.C. Lin, *J. Chromatogr. B: Biomed. Sci. Appl.* 657 (1994) 125.
- [65] R.V. Rele, P.J. Gurav, *Int. J. Pharma Bio Sci.* 3 (2012) 89.
- [66] H. Fernandez, F.J. Ruperez, C. Barbas, *J. Pharm. Biomed. Anal.* 31 (2003) 499.
- [67] L. Omar, M.I. El-Barghouthi, N.A. Masoud, A.A. Abdoh, O. Al, M.B. Zughul, A.A. Badwan, *J. Solution Chem.* 36 (2007) 605.

Publication IV: Main manuscript

- [68] ICH Harmonised Tripartite Guidelines, Validation of analytical procedures: text and methodology Q2(R1). <http://www.ich.org/products/guidelines/quality/article/quality-guidelines.html> (Accessed 01.06.2013)
- [69] F. Baeuml, T. Welsch, J. Chromatogr. A 961 (2002) 35.
- [70] L. Baur, C. Sanger-van de Griend, H. Watzig, J. Chromatogr. A 979 (2002) 97.
- [71] S. Lopez-Grio, J.J. Baeza-Baeza, M.C. Garcia-Alvarez-Coque, Chromatographia 48 (1998) 655.
- [72] H.J. Issaq, I.Z. Atamna, G.M. Muschik, G.M. Janini, Chromatographia 32 (1991) 155.
- [73] I. Orentaite, A. Maruska, U. Pyell, Electrophoresis 32 (2011) 604.
- [74] D.W. Fuerstenau, J. Phys. Chem. 60 (1956) 981.
- [75] R. Brechtel, W. Hohmann, H. Ruediger, H. Waetzig, J. Chromatogr. A 716 (1995) 97.
- [76] D.J. Pietrzyk, S. Chen, B. Chanthawat, J. Chromatogr. A 775 (1997) 327.
- [77] H. Waetzig, M. Degenhardt, A. Kunkel, Electrophoresis 19 (1998) 2695.
- [78] S.J. Williams, D.M. Goodall, J. Chromatogr. 629 (1993) 379.
- [79] J.E. Campbell, M. Hewins, R.J. Lynch, D.D. Shrewsbury, Chromatographia 16 (1982) 162.
- [80] K.D. Altria, H. Fabre, Chromatographia 40 (1995) 313.
- [81] J.C. Miller, J.N. Miller, Statistics and Chemometrics for Analytical Chemistry, 5th Edition, Pearson Education Limited, Harlow, England, 2005.
- [82] J. Mandel, The statistical analysis of experimental data, Wiley & Sons, Inc., New York, 1964.
- [83] G. Schmitt, M. Herbold, Institute of Forensic Medicine and Traffic Medicine, Heidelberg University Hospital, Heidelberg, Germany, 2002.

**Figure legends:**

**Figure 1.** Chemical structures of the studied analytes.

**Figure 2.** Electropherograms obtained with three injection volumes of LOR and DSL dissolved in four different sample matrices including (A) 10 mmol L<sup>-1</sup> phosphoric acid, pH 2.15, (B) 10% v/v methanolic solution of 10 mmol L<sup>-1</sup> phosphoric acid, pH 2.15, (C) 10% v/v methanolic solution of 10 mmol L<sup>-1</sup> sodium borate buffer, pH 9.30 and (D) BGE (non-sweeping condition). BGE: 10 mmol L<sup>-1</sup> sodium borate buffer, pH 9.30 containing 40 mmol L<sup>-1</sup> SDS and 20 mmol L<sup>-1</sup> HP-β-CD. Injection: hydrodynamic using pressure (A1,B1,C1,D1) 0.5 psi for 5 s, (A2,B2,C2,D2) 0.5 psi for 10 s, (A3,B3,C3,D3) 0.5 psi for 15 s. Analyte concentration: 10 μg mL<sup>-1</sup> each. For other experimental parameters see Figure 3 (temperature of the capillary and the sample tray 25°C).

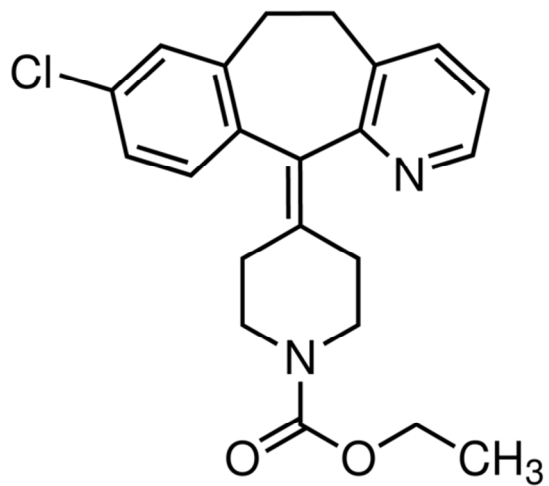
**Figure 3.** Electropherograms of LOR and DSL obtained for 10 subsequent runs under optimized experimental conditions with 4-ethylaniline as I.S. (analyte concentration: 10 μg mL<sup>-1</sup> each). BGE: 10 mmol L<sup>-1</sup> sodium borate buffer, pH 9.30 containing 40 mmol L<sup>-1</sup> SDS and 20 mmol L<sup>-1</sup> hydroxypropyl-β-CD; temperature of the capillary and the sample tray: 30°C; applied voltage: +25 kV; injection: hydrodynamic injection using pressure 0.5 psi for 5 s, detection wavelength: 200 nm, capillary dimensions: 50 μm × 503(401) mm.

**Figure 4.** Electropherogram of LOR and DSL in presence of the co-formulated drug pseudoephedrine under optimized experimental conditions (analyte concentration: 20 μg mL<sup>-1</sup> for LOR and DSL, 50 μg mL<sup>-1</sup> for pseudoephedrine, for experimental parameters refer to Figure 3).

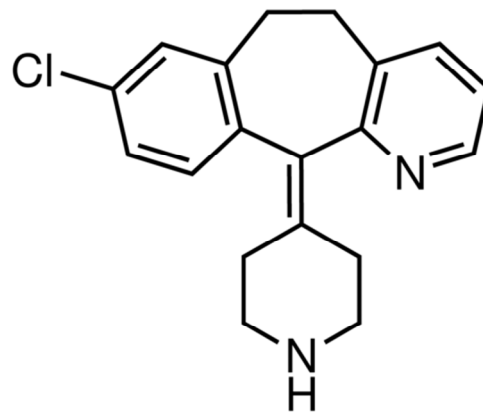
**Figure 5.** Electropherograms obtained from the application of the developed CD-MEKC method to the analysis of: (A) Lora-ADGC<sup>®</sup> tablets and (B) Aerius<sup>®</sup> film-coated tablets (analyte concentration: 25 μg mL<sup>-1</sup> each, for experimental parameters refer to Figure 3).

**Figure 6.** Electropherograms obtained from the application of the developed CD-MEKC method to the analysis of spiked human urine (I.S.= 2-phenylethylamine, for experimental parameters refer to Figure 3).

**Figure 7.** Electropherogram obtained from the application of the developed CD-MEKC method to analyze DSL spiked in LOR bulk powder at the stated pharmacopeia limit (analyte concentration: 5 μg mL<sup>-1</sup> for DSL and 5000 μg mL<sup>-1</sup> for LOR, for experimental parameters refer to Figure 3).



**Loratadine**



**Desloratadine**

Figure 1

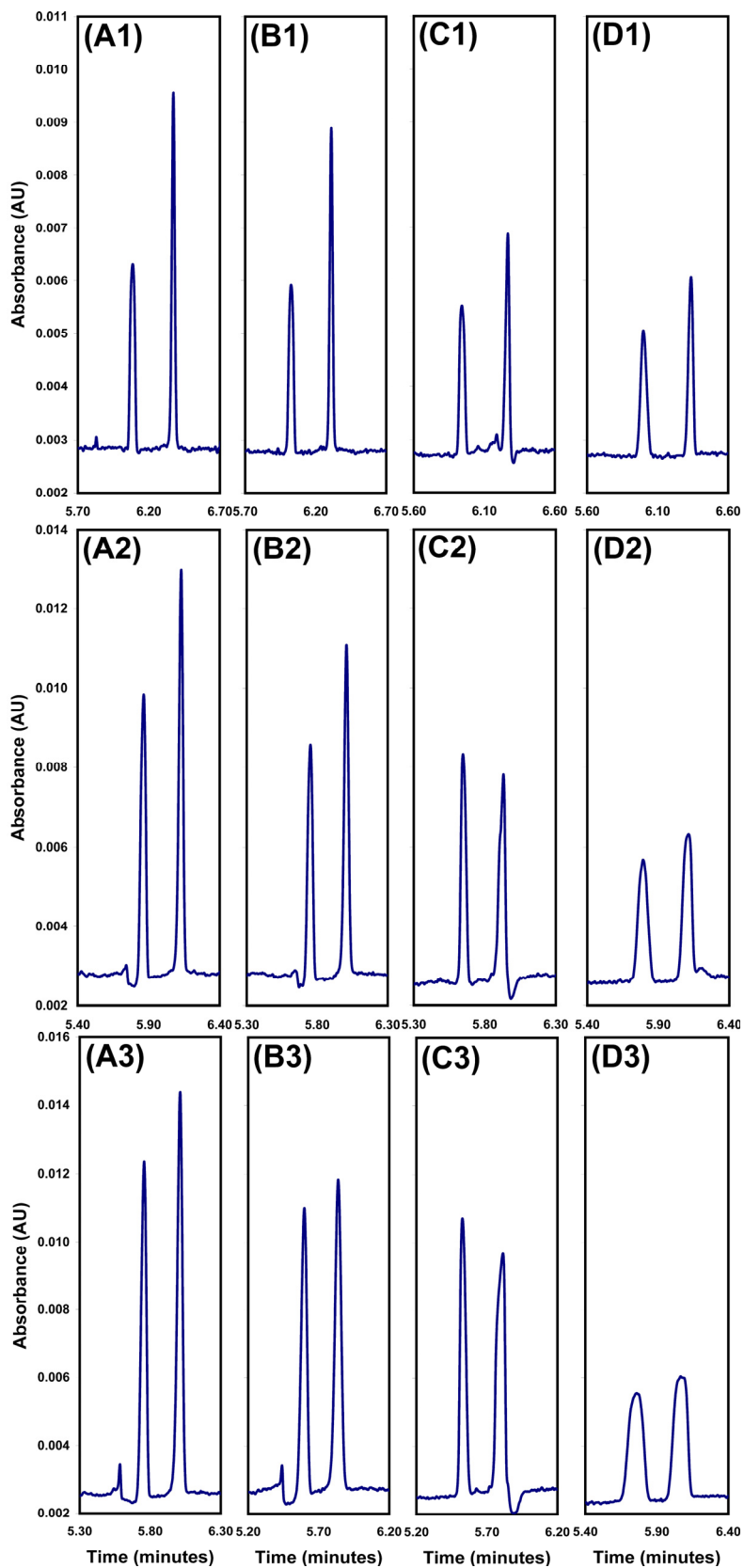


**Figure 2**

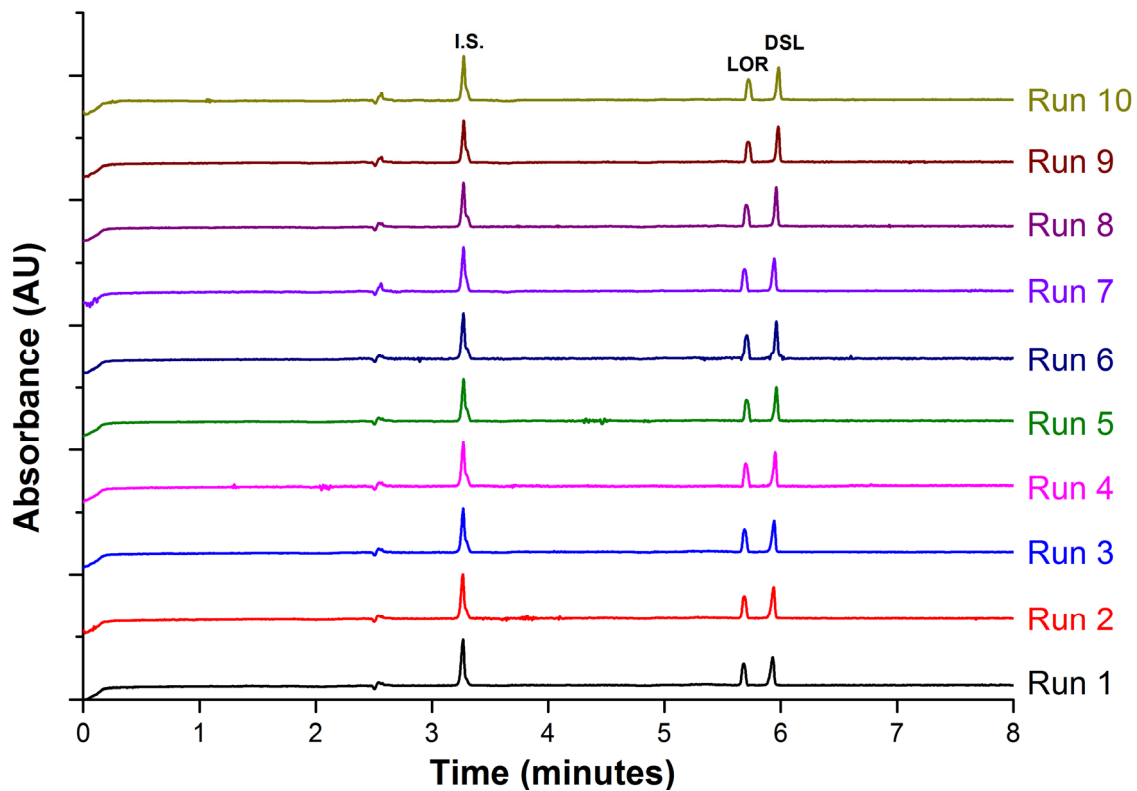
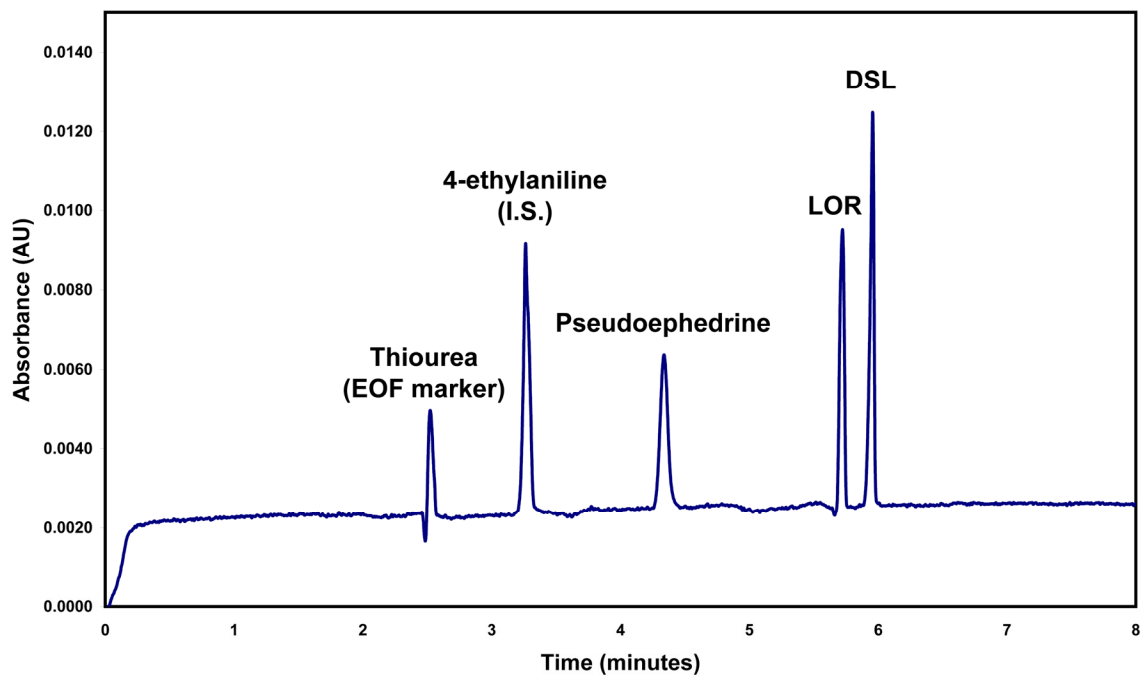
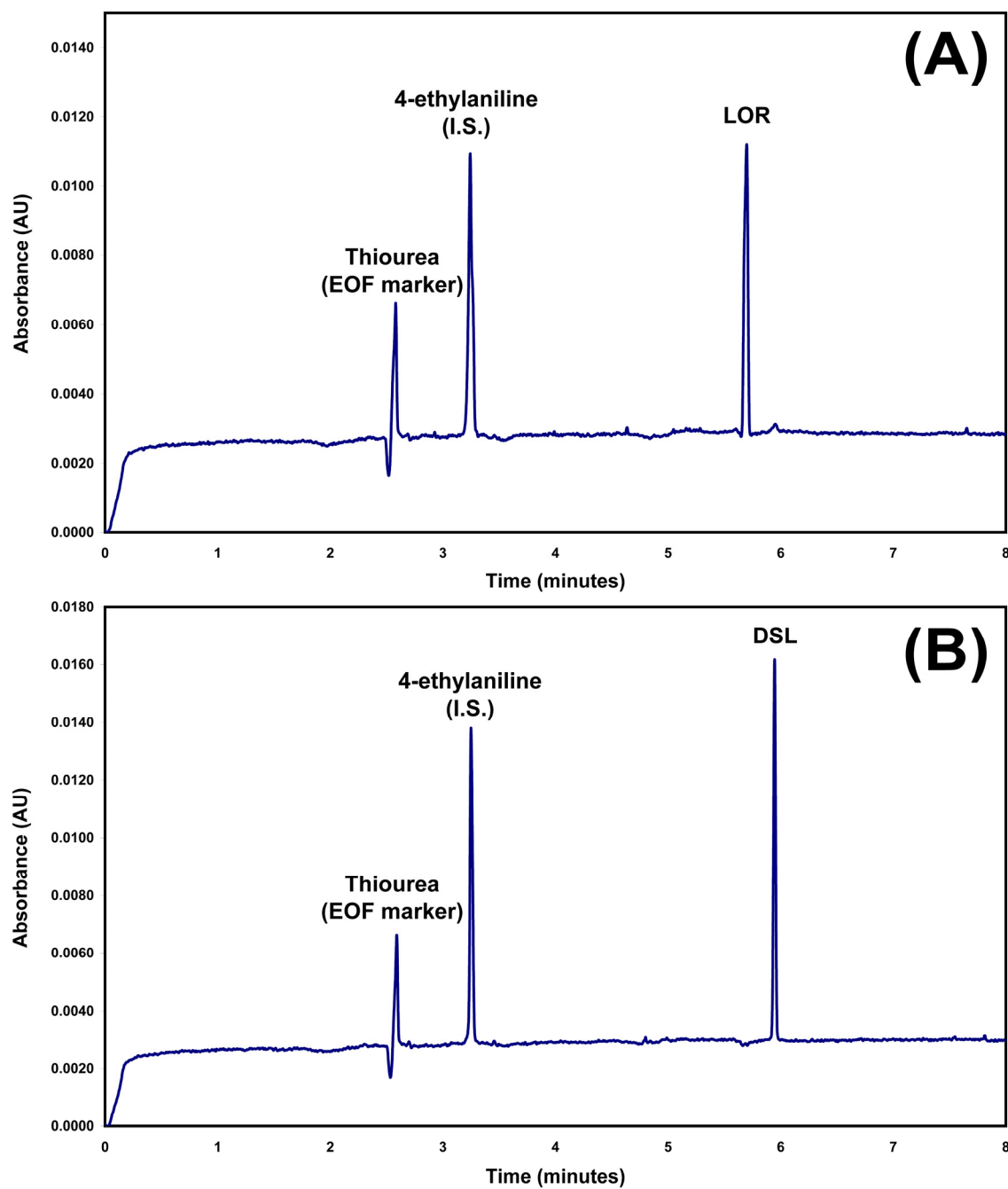


Figure 3



**Figure 4**



**Figure 5**

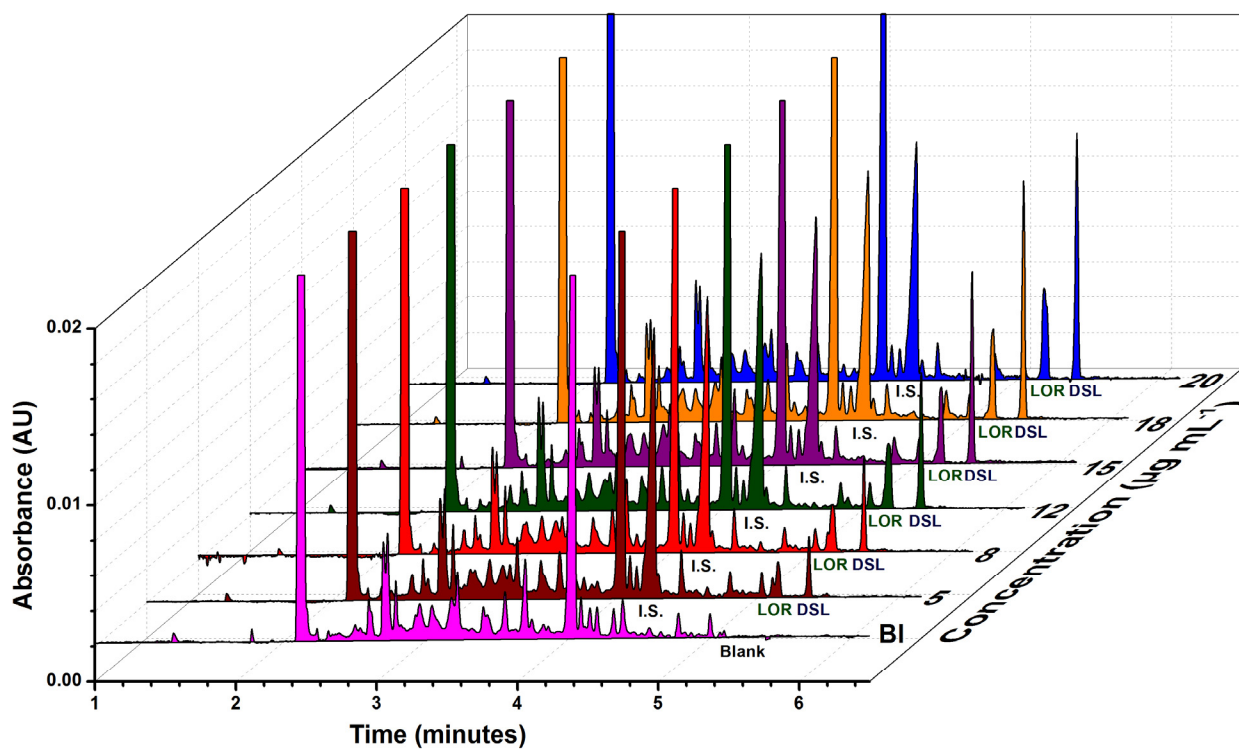


**Figure 6**

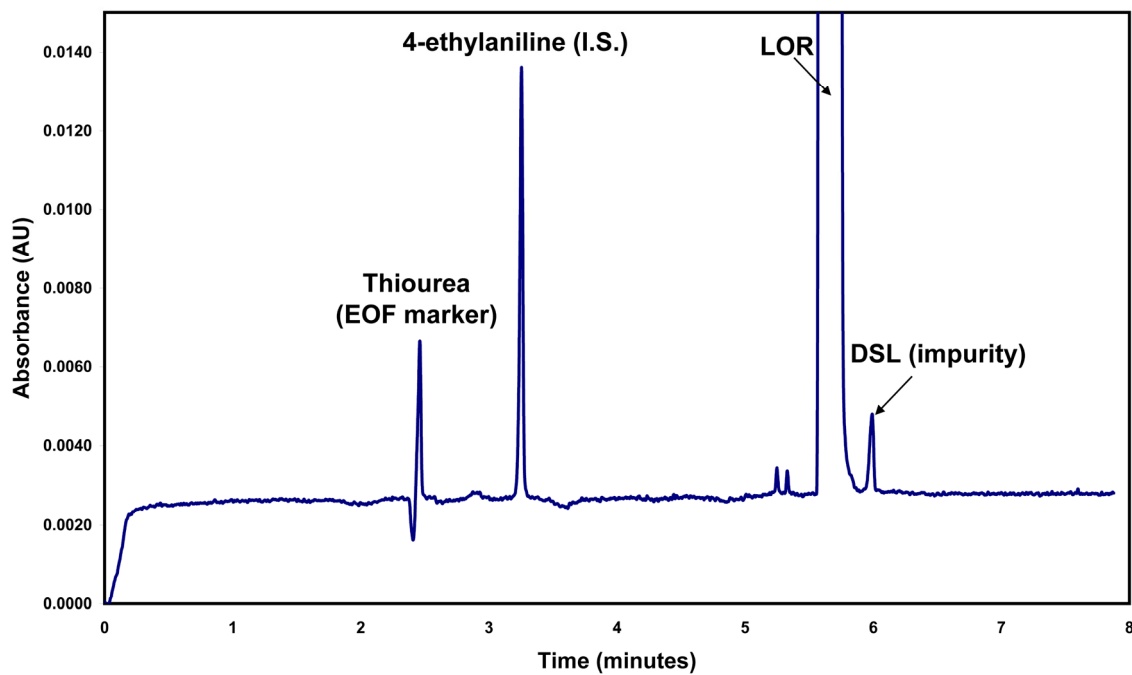


**Figure 7**

**Table 1.** Effect of concentration of SDS and  $\beta$ -CD/HP- $\beta$ -CD on the separation of LOR and DSL.<sup>a</sup>

SDS concentration (mmol L <sup>-1</sup> )	Type of CD	CD concentration (mmol L <sup>-1</sup> )	$\Delta t_r^b$	$R_s^b$	Total run time	Remark
30	$\beta$ -CD	20	0.14	1.2	5.8	
		25	0.28	1.8	6.2	
		30	---	---	---	Peak deformation <sup>c</sup>
	HP- $\beta$ -CD	20	0.50	4.2	5.6	Peak shoulder
		25	---	---	---	Peak deformation <sup>c</sup>
		30	---	---	---	Peak deformation <sup>c</sup>
40	$\beta$ -CD	20	0.07	0.7	6.2	
		25	0.12	1.1	6.3	
		30	0.21	1.7	6.4	
	HP- $\beta$ -CD	20	0.23	3.6	6.1	Optimum
		25	0.43	4.2	5.9	Peak shoulder
		30	---	---	---	Peak deformation <sup>c</sup>
50	$\beta$ -CD	20	0.04	0.3	6.5	
		25	0.07	0.9	6.6	
		30	0.12	1.2	6.7	
	HP- $\beta$ -CD	20	0.16	2.6	6.7	
		25	0.34	4.8	7.2	Peak shoulder
		30	---	---	---	Peak deformation

<sup>a</sup> This measurement series was performed using 5 mmol L<sup>-1</sup> sodium borate buffer and capillary temperature 25°C. Other experimental parameters see Figure 3.

<sup>b</sup>  $\Delta t_r$  = difference in migration time,  $R_s$  = peak resolution for LOR and DSL peaks.

<sup>c</sup> Peak deformation refers to peak splitting or complete peak distortion of LOR peak.

**Table 2.** Effect of borate buffer concentration and applied voltage on the separation of LOR and DSL.<sup>a</sup>

Borate buffer concentration (mmol L <sup>-1</sup> )	Applied voltage (kV)	$\Delta t_r^b$	$R_s^b$	Total run time	Remark
5	15	0.36	3.8	9.5	Optimum
	20	0.27	3.7	7.1	
	25	0.21	3.6	5.6	
10	15			10.8	Peak deformation <sup>c</sup>
	20	0.32	4.2	8.0	Peak shoulder
	25	0.25	4.2	6.2	Optimum
15	15	0.57	3.8	12.2	Peak shoulder
	20	0.43	4.1	9.0	Peak shoulder
	25	0.33	4.0	7.0	Peak shoulder

<sup>a</sup> This measurement series was performed using capillary temperature of 25°C. For other experimental parameters see Figure 3.

<sup>b</sup>  $\Delta t_r$  = difference in migration time,  $R_s$  = peak resolution for LOR and DSL peaks.

<sup>c</sup> Peak deformation refers to peak splitting or complete peak distortion of LOR peak.

**Table 3.** Effect of capillary temperature on the separation of LOR and DSL.<sup>a</sup>

Capillary temperature (°C)	Borate buffer concentration (mmol L <sup>-1</sup> )	$\Delta t_r^b$	$R_s^b$	Total run time	Remark
20	5	0.27	3.7	6.8	peak shoulder
	10	0.32	4.5	7.6	
25	5	0.24	3.6	5.9	peak shoulder
	10	0.28	4.2	6.6	
30	5	0.21	3.6	5.3	Optimum
	10	0.24	3.9	5.9	

<sup>a</sup> For other experimental parameters see Figure 3.

<sup>b</sup>  $\Delta t_r$  = difference in migration time,  $R_s$  = peak resolution for LOR and DSL peaks.

<sup>c</sup> Peak deformation refers to peak splitting or complete peak distortion of LOR peak.

**Table 4.** Validation parameters of LOR and DSL using the developed CD-MEKC method (see Figure 3) using different calibration response parameters.<sup>a</sup>

Parameter	LOR				DSL			
	Peak height ratio	Corr. peak area	Peak area ratio	Corr. peak area ratio	Peak height ratio	Corr. peak area	Peak area ratio	Corr. peak area ratio
Range ( $\mu\text{g mL}^{-1}$ )	3 - 35	3 - 60	3 - 60	3 - 60	2 - 35	2 - 60	2 - 60	2 - 60
Regression equation	$y = 0.0327x + 0.0458$	$y = 165.84x - 228.14$	$y = 0.0424x - 0.0374$	$y = 0.0244x - 0.0249$	$y = 0.0547x - 0.0036$	$y = 185.43x - 51.743$	$y = 0.0481x + 0.0277$	$y = 0.0263x + 0.0140$
Correlation coefficient ( $r$ )	0.9987	0.9981	0.9997	0.9997	0.9987	0.9951	0.9998	0.9998
$S_{y/x}$ <sup>b</sup>	0.0198	190.28	0.0184	0.0107	0.0332	327.94	0.0158	0.0082
$S_a$ <sup>b</sup>	0.0099	77.879	0.0075	0.0044	0.0146	133.63	0.0064	0.0033
$S_b$ <sup>b</sup>	0.0005	3.0639	0.0003	0.0002	0.0009	5.3088	0.0003	0.0001
%recovery (mean $\pm$ SD)	98.67 $\pm$ 8.10 (n=11)	102.14 $\pm$ 7.27 (n=13)	101.03 $\pm$ 1.81 (n=13)	102.59 $\pm$ 2.61 (n=13)	100.12 $\pm$ 6.41 (n=12)	104.62 $\pm$ 12.62 (n=14)	100.44 $\pm$ 2.50 (n=14)	101.71 $\pm$ 2.81 (n=14)
%RSD <sup>c</sup>	8.21	7.12	1.80	2.55	6.40	12.07	2.49	2.77
%Error <sup>c</sup>	2.47	1.97	0.50	0.71	1.85	3.22	0.66	0.74
DL ( $\mu\text{g mL}^{-1}$ ) <sup>d</sup>	1	1	1	1	0.6	0.6	0.6	0.6
QL ( $\mu\text{g mL}^{-1}$ ) <sup>d</sup>	3	3	3	3	2	2	2	2

<sup>a</sup> The results are based on the average of at least 3 replicate determinations. The measured responses are the corrected peak area (peak area of analyte/migration time), peak height ratio (analyte/ I.S.), peak area ratio (analyte/I.S.) or corrected peak area ratio (analyte/I.S.).

<sup>b</sup>  $S_{y/x}$  = standard deviation of the residuals,  $S_a$  = standard deviation of the intercept and  $S_b$  = standard deviation of the slope.

<sup>c</sup> %RSD = percentage relative standard and %Error = %RSD/ $\sqrt{n}$ .

<sup>d</sup> DL = detection limit and QL = quantitation limit.

**Table 5.** Assay results for the determination of LOR and DSL in pure form by the developed CD-MEKC method (see Figure 3) and the official method (see Supplementary Data).

	Developed method		Official method [36]
	Concentration added ( $\mu\text{g mL}^{-1}$ )	%Recovery <sup>a</sup>	
LOR	5	97.90	98.91
	30	98.56	100.25
	50	98.91	99.58
Mean $\pm$ SD		98.46 $\pm$ 0.51	99.58 $\pm$ 0.67
<i>t</i>		2.306 (2.78) <sup>b</sup>	
<i>F</i>		1.707 (19.00) <sup>b</sup>	
DSL	5	99.07	99.65
	30	99.55	101.02
	50	100.23	99.74
Mean $\pm$ SD		99.62 $\pm$ 0.58	100.14 $\pm$ 0.77
<i>t</i>		0.935 (2.78) <sup>b</sup>	
<i>F</i>		1.728 (19.00) <sup>b</sup>	

<sup>a</sup> Average of 3 replicate determinations.

<sup>b</sup> The figures between parentheses are the tabulated values of *t* and *F* at *P* = 0.05 [81].

**Table 6.** Intraday and interday precision data for the determination of LOR and DSL by the developed CD-MEKC method (for other experimental values refer to Figure 3).

Day	Run no.	LOR						DSL					
		7 µg mL <sup>-1</sup>		15 µg mL <sup>-1</sup>		35 µg mL <sup>-1</sup>		7 µg mL <sup>-1</sup>		15 µg mL <sup>-1</sup>		35 µg mL <sup>-1</sup>	
		migration time	Peak area ratio	migration time	Peak area ratio	migration time	Peak area ratio	migration time	Peak area ratio	migration time	Peak area ratio	migration time	Peak area ratio
Day 1	1	5.67	0.25	5.68	0.65	5.74	1.47	5.91	0.38	5.92	0.77	5.96	1.79
	2	5.72	0.26	5.74	0.61	5.75	1.44	5.96	0.40	5.98	0.74	5.97	1.78
	3	5.73	0.25	5.75	0.63	5.72	1.41	5.97	0.40	5.99	0.78	5.93	1.73
	Mean	5.71	0.26	5.72	0.63	5.74	1.44	5.95	0.39	5.96	0.76	5.95	1.77
	SD	0.03	0.00	0.03	0.02	0.02	0.03	0.03	0.01	0.04	0.02	0.02	0.03
	%RSD	0.49	1.19	0.59	3.24	0.30	2.19	0.51	2.59	0.63	2.74	0.40	1.75
Day 2	1	5.67	0.27	5.68	0.59	5.72	1.41	5.91	0.37	5.92	0.71	5.93	1.75
	2	5.70	0.28	5.70	0.59	5.74	1.45	5.94	0.36	5.92	0.69	5.96	1.69
	3	5.71	0.26	5.70	0.56	5.75	1.42	5.96	0.37	5.94	0.70	5.96	1.80
	Mean	5.69	0.27	5.69	0.58	5.73	1.43	5.93	0.37	5.92	0.70	5.95	1.75
	SD	0.02	0.01	0.01	0.01	0.01	0.02	0.03	0.01	0.01	0.01	0.02	0.05
	%RSD	0.40	3.96	0.18	2.32	0.25	1.57	0.43	2.06	0.18	1.08	0.33	3.09
Day 3	1	5.71	0.24	5.67	0.58	5.70	1.38	5.96	0.34	5.89	0.69	5.90	1.69
	2	5.72	0.23	5.72	0.57	5.71	1.31	5.97	0.37	5.96	0.67	5.91	1.60
	3	5.73	0.24	5.72	0.58	5.70	1.29	5.98	0.36	5.96	0.72	5.92	1.56
	Mean	5.72	0.24	5.70	0.58	5.70	1.33	5.97	0.36	5.94	0.69	5.91	1.62
	SD	0.01	0.01	0.03	0.01	0.01	0.05	0.01	0.01	0.04	0.03	0.01	0.06
	%RSD	0.11	3.04	0.48	1.20	0.12	3.66	0.15	3.57	0.66	3.79	0.10	3.95
Interday	Overall mean	5.71	0.25	5.71	0.60	5.72	1.40	5.95	0.37	5.94	0.72	5.94	1.71
	SD	0.02	0.01	0.03	0.03	0.02	0.06	0.02	0.02	0.03	0.04	0.03	0.08
	%RSD	0.38	5.65	0.45	4.88	0.35	4.38	0.42	4.74	0.55	5.42	0.44	4.88

**Table 7.** Robustness data for the determination of LOR and DSL by the developed CD-MEKC method (analyte concentration = 15  $\mu\text{g mL}^{-1}$  each, for experimental parameters refer to Figure 3).

Parameter	Levels	%RSD (n=6) <sup>a</sup>				
		$R_s^b$	$t_r^b$ (LOR)	Peak area ratio (LOR)	$t_r^b$ (DSL)	Peak area ratio (DSL)
Applied voltage	(+24, +25, +26) kV	2.02	3.96	1.26	3.96	0.53
Capillary temperature	(29, 30, 31) °C	3.17	2.06	0.80	2.05	1.04
SDS concentration	(39, 40, 41) mmol L <sup>-1</sup>	3.23	1.14	2.60	0.96	1.72
HP- $\beta$ -CD concentration	(19, 20, 21) mmol L <sup>-1</sup>	6.49	0.17	3.16	0.15	3.92
Borate buffer concentration	(9, 10, 11) mmol L <sup>-1</sup>	1.57	2.22	1.57	2.24	1.34
pH of borate buffer	(9.20, 9.30, 9.40)	2.00	0.92	2.91	1.06	1.93

<sup>a</sup> Duplicate measurements for each level.

<sup>b</sup>  $t_r$  = migration time,  $R_s$  = peak resolution for LOR and DSL.

**Table 8.** Assay results for the determination of LOR and DSL in tablets by the developed CD-MEKC method (see Figure 3) and the official method (see Supplementary Data).

	%Recovery <sup>a</sup>	
	Developed method	Official method [36]
Lora-ADGC® tablets	99.60	99.49
	98.70	100.81
	98.19	99.40
Mean±SD	98.83±0.71	99.90±0.79
<i>t</i>	1.741 (2.78) <sup>b</sup>	
<i>F</i>	1.222 (19.00) <sup>b</sup>	
Aerius® film-coated tablets	98.74	100.09
	98.35	99.74
	98.96	99.03
Mean±SD	98.68±0.31	99.62±0.54
<i>t</i>	2.607 (2.78) <sup>b</sup>	
<i>F</i>	3.057 (19.00) <sup>b</sup>	

<sup>a</sup> Average of 3 replicate determinations.

<sup>b</sup> The figures between parentheses are the tabulated values of *t* and *F* at *P* = 0.05 [81].

**Table 9.** Assay results for the determination of LOR and DSL in spiked human urine by the developed CD-MEKC method (for experimental parameters refer to Figure 3).

	Concentration added ( $\mu\text{g mL}^{-1}$ )	Concentration found ( $\mu\text{g mL}^{-1}$ )	%Recovery <sup>a</sup>
LOR	5	5.219	104.38
	8	7.482	93.53
	10	8.782	87.82
	12	11.18	93.17
	18	17.52	97.33
Mean $\pm$ SD			95.25 $\pm$ 6.13
%RSD			6.43
DSL	5	5.219	104.38
	8	7.770	97.13
	10	8.444	84.44
	12	11.27	93.92
	18	16.95	94.17
Mean $\pm$ SD			94.81 $\pm$ 7.17
%RSD			7.56

<sup>a</sup> Average of 3 replicate determinations.

**5.4.4. Robust analysis of hydrophobic basic analytes in pharmaceutical preparations and biological fluids by sweeping-micellar electrokinetic chromatography with retention factor gradient effect and dynamic pH junction.**

Mohamed El-Awady<sup>1</sup>, Fathalla Belal<sup>2</sup>, Ute Pyell<sup>1\*</sup>

<sup>1</sup>University of Marburg, Department of Chemistry, Hans-Meerwein-Straße, D-35032 Marburg, Germany

<sup>2</sup>Analytical Chemistry Department, Faculty of Pharmacy, Mansoura University, 35516 Mansoura, Egypt

\* corresponding author

### **Supplementary data**

- Measurement of retention factors of LOR and DSL.
- Optimization of injection volume for the developed CD-MEKC method.
- Calibration curves for LOR and DSL using the developed CD-MEKC.
- Experimental details of the reference pharmacopeial method.

**Measurement of retention factors of LOR and DSL**

To illustrate the effect of HP- $\beta$ -CD on the retention behavior of both LOR and DSL, the retention factors for both analytes were measured in a BGE containing 40 mmol L<sup>-1</sup> SDS and 20 mmol L<sup>-1</sup> HP- $\beta$ -CD dissolved in 5 mmol L<sup>-1</sup> sodium borate buffer, pH 9.30 and compared with those in the same BGE but without HP- $\beta$ -CD. In presence of CDs in the BGE, the direct measurement of retention factors using a single compound as a micelle marker is no longer reliable. That is because the prerequisite that the micelle marker should have a retention factor of infinity is no longer fulfilled. The difficulty of a direct measurement of the retention factors in the presence of CDs is similar to that observed by Chen *et al.* [Electrophoresis 16 (1995) 1457] during their study of the effect of organic modifier concentrations on the electrophoretic mobility of micelles in MEKC. Therefore, in these cases we have to use the iterative approach published by Bushey and Jorgenson [J. Microcolumn Sep. 1 (1989) 125, Anal. Chem. 61 (1989) 491] for the determination of the electrophoretic mobility of the micelles which is based on the Martin equation (valid for the retention factors of the members of a homologous series). In the present study, the homologous series of alkyl phenyl ketones namely acetophenone, propiophenone, butyrophenone, valerophenone and hexanophenone were used. The same homologous series was used by Chen *et al.* [Electrophoresis 16 (1995) 1457] for measuring the  $t_{mc}$  values in BGEs containing different organic modifiers.

In this iterative approach, hexanophenone is first assumed to be a micelle marker and the retention factor  $k$  for acetophenone, propiophenone, butyrophenone and valerophenone is calculated according to Eq. (1), where  $t_r$  is the migration time of the analyte and  $t_0$  is the migration time of the EOF marker (methanol used to solubilize the mixture of alkyl phenyl ketones).

$$k = \frac{t_s - t_0}{t_0(1 - t_s / t_{mc})} \quad (1)$$

where  $t_0$  = migration time of the EOF marker,  $t_s$  = migration time of the analyte,  $t_{mc}$  = migration time of the micelle marker.

Then  $\log k$  is plotted against the carbon number  $N_C$  of the alkyl group. Using this plot, a temporary value of  $k$  for hexanophenone is obtained from  $\log k$  at  $N_C = 6$  from which a new  $t_{mc}$  is calculated using Eq. (1). Then the values of  $\log k$  are re-calculated employing the improved estimation of  $t_{mc}$  and re-plotted against  $N_C$ . The iterative procedure is then repeated until a constant value of  $t_{mc}$  is obtained with the lowest possible sum of squared errors (SSE) and the highest possible squared correlation coefficient  $R^2$ . In all cases the convergence criterion was reached. The results are mentioned in Section 4.

**Optimization of injection volume for the developed CD-MEKC method**

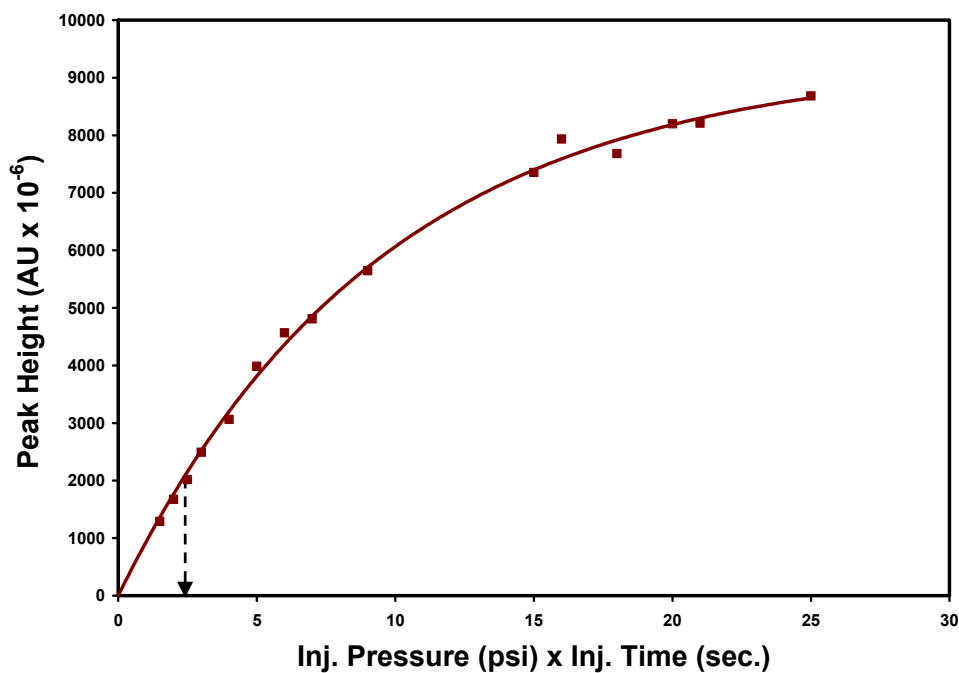


**Figure S1:** Peak height plotted against injected volume for **LOR** under optimized experimental conditions (for experimental parameters refer to Figure 3).

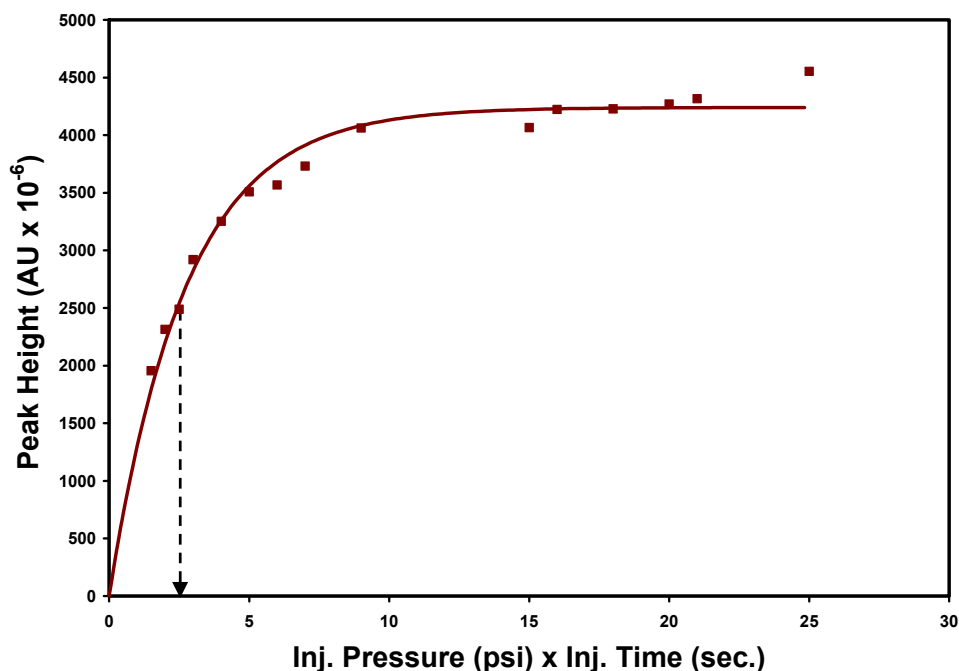


**Figure S2:** Peak height plotted against injected volume for **DSL** under optimized experimental conditions (for experimental parameters refer to Figure 3).

**Calibration curves for LOR and DSL using the developed CD-MEKC**

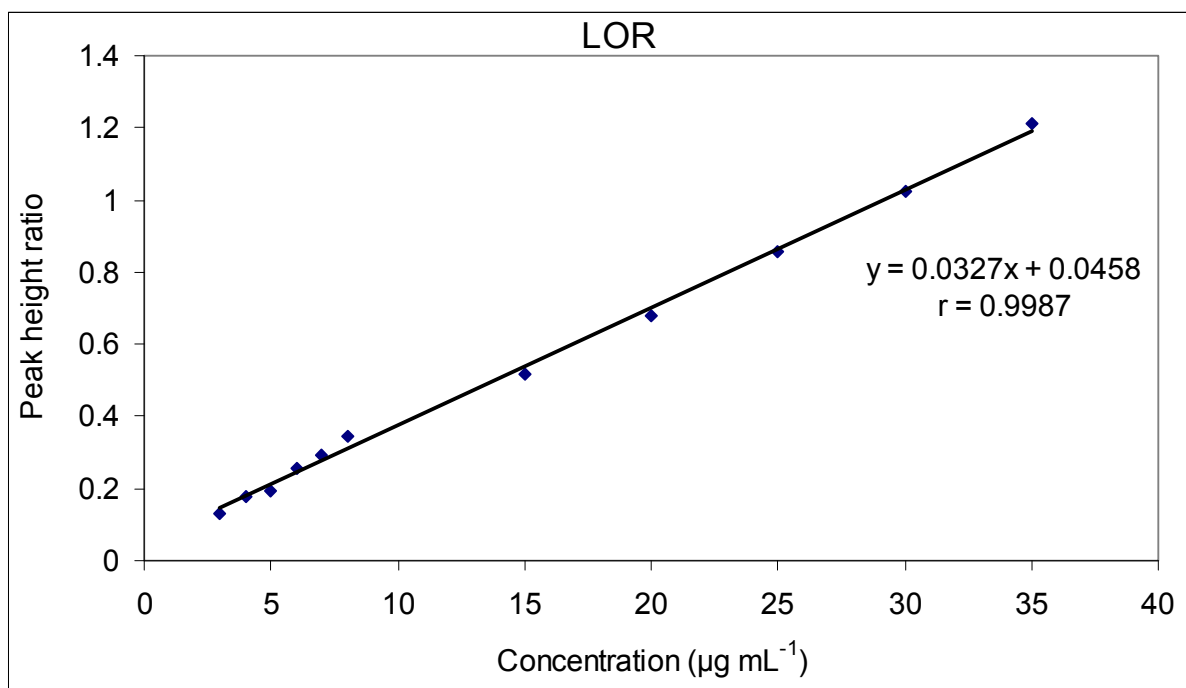


**Figure S3:** Calibration curve for LOR using **peak height ratio** as response parameter (for experimental conditions refer to Figure 3).

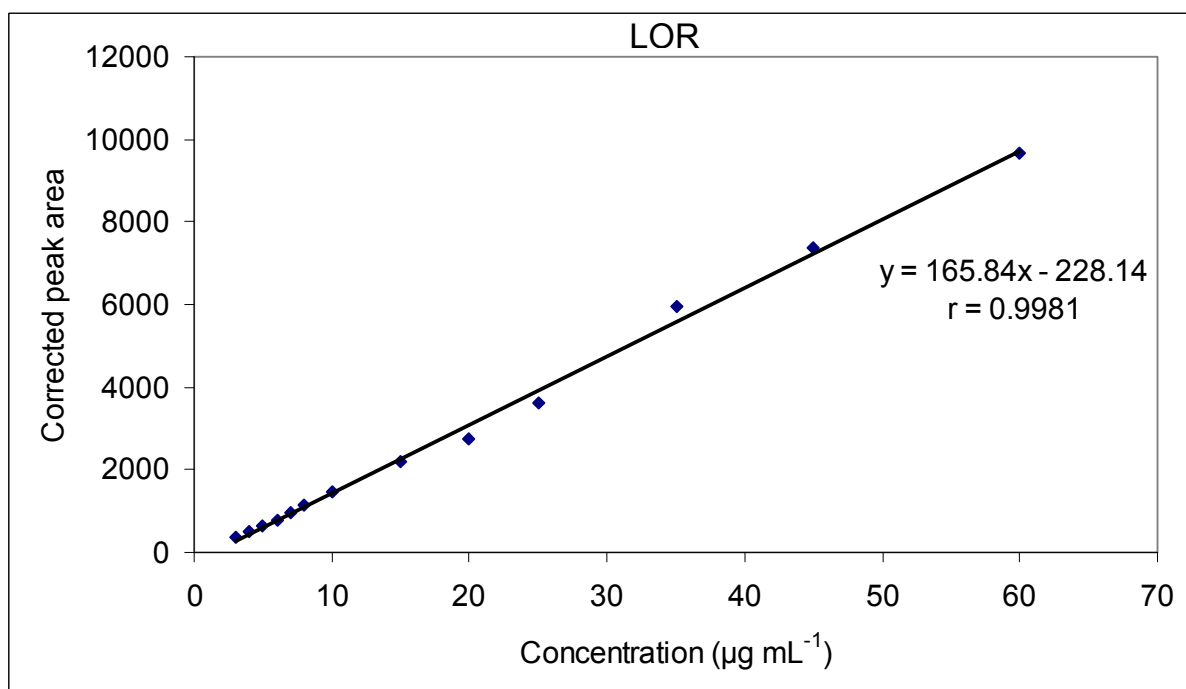


**Figure S4:** Calibration curve for LOR using **corrected peak area** as response parameter (for experimental conditions refer to Figure 3).

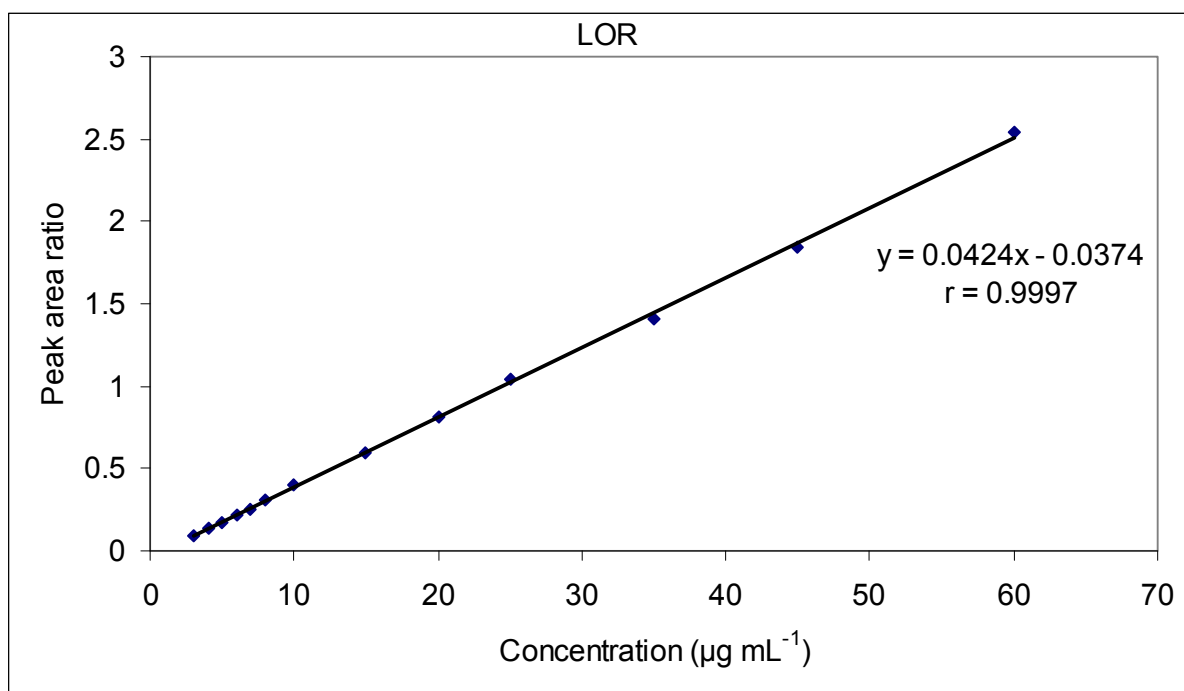


**Figure S5:** Calibration curve for LOR using **peak area ratio** as response parameter (for experimental conditions refer to Figure 3).

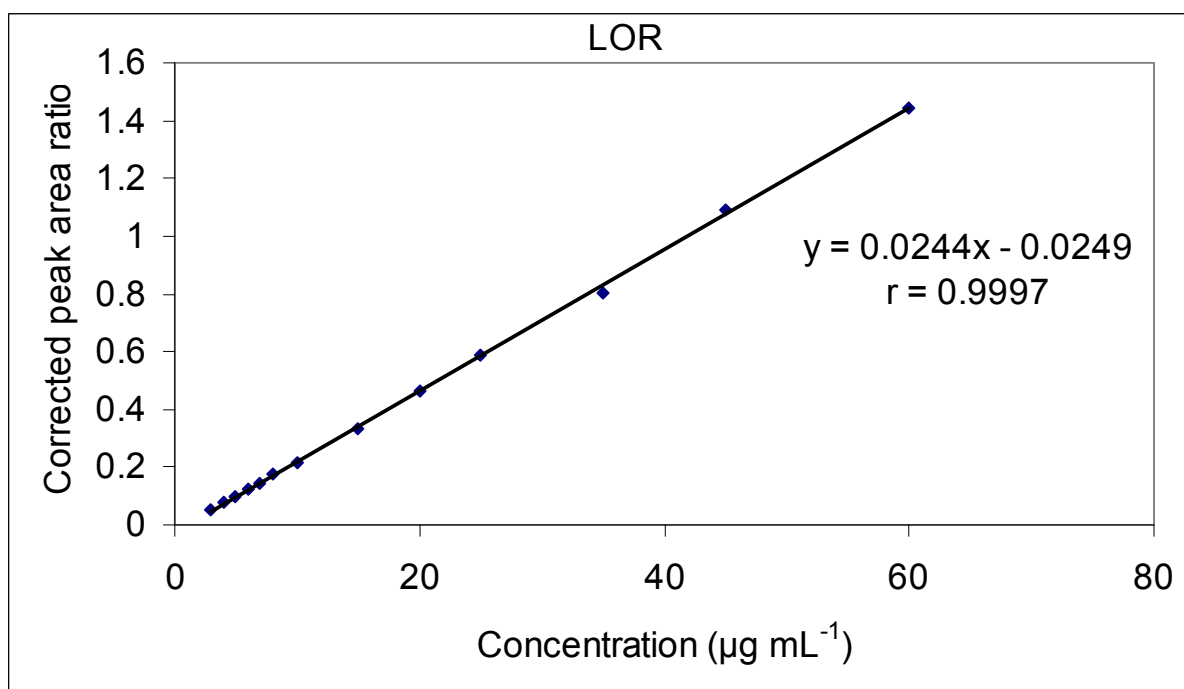


**Figure S6:** Calibration curve for LOR using **corrected peak area ratio** as response parameter (for experimental conditions refer to Figure 3).

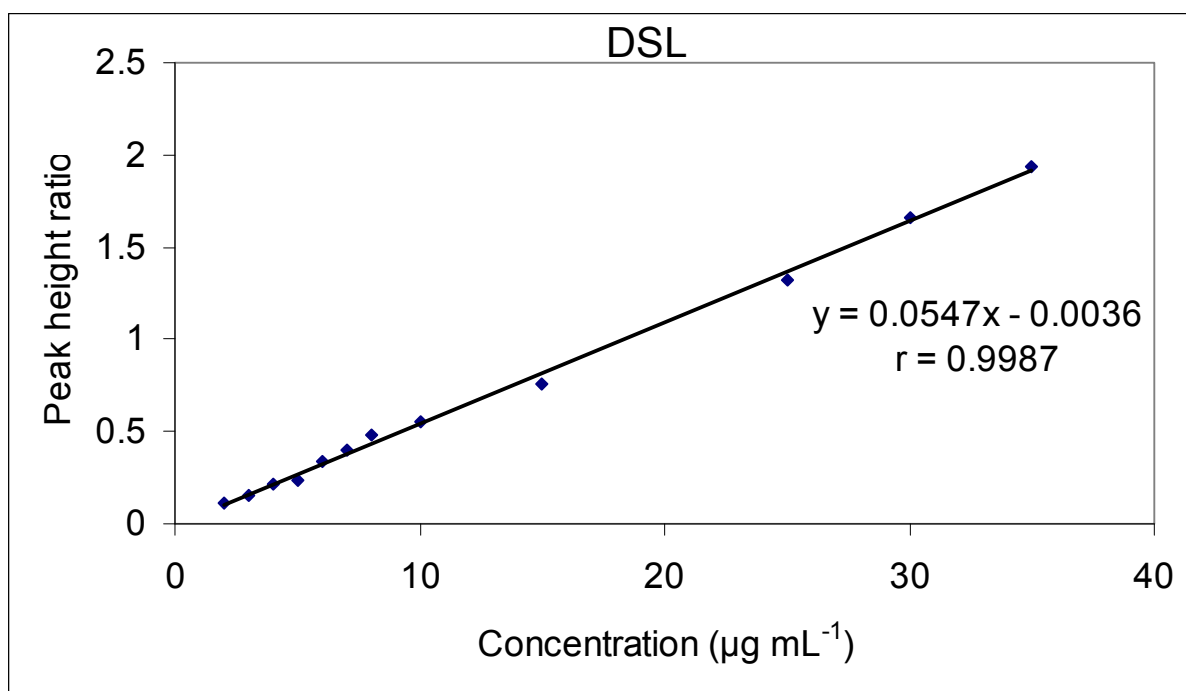


**Figure S7:** Calibration curve for **DSL** using **peak height ratio** as response parameter (for experimental conditions refer to Figure 3).

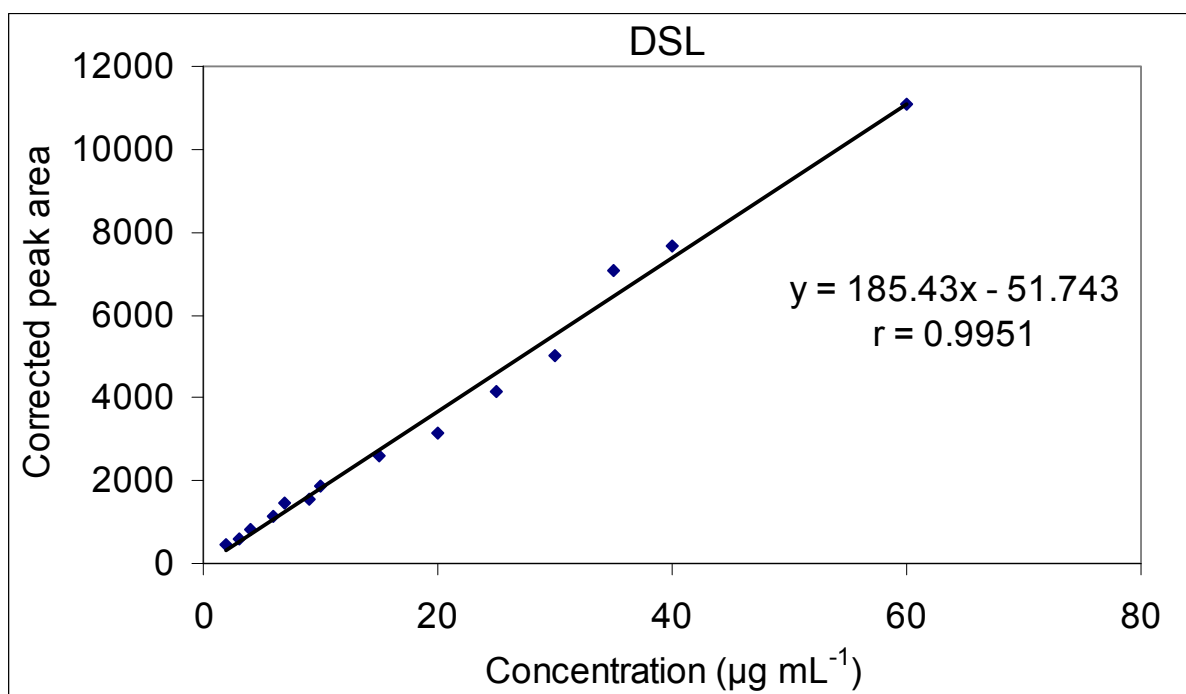


**Figure S8:** Calibration curve for **DSL** using **corrected peak area** as response parameter (for experimental conditions refer to Figure 3).

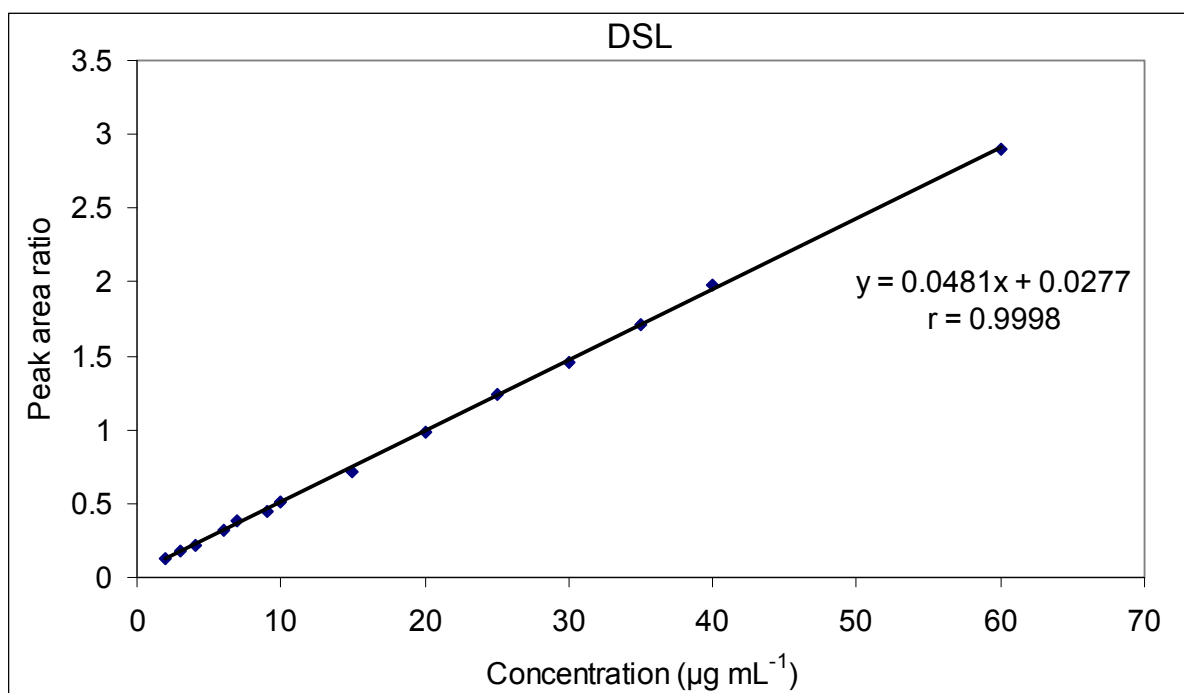


**Figure S9:** Calibration curve for **DSL** using **peak area ratio** as response parameter (for experimental conditions refer to Figure 3).

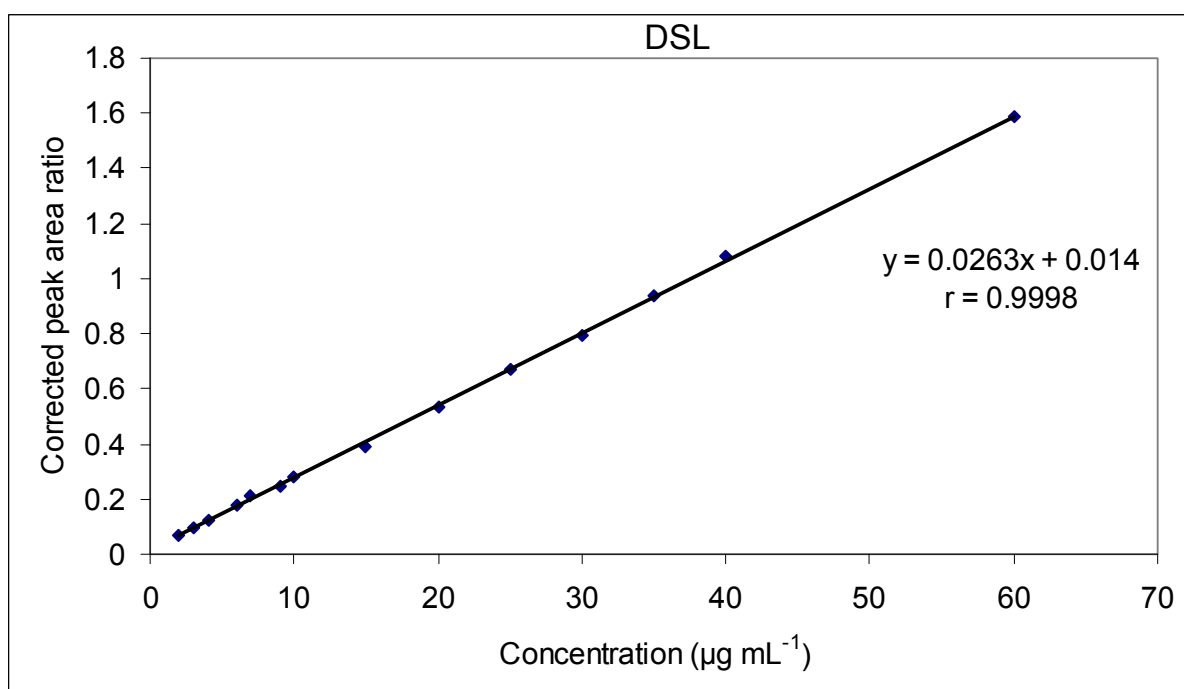


**Figure S10:** Calibration curve for **DSL** using **corrected peak area ratio** as response parameter (for experimental conditions refer to Figure 3).

**Calibration curves for LOR and DSL in spiked human urine using the developed CD-MEKC**

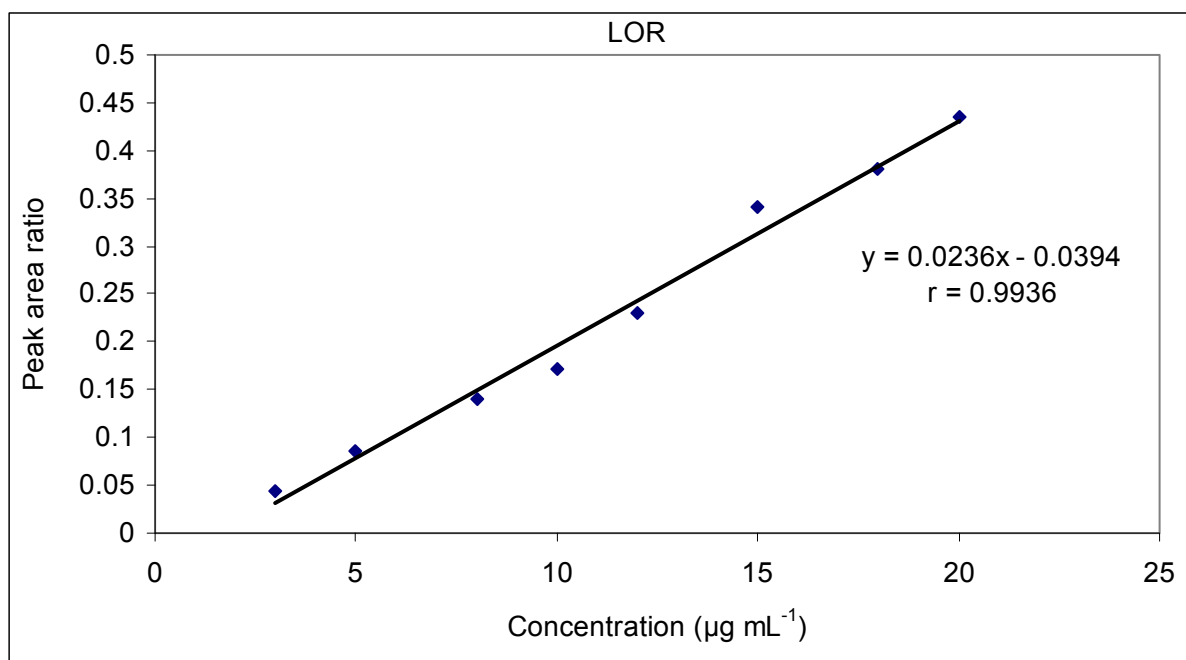


**Figure S11:** Calibration curve for **LOR** in spiked human urine using **peak area ratio** as response parameter (for experimental conditions refer to Figure 3).

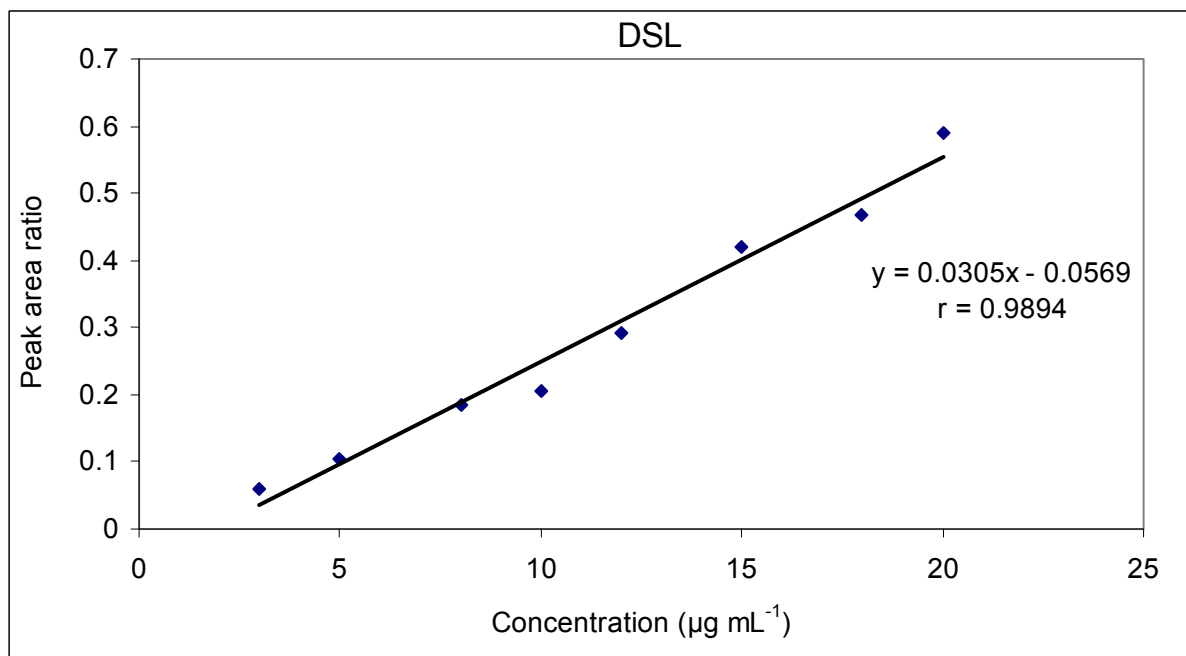


**Figure S12:** Calibration curve for **DSL** in spiked human urine using **peak area ratio** as response parameter (for experimental conditions refer to Figure 3).

### **Experimental details of the reference pharmacopeial method**

The reference comparison method is based on the liquid chromatographic method reported for the determination of related substances in the monograph of LOR in the European Pharmacopeia [7th Edition (7.8), Online Version, European directorate for the quality of medicines & healthcare (EDQM), Strasbourg, 2013]. The determination was based on one-point assay using peak area as the response parameter.

#### **Apparatus:**

All measurements were done with a Merck Hitachi Chromatograph model L-7100 equipped with a Rheodyne injector valve with a 20  $\mu\text{L}$  loop, and a Merck Hitachi L-7400 UV detector. The chromatograms were recorded on a Merck Hitachi D-7500 integrator. The mobile phase was degassed using Merck solvent L-7612 degasser. A Consort P-901 pH-meter was used for pH measurements. A Promosil ODS 100 A column (C18, 250 x 4.6 mm i.d., 5  $\mu\text{m}$  particle size), Agela Technologies, USA was used for the separation.

#### **Preparation of the mobile phase:**

The mobile phase was prepared by mixing 30 volumes of methanol, 35 volumes of a 6.8 g  $\text{L}^{-1}$  solution of potassium dihydrogen phosphate in water previously adjusted to pH  $2.80 \pm 0.05$  with phosphoric acid and 40 volumes of acetonitrile.

#### **Preparation of samples:**

Standard solution: 20  $\mu\text{g mL}^{-1}$  of LOR and DSL dissolved in the mobile phase.

For tablets: the finely powdered tablets of each analyte were dissolved in mobile phase so that the final concentration of the studied analyte is 20  $\mu\text{g mL}^{-1}$ . The solution is then sonicated for 30 min and filtered through a 0.45  $\mu\text{m}$  membrane filter.

#### **Chromatographic conditions:**

Column: C18, 250 x 4.6 mm i.d., 5  $\mu\text{m}$  particle size.

Temperature: 25°C.

Flow rate: 1.5  $\text{mL min}^{-1}$

Detection: UV detection at 220 nm.

Injection volume: 20  $\mu\text{L}$ .

**Chromatogram:**

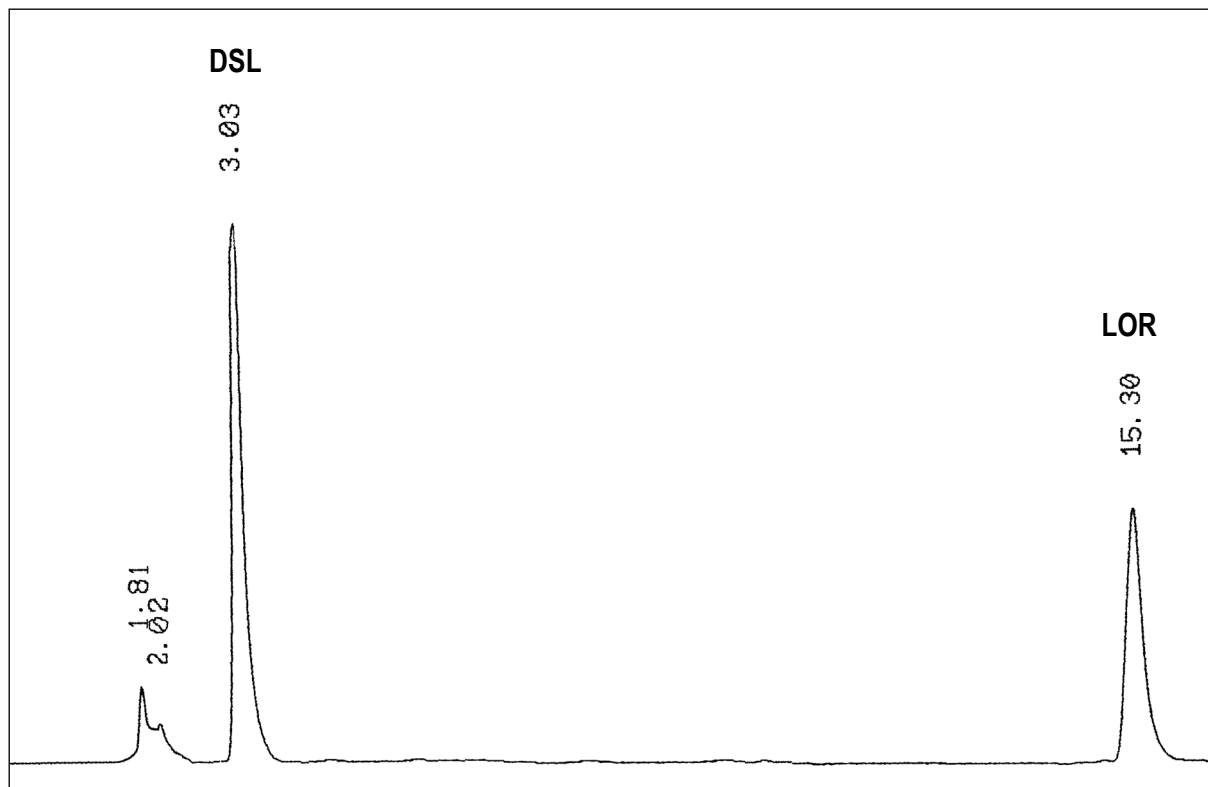


**Figure S13:** Chromatogram of LOR and DSL ( $20 \mu\text{g mL}^{-1}$  each) obtained with the reference pharmacopeial method.

## 6. Acknowledgement

My praise, gratitude and thanks to **God**, the Almighty, for guiding and helping me to achieve this work.

I am cordially indebted to **Prof. Dr. Ute Pyell**, for her supervision, valuable advices and moral support while performing this work. I appreciate her helpful scientific instructions and comments that she always offered to me. In the research group of Prof. Pyell, I have really learned how to thoroughly investigate the fundamentals of analytical techniques and how to apply my findings on real pharmaceutical applications. My sincere thanks and acknowledgement to her for providing all the facilities that helped me to complete this project.

Thanks to **Dr. Carolin Huhn** and **Dr. Pablo Kler** (Forschungszentrum Jülich, Germany) for their contribution in the first publication of this dissertation. My sincere thanks and gratitude to **Prof. Dr. Fathalla Belal** and **M.Sc. Heba Elmansi** (Faculty of Pharmacy, Mansoura University, Egypt) for their valuable contribution in the fourth publication of the dissertation.

Special acknowledgement to **Yousef-Jameel Foundation** for funding my PhD project, and offering all the required facilities. Thanks to **Frau Miriam Groß** (International Office, University of Marburg) for her care as the coordinator of Yousef-Jameel scholarship program in Marburg.

I would like also to express my thanks to my colleagues in the research group of Prof. Pyell especially **Ayat Allah Al-Massaedh** and **Azza Rageh** for their continuous support and valuable scientific discussion. I also thank my colleagues in the department of chemistry **Mohamed Abd El-Majeed**, **Yasser Assem**, **Haitham Abd El-Aal**, **Ahmed Bayoumi** and **Mustafa Zyadi** for their support and for the nice time that we spent in Marburg.

I owe special acknowledgement, deep appreciation and sincere thanks to my big family (**my father**, **my mother** and **my brothers**) and my small family (**my wife** and **my beloved children**) for their unlimited encouragement, continuous advices, and cordial assistance during my PhD project. Words can not express how grateful I feel to them for their unconditional love and emotional support.

Finally, I thank all those who might have had a hand in realizing this work in one way or another but it has not been possible to mention them by name.

*Mohamed El-Awady*



## 7. Curriculum Vitae

### M.Sc. Mohamed Ibraheem Mohamed El-Awady

University of Marburg, Department of Chemistry

Hans-Meerwein-Straße, 35032 Marburg, Germany

Tel: Office: +49 64212825411, Mobile: +49 17624977895, Fax: +49 64212822124

E-mail: [mohamedelawady2@yahoo.com](mailto:mohamedelawady2@yahoo.com), [elawadym@staff.uni-marburg.de](mailto:elawadym@staff.uni-marburg.de)

#### Academic degrees

- **M.Sc.** Pharmaceutical Analytical Chemistry, December 2007, Faculty of Pharmacy, Mansoura University, Mansoura, Egypt.  
Thesis title: "Determination of certain compounds or their related products in pharmaceutical preparations and biological fluids".
- **B.Sc.** Pharmaceutical Sciences, July 2000, Very Good, Honor, Faculty of Pharmacy, Mansoura University, Mansoura, Egypt.
- **High school degree**, July 1995, Talaat Harb Secondary School, El-Mehalla El-Koubra, Egypt.

#### Experience

- **Aug. 2009 to Present:** PhD student in the Department of Chemistry, University of Marburg, Marburg, Germany.
- **Jan. 2008 to Present:** Assistant Lecturer of Pharmaceutical Analytical Chemistry, Faculty of Pharmacy, Mansoura University, Mansoura, Egypt.
- **Oct. 2000 to 2007:** Graduate Teaching and Research Associate, Faculty of Pharmacy, Mansoura University, conducting research on the determination of pharmaceutical compounds and their formulations using chromatographic, fluorometric, spectrophotometric, polarographic and titrimetric methods. Also, I assisted in teaching pharmaceutical analytical chemistry to undergraduate students.
- **Mar. 2001 to Mar. 2002:** Quality Control Pharmacist during military service, Army Forces Pharmaceutical Company, Giza, Egypt.
- **Mar. 2006 to July 2009:** Member in E-learning Unit and in Quality Assurance & Accreditation Unit, Faculty of Pharmacy, Mansoura University, Mansoura, Egypt.
- **Aug. 1999 to Sep. 1999:** Training in Quality Control Department, EIPICO Pharmaceutical Company, 10<sup>th</sup> of Ramadan City, Egypt.

## **List of Publications**

### **PhD publications**

1. Processes involved in sweeping under inhomogeneous electric field conditions as sample enrichment procedure in micellar electrokinetic chromatography.  
Mohamed El-Awady, Carolin Huhn, Ute Pyell,  
*Journal of Chromatography A*, 1264 (2012) 124-136 [doi: 10.1016/j.chroma.2012.09.044].
2. Sweeping as a multistep enrichment process in micellar electrokinetic chromatography: The retention factor gradient effect.  
Mohamed El-Awady, Ute Pyell,  
*Journal of Chromatography A*, 1297 (2013) 213-225 [doi: 10.1016/j.chroma.2013.04.069].
3. Processes involved in sweeping as sample enrichment method in cyclodextrin-modified micellar electrokinetic chromatography of hydrophobic basic analytes.  
Mohamed El-Awady, Ute Pyell,  
*Submitted to: Electrophoresis*.
4. Robust analysis of hydrophobic basic analytes in pharmaceutical preparations and biological fluids by sweeping-micellar electrokinetic chromatography with retention factor gradient effect and dynamic pH junction.  
Mohamed El-Awady, Fathalla Belal, Ute Pyell,  
*Submitted to: Journal of Chromatography A*.

### **M.Sc. publications**

1. Spectrophotometric analysis of a mixture of glyburide and metformin HCl in pharmaceutical preparations.  
Fathalla Belal, Mohie Sharaf El-Din, Fatma Aly, Mohamed Hefnawy, Mohamed El-Awady,  
*Der Pharma Chemica*, 3 (2011) 53-64.
2. Spectrophotometric determination of 2-amino-4-chlorophenol as a potential impurity in chlorzoxazone bulk drug.  
Fathalla Belal, Mohie Sharaf El-Din, Fatma Aly, Mohamed El-Awady,  
*International Journal of Pharmaceutical Sciences and Research*, 2 (2011) 829-838.
3. Fluorometric determination of bopindolol and celiprolol in pharmaceutical preparations and biological fluids.  
Fathalla Belal, Mohie Sharaf El-Din, Fatma Aly, Mohamed Hefnawy, Mohamed El-Awady,  
*Journal of Fluorescence*, 22 (2012) 1141-1150 [doi: 10.1007/s10895-012-1053-1].
4. Stability-indicating HPLC method for the determination of atenolol in pharmaceutical preparations.  
Fathalla Belal, Mohie Sharaf El-Din, Fatma Aly, Mohamed Hefnawy, Mohamed El-Awady,  
*Journal of Chromatography and Separation Techniques*, 4 (2013), 1-7 [doi: 10.4172/2157-7064.1000164].

### **Conferences**

1. The 39th International Symposium on High Performance Liquid Phase Separations and Related Techniques (HPLC2013), June 16-20, 2013, Amsterdam, the Netherlands [Poster Presentation].
2. The 27<sup>th</sup> International Symposium on MicroScale Bioseparations and Analyses (MSB2012), February 12-15, 2012, Geneva, Switzerland [Poster Presentation].
3. CE Forum: Capillary Electromigration Separation Techniques in Chemistry, Food Chemistry and Pharmacy, October 12-13, 2010, Jülich Research Center, Jülich, Germany [Poster Presentation].
4. The 1<sup>st</sup> International Pharmaceutical Sciences Conference, November 18-19, 2009, Tanta University, Tanta, Egypt [Poster Presentation].
5. The 34<sup>th</sup> International Symposium on High Performance Liquid Phase Separations and Related Techniques (HPLC2009), June 28 - July 2, 2009, Dresden, Germany [Poster Presentation].
6. The 5<sup>th</sup> International Conference on Chemistry "Green and Sustainable Chemistry for Developing Countries" (Chem05), March 3-6, 2008, Cairo University, Cairo, Egypt [Poster Presentation].
7. Al-Azhar 4<sup>th</sup> International Conference for Pharmaceutical and Biological Sciences, February 13-15, 2006, Al-Azhar University, Cairo, Egypt [Poster Presentation].

### **Oral presentation**

Oral presentation on my PhD work in the weekly seminar of the research groups of analytical chemistry in the Department of Chemistry, University of Marburg, February 7, 2012, Marburg, Germany.

### **Courses and Workshops**

1. "Agilent Forum for Capillary Electrophoresis" workshop, April 10, 2013, Agilent Technologies, Waldbronn, Germany.
2. "Capillary Electrophoresis: Method Development and Validation" training course, November 6-7, 2012, Kantisto Separation Sciences BV, Amsterdam, the Netherlands.
3. "Current Issues of Instrumental Analysis" workshop, July 6, 2012, Agilent Technologies, Waldbronn, Germany.
4. "Sample Preparation of Whole Blood for Microscale Bioseparations" workshop, February 12-15, 2012, Geneva, Switzerland.
5. "CE-MS: New developments and Applications" workshop, February 12-15, 2012, Geneva, Switzerland.
6. "Electromigration Separation Techniques" course by Prof. Dr. Ute Pyell, Winter semester (October 2011-March 2012), Department of Chemistry, University of Marburg, Germany.
7. "Chromatographic Analysis" training course, July 21-24, 2007, Faculty of Science, Ain-Shams University, Cairo, Egypt.
8. "Research Methodology" workshop, February 5-8, 2006, Mansoura University, Mansoura, Egypt.
9. "High Performance Liquid Chromatography" training course, May 5-8, 2003, Faculty of Pharmacy, Alexandria University, Alexandria, Egypt.

### **Membership**

- Member in the German Chemical Society (GDCh).
- Member in Marburg University Research Academy (MARA).

### **Grants**

- Yousef-Jameel PhD scholarship, August 2009-July 2013, Department of Chemistry, University of Marburg, Germany.
- German Chemical Society (GDCh) scholarship for the CE Forum: Capillary Electromigration Separation Techniques in Chemistry, Food Chemistry and Pharmacy, October 12-13, 2010, Jülich Research Center, Jülich, Germany.
- German Chemical Society (GDCh) scholarship for the 27<sup>th</sup> International Symposium on MicroScale Bioseparations and Analyses (MSB2012), February 12-15, 2012, Geneva, Switzerland

### **Teaching Experiences**

- Undergraduate Studies: Qualitative inorganic analysis, quantitative chemical analysis, instrumental analysis, and applied analysis (analysis of water, oils, fats and pharmaceutical preparations).
- Postgraduate Studies: Instrumental analysis for quality control diploma students.

### **Skills**

- Good command of English [TOEFL (ibt) score 80 equivalent to TOEFL (cbt) score 550].
- Advanced computer skills [International Computer Driving License (ICDL)].

### **References**

- **Prof. Dr. Ute Pyell**  
University of Marburg  
Department of Chemistry  
Hans-Meerwein-Straße  
35032 Marburg, Germany.  
E-mail: [pyellu@staff.uni-marburg.de](mailto:pyellu@staff.uni-marburg.de)
- **Prof. Dr. Fathalla Belal**  
Mansoura University  
Faculty of Pharmacy  
Department of Analytical Chemistry,  
Mansoura 35516, Egypt.  
E-mail: [ffbelal@yahoo.com](mailto:ffbelal@yahoo.com)